Dipartimento Interateneo di Fisica M. Merlin

Ph.D. Degree in Physics

Cycle XXXVIII

Ph.D. Thesis in Theoretical Physics

Scientific Disciplinary Sector: FIS/02

Cosmological primordial gravitational waves from pre-Big Bang

Supervisors:

Prof. Luigi Tedesco

Prof. Giuseppe Fanizza

Coordinator:

Prof. Vincenzo Spagnolo

Candidate:

Eliseo Pavone

A.Y. 2024/2025

FINAL EXAM 2026

Dipartimento Interateneo di Fisica M. Merlin

Ph.D. Degree in Physics

Cycle XXXVIII

Ph.D. Thesis in Theoretical Physics

Scientific Disciplinary Sector: FIS/02

Cosmological primordial gravitational waves from pre-Big Bang

Supervisors:

Prof. Luigi Tedesco

Prof. Giuseppe Fanizza

Coordinator:

Prof. Vincenzo Spagnolo

Candidate:

Eliseo Pavone

A.Y. 2024/2025

FINAL EXAM 2026

I hear it's amazing when the famous purple stuffed worm in flap-jaw space with the tuning fork does a raw blink on Hara-Kiri Rock. I need scissors! 61!

Acknowledgments

Desidero esprimere la mia più profonda gratitudine al Professor Gabriele Veneziano e al Professor Maurizio Gasperini, per avermi guidato con costante attenzione durante il mio percorso di ricerca. I loro insegnamenti, i preziosi suggerimenti e la disponibilità al confronto hanno rappresentato per me una fonte inesauribile di ispirazione scientifica e di crescita personale. Senza il loro supporto e la loro fiducia questo lavoro non avrebbe potuto prendere forma.

Ringrazio il Professor Gabriele Veneziano, per la sua disponibilità e per l'ospitalità durante il mio periodo di visiting al CERN. La possibilità di lavorare in un ambiente così stimolante e di confrontarmi direttamente con lui ha rappresentato un'esperienza di grande arricchimento, sia sul piano scientifico che personale.

Vorrei ringraziare Maurizio Gasperini, che più di ogni altro ha segnato il mio percorso di formazione. È stato lui ad accompagnarmi, passo dopo passo, nella scoperta della relatività ristretta e generale, nella comprensione della cosmologia e persino nell'affascinante avventura della teoria delle stringhe. Con le sue lezioni mi ha aperto le porte alla conoscenza della gravità e del funzionamento del cosmo, trasmettendomi non soltanto nozioni, ma anche il senso profondo della ricerca e della meraviglia che essa porta con sé. Negli anni successivi ho avuto la fortuna di averlo accanto anche come guida nella ricerca, sempre disponibile al confronto e attento ai dettagli, capace di indicarmi la strada senza mai togliere spazio alla mia curiosità. La sua presenza è stata per me un punto di riferimento costante e prezioso, che ha reso più ricco e significativo questo cammino.

Desidero inoltre ringraziare i miei supervisori, il Professor Luigi Tedesco e il Professor Giuseppe Fanizza, per il loro sostegno durante gli anni del dottorato. In particolare, a Luigi va la mia sincera riconoscenza non solo per i consigli scientifici e per l'attenzione riservata al mio lavoro, ma soprattutto per il supporto umano, la disponibilità e l'incoraggiamento costante che mi hanno accompagnato lungo questo percorso, ma anche per le birre offerte al CERN. A Giuseppe sono grato per i consigli e le indicazioni che mi ha dato lungo il percorso, in particolare nell'aiutarmi a orientarmi meglio tra conferenze e occasioni di confronto con la comunità scientifica.

Una menzione specialissima va al Dottor Pietro Conzinu, con cui è sempre un piacere collaborare, ma anche bere ad R1. Sono certo ci aspetteranno ancora videocall infinite di lavoro, ma sono contento di farle con lui.
Un pensiero speciale è per i miei genitori e per mio fratello. Mi hanno accompagnato in ogni fase di questo percorso con un sostegno silenzioso ma costante, con la loro fiducia e il loro affetto incondizionato. Hanno condiviso con me le difficoltà e le fatiche di questi anni, ma anche le gioie e le piccole conquiste quotidiane, ricordandomi sempre chi sono e da dove vengo. A loro devo la poca forza e la poca serenità che mi hanno permesso di arrivare fin qui.
Ringrazio gli amici di dipartimento, tutti, ma in particolar modo Fabio, Dent e Cip. Ognuno di voi ha avuto un differente ruolo in questi 3 anni di dottorato. L'unico problema è che ci sono squilibri mentali in tutti noi e non è uno di quei casi in cui vale il terzo principio della dinamica.
Ringrazio me e la mia tenacia nell'aver retto psicologicamente questi anni difficili, inoltre vorrei dedicare un pensiero di supporto a tutti i dottorandi che faticano a mantenere un equilibrio psico-fisico adeguato.
Rinnovo i miei più sentiti ringraziamenti per Francesco Rotondo, Hideo Kojima, mio cugino Tommaso di Gravina e ad Ascanio, sempre fonte di immensa ispirazione, linfa vitale di filosofia contemporanea.
Come sempre anche in questa occasione rinnovo il mio ringraziamento più sentito a tutti
"Conosco la metà di voi solo a metà e nutro per meno della metà di voi metà dell'affetto che meritate."

This thesis is based on the following publications of the author

PUBLICATIONS

1. E. Pavone, L. Tedesco, *Viscosity in Isotropic Cosmological Backgrounds in General Relativity and Starobinsky Gravity,* JCAP **09**, 065 (2025). [1]

2. P. Conzinu, M. Gasperini, E. Pavone, *A simple example of non-minimal Pre-Big Bang scenario,* JCAP **11**, 027 (2025). [2]

3. P. Conzinu, G. Fanizza, M. Gasperini, E. Pavone, L. Tedesco, G. Veneziano, *Constraints on the Pre-Big Bang scenario from a cosmological interpretation of the NANOGrav data,* JCAP **02**, 039 (2025). [3]

4. I. Ben-Dayan, G. Calcagni, M. Gasperini, A. Mazumdar, E. Pavone, U. Thattarampilly, A. Verma, *Gravitational-wave background in bouncing models from semi-classical, quantum and string gravity,* JCAP **09**, 058 (2024). [4]

5. P. Conzinu, G. Fanizza, M. Gasperini, E. Pavone, L. Tedesco, G. Veneziano, *From the string vacuum to FLRW or de Sitter via α' corrections,* JCAP **12**, 019 (2023). [5]

6. G. Fanizza, M. Gasperini, E. Pavone, L. Tedesco, *Linearized propagation equations for metric fluctuations in a general (non-vacuum) background geometry*, JCAP **07**, 021 (2021). [6]

OTHER PUBLICATIONS

7. G. Fanizza, E. Pavone, L. Tedesco, *Freeze-out and spectral running of primordial gravitational waves in viscous cosmology*, submitted to JCAP (2025). [7]

8. G. Fanizza, E. Pavone, L. Tedesco, *Gravitational-wave luminosity distance in viscous cosmological models*, JCAP **08**, 064 (2022). [8]

9. S. Longo, G. Micca Longo, E. Pavone, F. Schiavone, *Deterministic models of minority neutral particle kinetics close to a catalytic surface, based on the formalism of radiative transfer,* Plasma Sources Sci. Technol. **28**, 125008 (2019). [9]

Contents

Introduction

In recent years, cosmology and astrophysics have entered a new era of multi-messenger observations, where Gravitational Waves and electromagnetic signals are studied together to provide a more comprehensive picture of the Universe. In particular, gravitational waves (GWs) might offer new insights on the earliest phases of evolution of the Universe and open a possible observational window on the interplay between Quantum Mechanics and General Relativity, the so-called *Quantum Gravity*. With the forthcoming advent of new generation GW antennas it will be possible in principle to probe primordial cosmological models via primordial Gravitational Waves (pGW) that are generated in the earliest epochs of the Universe, and they evolve unaltered to our epoch, since gravitational waves couple very weakly to matter, and might be able to shed light to cosmological epochs that are currently not directly observable via electromagnetic (EM) signals.
Several classes of theoretical models predict the existence of a stochastic background of pGWs, each with distinct spectral features. Among the most widely studied are inflationary models, where quantum fluctuations of the metric are amplified and stretched to cosmological scales [10–16] by a mechanism akin to the one that generates Hawking radiation of black holes [17]. The mechanism responsible for the "classicalization" of the quantum vacuum metric fluctuations which is responsible for the generation of pGWs is the same as the one that generates curvature perturbations, that are the seeds of late time structure formation in the Universe. The latter is indirectly probed via Large Scale Structure (LSS) surveys and via Cosmic Microwave Background (CMB) anisotropies, hinting that a naïve quantization of the geometry is able to reproduce the observed two point correlation function of the curvature power spectrum, and the existence of a quantum mechanical description for the space-time geometry able to explain the macroscopic observations. The mechanism responsible for the inhomogeneities of our observed Universe (galaxies, clusters,...) has its origin in the earliest epochs of the

yet to be completely known evolution of the Universe, but the same mechanism consistently generates also a Stochastic Gravitational Wave Background (SGWB) that should be present today and in some primordial cosmological models, detectable by future gravitational antennas.

With these premises, this thesis focuses on an alternative paradigm to the slow-roll inflationary one [18], the so-called pre-Big Bang scenario [19–21] inspired by string theory and its dualities (S and T-duality), that neatly connect expanding and contracting geometries (T-duality), and links tensor (pGW) and scalar power spectra (S-duality), providing qualitatively different predictions for the tensor and scalar spectra with respect to standard inflationary cosmology. Disentangling these signatures represents both a theoretical challenge and a promising observational target which may lead to some indirect evidence for string theory.
From the observational side, the next generation of ground- and space-based interferometers, including LISA [22–24], the Einstein Telescope [25, 26], and DECIGO [27–29] will greatly extend the accessible frequency range and forecasted sensitivities, enhancing the prospects of directly probing the early Universe with gravitational waves. Moreover, recent results from Pulsar Timing Array (IPTA) col- laborations, including NANOGrav [30, 31], the Parkes PTA (PPTA) [32, 33], the European PTA (EPTA) in partnership with the Indian PTA (InPTA) [34, 35], and the Chinese PTA (CPTA) [36], have provided tantalizing hints of the presence of a common-spectrum stochastic process, potentially consistent with a gravitational wave background in the nanohertz frequency band. While astrophysical sources, such as supermassive black hole binaries, offer a compelling explanation, the possibility that this signal has a cosmological origin remains an exciting and actively investigated hypothesis.

In this context, it becomes crucial to refine the theoretical predictions for primordial gravitational wave spectra stemming from the pre-Big Bang scenario. The thesis has two main focuses, the first more technical which aims to address the bouncing transition from the pre-Big Bang epoch to a standard phase cosmological evolution, where a full non-perturbative description of string theory, both in the string length α', and string coupling g_s expansions, is required. The second focus is what are the phenomenological consequences on the pGW spectrum produced in this scenario.
The thesis is organized as follows:

In **Chapter I**, a discussion on gravitational wave propagation in general non vacuum background is given (partially based on [6]), this Chapter also serves to clarify the conventions used throughout the thesis. For later application the neat example of GW propagation in an FLRW geometry in the presence of viscous fluids is presented.

In **Chapter II**, a brief review of the standard cosmological model is given, with particular emphasis on the standard known flatness, horizon and curvature problems. Moreover the mechanism of amplification of tensor vacuum fluctuations in primordial epochs is presented.

In **Chapter III**, a concise introduction to the effective action of the massless multiplet of string theory is given and a basic introduction to the pre-Big Bang scenario.

In **Chapter IV** [5], I show how a smooth bouncing transition from the Dilaton Driven phase (DDI) of string cosmology to a standard cosmological epoch is achievable by implementing all order α' corrections and a non-perturbative dilaton potential.

In **Chapter V** [4], the phenomenological imprints on the SGWB of the "minimal" pre-Big-Bang scenario is calculated and analyzed in light of the future gravitational wave antennas (LISA, ET, DECIGO), showing that a detectable signal can be produced in the forecasted working frequencies and sensitivities.

In **Chapter VI** [3], I show that the breaking of S-duality in the high-curvature phase on the pre-Big Bang (called the string phase) can lead to pGW spectrum compatible both with the observed PTA signal and with the future gravitational antennas sensitivities.

In order to give a concrete realization of the S-duality breaking mechanism in terms of viscosity, in **Chapter VII** [1] I analyze the effects of viscosity in isotropic but not necessarily homogeneous cosmological space-time.

Finally in **Chapter VIII** [2] I show some physically motivated scenarios (in the context of string cosmology) where a signal compatible with PTA is produced using anisotropic cosmological fluids and viscous fluids.

In summary, this thesis aims to contribute to our understanding of the interplay between string theory, cosmology, and gravitational-wave physics, with the hope

that forthcoming observations will allow us to confront fundamental ideas about the origin of our Universe with data for the first time.

Chapter 1

General Relativity and Gravitational Wave propagation in a generic curved space-time

In this section I will give a brief review of the main features of the Einstein's theory of gravitation, namely General Relativity (GR) and its formalism. Given that one the main foci of this thesis will be the analysis of the tensorial perturbations on a given generic curved background, this section will also discuss some basic, yet relevant features concerning this topic. Part of the results of this Chapter can be found in full details in [6].

Let us suppose that the space-time is described by a pseudo-Riemannian 4-dimensional manifold $\mathcal{M}_4$, characterized by a metric $g_{\mu\nu}$, with signature $(+,-,-,-)$, that controls how the invariant interval is evaluated

$$ds^2 = g_{\mu\nu}(x)dx^\mu dx^\nu, \tag{1.1}$$

where the coordinates $x^\mu,\ \mu = 0,\dots,3$ are a parametrization of $\mathcal{M}_4$ called "chart" and the 0-th component is a time-like coordinate. One of the cornerstones of GR consists of the general covariance principle. This states that physical laws must retain the same form regardless of the coordinate system adopted to describe them. From the technical viewpoint, if two different coordinate systems x and x' are linked by

$$x^\mu \to x'^\mu = f^\mu(x), \tag{1.2}$$

where the functions f^μ are invertible, continuous, differentiable and with differentiable inverse, namely diffeomorphisms, then theories must be formulated in terms of geometrical objects that belong to the tensorial representation of the diffeomorphism group. In particular a geometric object T is represented by a contravariant tensor of rank r (total number of indices) if under the action of a diffeomorphism, transforms in the following way

$$T^{\mu\nu\dots}(x) \to T'^{\mu\nu\dots}(x') = \frac{\partial x'^\mu}{\partial x^\alpha}\frac{\partial x'^\nu}{\partial x^\beta}\dots T^{\alpha\beta\dots}(x), \tag{1.3}$$

where $\frac{\partial x'^\mu}{\partial x^\alpha}$ is the Jacobian matrix of the given transformation. The dual representation of the same geometrical object T is called the covariant representation and transforms as follows

$$T_{\mu\nu\dots}(x) \to T'_{\mu\nu\dots}(x') = \frac{\partial x^\alpha}{\partial x'^\mu}\frac{\partial x^\beta}{\partial x'^\nu}\dots T_{\alpha\beta\dots}(x), \tag{1.4}$$

with $\frac{\partial x^\alpha}{\partial x'^\mu}$ the inverse Jacobian transformation. The scalar products are performed by "contracting" (summing over) pairs of covariant and contravariant indices

$$T^{\mu\nu\dots}(x)T_{\mu\nu\dots}(x) = T'^{\mu\nu\dots}(x')T'_{\mu\nu\dots}(x'). \tag{1.5}$$

Moreover, also *mixed* forms (n, m) behaving as rank n tensors with respect to the contravariant representation and as rank m covariant tensors are allowed, and transform as follows

$$T'^{\mu\nu\dots}{}_{\rho\sigma\dots}(x') = \frac{\partial x'^\mu}{\partial x^\alpha}\frac{\partial x'^\nu}{\partial x^\beta}\dots\frac{\partial x^\lambda}{\partial x'^\rho}\frac{\partial x^\gamma}{\partial x'^\sigma}\dots T^{\alpha\beta\dots}{}_{\lambda\gamma\dots}(x). \tag{1.6}$$

It is important to remember that the tensorial representations are a subclass of geometrical objects called *tensorial densities* that are characterized by two parameters, the rank r and the weight w. The transformation law for these objects is given by

$$V^{\mu\nu\dots}(x) \to V'^{\mu\nu\dots}(x') = \frac{\partial x'^\mu}{\partial x^\alpha}\frac{\partial x'^\nu}{\partial x^\beta}\dots V^{\alpha\beta\dots}(x)\left|\frac{\partial x'}{\partial x}\right|^w, \tag{1.7}$$

where $\left|\frac{\partial x'}{\partial x}\right| = \det\left(\frac{\partial x'}{\partial x}\right)$. The most relevant example of a tensorial density with $w = 1$ is provided by the infinitesimal 4-dimensional volume element

$$d^4x \to d^4x' = d^4x\left|\frac{\partial x'}{\partial x}\right|. \tag{1.8}$$

1.1 Metric, connection and the covariant derivative

The basic hypothesis of the Riemannian geometry is that the infinitesimal line element ds^2 is represented by a quadratic homogeneous form of the coordinates which is also invariant under diffeomorphisms

$$ds'^2 = ds^2 \Rightarrow g'_{\alpha\beta}(x')dx'^{\alpha}dx'^{\beta} = g_{\mu\nu}(x)dx^{\mu}dx^{\nu}. \tag{1.9}$$

A direct consequence of this requirement is the following transformation rule for the metric

$$g'_{\mu\nu}(x') = \frac{\partial x^{\alpha}}{\partial x'^{\mu}}\frac{\partial x^{\beta}}{\partial x'^{\nu}}g_{\alpha\beta}(x), \tag{1.10}$$

thus the metric transforms as a rank 2 covariant tensor. Moreover it can be easily shown that the determinant $g = \det(g_{\mu\nu})$ transforms as follows

$$g' = \left|\frac{\partial x'}{\partial x}\right|^{-2} g. \tag{1.11}$$

It is crucial to notice that the determinant is negative, so that $-g$ is positive, we then have that

$$\sqrt{-g'} = \sqrt{-g}\left|\frac{\partial x'}{\partial x}\right|^{-1}, \tag{1.12}$$

and the combination $d^4x\sqrt{-g}$ that defines the invariant volume element, transforms as a scalar. Aside from ds^2, all the scalar products must be invariant under diffeomorphisms and can be defined using the metric tensor

$$A^{\mu\nu\ldots}B_{\mu\nu\ldots} \equiv A^{\mu\nu\ldots}g_{\mu\alpha}g_{\nu\beta}\ldots B^{\alpha\beta\ldots} \equiv A_{\alpha\beta\ldots}g^{\mu\alpha}g^{\nu\beta}\ldots B_{\mu\nu}. \tag{1.13}$$

The main consequences are that the metric can raise and lower indices

$$A_{\alpha} = g_{\alpha\nu}A^{\nu} \qquad A^{\mu} = g^{\mu\alpha}A_{\alpha}\ , \tag{1.14}$$

and from $A_{\mu} = g_{\mu\nu}A^{\nu} = g_{\mu\nu}g^{\nu\alpha}A_{\alpha}$

$$g_{\mu\nu}g^{\nu\alpha} = \delta^{\alpha}_{\mu}. \tag{1.15}$$

It is important to remember that the differential of a vector in this context does not transform as a vector, in fact

$$A^\mu = \frac{\partial x^\mu}{\partial x'^\nu} A'^\nu, \tag{1.16}$$

differentiating both sides we get

$$dA^\mu = \frac{\partial x^\mu}{\partial x'^\nu} dA'^\nu + \frac{\partial^2 x^\mu}{\partial x'^\alpha \partial x'^\nu} A'^\nu dx'^\alpha. \tag{1.17}$$

The second quantity (the one with double derivatives) is vanishing if the transformation $x^\mu(x')$ is linear i.e. Lorentz transformations, and only in this case the differential transforms as the vector itself. However in general it is required a new definition of the differential that preserves the geometric nature of the differentiated object, such that the differential of a vector transforms as a vector, the differential of a tensor transforms as a tensor and so on. To this aim we introduce the *affine connection* $\Gamma_{\alpha\beta}{}^\mu(x)$ that acts as a gauge field and define the covariant differential D as

$$DA^\mu = dA^\mu + \delta A^\mu \equiv dA^\mu + \Gamma_{\alpha\beta}{}^\mu dx^\alpha A^\beta. \tag{1.18}$$

We impose the covariant transformation property so that

$$DA^\mu = \frac{\partial x^\mu}{\partial x'^\nu} (DA^\nu)' \equiv \frac{\partial x^\mu}{\partial x'^\nu} \left(dA'^\nu + \Gamma'_{\alpha\beta}{}^\nu dx'^\alpha A'^\beta \right). \tag{1.19}$$

Using Eq. (1.18) in the latter, we are able to define the transformation law of the affine connection

$$\Gamma'_{\alpha\beta}{}^\mu = \frac{\partial x'^\mu}{\partial x^\gamma} \frac{\partial x^\lambda}{\partial x'^\alpha} \frac{\partial x^\rho}{\partial x'^\beta} \Gamma_{\lambda\rho}{}^\gamma + \frac{\partial x'^\mu}{\partial x^\gamma} \frac{\partial^2 x^\gamma}{\partial x'^\alpha \partial x'^\beta}. \tag{1.20}$$

It is easy to notice that Γ does not transform as a tensor, but its antisymmetric part does, namely $\Gamma_{[\alpha\beta]}{}^\gamma = \frac{\Gamma_{\alpha\beta}{}^\gamma - \Gamma_{\beta\alpha}{}^\gamma}{2} \equiv Q_{\alpha\beta}{}^\gamma$ which is called the "torsion". From Eq. (1.18) we can now define the covariant derivative as

$$\nabla_\alpha A^\mu = \partial_\alpha A^\mu + \Gamma_{\alpha\beta}{}^\mu A^\beta, \tag{1.21}$$

and

$$\nabla_\alpha A_\mu = \partial_\alpha A_\mu - \Gamma_{\alpha\mu}{}^\nu A_\nu. \tag{1.22}$$

In general for a mixed tensor we obtain

$$\begin{aligned}\nabla_\alpha T^{\mu\nu\ldots}{}_{\beta\gamma\ldots} =& \partial_\alpha T^{\mu\nu\ldots}{}_{\beta\gamma\ldots} + \Gamma_{\alpha\rho}{}^{\mu} T^{\rho\nu\ldots}{}_{\beta\gamma\ldots} + \Gamma_{\alpha\rho}{}^{\nu} T^{\mu\rho\ldots}{}_{\beta\gamma\ldots} + \ldots \\ & - \Gamma_{\alpha\beta}{}^{\rho} T^{\mu\nu\ldots}{}_{\rho\gamma\ldots} - \Gamma_{\alpha\gamma}{}^{\rho} T^{\mu\nu\ldots}{}_{\beta\rho\ldots} - \ldots .\end{aligned} \tag{1.23}$$

To fix completely the geometric structure of the space-time we can impose two constraints on the affine connection. The first one is the torsion-free condition, which implies that the connection is symmetric in the first two indices

$$\Gamma_{[\alpha\beta]}{}^{\gamma} = 0, \tag{1.24}$$

and the second is the metricity condition

$$\nabla_\alpha g_{\mu\nu} = \partial_\alpha g_{\mu\nu} - \Gamma_{\alpha\mu}{}^{\rho} g_{\rho\nu} - \Gamma_{\alpha\nu}{}^{\rho} g_{\mu\rho} = 0. \tag{1.25}$$

By circularly permuting the indices of the latter it can be proven that

$$\Gamma_{\mu\nu}{}^{\alpha} \equiv \left\{ \begin{array}{c} \alpha \\ \mu\nu \end{array} \right\} = \frac{1}{2} g^{\alpha\rho} \left(\partial_\mu g_{\nu\rho} + \partial_\nu g_{\mu\rho} - \partial_\rho g_{\mu\nu} \right), \tag{1.26}$$

which defines the so-called *Christoffel connection,* and it will be used from now on.

It will be useful for the next sections to give some remarks on the covariant divergence, the covariant D'Alembertian, and the covariant Gauss theorem. First of all let us evaluate the covariant divergence of a vector

$$\nabla_\mu V^\mu = \partial_\mu V^\mu + \Gamma_{\mu\alpha}{}^{\mu} V^\alpha. \tag{1.27}$$

By means of Eq. (1.26), we have

$$\Gamma_{\mu\alpha}{}^{\mu} \equiv \frac{1}{2} g^{\mu\nu} \partial_\alpha g_{\mu\nu}. \tag{1.28}$$

Moreover using the known relationship between the determinant and the trace

$$\det(A) = e^{\mathrm{Tr}(\ln(A))}, \tag{1.29}$$

it is easy to show that the differential of the determinant of the metric is

$$\delta\sqrt{-g} = \frac{\delta(-g)}{2\sqrt{-g}} = \frac{\sqrt{-g}}{2} g^{\mu\nu} \delta(g_{\mu\nu}) = -\frac{\sqrt{-g}}{2} g_{\mu\nu} \delta(g^{\mu\nu}). \tag{1.30}$$

The last equality is obtained using $\delta\left(g^{\mu\nu}g_{\mu\nu}\right) = \delta\left(\delta^{\mu}_{\mu}\right) = \delta(4) = 0$. Using Eq. (1.30) in Eq. (1.27) we finally arrive at

$$\nabla_\mu V^\mu = \partial_\mu V^\mu + \frac{1}{\sqrt{-g}}\left(\partial_\alpha\sqrt{-g}\right)V^\alpha = \frac{1}{\sqrt{-g}}\partial_\alpha\left(\sqrt{-g}V^\alpha\right). \tag{1.31}$$

The evaluation of the covariant D'Alembertian is straightforward and yields

$$\nabla_\mu\nabla^\mu\psi = \frac{1}{\sqrt{-g}}\partial_\mu\left(\sqrt{-g}g^{\mu\nu}\partial_\nu\psi\right). \tag{1.32}$$

To conclude we show how the Gauss theorem can be stated in this context. First of all, as we have already stated previously, the invariant space-time volume element is given by $d^4x\sqrt{-g}$, so this is the correct measure to be used while stating the Gauss's theorem

$$\int_\Omega d^4x\sqrt{-g}\nabla_\mu V^\mu = \int_\Omega d^4x\partial_\mu\left(\sqrt{-g}V^\mu\right) = \int_{\partial\Omega} dS_\mu\sqrt{-g}V^\mu, \tag{1.33}$$

where Ω is a closed hypervolume in 3+1 dimensions bounded by an orientable hypersurface $\partial\Omega$, and dS_μ is taken to be outgoing with respect to the same hypersurface.

1.2 Geodesic curves and the curvature tensors

Let us consider a curve in the space-time $\mathcal{M}_4$, described by the parametric equation $x^\mu = \xi^\mu(\tau)$, where τ is a scalar (invariant under diffeomorphisms). The tangent vector to the trajectory is expressed as usual as $u^\mu = \frac{d\xi^\mu}{d\tau}$. The covariant differential is given by

$$Du^\mu = du^\mu + \Gamma_{\alpha\beta}{}^\mu d\xi^\alpha u^\beta, \tag{1.34}$$

and the curve is called "self-parallel" or geodesic if $Du^\mu = 0$,

$$\frac{Du^\mu}{d\tau} = \frac{du^\mu}{d\tau} + \Gamma_{\alpha\beta}{}^\mu u^\alpha u^\beta = 0. \tag{1.35}$$

It can be shown that this is the equation that describes the motion of a free particle in a given space-time geometry, but for the sake of brevity we will avoid to provide a proof for this statement. The geodesic equation can be rewritten in the following way (the dot will denote the derivative with respect to the scalar

parameter)

$$\ddot{\xi}^{\mu} + \Gamma_{\alpha\beta}{}^{\mu}\dot{\xi}^{\alpha}\dot{\xi}^{\beta} = 0. \tag{1.36}$$

It is crucial to notice that locally Γ can be set to 0, giving the Newton's second law for a free particle. The real effects of gravity can be calculated only taking into account tidal forces, that act on extended bodies. To this aim let us consider two nearby test particles with the trajectory described by $\xi^{\mu}(\tau)$ and $\xi^{\mu}(\tau) + \Delta^{\mu}(\tau)$, where $\Delta^{\mu}(\tau)$ is the displacement. Writing the geodesic equations for both and subtracting, it is possible to obtain the so called *equation of geodesic deviation*

$$\frac{D^2\Delta^{\mu}(\tau)}{d\tau^2} = -\Delta^{\nu} R_{\nu\alpha\beta}{}^{\mu}\dot{\xi}^{\alpha}\dot{\xi}^{\beta}, \tag{1.37}$$

where the Riemann curvature tensor is defined as

$$R_{\mu\nu\alpha}{}^{\beta} = 2\partial_{[\mu}\Gamma_{\nu]\alpha}{}^{\beta} + 2\Gamma_{[\mu|\rho}{}^{\beta}\Gamma_{|\nu]\alpha}{}^{\rho}, \tag{1.38}$$

where we use the following notation for the symmetric and antisymmetric part of a tensor

$$\begin{aligned} C_{[\mu\nu]} &= \tfrac{C_{\mu\nu}-C_{\nu\mu}}{2} \\ C_{(\mu\nu)} &= \tfrac{C_{\mu\nu}+C_{\nu\mu}}{2}. \end{aligned} \tag{1.39}$$

The Riemann tensor can also be written as follows, for a generic vector A^{β}

$$[\nabla_{\mu}, \nabla_{\nu}] A^{\beta} = R_{\mu\nu\alpha}{}^{\beta} A^{\alpha}. \tag{1.40}$$

After all the technical definitions it is necessary to give some physical interpretations about the basic assumptions of the Einstein formalism. First of all the diffeomorphism invariance allows us to perform a local coordinate transformation that is able to recast $g'_{\mu\nu}(x_0) = \eta_{\mu\nu}$, where $\eta_{\mu\nu}$ is the usual Minkowskian metric. Moreover since we have chosen Γ to be torsion-less, it can be seen from Eq. (1.20) that the Christoffel connection does not transform as a tensor, so it is possible to set it locally equal to 0. These two properties are the mathematical features that encodes the property of gravity to be locally eliminable by a coordinate transformation. On the other hand the Riemann tensor is able to highlight without ambiguities the presence of gravity, because cannot be set locally to 0, so it is

the geometric property of space-time that represents the physical effects due to gravitational fields.

Properties of the Riemann tensor

From the definition given in Eq. (1.38) the following properties can be proven

$$R_{\mu\nu\alpha\beta} = R_{\alpha\beta\mu\nu} \tag{1.41}$$

and

$$R_{\mu\nu\alpha\beta} = -R_{\nu\mu\alpha\beta} = -R_{\mu\nu\beta\alpha} = R_{[\mu\nu][\alpha\beta]}. \tag{1.42}$$

Moreover the Riemann tensor satisfies the two *Bianchi identities:*

1st Bianchi identity

$$R_{[\mu\nu\alpha]}{}^{\beta} = 0 \tag{1.43}$$

2nd Bianchi identity

$$\nabla_{[\lambda} R_{\mu\nu]\alpha}{}^{\beta} = 0. \tag{1.44}$$

By contracting the indices of the Riemann tensor it is possible to construct lower rank tensors that still encodes the curvature properties of the space-time. We can define the *Ricci tensor*

$$R_{\nu\alpha} \equiv R_{\mu\nu\alpha}{}^{\mu} = R_{\alpha\nu} \tag{1.45}$$

and the *Ricci scalar* as

$$R \equiv g^{\mu\nu} R_{\mu\nu}. \tag{1.46}$$

To conclude we can define the *Einstein tensor*

$$G_{\mu\nu} = R_{\mu\nu} - \frac{1}{2} g_{\mu\nu} R \tag{1.47}$$

that satisfies the *Contracted Bianchi identity*

$$\nabla_\nu G^{\mu\nu} = 0. \tag{1.48}$$

This last equality is crucial to preserve the consistence of the Einstein field equations with the diffeomorphism invariance. Now we have all the necessary ingredients to find the equations governing gravity, namely the Einstein equations.

1.3 The Einstein equations and the second order variation of the gravitational action

Throughout this thesis we will use $\hbar = c = k_b = 1 \Rightarrow \lambda_p^2 = 8\pi G$. The action is given by

$$S = S_{EH} + S_m + S_{YGH}, \tag{1.49}$$

where

$$S_{EH} = -\frac{1}{2\lambda_p^2}\int_\Omega d^4x\,\sqrt{-g}R \tag{1.50}$$

and

$$S_m = \int_\Omega d^4x\,\sqrt{-g}\mathcal{L}_m\left(\psi, \nabla\psi, g\right). \tag{1.51}$$

The matter Lagrangian density $\mathcal{L}_m$ is obtained by the special relativity one with the substitutions $\partial_\mu \to \nabla_\mu$ and $\eta_{\mu\nu} \to g_{\mu\nu}$. The York-Gibbons-Hawking action S_{YGH} is required to compensate for the boundary terms that appear in S_{EH} because it contains in addition to the standard kinetic terms $\sim (\partial g)^2$, terms that do not vanish on the boundary $\sim \partial^2 g$. In order to recover the Einstein equations from the action we will proceed with a standard variational technique, but we will perform it up to the second order, in order to find the evolution equations for the metric perturbations.
Let us define the full metric to be the superposition of a background and a perturbation on top of it

$$g_{\mu\nu} \to \bar{g}_{\mu\nu} = g_{\mu\nu} + \delta g_{\mu\nu} = g_{\mu\nu} + h_{\mu\nu} \tag{1.52}$$

and we impose the action to be stationary, namely $\delta S = 0$. First of all it is convenient to apply the formalism of functional derivatives and expand the action in Taylor series around the background metric $g_{\mu\nu}$. Given an arbitrary function $A = A\left(g, \partial g, \dots\right)$,we perform the metric expansion (1.52) so

$$A\left(\bar{g}, \partial\bar{g}, \dots\right) = A\left(g, \partial g, \dots\right) + \delta^{(1)}A + \delta^{(2)}A + \dots, \tag{1.53}$$

where

$$\delta^{(1)}A = \left(\frac{\delta A}{\delta \bar{g}_{\mu\nu}}\right)_0 \delta g_{\mu\nu} \tag{1.54}$$

$$\delta^{(2)}A = \frac{1}{2}\left(\frac{\delta}{\delta \bar{g}_{\rho\sigma}}\frac{\delta A}{\delta \bar{g}_{\mu\nu}}\right)_0 \delta g_{\rho\sigma}\delta g_{\mu\nu}, \tag{1.55}$$

and the subscript "0" denotes the evaluation has to be done on the unperturbed metric $g_{\mu\nu}$. Moreover the functional derivative is defined in the common way

$$\frac{\delta A\left(g, \partial g, \dots\right)}{\delta g_{\mu\nu}} \equiv \frac{\partial A}{\partial g_{\mu\nu}}\delta g_{\mu\nu} + \frac{\partial A}{\partial\left(\partial_\lambda g_{\mu\nu}\right)}\partial_\lambda \delta g_{\mu\nu} + \dots, \tag{1.56}$$

where we used the commutation property $\delta\partial_\lambda g_{\mu\nu} = \partial_\lambda \delta g_{\mu\nu}$. As a useful example we give an evaluation of the functional derivatives of the contravariant metric tensor $A = \bar{g}^{\mu\nu}$

$$\delta^{(1)}\bar{g}^{\mu\nu} = \left(\frac{\delta \bar{g}^{\mu\nu}}{\delta \bar{g}_{\alpha\beta}}\right)_0 \delta g_{\alpha\beta} = \left(\frac{\delta \bar{g}^{\mu\nu}}{\delta \bar{g}_{\alpha\beta}}\right)_0 \delta g_{\alpha\beta} = -g^{\mu\lambda}g^{\nu\rho}\left(\frac{\delta \bar{g}_{\lambda\rho}}{\delta \bar{g}_{\alpha\beta}}\right)_0 \delta g_{\alpha\beta} = -h^{\mu\nu} \tag{1.57}$$

and

$$\begin{aligned}\delta^{(2)}\bar{g}^{\mu\nu} &= \frac{1}{2}\left(\frac{\delta}{\delta \bar{g}_{\rho\sigma}}\frac{\delta \bar{g}^{\mu\nu}}{\delta \bar{g}_{\alpha\beta}}\right)_0 \delta g_{\rho\sigma}\delta g_{\alpha\beta} \\ &= \frac{1}{2}\left(g^{\mu\rho}g^{\alpha\sigma}g^{\nu\beta} + g^{\mu\alpha}g^{\nu\rho}g^{\beta\sigma}\right)\delta g_{\rho\sigma}\delta g_{\alpha\beta} = h^{\mu\alpha}h_\alpha{}^\nu.\end{aligned} \tag{1.58}$$

Using these last two equations in Eq. (1.53), we get

$$\bar{g}^{\mu\nu} = g^{\mu\nu} - h^{\mu\nu} + h^{\mu\alpha} h_{\alpha}{}^{\nu} + \dots, \tag{1.59}$$

and it can be easily checked that Eq. (1.15) holds up to $\mathcal{O}(h^3)$

$$\bar{g}_{\alpha\mu}\bar{g}^{\mu\nu} = (g_{\alpha\mu} + h_{\alpha\mu})\left(g^{\mu\nu} - h^{\mu\nu} + h^{\mu\alpha} h_{\alpha}{}^{\nu}\right) = \delta_{\alpha}{}^{\nu} + \mathcal{O}(h^3). \tag{1.60}$$

From now on we will neglect the boundary terms given by the York-Gibbons-Hawking action, and we will focus only on the gravitational and matter action, given that every non-vanishing boundary term is balanced. The action reads

$$S = \frac{1}{2\lambda_p^2}\int_{\Omega} d^4x\sqrt{-g}\left[-R + 2\lambda_p^2\mathcal{L}_m\right] \tag{1.61}$$

and its variation

$$\begin{aligned}\delta S = \delta^{(1)}S + \delta^{(2)}S + \dots = &\frac{1}{2\lambda_p^2}\int_{\Omega} d^4x\,\delta^{(1)}\left[-\sqrt{-g}R + 2\lambda_p^2\sqrt{-g}\mathcal{L}_M\right] \\ &+ \delta^{(2)}\left[-\sqrt{-g}R + 2\lambda_p^2\sqrt{-g}\mathcal{L}_m\right] + \dots = 0\end{aligned} \tag{1.62}$$

In the next two sections the two terms will be evaluated, following the arguments in [6], showing how the first reproduces, as expected, the standard Einstein equations, while the second is the actual action for the metric perturbations.

1.3.1 The 1st order variation of the gravitational action: Einstein equations

Starting from Eq. (1.62) we are interested in the first term

$$\delta^{(1)}S = \frac{1}{2\lambda_p^2}\int_{\Omega} d^4x\,\delta^{(1)}\left[-\sqrt{-g}R + 2\lambda_p^2\sqrt{-g}\mathcal{L}_m\right], \tag{1.63}$$

and we define the dynamical stress-energy tensor as

$$\frac{\delta\sqrt{-g}\mathcal{L}_m}{\delta g_{\mu\nu}} \equiv -\frac{1}{2}\sqrt{-g}T^{\mu\nu}. \tag{1.64}$$

Writing the Ricci scalar as in Eq. (1.46) and using Eqs. (1.30) and (1.64), the variation of the action (1.63) becomes

$$\delta^{(1)}S = \frac{1}{2\lambda_p^2}\int_\Omega d^4x\,\sqrt{-g}\left[\left(R^{\mu\nu} - \frac{1}{2}g^{\mu\nu}R - \lambda_p^2 T^{\mu\nu}\right)\delta g_{\mu\nu} - g^{\mu\nu}\delta^{(1)}R_{\mu\nu}\right] = 0. \tag{1.65}$$

The last term is the afore mentioned non-vanishing boundary term that is compensated by an appropriate boundary action. To show this let us rewrite the term $\delta^{(1)}R_{\mu\nu}$ using the "contracted Palatini identity" [37]

$$\delta^{(1)}R_{\mu\nu} = \nabla_\alpha\left(\delta^{(1)}\Gamma_{\mu\nu}{}^\alpha\right) - \nabla_\mu\left(\delta^{(1)}\Gamma_{\alpha\nu}{}^\alpha\right) \tag{1.66}$$

where the covariant derivative is performed with respect to the background metric $g_{\mu\nu}$. Moreover the explicit computation of $\delta^{(1)}\Gamma_{\mu\nu}{}^\alpha$ (see [6]) yields

$$\delta^{(1)}\Gamma_{\mu\nu}{}^\alpha = \frac{1}{2}g^{\alpha\rho}\left(\nabla_\mu h_{\nu\rho} + \nabla_\nu h_{\mu\rho} - \nabla_\rho h_{\mu\nu}\right). \tag{1.67}$$

Inserting Eq. (1.66) in Eq. (1.65) and using the metricity condition (1.25) and the covariant Gauss's theorem

$$\begin{aligned}\int_\Omega d^4x\,\sqrt{-g}g^{\mu\nu}\delta^{(1)}R_{\mu\nu} &= \int_\Omega d^4x\,\sqrt{-g}\nabla_\alpha\left(g^{\mu\nu}\delta^{(1)}\Gamma_{\mu\nu}{}^\alpha - g^{\alpha\nu}\delta^{(1)}\Gamma_{\rho\nu}{}^\rho\right)\\ &= \int_{\partial\Omega} dS_\alpha\,\sqrt{-g}\left(g^{\mu\nu}\delta^{(1)}\Gamma_{\mu\nu}{}^\alpha - g^{\alpha\nu}\delta^{(1)}\Gamma_{\rho\nu}{}^\rho\right).\end{aligned} \tag{1.68}$$

Aside from terms $\sim \delta g$ that vanish on the boundary, there are terms $\sim \partial\delta g$ that are non-vanishing, but compensated by the boundary action S_{YGH}. Finally we can conclude that the first order stationary condition $\delta^{(1)}S = 0$ for the action yields the famous Einstein equations

$$R^{\mu\nu} - \frac{1}{2}g^{\mu\nu}R = \lambda_p^2 T^{\mu\nu}. \tag{1.69}$$

From this last equation another useful relation between the Ricci scalar and the trace of the energy-momentum tensor $T = g_{\mu\nu}T^{\mu\nu}$ can be retrieved

$$\lambda_p^2 T = -R \tag{1.70}$$

Since we are interested in the cosmological applications of the Einstein theory, it is worth to mention that in the Einstein-Hilbert action (1.50), it is possible to add

a constant term Λ, usually referred as cosmological constant, that does not violate the diffeomorphism invariance of the theory

$$S_\Lambda = -\int_\Omega d^4x\sqrt{-g}\Lambda, \tag{1.71}$$

whose variation leads to an additional term in Eq. (1.69) that becomes

$$R^{\mu\nu} - \frac{1}{2}g^{\mu\nu}R = \lambda_p^2\left(T^{\mu\nu} + \Lambda g^{\mu\nu}\right). \tag{1.72}$$

It is worth to mention that the cosmological constant term is the currently accepted form of Dark Energy. To conclude let us state that the "contracted Bianchi identity" Eq. (1.48) forces $\nabla_\nu T^{\mu\nu} = 0$ for consistency. This property is verified if and only if the on-shell energy-momentum tensor is invariant under diffeomorphism.

1.3.2 The 2nd order variation of the gravitational action: evolution of the metric perturbation and gravitational waves

Let us now compute the second order variation of the action (1.62)

$$\delta^{(2)}S = \frac{1}{2\lambda_p^2}\int_\Omega d^4x\delta^{(2)}\left[-\sqrt{-g}R + 2\lambda_p^2\sqrt{-g}\mathcal{L}_m\right]. \tag{1.73}$$

From the definition of the second order expansion term from Eq. (1.55), the stationarity condition becomes

$$\delta^{(2)}S = \frac{1}{4\lambda_p^2}\int_\Omega d^4x\left[\frac{\delta}{\delta\bar{g}_{\rho\sigma}}\frac{\delta}{\delta\bar{g}_{\mu\nu}}\left(-\sqrt{-g}R + 2\lambda_p^2\sqrt{-g}\mathcal{L}_m\right)\right]_0 \delta g_{\rho\sigma}\delta g_{\mu\nu} = 0. \tag{1.74}$$

We can exploit the results of the previous section, in particular Eq. (1.65) to rewrite the last equation as

$$\delta^{(2)}S = \frac{1}{4\lambda_p^2}\int_\Omega d^4x \left[\delta^{(1)}\left(\sqrt{-g}R^{\mu\nu} - \frac{1}{2}\sqrt{-g}g^{\mu\nu}R - \lambda_p^2\sqrt{-g}T^{\mu\nu}\right)\right]\delta g_{\mu\nu} \\ - \frac{1}{4\lambda_p^2}\int_\Omega d^4x \left[\delta^{(1)}\left(\sqrt{-g}g^{\mu\nu}\right)\delta^{(1)}R_{\mu\nu} + 2\sqrt{-g}g^{\mu\nu}\delta^{(2)}R_{\mu\nu}\right] = 0. \tag{1.75}$$

In Ref.[6] we have shown that the last two terms cancel out because are equal but with opposite signs. Factoring out $\delta^{(1)}\left(g^{\alpha\mu}g^{\beta\nu}\sqrt{-g}\right)$ we have as equation of motion for the metric perturbations, the following

$$\delta^{(1)}\left(R_{\alpha\beta} - \frac{1}{2}g_{\alpha\beta}R\right) = \lambda_p^2\delta^{(1)}T_{\alpha\beta}. \tag{1.76}$$

The latter are exactly the perturbed Einstein equations (1.69). Eq. (1.76) can be expanded and recast as

$$\delta^{(1)}R_{\alpha\beta} - \frac{1}{2}\delta^{(1)}\left(g_{\alpha\beta}g^{\mu\nu}R_{\mu\nu}\right) = \lambda_p^2\delta^{(1)}T_{\alpha\beta} \Rightarrow$$

$$\Rightarrow \delta^{(1)}R_{\alpha\beta} - \frac{1}{2}h_{\alpha\beta}R + \frac{1}{2}g_{\alpha\beta}h^{\mu\nu}R_{\mu\nu} - \frac{1}{2}g_{\alpha\beta}g^{\mu\nu}\delta^{(1)}R_{\mu\nu} = \lambda_p^2\delta^{(1)}T_{\alpha\beta}. \tag{1.77}$$

To write explicitly all the terms in the last equation, we recall that from Eqs. (1.66) and (1.67), the following identities can be easily checked

$$\delta^{(1)}R_{\alpha\beta} = \frac{1}{2}\left(\nabla_\mu\nabla_\alpha h_\beta{}^\mu + \nabla_\mu\nabla_\beta h_\alpha{}^\mu - \nabla^2 h_{\alpha\beta} - \nabla_\alpha\nabla_\beta h\right) \tag{1.78}$$

and

$$g^{\mu\nu}\delta^{(1)}R_{\mu\nu} = \nabla_\mu\nabla_\nu h^{\mu\nu} - \nabla^2 h, \tag{1.79}$$

where we have set $h = g^{\mu\nu}\delta g_{\mu\nu} = g^{\mu\nu}h_{\mu\nu}$ and the D'Alembert operator is $\nabla^2 = g^{\mu\nu}\nabla_\mu\nabla_\nu$. Moreover it is useful to rewrite the first two terms of Eq. (1.78) using the commutation rule for the covariant derivatives on mixed tensors. The formula can be obtained by exploiting the result in Eq. (1.40) and writing a generic mixed tensor $C_\beta{}^\nu = A_\beta B^\nu = g_{\rho\beta}A^\rho B^\nu$

$$\begin{aligned}[\nabla_\mu, \nabla_\alpha] C_\beta{}^\nu &= [\nabla_\mu, \nabla_\alpha] g_{\rho\beta} A^\rho B^\nu = B^\nu [\nabla_\mu, \nabla_\alpha] g_{\rho\beta} A^\rho + g_{\rho\beta} A^\rho [\nabla_\mu, \nabla_\alpha] B^\nu \\ &= g_{\rho\beta} \left(R_{\mu\alpha\delta}{}^\rho A^\delta B^\nu + R_{\mu\alpha\delta}{}^\nu A^\rho B^\delta \right) = R_{\mu\alpha\delta\beta} C^{\delta\nu} + R_{\mu\alpha\delta}{}^\nu C_\beta{}^\delta,\end{aligned} \tag{1.80}$$

where we have used the metricity condition. We can write the first two terms in Eq. (1.78) using the last equality and the properties (1.41) and (1.42) as

$$\nabla_\mu \nabla_\alpha h_\beta{}^\mu + \nabla_\mu \nabla_\beta h_\alpha{}^\mu = \nabla_\alpha \nabla_\mu h_\beta{}^\mu + \nabla_\beta \nabla_\mu h_\alpha{}^\mu - 2R_{\mu\alpha\beta\nu} h^{\mu\nu} + R_{\alpha\nu} h_\beta{}^\nu + R_{\nu\beta} h_\alpha{}^\nu. \tag{1.81}$$

Finally after substituting Eqs. (1.78), (1.79) and (1.81) in (1.77), we find the evolution equations for the metric perturbations in an arbitrary background metric

$$\nabla^2 h_{\alpha\beta} + 2R_{\mu\alpha\beta\nu} h^{\mu\nu} + R h_{\alpha\beta} - g_{\alpha\beta} h^{\mu\nu} R_{\mu\nu} - h_\alpha{}^\nu R_{\nu\beta} - h_\beta{}^\nu R_{\nu\alpha} - \nabla_\beta \nabla_\mu h_\alpha{}^\mu +$$

$$- \nabla_\alpha \nabla_\mu h_\beta{}^\mu + \nabla_\alpha \nabla_\beta h - g_{\alpha\beta} \left(\nabla^2 h - \nabla_\mu \nabla_\nu h^{\mu\nu} \right) = -2\lambda_p^2 \delta^{(1)} T_{\alpha\beta}. \tag{1.82}$$

For a vacuum geometry ($R_{\mu\nu} = 0 = R,\ T_{\mu\nu} = 0 = \delta^{(1)} T_{\mu\nu}$), Eq. (1.82) simplifies significantly

$$\nabla^2 h_{\alpha\beta} + 2R_{\mu\alpha\beta\nu} h^{\mu\nu} = 0. \tag{1.83}$$

However the main topic of this thesis is the analysis of the evolution of Gravitational Waves (GW) in a cosmological scenario, where the geometry is not the vacuum one. To this aim let us introduce the so called "TT gauge" conditions, where TT stands for Transverse and Traceless

$$\nabla_\nu h^{\mu\nu} = 0 \qquad h = g^{\mu\nu} h_{\mu\nu} = 0\ . \tag{1.84}$$

It is crucial to remember that the diffeomorphism invariance always allows for additional constraints, but it is not guaranteed that these constraints can be imposed. Using Eq. (1.84) in (1.82) we are left with

$$\nabla^2 h_{\alpha\beta} + 2R_{\mu\alpha\beta\nu}h^{\mu\nu} + Rh_{\alpha\beta} - h_\alpha{}^\nu R_{\nu\beta} - h_\beta{}^\nu R_{\nu\alpha} = -2\lambda_p^2 \delta^{(1)} T_{\alpha\beta}. \tag{1.85}$$

Taking the trace of this last equation we find, for consistency with the gauge conditions, that the following condition must be satisfied (this condition is necessary, but not sufficient to impose the TT gauge)

$$2R_{\alpha\beta}h^{\alpha\beta} = g^{\alpha\beta}\lambda_p^2 \delta^{(1)} T_{\alpha\beta}. \tag{1.86}$$

Finally we can rewrite Eq. (1.85) in a simpler form, using the Einstein equations

$$\nabla^2 h_{\alpha\beta} + 2R_{\mu\alpha\beta\nu}h^{\mu\nu} = \lambda_p^2 \left(h_\alpha{}^\nu T_{\nu\beta} + h_\beta{}^\nu T_{\nu\alpha} + \frac{1}{2} g_{\alpha\beta} g^{\mu\nu} \delta^{(1)} T_{\mu\nu} - 2\delta^{(1)} T_{\alpha\beta} \right). \tag{1.87}$$

It is clear that GWs propagate differently in a general non-vacuum background with respect to the vacuum one. As a useful example hereafter I am presenting the science case of the propagation equation in an FLRW geometry in the presence of a viscous fluid since this source will be taken into account in Chapter VI and specialized in the string phase of the pre-Big Bang scenario.

Chapter 2

The Standard Model of Cosmology

In this chapter I will give a brief review of the standard model of cosmology and its assumptions. The so-called concordance model has been extremely successful in describing our current observations of the Universe, but recent observations seem to indicate that some problems are arising with the improvements of measurements, such as the Hubble tension [38–44] and the recently possible evidence from DESI of the time dependence of the Dark Energy equation of state [45].
First of all, the most relevant question that has to be asked is: why is a relativistic theory of gravity needed in order to construct a model of the cosmos? It is known that the Newtonian gravity can be successfully used to study the effects of gravity from laboratory scales up to galactic distances, however this *approximation* fails on length scales of the order of the Hubble radius $R_H = c/H_0 \sim 10^{28}$cm, which is the maximum distance we are able to observe. Let us evaluate the mass M within a sphere of radius R_H, defining the mean energy density today as $\rho_0 = \rho(t_0)$

$$M = \frac{4\pi}{3}\frac{\rho_0}{c^2}\left(\frac{c}{H_0}\right)^3. \tag{2.1}$$

The absolute value of the Newtonian potential is given by

$$|\phi| = \frac{GM}{R_H} = \frac{4\pi}{3}\frac{G\rho_0}{H_0^2}. \tag{2.2}$$

The Newtonian approximation is valid as long as the gravitational potential energy of a test mass is negligible with respect to its rest energy, namely

$$\frac{|\phi|}{c^2} \ll 1, \tag{2.3}$$

but using the current observed value of $\rho_0/c^2 \sim 10^{-29}\mathrm{g\,cm^{-3}}$ and $H_0 \sim 10^{-18}\mathrm{s^{-1}}$, we get

$$\frac{|\phi|}{c^2} = \frac{4\pi}{3}\frac{G\rho_0}{c^2 H_0^2} \sim 1. \tag{2.4}$$

The last result clearly underlines the necessity of using GR to build a cosmological model, or of a modified version of it coming from string theory [46, 47] and its higher curvature corrections [48–50], or $f(R)$ models [51, 52], or others.

The main assumptions of the concordance model are the following:

1. The unique force that drives the evolution of the Universe on large scale is gravity and it is correctly described by GR.

2. On large scales, the energy content of the Universe is homogeneous and isotropic. On smaller scales, where inhomogeneities and anisotropies occur, still homogeneity and isotropy are restored in a weaker statistical sense. This allows us to describe the Universe as made of perturbations built on top of a homogeneous and isotropic background, i.e. FLRW metric.

3. The matter sources of the gravitational field are non-interacting, barotropic perfect fluids. The main components of the cosmological fluid are:
   i) a pressureless fluid, also known as matter fluid, with equation of state (EoS) $p = 0$,
   ii) a radiation fluid with EoS $p = \frac{\rho}{3}$ and,
   iii) the Dark Energy fluid, with EoS $p = -\rho = -\Lambda$, that is equivalent to the cosmological constant of Eq. (1.72).

4. The radiation is in thermal equilibrium.

The third assumption will be dropped later in this thesis, allowing for dissipative barotropic fluids as a source for the geometry. The dissipative properties will be encoded in two parameters called the shear viscosity η and the bulk viscosity ζ, as we shall see in the next sections.

2.1 The Friedmann-Lemaître-Robertson-Walker geometry

Let us begin by embedding a space-like N-dimensional hypersurface Σ_n with constant curvature in a $(N+1)+1$-dimensional Minkowskian space, parametrized by the coordinates X^A. The line element in the $(N+1)+1$ dimensional manifold is given by

$$ds^2 = \eta_{AB} dX^A dX^B \qquad A, B = 0, 1, \ldots, N+1 \ , \tag{2.5}$$

with the constraint

$$f(X^A) = 0 \quad \equiv \quad \delta_{ij} X^i X^j = \tfrac{1}{k} \quad i, j = 1, \ldots, N+1. \tag{2.6}$$

If $k > 0$ the equation describes a hypersphere with radius $R^2 = 1/k$, conversely if $k < 0$ it describes an $N+1$-dimensional hyperboloid. Our aim is to evaluate the induced metric on the embedded manifold Σ_n. In order to do so we introduce the "stereographic" coordinates, $\{x^a, a = 1, \ldots, N\}$

$$\begin{aligned} X^A &= \delta^A_a x^a \quad A = 1, \ldots, N \\ X^{N+1} &= y. \end{aligned} \tag{2.7}$$

From the condition Eq. (2.6), the $N+1$ coordinate is constrained to be

$$y^2 = -\delta_{ab} x^a x^b + \frac{1}{k}, \tag{2.8}$$

and differentiating

$$y dy = -\delta_{ab} x^a dx^b, \tag{2.9}$$

finally we get

$$dy^2 = k \frac{x_a x_b dx^a dx^b}{1 - k x_a x^a}. \tag{2.10}$$

The induced line element on Σ_n is then

$$ds^2 = \tau_{AB} dX^A dX^B = b^2(t')dt'^2 - a^2(t') \left[\delta_{ab} + \frac{k x_a x_b}{1 - k x_c x^c} \right] dx^a dx^b. \tag{2.11}$$

The two functions $b(t')$, $a(t')$ can be inserted because they do not change the symmetries of the spatial part of the metric and moreover can take into account the expansion of the Universe. The symmetry group of the spatial part of this metric is $SO(N)$ and the translation group, so there exist in general $\frac{N(N-1)}{2} + N = \frac{N(N+1)}{2}$ Killing vectors. A Killing vector ξ^μ is the generator of a transformation that leaves the metric locally invariant, namely $g'^{\mu\nu}(x) = g^{\mu\nu}(x)$.
Let us consider a space-time manifold $\mathcal{M}_4$ with $D = 4$ dimensions and with space sections that are 3-dimensional manifolds with constant curvature, thus maximally symmetric. It can be written from Eq. (2.11) the following line element

$$ds^2 = b^2(t')dt'^2 - a^2(t') \left[|d\mathbf{x}|^2 + \frac{k\,(\mathbf{x} \cdot d\mathbf{x})}{1 - k|\mathbf{x}|^2} \right], \tag{2.12}$$

or in spherical coordinates ($x^1 = r\cos\phi\sin\theta$, $x^2 = r\sin\theta\sin\phi$, $x^3 = r\cos\theta$)

$$ds^2 = b^2(t')dt'^2 - a^2(t') \left[\frac{dr^2}{1 - kr^2} + r^2 d\Omega^2 \right]$$

$$d\Omega^2 = d\theta^2 + \sin^2\theta d\phi^2. \tag{2.13}$$

The coordinate system in which the line element assumes the expression in (2.12) is called "comoving" because an initially static observer $u^\mu = (\frac{1}{b(t')}, \mathbf{0})$ remains static during the evolution. In other words a static observer has no relative motion with respect to the coordinate system.

2.1.1 Synchronous and conformal gauge

The use of comoving coordinates to parametrize the FLRW geometry identifies the comoving observers as privileged in this geometry and can be used to synchronize clocks. We can parametrize the time coordinate to coincide with the proper time of these observers

$$b^2(t')dt'^2 = dt^2. \tag{2.14}$$

This choice of coordinates is called the *Synchronous gauge* and the time coordinate t, the *cosmic time.* In this frame the line element takes the form

$$ds^2 = dt^2 - a^2(t)\left[|d\mathbf{x}|^2 + \frac{k\,(\mathbf{x}\cdot d\mathbf{x})}{1-k|\mathbf{x}|^2}\right], \tag{2.15}$$

or

$$ds^2 = dt^2 - a^2(t)\left[\frac{dr^2}{1-kr^2} + r^2 d\Omega^2\right]. \tag{2.16}$$

Another viable option that results to be particularly convenient when the curvature is null (it happens to be negligible), is the so-called *Conformal gauge.* The conformal time is defined by the following relation with the cosmic time

$$a(\tau)d\tau = dt \Rightarrow \tau = \int_0^t \frac{dt'}{a(t')}. \tag{2.17}$$

Neglecting the curvature, the line element takes the form

$$ds^2 = a^2(\tau)\left[d\tau^2 - |d\mathbf{x}|^2\right]. \tag{2.18}$$

Given the simple form, we will use the conformal time extensively throughout the thesis.

2.1.2 Cosmological horizons

Another interesting kinematic effect due to the FLRW expanding geometry concerns the possible presence of causal horizons. We first illustrate what a*particle horizon* is: let us consider a light-like signal emitted from the position r_1 at a cosmic time t_1 and received at a position $r = 0$ at time t_0, with $t_1 < t_0$. Since $ds^2 = 0$ and $d\Omega^2 = 0$, from Eq. (2.16) we arrive at

$$\int_0^{r_1} \frac{dr}{\sqrt{1-kr^2}} = \int_{t_1}^{t_0} \frac{dt'}{a(t')}. \tag{2.19}$$

Suppose now that we can extend Eq. (2.19) to the earliest time in the past t_{min} reachable along the manifold such that $t_1 \to t_{min}$. We then have that the corresponding source at that time has proper distance given by

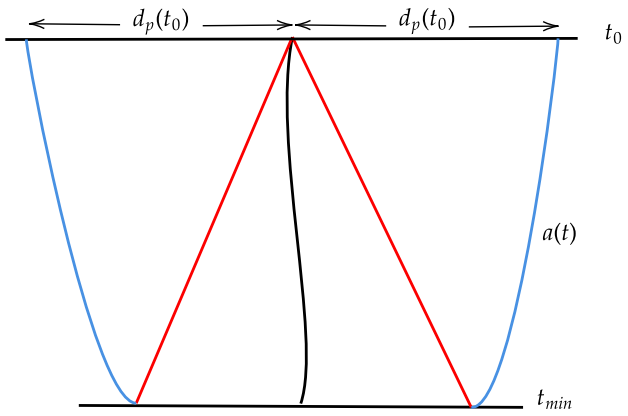

FIGURE 2.1: Graphic interpretation of the particle horizon.

$$d_p(t_0) = a(t_0) \int_{t_{min}}^{t} \frac{dt'}{a(t')}. \tag{2.20}$$

If this distance is finite, we then say that the Universe admits a particle horizon. Since this quantity regards light-like signals reaching the observer from the past, this quantity can be intuitively thought as the radius of the past light-cone.

Another important horizon is called the *event horizon.* First of all let us imagine that a signal is emitted today t_0 from the position r_2, and it propagates towards the origin $r = 0$ and it reaches it at $t = t_2 > t_0$. The proper distance between the receiver and the emitter at the time t_0 is given by

$$d(t_0) = a(t_0) \int_0^{r_2} \frac{dr}{\sqrt{1 - kr^2}} = a(t_0) \int_{t_0}^{t_2} \frac{dt'}{a(t')}. \tag{2.21}$$

If we extend Eq. (2.21) to the maximum future time t_{max} reachable along the manifold such that $t_2 \to t_{max}$, we have that the corresponding source at the time t_0 has proper distance given by

$$d_e(t_0) = a(t_0) \int_{t_0}^{t_{max}} \frac{dt'}{a(t')}. \tag{2.22}$$

To conclude this section, we observe that the presence of horizons depends on $a(t)$ (i.e. the energy content of the Universe) and on the temporal domain of the manifold $t_{min} < t < t_{max}$.

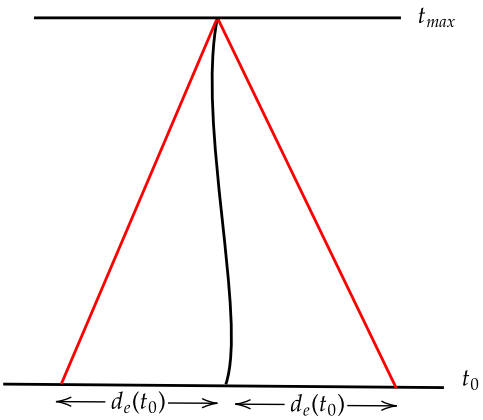

FIGURE 2.2: Graphic interpretation of the event horizon.

2.2 The material content of the Universe: the ΛCDM model

As for now we have only described the geometry that is commonly used to describe the Universe, but no mention of what material sources should be responsible for its expansion has been presented. The main aim of this section will be to give a brief review of the energy content that will allow us to determine the parameters describing a FLRW geometry, namely the curvature k and the scale factor $a(t)$. According to this model, the Universe used to be warmer in the past, allowing for thermonuclear reactions to take place that produced the elements that we observe today (this process takes place at energy scales of the order of the MeV). Moreover the expansion described by the FLRW geometry allows us to interpret in a natural way the Cosmic Microwave Background (CMB) and the redshift that characterizes the cosmological sources as a function of the distance (the Hubble law). Despite all these outstanding results, the so-called ΛCDM model is far from being complete, as it lacks an explanation for the isotropy of the CMB, increasing evidence points to a large discrepancy of the value of the Hubble's constant measured using different techniques (the H_0 tension), novel evidence is pointing towards a non-constant Dark Energy source, and it predicts a singularity in the past (i.e. the geometry is not geodesically complete).

2.2.1 The Friedmann-Lemaitre-Robertson-Walker equations

To fully solve for the scale factor the Einstein field equations must be solved

$$R_{\mu}{}^{\nu} = \lambda_p^2 \left(T_{\mu}{}^{\nu} - \frac{1}{2}\delta_{\mu}^{\nu} T \right). \tag{2.23}$$

In order to solve these equations, some assumptions must be made on the energy-momentum tensor. In the ΛCDM model all the energy sources are modelled as barotropic perfect fluids whose energy momentum tensor is given by

$$T_{\mu\nu} = (\rho + p)\, u_\mu u_\nu - p g_{\mu\nu}, \tag{2.24}$$

where $\rho = \rho(t)$ is the energy density, $p = p(t)$ is the pressure and u_μ is the velocity field. A derivation of the above formula will be given in the section dedicated to the relativistic fluid dynamics. To be consistent with the homogeneity assumption, both the energy density and the pressure do not depend on the spatial coordinates. The velocity field u_μ is taken to be time-like, since it is taken to be comoving with the geodesic of test-particles. We hence have to a physical observer that moves inside the light cone of the fluid

$$g_{\mu\nu} u^\mu u^\nu = 1. \tag{2.25}$$

This implies that the velocity field is given by $u^\mu = (u^0, \mathbf{0})$, with $u^0 = 1$ as a consequence of Eq. (2.25). Rising one of the indices, we can finally write

$$T_{\mu}{}^{\nu} = \mathrm{diag}(\rho, -p, -p, -p) \tag{2.26}$$

and

$$T = \rho - 3p. \tag{2.27}$$

In order to find the Einstein equations, we still have to evaluate all the Christoffel symbols of the metric (2.16) in order to compute the Ricci tensor. For the sake of conciseness, we only report the non-null component of $R_{\mu}{}^{\nu}$ [53, 54]

$$
\begin{aligned}
R_0{}^0 &= -3\frac{\ddot{a}}{a}, \\
R_i{}^j &= -\left(\frac{\ddot{a}}{a} + 2H^2 + 2\frac{k}{a^2}\right)\delta_i^j, \\
R_\alpha{}^\beta &= 0 \quad \text{if } \alpha \neq \beta.
\end{aligned}
\tag{2.28}
$$

where

$$
H(t) \equiv \frac{\dot{a}(t)}{a(t)} \tag{2.29}
$$

is the *Hubble parameter* that plays a pivotal role in the dynamics of a FLRW geometry.
The r.h.s. of Eq. (2.23) is readily written from Eqs. (2.26) and (2.27) as

$$
\begin{aligned}
T_0{}^0 - \frac{1}{2}T &= \frac{1}{2}(\rho + 3p) \\
T_i{}^j - \frac{1}{2}T\delta_i^j &= -\frac{1}{2}(\rho - p)\,\delta_i^j
\end{aligned}
\tag{2.30}
$$

The combination of Eqs. (2.30) and (2.28) yields the Friedmann equations

$$
\frac{\ddot{a}}{a} = -\frac{\lambda_p^2}{6}(\rho + 3p) \tag{2.31}
$$

$$
\frac{\ddot{a}}{a} + 2H^2 + 2\frac{k}{a^2} = \frac{\lambda_p^2}{2}(\rho - p)\,. \tag{2.32}
$$

Once the equation of state $p = p(\rho)$ and the curvature k are known, the Friedmann equations can give the evolution of the energy density $\rho(t)$ and of the scale factor $a(t)$. The two equations above can be rewritten eliminating the explicit dependence upon $\frac{\ddot{a}}{a}$ by using the relation $\dot{H} = \frac{\ddot{a}}{a} - H^2$. Doing so the Friedmann equations take the more familiar form

$$
H^2 + \frac{k}{a^2} = \frac{\lambda_p^2}{3}\rho \tag{2.33}
$$

and

$$
2\dot{H} + 3H^2 + \frac{k}{a^2} = -\lambda_p^2 p. \tag{2.34}
$$

A third equation has to be added to these two, the covariant conservation law for the energy-momentum tensor, $\nabla_\nu T_\mu{}^\nu = 0$, but this equation is not independent from Eqs. (2.33) and (2.34). The spatial components of this equation are identically satisfied while the 0-th component reads

$$\dot{\rho} + 3H(\rho + p) = 0, \tag{2.35}$$

which can be interpreted as the adiabatic evolution ($TdS = dU + pdV = 0$) for a fluid in a comoving patch of volume $V = L^3 a^3$, where L is a fixed coordinate distance of the patch of Universe under consideration.
We end this section by rewriting the Friedmann equation in conformal time. From Eq. (2.17) we have

$$\mathcal{H}^2 + k = \frac{\lambda_p^2}{3}\rho a^2, \tag{2.36}$$

$$2\mathcal{H}' + \mathcal{H}^2 + k = -\lambda_p^2 p a^2 \tag{2.37}$$

and

$$\rho' + 3\mathcal{H}(\rho + p) = 0. \tag{2.38}$$

, where we denote with " $'$ " the derivative with respect to the conformal time and $\mathcal{H} = a'/a$.

2.2.2 The cosmological fluids

In the context of the standard cosmological model, all the fluids are perfect, non-interacting and barotropic, namely the total energy density, the pressures and the equations of state are given by the following identities

$$\rho = \sum_n \rho_n \qquad p = \sum_n p_n \qquad p_n = w_n \rho_n \ . \tag{2.39}$$

The assumption that each fluid does not interact with another corresponds to the fact that each component satisfies its own energy conservation law

$$\dot{\rho}_n + 3H\rho_n(1 + w_n) = 0. \tag{2.40}$$

The solution to this equation is straightforward (after recalling the definition of H) and reads

$$\rho_n = \rho_{0n} \left(\frac{a}{a_0} \right)^{-3(1+w_n)} . \tag{2.41}$$

According to the last solution each fluid component of the mixture dilutes in a different way, so in general there is always one component prevailing over the others. Each of these stages takes the name of *Cosmological Epoch.* Moreover this simplification allow us to solve the Friedmann equation (2.33) when the curvature contribution k is negligible

$$\left(\frac{da}{dt} \right)^2 = \frac{\lambda_p^2}{3} \left(\frac{a}{a_0} \right)^{2-3(1+w_n)} \Rightarrow a(t) = a_0 \left(\pm \frac{t}{t_0} \right)^{\frac{2}{3(1+w_n)}} , \tag{2.42}$$

where t_0 is a fixed cosmic time and $a_0 = a(t_0)$. It is customary to set t_0 as the cosmic time today, also known as the age of the universe and $a_0 = a(t_0) = 1$. The $\pm$ appears because the Einstein equations are symmetric under time-reversal transformations, but we will consider only the positive branch that represents an expanding universe.

For completeness reasons we give the same solution in terms of the conformal time τ because it will be useful later

$$a(\tau) = a_0 \left(\pm \frac{\tau}{\tau_0} \right)^{\frac{2}{1+3w_n}} , \tag{2.43}$$

where

$$\tau_0 = \int_0^{t_0} \frac{dt'}{a(t')}. \tag{2.44}$$

The matter fluid

The matter in the Universe is modelled after a pressureless perfect fluid with EoS $p_m = 0 \Rightarrow w_m = 0$. It is important to stress that by matter we mean every astrophysical object that is non-relativistic, including cold dark matter. The simple reason behind this assumption is an observational fact, the matter

we observe is non-relativistic. From the equation of a perfect gas in thermal equilibrium we have

$$pV = NT, \tag{2.45}$$

with $k_b = 1$ and T the temperature. From statistical thermodynamics we know that

$$T \sim mv^2, \tag{2.46}$$

thus remembering the relation between the mass and the energy $E = Mc^2$ with $M = Nm$, Eq. (2.45) becomes

$$p_m \sim \rho_m \frac{v^2}{c^2} \sim 0, \tag{2.47}$$

hence the assumption of a pressureless fluid.
For a matter dominated universe we can write how the scale factor evolves over time using Eq. (2.42)

$$a(t) \sim t^{\frac{2}{3}} \tag{2.48}$$

and in conformal time

$$a(\tau) \sim \tau^2 \tag{2.49}$$

To conclude, using Eq. (2.41) the matter fluid scales with the scale factor as

$$\rho_m = \rho_{0m} \left(\frac{a}{a_0} \right)^{-3} \tag{2.50}$$

The radiation fluid

The radiation contribution in the Universe is modelled with a traceless energy-momentum tensor

$$T_\mu{}^\mu = 0. \tag{2.51}$$

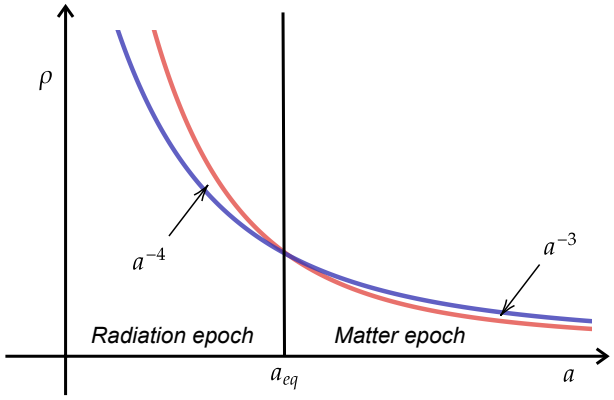

FIGURE 2.3: Energy density evolution as a function of the scale factor for a matter fluid $w_m = 0$ and a radiation fluid $w_r = \frac{1}{3}$.

By radiation we mean every massless particle (photons, gravitons) and every ultra-relativistic massive particle like neutrinos. Eqs. (2.27) and (2.51) yield

$$p_r = \frac{\rho_r}{3} \Rightarrow w_r = \frac{1}{3} \tag{2.52}$$

Using the last equality in Eqs. (2.42) and (2.43) we can write the following expressions for the scale factor in cosmic time and conformal time in a radiation dominated Universe

$$a(t) \sim t^{\frac{1}{2}} \tag{2.53}$$

$$a(\tau) \sim \tau \tag{2.54}$$

To conclude, using Eq. (2.41) the radiation fluid scales with the scale factor as

$$\rho_r = \rho_{0r} \left(\frac{a}{a_0} \right)^{-4} . \tag{2.55}$$

As can be seen from Fig. (2.3) the Universe had been dominated by the radiation fluid until the scale factor reached a_{eq}. Only after this equality time matter energy density starts to drive the cosmic expansion.

The Λ fluid, Dark Energy or cosmological constant

Recent observations [55] have discovered that the Universe is undergoing an accelerate expansion. According to the matter plus radiation fluids, neither of the two cosmological sources makes the Universe accelerate. In fact given a generic scale factor $a(t) \sim t^{\frac{2}{3(1+w_n)}}$, we have that

$$\frac{\ddot{a}}{a} = -\frac{2\left(1+3w_n\right)}{9\left(1+w_n\right)^2 t^2} > 0, \tag{2.56}$$

so to have an accelerated expansion, the condition $w_n < -\frac{1}{3}$ must be met. Clearly this condition is not fulfilled neither by the matter fluid $w_m = 0$ nor the radiation one $w_r = \frac{1}{3}$. The observed value for this fluid component is $w_\Lambda \approx -1$, although recent observations from DESI [45] suggest that the Dark Energy component might be evolving as $w = w_0 + w_a(1-a)$, with $w_0 > -1$ and $w_a < 0$. Interestingly enough the interpretation of this exotic component is not yet understood and could be just the manifestation of one of the assumption of the cosmological model being wrong. Some attempts have been carried out to interpret dark energy as the quantum vacuum energy, however when doing the calculation, the theoretical value is wrong by 120 orders of magnitude [56]! The current concordance model assumes the presence of a dark energy as a cosmological constant component; in the following a Λ dominated Universe will be studied. Nevertheless it is important to stress that we are not living currently in a dark energy dominated universe, even though its contribution is greater than the one from the matter fluid, their orders of magnitude are comparable.

Given the particular value of $w_\Lambda = -1$, all the already evaluated formulas for the scale factor cannot be applied because every exponent diverges. The energy momentum tensor for the cosmological constant is given by ($\rho_\Lambda = \Lambda$)

$$T_\mu{}^\nu = \mathrm{diag}(\Lambda, \Lambda, \Lambda, \Lambda). \tag{2.57}$$

Inserting $p = -\Lambda$ into Eq. (2.35) yields an interesting property of this fluid, namely it does not dilute over time

$$\dot{\rho}_\Lambda = 0 \Rightarrow \rho_\Lambda = \Lambda. \tag{2.58}$$

The scale factor can be evaluated from Eq. (2.33) as

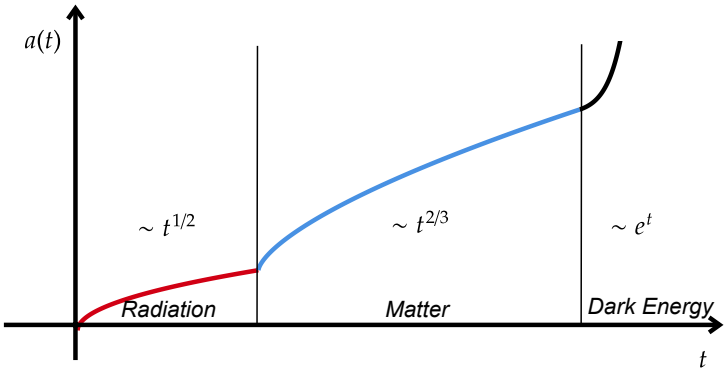

FIGURE 2.4: Evolution of the scale factor throughout the standard phases of the ΛCDM model

$$a(t) = a_0 e^{\sqrt{\frac{\lambda_p^2}{3}\Lambda}(t-t_0)} \equiv a_0 e^{H_\Lambda (t-t_0)}, \tag{2.59}$$

where we have defined $H_\Lambda \equiv \sqrt{\frac{\lambda_p^2}{3}\Lambda}$. To evaluate how the scale factor evolves in terms of the conformal time we use Eq. (2.43)

$$a(\tau) \sim (-H_\Lambda \tau)^{-1}\,. \tag{2.60}$$

The minus sign is necessary because $a \in [0, +\infty) \Rightarrow \tau \in (-\infty, 0)$.

Final remarks on the ΛCDM model

We can conclude this section giving a summary about the full ΛCDM model. At the beginning, the Universe was smaller and radiation dominated, as it expanded, the matter energy density prevailed, leading to a subsequent matter domination phase and recently, the Dark Energy contribution took over starting the exponential expansion.

It is crucial to remark that this model cannot account for a mechanism able to explain the isotropy of the blackbody radiation of the CMB [57] that was generated during the recombination era. Moreover it predicts an initial singularity, because ρ_m, ρ_r and the curvature tensors and scalar diverge for $t \to 0$. Although we do not have a unique formulation for a Quantum Gravity theory, it is expected that at such high curvature and high energies regimes, quantum behaviors should play a crucial role, making the predictions of a "classical" theory of gravity such as GR not reliable.

2.3 The early Universe: the Inflation mechanism

In this section we will show some of the main problems at early times of the concordance model and how an initial period of accelerated expansion called *inflationary period* can solve them. Firstly we will provide a brief analysis of the possible scale factors able to solve the problems linked to the early phases of the ΛCDM model and then we will focus on two possible models, the de Sitter inflation and the more realistic slow roll inflation.

2.3.1 The flatness problem

The flatness problem is a fine tuning problem that arises when we analyse how the ratio between the spatial curvature and the space-time curvature evolve over time. In an FLRW geometry the curvature parameter k is related to the square of the inverse of the spatial curvature, namely $k = \frac{1}{R^2}$. However we know that a proper length scales as the scale factor, so we can introduce a proper length $L_k(t)$ that characterizes the radius of curvature

$$L_k(t) = \left(\frac{a^2}{|k|}\right)^{\frac{1}{2}}. \tag{2.61}$$

On the other hand, by direct computations of the curvatures of the FLRW geometry, it is possible to associate to the space-time curvature a proper length L_H that is related to the so-called Hubble radius

$$L_H(t) = R_H = |H|^{-1}. \tag{2.62}$$

If we consider the ratio of the two we have

$$r(t) = \frac{L_H}{L_k} \sim \frac{spatial\ curvature}{space - time\ curvature}, \tag{2.63}$$

and its square coincides with the modulus of $\Omega_k(t)$. The experimental result suggest that today the spatial curvature is smaller than the space-time one, $r_0 \lesssim 0.1$. Going back in the past and assuming a scale factor $a(t) \sim t^\alpha$, with $0 < \alpha < 1$ (recalling that $\alpha = \frac{1}{2}$ radiation, $\alpha = \frac{2}{3}$ matter), we can evaluate Eq. (2.63)

$$r(t) \sim \frac{k}{aH} \sim \frac{1}{\dot{a}} \sim t^{1-\alpha} \underset{t\to 0}{\longrightarrow} 0. \tag{2.64}$$

As a consequence the Universe was highly asymmetric during its early stages and at the Planck time $r_p \lesssim 10^{-31}$. This asymmetry should be understood as a spatial curvature strongly suppressed with respect to the space-time one, giving rise to a *Fine-tuning problem.* Starting from more "natural" conditions given by $r \sim 1$, we can suppress r to suitable values that are required to preserve the small value of r observed today. The problem can be solved with a phase of accelerated expansion $a(t) \sim t^\beta$ with $\beta > 1$, in fact in this case we have

$$r(t) \sim t^{1-\beta} \underset{t\to 0}{\longrightarrow} \infty. \tag{2.65}$$

A phase with this property is called inflationary because it corresponds to an accelerated scale factor

$$H = \frac{\dot{a}}{a} = \frac{\beta}{t} > 0 \qquad \frac{\ddot{a}}{a} = \frac{\beta(\beta-1)}{t^2} > 0. \tag{2.66}$$

2.3.2 The horizon problem

A more severe problem arises while analyzing the isotropy and the thermal equilibrium of the CMB. According to the ΛCDM model not all the regions that we are able to observe today were not causally connected in the past. How did they thermalize without the possibility of information exchange? This conundrum is called the *Horizon problem,* and it can be solved by an initial period of inflation as well.

Let us begin by considering the region of space inside the particle horizon at time t, in a FLRW geometry with scale factor $a(t) \sim t^\alpha$, $0 < \alpha < 1$. By Eq. (2.20) we get

$$d_p(t) = a(t) \int_0^t \frac{dt'}{a(t')} = \frac{t}{1-\alpha} = \frac{\alpha}{1-\alpha} H^{-1}(t). \tag{2.67}$$

On the other hand the radius of the trhee-dimensional sphere enclosed in the particle horizon evolves as the scale factor $\sim t^\alpha$. As a consequence we have that the ratio of the particle horizon and the radius gets smaller as we go back in time

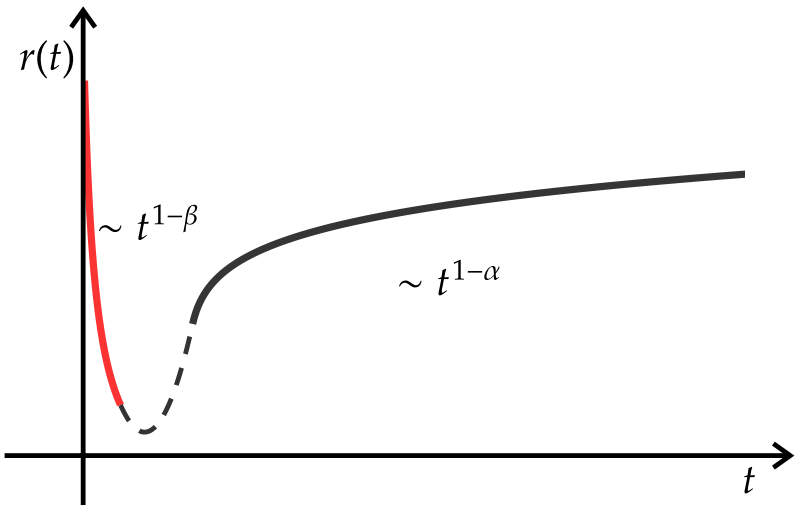

FIGURE 2.5: Evolution of $r(t)$ to solve the flatness and horizon problems.

$$\frac{horizon\ radius}{radius\ space\ region} \sim \frac{H^{-1}}{a} \sim r(t) \sim t^{1-\alpha} \underset{t\to 0}{\longrightarrow} 0. \tag{2.68}$$

The direct consequence is that the space accessible to our observations was bigger than the particle horizon, so it contained regions separated by $d > d_p$ and so causally disconnected. The problem once again can be solved by an initial period of accelerated expansion $a(t) \sim t^\beta$ with $\beta > 1$, that allows for thermalization to take place before the region becomes causally disconnected.

It is important to notice that a fluid with $p < -\frac{\rho}{3}$ could, at least in principle, resolve also the initial singularity problem. A *necessary condition* (but not sufficient) for a space-time manifold to be "geodesically complete" (without singularities) requires that for each time-like or light-like geodesic the following constraint must be met

$$R_{\mu\nu}u^\mu u^\nu < 0, \quad u^\mu u_\mu \geq 0, \tag{2.69}$$

where u^μ is the 4-vector tangent to the geodesic curve. Using the Einstein field equation to rewrite the Ricci tensor and the velocity field of a comoving fluid $u_\mu u^\mu = 1$ and $u^\mu = (1, \mathbf{0})$, Eq. (2.69) becomes

$$T_{\mu\nu}u^\mu u^\nu - \frac{T}{2} < 0. \tag{2.70}$$

From the energy-momentum tensor of the perfect fluid Eqs. (2.26) and (2.27) we have

$$\frac{1}{2}(\rho + 3p) < 0 \Rightarrow p < \frac{\rho}{3}. \tag{2.71}$$

Interestingly enough, the condition to have an accelerated expansion from Eq. (2.31) is the same.

In the next section we will analyze all the possible scale factors that can solve the problems at early time of the concordance model.

2.3.3 Inflationary kinematics

In the previous section we have seen that the early times problems of the ΛCDM can solved by a decreasing $r = \frac{1}{\dot{a}}$ factor.

As a first attempt, we can consider a *power-law* scale factor with $\beta > 1$

$$\begin{aligned} a &\sim t^{\beta}, & \beta &> 1 \\ H &= \frac{\beta}{t} > 0, & 0 \leq t &< +\infty \\ \dot{H} &= -\frac{\beta}{t^2} < 0, & & \\ \frac{\ddot{a}}{a} &= \frac{\beta(\beta-1)}{t^2} > 0, & & \\ r(t) &= t^{1-\beta}, & & \end{aligned} \tag{2.72}$$

This phase is characterized by an accelerated expansion, while the curvature is decreasing since both the moduli of both H and $\dot{H}$ goes to 0 as $t \to +\infty$. These models can have an initial singularity for $t \to 0^+$.

The r parameter can be decreasing also for power law behaviors (with $\beta < 0$) but with negative cosmic time, in particular

$$\begin{aligned} a &\sim (-t)^{\beta}, & \beta &< 0, \\ H &= -\frac{\beta}{(-t)} > 0, & -\infty < t &< 0, \\ \dot{H} &= -\frac{\beta}{t^2} < 0, & & \\ \frac{\ddot{a}}{a} &= \frac{\beta(\beta-1)}{t^2} > 0, & & \\ |r(t)| &= (-t)^{1-\beta}, & & \end{aligned} \tag{2.73}$$

In this case both H and $\dot{H}$ grow for t approaching 0 from the left, evolving towards a final singularity for $t \to 0^-$. This inflationary scenario is called *superinflation* because we have an accelerated expansion with an increasing curvature.
Finally the r factor can be decreasing even for a contracting universe, in particular for $(0 < \beta < 1)$

$$\begin{aligned} a &\sim (-t)^{\beta}, & 0 < \beta &< 1, \\ H &= -\frac{\beta}{(-t)} > 0, & -\infty < t &< 0, \\ \dot{H} &= -\frac{\beta}{t^2} < 0, & & \\ \frac{\ddot{a}}{a} &= \frac{\beta(\beta-1)}{t^2} > 0, & & \\ |r(t)| &= (-t)^{1-\beta}. & & \end{aligned} \tag{2.74}$$

Also in this case the curvature increases during the inflationary phase towards a singularity in the limit $t \to 0^-$ and moreover there is an accelerated contraction.
For future practical applications it is convenient to express all these different scale factors in conformal time

$$a(\tau) \sim (-\tau)^{\alpha}, \qquad -\infty < \alpha < +\infty, \qquad -\infty < \tau < 0. \tag{2.75}$$

Our aim is to link the range of values β for the scale factors expressed in cosmic time to the exponent α. For this reason we use the relation between the conformal time and the cosmic time given in Eq. (2.17) $(dt = a\, d\tau)$ and integrate both sides to obtain

$$-(1+\alpha)\, t \sim (-\tau)^{1+\alpha}, \tag{2.76}$$

so

$$a \sim (-\tau)^{\alpha} \sim [-(1+\alpha)\, t]^{\beta}, \qquad \beta = \tfrac{\alpha}{1+\alpha}. \tag{2.77}$$

In the table we summarize all the possible models both in conformal time and cosmic time with their exponents.

Inflationary models	Cosmic time $a = \|t\|^\beta$	Conformal time $a = (-\tau)^\alpha$
Power law	$\beta > 1, \quad t > 0$	$\alpha < -1, \quad \tau < 0$
De Sitter	$\beta = +\infty, \quad -\infty < t < +\infty$	$\alpha = -1, \quad \tau < 0$
Superinflation	$\beta < 0, \quad t < 0$	$-1 < \alpha < 0, \quad \tau < 0$
Accelerated contraction	$0 < \beta < 1, \quad t < 0$	$\alpha > 0, \quad \tau < 0$

TABLE 2.1: Four possible cases of inflationary kinematics.

In the next section we will analyze the simplest inflationary model which describes a space-time with constant curvature, geodesically complete and regular, the de Sitter model.

2.3.4 de-Sitter inflation

The simplest model of inflationary phase can be realised by taking as source a perfect fluid that behaves like the cosmological constant (see Eq. (2.57)). Hence, in order to obtain the EoS $p = -\rho$, we need to investigate whether there exists any kind of (exotic) dynamical degree of freedom whose EoS is the one of Λ. The system we are looking for is a self-interacting scalar field minimally coupled with the geometry, whose lagrangian density is given by

$$\mathcal{L}_m = \frac{1}{2}\nabla_\mu\phi\nabla^\mu\phi - V(\phi), \tag{2.78}$$

when frozen in the minimum of its potential. Given that the covariant derivatives act on a scalar field we can write

$$\nabla_\mu\phi\nabla^\mu\phi = g^{\mu\nu}\partial_\mu\phi\partial_\nu\phi. \tag{2.79}$$

For completeness and later use let us write the whole action

$$S = -\frac{1}{2\lambda_p^2}\int_\Omega d^4x\,\sqrt{-g}R + \int_\Omega d^4x\,\sqrt{-g}\frac{1}{2}g^{\mu\nu}\partial_\mu\phi\partial_\nu\phi - V(\phi). \tag{2.80}$$

We have to check if a scalar field in the minimum of its potential is able to solve its equation of motion (EoM). The equation of motion for the field ϕ is given by the usual Euler-Lagrange equations

$$\frac{\delta S}{\delta \phi} = 0, \tag{2.81}$$

thus:

$$\frac{\partial \sqrt{-g}\mathcal{L}_m}{\partial \phi} - \partial_\mu \frac{\partial \sqrt{-g}\mathcal{L}_m}{\partial_\mu \phi} = 0. \tag{2.82}$$

An easy and direct calculation yields

$$\partial_\mu \left(\sqrt{-g} g^{\mu\nu} \partial_\nu \phi\right) + \sqrt{-g}\frac{\partial V}{\partial \phi} = 0, \tag{2.83}$$

and using the definition of the D'Alembert operator in a curved space-time (1.32)

$$\nabla_\mu \nabla^\mu \phi + \frac{\partial V}{\partial \phi} = 0. \tag{2.84}$$

If $V(\phi)$ has a minimum for $\phi = cost = \phi_0$, we have $\left(\frac{\partial V}{\partial \phi}\right)_{\phi=\phi_0} = 0$ and it is a solution of the equation of motion (2.84)

$$\phi = \phi_0, \qquad \left(\frac{\partial V}{\partial \phi}\right)_{\phi=\phi_0} = 0, \qquad V(\phi_0) = \Lambda_{\text{inf}}, \tag{2.85}$$

where Λ_{inf} is not the same as the cosmological constant! The last step is to evaluate the energy-momentum tensor and verify that the constant solution reproduce the one of a perfect fluid with coefficient $w = -1$. From Eq. (1.64) we get

$$T_{\mu\nu} = \frac{2}{\sqrt{-g}} \frac{\delta \sqrt{-g}\mathcal{L}_m}{\delta g^{\mu\nu}}, \tag{2.86}$$

and after evaluating the derivatives using Eq. (1.30), we are left with

$$T_{\mu\nu} = \frac{2}{\sqrt{-g}} \left[-\frac{\sqrt{-g}}{2} g_{\mu\nu} \left(\frac{1}{2} g^{\alpha\beta} \partial_\alpha \phi \partial_\beta \phi - V(\phi) \right) + \frac{\sqrt{-g}}{2} \delta^\alpha_\mu \delta^\beta_\nu \partial_\alpha \phi \partial_\beta \phi \right]$$

$$T_{\mu\nu} = \partial_\mu \phi \partial_\nu \phi - \frac{g_{\mu\nu}}{2} (\partial \phi)^2 + g_{\mu\nu} V(\phi), \tag{2.87}$$

where $(\partial\phi)^2 = g^{\alpha\beta}\partial_\alpha\phi\partial_\beta\phi = \nabla_\alpha \nabla^\alpha \phi$. Using Eq. (2.85) in the energy-momentum tensor formula for a scalar field we arrive at

$$T_\mu{}^\nu = V(\phi_0)\delta_\mu^\nu = \Lambda_{\rm inf}\delta_\mu^\nu = \mathrm{diag}\left(\Lambda_{\rm inf}, \Lambda_{\rm inf}, \Lambda_{\rm inf}, \Lambda_{\rm inf}\right). \tag{2.88}$$

The kinematic properties of the cosmic geometry have been already discussed for this particular case when we were describing a cosmological constant dominated Universe Eqs. (2.59) and (2.60). However we report once again the results in this section because, although they are equal from the mathematical point of view, their physical meaning is completely different. The dark energy contribution is not equal to the de Sitter vacuum energy despite the fact we have used the same letter (Λ) to refer to their energy densities,

$$\begin{aligned} a(t) &= e^{H_{\Lambda_{\rm inf}}t}, \quad H_{\Lambda_{\rm inf}} = \left(\tfrac{\Lambda_{\rm inf}\lambda_p^2}{3}\right)^{\frac{1}{2}}, \\ H(t) &= H_{\Lambda_{\rm inf}}, \qquad \frac{\ddot{a}}{a} = H_{\Lambda_{\rm inf}}^2, \end{aligned} \qquad -\infty < t < +\infty \tag{2.89}$$

with the line element given by

$$ds^2 = dt^2 - e^{2\Lambda_{\rm inf}\, t}|d\mathbf{x}|^2. \tag{2.90}$$

In conformal time

$$\begin{aligned} a(\tau) &= -\frac{1}{H_{\Lambda_{\rm inf}}\tau}, \quad H_{\Lambda_{\rm inf}} = \left(\frac{\Lambda_{\rm inf}\lambda_p^2}{3}\right)^{\frac{1}{2}}, \\ \mathcal{H}(\tau) &= -\frac{1}{\tau}, \qquad \frac{a''}{a} = \frac{1}{\tau^2}, \end{aligned} \qquad -\infty < \tau < 0 \tag{2.91}$$

with the line element in the conformal gauge

$$ds^2 = \frac{1}{\left(H_{\Lambda_{\rm inf}}\tau\right)^2}\left(d\tau^2 - |d\mathbf{x}|^2\right). \tag{2.92}$$

The main drawback of this inflationary scenario is the absence of a mechanism to exit from the inflationary period. Once the scalar field, called the Inflaton from now on, is in a minimum of its potential the inflationary period lasts forever. Some efforts have been done to implement some kind of macroscopic tunneling effect from a metastable state to a stable state at lower energy, but they were not successful.

2.3.5 Slow-roll inflation

A possible way out from the endless inflation previously described can be provided by relaxing the stationarity condition for the Inflaton field. Supposing that the field is "slow rolling" along a potential that is varying slowly $\frac{\partial V}{\partial \phi} = V_\phi \approx 0$, it is possible to achieve a quasi-exponential expansion with decreasing curvature, while resolving the problem of the inflation exit. The main aim of this section is to describe the main features of a slow roll scenario in a spatially flat FLRW metric and the evaluation of the scale factor $a(t)$.
Let us begin with some assumptions, since we have an homogeneous background metric, we assume the same property for the Inflaton field, namely

$$\phi = \phi(t). \tag{2.93}$$

Moreover from Eq. (2.87) it is possible to write its energy-momentum tensor, that is necessary in order to be able to write the Friedmann equations (Eqs. (2.33) and (2.34)) and the EoM for the field (Eq. (2.84))

$$T_0{}^0 = \tfrac{1}{2}\dot{\phi}^2 + V \qquad T_i{}^j = -\delta_i^j \left(\tfrac{1}{2}\dot{\phi}^2 - V\right) . \tag{2.94}$$

The direct comparison with the energy-momentum tensor of a perfect fluid given in Eq. (2.26) yields

$$\rho(t) = \tfrac{1}{2}\dot{\phi}^2 + V \qquad p(t) = \tfrac{1}{2}\dot{\phi}^2 - V \ . \tag{2.95}$$

Having the expressions for the energy density and the pressure, we can substitute into the Friedmann equations (Eqs. (2.33) and (2.34)) setting $k = 0$

$$3H^2 = \lambda_p^2 \left(\frac{1}{2}\dot{\phi}^2 + V\right), \tag{2.96}$$

and using the last equality together with (2.95) in (2.34):

$$2\dot{H} = -\lambda_p^2 \dot{\phi}^2. \tag{2.97}$$

This set of equations has to be completed with the EoM for the scalar field Eq. (2.84), but unless $\dot{\phi} = 0$ which implies the de Sitter inflation, the equation of motion is not linearly independent from the Friedmann equations

$$\nabla_\mu \nabla^\mu \phi + V_\phi = 0 \Rightarrow g^{\mu\nu} \left(\partial_\mu \partial_\nu - \Gamma_{\mu\nu}{}^{\alpha} \partial_\alpha \right) \phi + V_\phi = 0. \tag{2.98}$$

From the homogeneity of the inflaton field and the Christoffel connection for a spatially flat FLRW metric, the latter becomes

$$\ddot{\phi} + 3H\dot{\phi} + V_\phi = 0. \tag{2.99}$$

The slow roll conditions

Let us suppose that the Hubble parameter varies slowly with time. We can introduce the slow parameter ε such that

$$\varepsilon = -\frac{\dot{H}}{H^2} \ll 1, \qquad \dot{\varepsilon} \approx 0 \ . \tag{2.100}$$

A direct double integration of the above Eq. (2.100) leads to

$$a(t) \sim t^{\frac{1}{\varepsilon}}. \tag{2.101}$$

It is not clear if this power behavior leads to a quasi-exponential expansion, but writing the scale factor in conformal time using Eq. (2.17)

$$a(\tau) \sim (-\tau)^{-\frac{1}{1-\varepsilon}} \sim (-\tau)^{-1-\varepsilon}, \tag{2.102}$$

it can be easily seen that for $\varepsilon = 0$ we retrieve the de Sitter solution (2.91) so an exponential expansion in cosmic time.

To better characterize the slow roll phase, additional constraints must be imposed on the Inflaton field. A slow evolution requires that the following conditions have to be met

$$|\dot{H}| \ll H^2, \quad |\ddot{\phi}| \ll |H\dot{\phi}|, \quad \dot{\phi}^2 \ll V \ . \tag{2.103}$$

Under these assumptions we can rewrite Eqs. (2.96) and (2.99) to link the slow roll parameter ε to the properties that the potential has to satisfy

$$3H^2 = \lambda_p^2 V \tag{2.104}$$

$$3H\dot{\phi} = -V_\phi. \tag{2.105}$$

If we differentiate the first equation by ϕ and divide by $3H^2$ we obtain

$$\frac{H_\phi}{H} = \frac{1}{2}\frac{V_\phi}{V}, \tag{2.106}$$

and using the chain rule on the definition of ε (2.100) and Eqs. (2.104), (2.105) and (2.106):

$$\varepsilon = -\frac{\dot{H}}{H^2} = -\frac{H_\phi}{H}\frac{\dot{\phi}}{H} = \frac{1}{2}\frac{V_\phi}{V}\frac{V_\phi}{3H^2}$$

$$\varepsilon = \frac{1}{2\lambda_p^2}\left(\frac{V_\phi}{V}\right)^2. \tag{2.107}$$

The kinematic request of $\varepsilon \ll 1$ implies that the logarithmic derivative of the potential with respect to the field must be far smaller than the Planck's length! Finally the request $|\ddot{\phi}| \ll |H\dot{\phi}|$ gives rise to a second slow roll parameter denoted with η

$$\eta = \tfrac{1}{\lambda_p^2}\left(\tfrac{V_{\phi\phi}}{V}\right) \qquad |\eta| \ll 1\ . \tag{2.108}$$

The last equation states, similarly to Eq. (2.107) that the convexity of the potential, with respect to the potential itself is smaller than the square of the Planck length.

Whether the nature of the primordial phase preceding the standard Hot Big Bang (the onset of the standard radiation epoch), it is widely believed that the source of the seeds of structure formation in our Universe should be traced back to quantum vacuum fluctuation in this epoch. In the following I am going to present some of the basic ingredients of Cosmological Perturbation Theory.

2.4 Cosmological Perturbation Theory

An inflationary phase preceding the standard evolution of the cosmos is able to explain also the small anisotropies that we observe in the CMB and the galactic and intergalactic structures formation. The origin and the growth of these fluctuations requires some mechanism outside the standard model of cosmology. The answer to this problem can be found in a classicalization mechanism of the primordial quantum fluctuations of the matter and geometry that are amplified during the inflationary epoch. Although it is possible to apply perturbation theory in order to study the scalar, the vector and the tensorial primordial perturbations (primordial Gravitational Waves), to the aim of this thesis we will focus only on the latter. However it is crucial to analyze in the first place the techniques required to develop a full and consistent perturbation theory in cosmology. The main focus of this section will be to evaluate the so-called power spectrum of the tensorial perturbations.

Acknowledging that General Relativity is invariant under diffeomorphism, it is necessary to underline that not every quantity we are able to define is identified uniquely and without ambiguities. We are always allowed to do a gauge transformation (general coordinate transformation at fixed space-time point) in order to impose additional constraints. The direct consequence of this feature (shared by all gauge theories in general) is that only invariant objects can be identified with measurable physical quantities.
First of all let us write the perturbed, spatially flat FLRW geometry in conformal time

$$\bar{g}_{\mu\nu}(\tau, \mathbf{x}) = g_{\mu\nu}(\tau) + \delta g_{\mu\nu}(\tau, \mathbf{x}), \tag{2.109}$$

where the unperturbed metric is given by

$$g_{\mu\nu} = a^2(\tau)\,\eta_{\mu\nu}, \tag{2.110}$$

with $\eta_{\mu\nu} = \mathrm{diag}(1, -1, -1, -1)$. As we have already seen, the FLRW spatial part of the geometry is invariant under $SO(3)$, so we can decompose the perturbation in irreducible representations of the group (this is a generalization of the Helmholtz decomposition of a vector field). In general $\delta g_{\mu\nu}$ has 10 degrees of freedom, and we can decompose the perturbation as follows:

- $\delta g_{00} = 2\varphi$, that transforms as a scalar under $SO(3)$;
- $\delta g_{i0} = -2\left(V_i + \partial_i B\right)$,where V_i is a divergence-less vector (2 vector degrees of freedom) and B is a scalar for a total of 3 degrees of freedom;
- $\delta g_{ij} = -\left[-2\psi\delta_{ij} + 2\partial_i\partial_j E + 2\partial_{(i}F_{j)} - h_{ij}\right]$, where ψ and E are two scalars, F_j is a divergence-less vector (2 vector degrees of freedom) and h_{ij} is a transverse ($\partial_j h^{ij} = 0$) and traceless ($g_{ij}h^{ij} = 0$) tensor (2 tensor degrees of freedom), for a total of 6 degrees of freedom.

With this decomposition the perturbed metric takes the form

$$\begin{aligned}\left(g_{\mu\nu} + \delta g_{\mu\nu}\right) dx^\mu dx^\nu = a^2\left(1 + 2\tfrac{\varphi}{a^2}\right) d\tau^2 - 2\left(V_i + \partial_i B\right) dx^i d\tau \\ - \left[\left(a^2 - 2\psi\right)\delta_{ij} + 2\partial_i\partial_j E + 2\partial_{(i}F_{j)} - h_{ij}\right] dx^i dx^j.\end{aligned} \tag{2.111}$$

The scalar, vector and tensor metric perturbations satisfy evolution equations which are decoupled at the first order, so they evolve independently. Moreover in the particular model we are considering, where the sources are perfect fluids and/or scalar fields [1], the tensor perturbations h_{ij} are not coupled directly with the sources. These perturbations describe the relic gravitational waves background that is amplified by the inflationary mechanism.
The perturbed scalar field is given by

$$\begin{aligned}\phi(\tau) \to \phi\left(\tau, \mathbf{x}\right) = \phi(\tau) + \delta\phi\left(\tau, \mathbf{x}\right) \\ \delta\phi\left(\tau, \mathbf{x}\right) = \chi,\end{aligned} \tag{2.112}$$

whereas for the perfect fluid from Eq. (2.24) we have

$$\begin{aligned}T_\mu{}^\nu\left(\tau\right) \to T_\mu{}^\nu\left(\tau, \mathbf{x}\right) = T_\mu{}^\nu\left(\tau\right) + \delta T_\mu{}^\nu\left(\tau, \mathbf{x}\right) \\ T_\mu{}^\nu\left(\tau, \mathbf{x}\right) = \left(\delta\rho + \delta p\right) u_\mu u^\nu + \left(\rho + p\right)\left(\delta u_\mu u^\nu + u_\mu \delta u^\nu\right) - \delta p \delta^\nu_\mu.\end{aligned} \tag{2.113}$$

It is clear that each perturbation is either scalar $(\delta\rho, \delta p, \chi, \delta u^0)$ or vector (δu^i) and it can be shown that they do not couple in the equation of motion with the tensor perturbations h_{ij}, so it is enough to use the evolution equations Eq. (1.87)

[1] This is valid also for viscous fluids

(notice that in that equation the symbol δT represents the energy momentum tensor with the perturbed metric, not perturbed sources!). However if we were interested in the scalar or vector perturbations it would be necessary to analyze how each variable transforms under a gauge transformation and construct from those new gauge invariant quantities called Bardeen potentials, and proceed with a gauge fixing procedure on those.

2.4.1 The perturbed action for tensorial perturbations in the TT gauge

Reproducing the calculations already present in [6] we have to compute the perturbative action for the tensorial perturbations. In Eq. (1.82) we wrote the EoM, and it is easy to show that they come from the following action

$$\begin{aligned}\delta^{(2)}S = -\frac{1}{8\lambda_p^2}\int_\Omega d^4x\Big[&\nabla^2 h_{\alpha\beta} + 2R_{\sigma\alpha\beta\lambda}h^{\sigma\lambda} + R\,h_{\alpha\beta} - g_{\alpha\beta}h^{\sigma\lambda}R_{\sigma\lambda} + \\ &- h_\alpha{}^\sigma R_{\sigma\beta} - h_\beta{}^\sigma R_{\sigma\alpha} - \nabla_\beta\nabla_\lambda h_\alpha{}^\lambda - \nabla_\alpha\nabla_\lambda h_\beta{}^\lambda + \nabla_\alpha\nabla_\beta h + \\ &- g_{\alpha\beta}\left(\nabla^2 h - \nabla_\sigma\nabla_\lambda h^{\sigma\lambda}\right) - 2\lambda_p^2\delta^{(1)}\sum_A T^A_{\alpha\beta}\Big]\left(\sqrt{-g}g^{\mu\alpha}g^{\nu\beta}\right)\delta g_{\mu\nu},\end{aligned} \tag{2.114}$$

where A denotes the two different background sources, namely the fluid which may be also imperfect and the scalar field. Let us deal with the two contributions separately and analyze under what circumstances the TT gauge conditions can be applied. It is important to underline that the following arguments can be extended to an arbitrary number of scalar field and perfect fluid sources.

The scalar field source

Let us recall that the energy-momentum tensor for a scalar field is given by Eq. (2.78). Using the theoretical apparatus exposed in Chap. I, we can easily write

$$\delta^{(1)}T_{\alpha\beta} = \delta^{(1)}\left[\partial_\alpha\phi\partial_\beta\phi - g_{\alpha\beta}\left(\frac{1}{2}g^{\rho\sigma}\partial_\rho\phi\partial_\sigma\phi - V(\phi)\right)\right] \tag{2.115}$$
$$= h_{\alpha\beta}\left(V(\phi) - \frac{1}{2}\partial_\mu\phi\partial^\mu\phi\right) + \frac{1}{2}g_{\alpha\beta}h^{\mu\nu}\partial_\mu\phi\partial_\nu\phi.$$

For consistency with the TT gauge conditions ($\nabla_i h^{ij} = 0,\ g^{ij}h_{ij} = 0,\ h^{0\mu} = 0$) given in Eq. (1.86) we have

$$h^{\alpha\beta}R_{\alpha\beta} = \lambda_p^2 h^{\alpha\beta}\partial_\alpha\phi\partial_\beta\phi. \tag{2.116}$$

Given that the background geometry is a spatially flat FLRW, $R_{ij} \propto g_{ij}$ the LHS is vanishing for the traceless condition. As a consequence $\partial_i\phi = 0$, which represents an homogeneous scalar source. Using these results we can write Eq. (2.115) as follows

$$\delta^{(1)}T_{\alpha\beta} = -h_{\alpha\beta}\left(\frac{1}{2}\dot{\phi}^2 - V(\phi)\right). \tag{2.117}$$

We notice that the quantity in parenthesis is the pressure of the scalar field given in Eq. (2.95) and, as we will see in the next subsection, the same is true for the perfect fluid.

The perfect fluid source

Using the energy momentum tensor for a perfect fluid given in Eq. (2.24) we can evaluate the first order perturbation in the metric as

$$\delta^{(1)}T_{\alpha\beta} = -ph_{\alpha\beta} + \frac{1}{2}(\rho + p)\, g_{\alpha\beta}h_{\mu\nu}u^\mu u^\nu + (\rho + p)\left(u_\alpha u^\nu h_{\nu\beta} + u_\beta u^\nu h_{\nu\alpha}\right), \tag{2.118}$$

with the standard condition $g_{\mu\nu}u^\mu u^\nu = 1$. Using the consistency relation given in Eq. (1.86) we obtain the following necessary condition for the TT gauge

$$h^{\alpha\beta}R_{\alpha\beta} = 2\lambda_p^2(\rho + p)\left(h_{\mu\nu}u^\mu u^\nu\right). \tag{2.119}$$

Again the l.h.s in a FLRW geometry is vanishing, and the consistency relation can be satisfied by a dark fluid $p = -\rho$ and/or by a comoving fluid $u^\mu = (1, \mathbf{0})$.

Taking a comoving fluid we can recast the first order perturbation of the energy momentum tensor as

$$\delta^{(1)}T_{\alpha\beta} = -ph_{\alpha\beta}. \tag{2.120}$$

The viscous fluid source

Using the energy momentum tensor of a viscous fluid

$$T^{\text{vis}}_{\mu\nu} = (\rho + \bar{p})u_\mu u_\nu - \bar{p}g_{\mu\nu} - 2\eta_V \left(u_{(\mu|}u^\alpha \nabla_\alpha u_{|\nu)} - \nabla_{(\mu|}u_{|\nu)} + \frac{1}{3}(g_{\mu\nu} - u_\mu u_\nu)\nabla_a u^\alpha \right) \tag{2.121}$$

where $\bar{p} = p - \zeta \nabla_\mu u^\mu$ is the effective pressure and ζ and η_V are the bulk and shear viscosity respectively. Also in this case as long as the fluid is comoving the TT gauge condition can be applied and we obtain

$$\delta^{(1)}T^{\text{vis}}_{\alpha\beta} = -h_{\alpha\beta}(\bar{p} + 2H\eta_V) + \eta_V \dot{h}_{\alpha\beta}. \tag{2.122}$$

The perturbative action

Including an arbitrary number of comoving viscous sources with different viscosities, ideal fluid sources and scalar fields with different potentials, we get

$$\sum_A \delta^{(1)}T^A_{\alpha\beta} = \sum_i \delta^{(1)} \left(T^{\text{ideal}}_{\alpha\beta}\right)_i + \sum_j \delta^{(1)} \left(T^{\text{scalar}}_{\alpha\beta}\right)_j + \sum_k \delta^{(1)} \left(T^{\text{vis}}_{\alpha\beta}\right)_k, \tag{2.123}$$

where the indices i, j, k run over the different sources of each kind contributing to the total energy-momentum tensor. Using Eqs. (2.117), (2.120) and (2.122), the last equality becomes

$$\begin{aligned} \textstyle\sum_A \delta^{(1)}T^A_{\alpha\beta} = -h_{\alpha\beta} \left[\sum_i p_i + \sum_j \left(\tfrac{1}{2}\dot{\phi}_j^2 - V_j(\phi_j) \right) + \sum_k (p_k - 3H\zeta_k + 2H\eta_k) \right] \\ + \textstyle\sum_k \eta_{V_k} \dot{h}_{\alpha\beta}. \end{aligned} \tag{2.124}$$

The last terms that we have to evaluate in the action given in Eq. (2.89) are

$$Rh_{\alpha\beta} = -h_{\alpha\beta}\lambda_p^2\left[\sum_i(\rho_i - 3p_i) + \sum_j\left(\rho_{\phi_j} - 3p_{\phi_j}\right) + \sum\rho_k - 3(p_k - 3H\zeta_k)\right], \tag{2.125}$$

and

$$\begin{aligned} h_{\alpha\sigma}R_\beta{}^\sigma = \lambda_p^2\Bigg(&-\frac{1}{2}h_{\alpha\sigma}\delta_\beta{}^\sigma\left[\sum_i(\rho_i - 3p_i) + \sum_j\left(\rho_{\phi_j} - 3p_{\phi_j}\right)\right. \\ &\left. + \sum_k(\rho_k - 3(p_k - 3H\zeta_k))\right] + h_{\alpha\sigma}\sum_A T_\beta^{A\,\sigma}\Bigg), \end{aligned} \tag{2.126}$$

where $\rho_{\phi_j} = \frac{1}{2}\dot{\phi}_j^2 + V_j(\phi_j)$ and $p_{\phi_j} = \frac{1}{2}\dot{\phi}_j^2 - V_j(\phi_j)$. Inserting all the above quantities in the action we arrive at

$$\begin{aligned} \delta^{(2)}S = -\frac{1}{8\lambda_p^2}\int_\Omega d^4x\Bigg[&\nabla^2 h_{\alpha\beta} + 2R_{\sigma\alpha\beta\lambda}h^{\sigma\lambda} \\ &+ \lambda_p^2 h_{\alpha\beta}\left(4\sum_k\eta_k\right)H + 2\lambda_p^2\sum_k\eta_{V_k}\dot{h}_{\alpha\beta}\Bigg]\left(\sqrt{-g}g^{\mu\alpha}g^{\nu\beta}\right)\delta g_{\mu\nu}, \end{aligned} \tag{2.127}$$

which leads to the following evolution equation

$$\nabla^2 h_{\alpha\beta} + 2R_{\sigma\alpha\beta\lambda}h^{\sigma\lambda} + \lambda_p^2 h_{\alpha\beta}(4\sum_k\eta_{V_k})H + 2\lambda_p^2\sum_k\eta_{V_k}\dot{h}_{\alpha\beta} = 0. \tag{2.128}$$

The equation of motion for the gravitational waves is modified by the presence of shear viscous fluids, via the sum of all their shear viscosities $\sum_k\eta_{V_k} \equiv \eta_V$. Also the bulk viscosity modifies the evolution of waves but in a more subtle way, because the Hubble parameter H in Eq. (2.128) depends on it[2]. However as we have already mentioned, we will neglect bulk viscous contributions to avoid changes in the standard cosmological evolution phases.

To conclude this subsection we rewrite Eq. (2.128) for the mixed components

[2]The Friedmann equations in the presence of a bulk viscous fluid are formally the same upon the substitution $p \to p - 3H\zeta$.

$$\ddot{h}_i{}^j + \left(3H + 2\eta\lambda_p^2\right)\dot{h}_i{}^j - \frac{(\partial_k)^2}{a^2}h_i{}^j = 0, \tag{2.129}$$

and in conformal time

$$h_i''{}^j + \left(2\mathcal{H} + 2\lambda_p^2\,\eta_V\,a\right)h_i'{}^j - (\partial_k)^2\,h_i{}^j = 0. \tag{2.130}$$

By comparison with the equation without shear viscosity ($\eta_V = 0$), it is clear that its presence becomes relevant when $H \sim \lambda_p^2\eta_V$. The viscous term introduces an additional friction contribution that tends to attenuate the amplitude of the waves during their evolution.

The quantum fluctuations

In order to be able to proceed with a standard quantization scheme for the tensor perturbations, it is necessary to build a perturbative action for the field $h_{\alpha\beta}$. To this aim it is enough to notice that the following action reproduce the EoM (2.130)

$$\delta^{(2)}S = \frac{1}{8\lambda_p^2}\int_\Omega d^3x\,d\tau\,\tilde{a}^2\left(h_i'{}^j h_j'{}^i + h_i{}^j\partial_k^2 h_j{}^i\right), \tag{2.131}$$

where

$$\frac{\tilde{a}'}{\tilde{a}} = \mathcal{H} + \lambda_p^2\eta_V a, \tag{2.132}$$

and $h_i{}^j$ has 6 degrees of freedom. Imposing the TT gauge conditions

$$\partial_j h_i{}^j = 0 \qquad g^{ij}h_{ij} = 0\ , \tag{2.133}$$

we are left with only two of them. We can exploit this property to rewrite the tensor perturbation as

$$h_{ij} = \begin{pmatrix} h_+ & h_\times & 0 \\ h_\times & -h_+ & 0 \\ 0 & 0 & 0 \end{pmatrix} = h_+ e_{ij}^+ + h_\times e_{ij}^\times. \tag{2.134}$$

The $+$ and $\times$ represent the two possible independent polarizations modes of a wave propagating in the $\hat{z}$ direction. Using the Pauli matrices, Eq. (2.134) can be

rewritten as

$$h_{ij} = h_+ \begin{pmatrix} \sigma_z & 0 \\ 0 & 0 \end{pmatrix} + h_\times \begin{pmatrix} \sigma_x & 0 \\ 0 & 0 \end{pmatrix}, \tag{2.135}$$

and from the properties of the Pauli matrices it can be easily checked that

$$e^A_{ij} e^{ij}_B = 2\delta^A{}_B, \qquad A, B = +, \times. \tag{2.136}$$

Exploiting this decomposition, the action (2.131) can be recasted as ($\partial_k^2 = \nabla^2$)

$$\delta^{(2)} S = \frac{1}{4\lambda_p^2} \sum_{A=+,\times} \int_\Omega d^3x\, d\tau\, \tilde{a}^2 \left(h'_A h'_A + h_A \nabla^2 h_A \right) = S_+ + S_\times. \tag{2.137}$$

To proceed to the quantization, it is mandatory to rewrite the action in a canonical form, so to this aim let us introduce the canonical variable

$$v_A = \xi h_A \tag{2.138}$$

where

$$\xi = \frac{\tilde{a}}{\sqrt{2}\lambda_p} \tag{2.139}$$

is the so-called pump-field of the tensor perturbations. After this substitution the action can be rewritten, up to a total derivative in the conformal time, as

$$\delta^{(2)} S = \frac{1}{2} \int d^3x\, d\tau \left(v'^2 + v \nabla^2 u + \frac{\xi''}{\xi} v^2 \right) \tag{2.140}$$

where we have dropped the polarization subscript because the following computations will be valid for both the polarizations. The last action represents a Klein-Gordon field with a non-constant mass term, whose equation of motion is

$$v'' - \left(\nabla^2 + \frac{\xi''}{\xi} \right) v = 0. \tag{2.141}$$

This last equation is known as the Mukhanov-Sasaki equation.

2.4.2 Mukhanov quantization and inflation driven classicalization

In this section we will define and evaluate the primordial Gravitational Waves (pGW) power spectrum arising from the vacuum fluctuations during an inflationary period without shear viscous sources (i.e. $\tilde{a} = a$). In order to do so we will start by quantizing the field $v(\tau, \mathbf{x})$. Going to the Fourier space, where the Fourier transform is defined as

$$v\left(\tau, \mathbf{x}\right) = \frac{1}{\left(2\pi\right)^3} \int_{-\infty}^{+\infty} d^3x \, e^{i\mathbf{k}\cdot\mathbf{x}} \, v_{\mathbf{k}}\left(\tau\right), \tag{2.142}$$

and assuming

$$a(\tau) = \left(-\frac{\tau}{\tau_I}\right)^{\alpha}, \tag{2.143}$$

Eq. (2.141) becomes

$$v_k'' + \left(k^2 - \frac{\alpha\left(\alpha - 1\right)}{\tau^2}\right) v_k = 0. \tag{2.144}$$

The most general solution can be expressed in terms of Hankel's functions of the first and second kind ($\nu = \frac{1}{2} - \alpha$)

$$v_k(\tau) = \sqrt{\tau}\left[A_k H_\nu^{(2)}\left(k\tau\right) + B_k H_\nu^{(1)}\left(k\tau\right)\right]. \tag{2.145}$$

2.4.2.1 Canonical variable quantization

To determine the normalization constants, we must quantize the field and choose a suitable vacuum state. Let us expand the canonical variable in terms of eigenfunctions of the Laplace operator $\nabla^2\psi_{\mathbf{k}}(\mathbf{x}) = -k^2\psi_{\mathbf{k}}(\mathbf{x})$

$$v(\mathbf{x}, \tau) = \frac{1}{\left(2\pi\right)^3} \int d^3k \, v_{\mathbf{k}}(\tau)\psi_{\mathbf{k}}(\mathbf{x}) \tag{2.146}$$

where:

$$\psi_{\mathbf{k}}(\mathbf{x}) = a_{\mathbf{k}} e^{-i\mathbf{k}\cdot\mathbf{x}} + b_{\mathbf{k}} e^{i\mathbf{k}\cdot\mathbf{x}} \tag{2.147}$$

and $v_{\mathbf{k}}(\tau)$ satisfies Eq. (2.144). Since $v(\mathbf{x},\tau)$ is real, the following relation holds true

$$v_{\mathbf{k}}^{\star}(\tau)a_{\mathbf{k}}^{\star} = v_{\mathbf{k}}(\tau)b_{\mathbf{k}}. \tag{2.148}$$

Promoting the canonical variable to an operator, we have

$$v(\mathbf{x},\tau) = \frac{1}{(2\pi)^3}\int d^3k\, v_{\mathbf{k}}(\tau)\hat{a}_{\mathbf{k}}e^{-i\mathbf{k}\cdot\mathbf{x}} + v_{\mathbf{k}}^{\star}(\tau)\hat{a}_{\mathbf{k}}^{\dagger}e^{i\mathbf{k}\cdot\mathbf{x}}. \tag{2.149}$$

We want to interpret $\hat{a}_{\mathbf{k}}$ and $\hat{a}_{\mathbf{k}}^{\dagger}$ as creator and annihilation operators, so we follow the canonical quantization scheme for a bosonic field, imposing the following commutation relations

$$\begin{gathered}\left[\hat{a}_{\mathbf{k}},\hat{a}_{\mathbf{k}'}\right] = \left[\hat{a}_{\mathbf{k}}^{\dagger},\hat{a}_{\mathbf{k}'}^{\dagger}\right] = 0 \\ \left[\hat{a}_{\mathbf{k}},\hat{a}_{\mathbf{k}'}^{\dagger}\right] = \delta^3\left(\mathbf{k}-\mathbf{k}'\right),\end{gathered} \tag{2.150}$$

moreover from the action Eq. (2.140) we obtain the conjugate field:

$$\pi(\mathbf{x},\tau) = \frac{\partial\mathcal{L}}{\partial v'} = v'\left(\mathbf{x},\tau\right), \tag{2.151}$$

and the equal time commutation relation of the field and its conjugate is

$$\left[v\left(\mathbf{x},\tau\right),\pi(\mathbf{x}',\tau)\right] = i\delta^3\left(\mathbf{x}-\mathbf{x}'\right). \tag{2.152}$$

Using Eq. (2.149), the commutation relations Eqs. (2.150) and imposing that the last equality is fulfilled, we get the following normalization constraint

$$v_{\mathbf{k}}(\tau)v_{\mathbf{k}}^{\star\prime}(\tau) - v_{\mathbf{k}}^{\star}(\tau)v_{\mathbf{k}}'(\tau) = i. \tag{2.153}$$

At this point, we introduce the *Bunch-Davies vacuum*. This is the state in the Fock space which is annihilated by the operators $\hat{a}_{\mathbf{k}}$, in the limit $\tau\to-\infty$

$$\hat{a}_{\mathbf{k}}|0\rangle = 0 \qquad \forall\mathbf{k} \tag{2.154}$$

and minimizes the vacuum energy

$$E_{vac} = \int d^3x\,\langle 0|\hat{\mathscr{H}}|0\rangle, \tag{2.155}$$

where the Hamiltonian density is given by

$$\hat{\mathscr{H}} = \frac{\partial \mathcal{L}}{\partial v'} v' - \mathcal{L} \overset{\tau \to -\infty}{\to} \frac{1}{2} \left(v'^2 + (\nabla v)^2 \right). \tag{2.156}$$

We want to find the expression of $v_{\mathbf{k}}(\tau)$ in order to minimize the vacuum energy. First of all let us suppose that $v_{\mathbf{k}}(\tau) = v_k(\tau)$, substitute Eq. (2.149) in Eq. (2.155), acting with the creation and annihilation operators, using the Fourier representation of the Dirac's delta and performing the integration over the solid angle, we arrive at

$$E_{vac} = \frac{1}{(2\pi)^2} \int_0^{+\infty} dk\, k^2 \left(|v_k'|^2 + k^2 |v_k|^2 \right). \tag{2.157}$$

We use the following Ansatz

$$v_k(\tau) = r_k(\tau) e^{i\alpha_k(\tau)} \tag{2.158}$$

and we minimize the contribution given by each mode k to the energy. Inserting the last equality in Eq. (2.153) yields

$$\alpha_k' = -\frac{1}{2|r_k|^2}. \tag{2.159}$$

We obtain

$$|v_k'|^2 + k^2 |v_k|^2 = |r_k'|^2 + \frac{1}{4|r_k|^2} + k^2 |r_k|^2 \tag{2.160}$$

and minimizing with respect to $|r_k|$ and $|r_k'|$ we arrive at

$$\begin{cases} r_k' = 0 \\ r_k = \frac{1}{\sqrt{2k}} \\ \alpha_k = -k\tau + const. \end{cases} \tag{2.161}$$

In conclusion, up to an arbitrary phase

$$v_k(\tau) = \frac{1}{\sqrt{2k}} e^{-ik\tau}. \tag{2.162}$$

Using the following asymptotic relations for the Hankel functions when ν is real and for large values of $|z|$

$$H_\nu^{(1)}(z) \sim \sqrt{\frac{2\pi}{z}} e^{i\left(z-\nu\frac{\pi}{2}-\frac{\pi}{4}\right)}$$
$$H_\nu^{(2)}(z) \sim \sqrt{\frac{2\pi}{z}} e^{-i\left(z-\nu\frac{\pi}{2}-\frac{\pi}{4}\right)}, \tag{2.163}$$

we have, by comparing with the Bunch-Davies vacuum solution Eq. (2.161), with the general solution given by Eq. (2.145), that

$$A_k = \sqrt{\frac{\pi}{4}},$$
$$B_k = 0. \tag{2.164}$$

Finally:

$$v_k(\tau) = \sqrt{\frac{\pi\tau}{4}} H_\nu^{(2)}(k\tau). \tag{2.165}$$

This last equation allows us to evaluate the pGW power spectrum produced during the inflationary period.

2.5 The two point correlation function and the pGW power spectrum

In this section we will evaluate the exact analytical form of the pGW power spectrum produced during an inflationary epoch. In order to do so we have to give some preliminary definitions that are necessary to define the quantity of interest. Given a field $\phi(\mathbf{x}, \tau)$, we define the two point correlation function as the equal time expected value at different positions, where the averaging procedure can be classical or quantum mechanical

$$\xi_\phi(\mathbf{r}) = \langle \phi(\mathbf{x}, \tau)\phi(\mathbf{x}+\mathbf{r}, \tau)\rangle$$

$$\xi_\phi(\mathbf{r}) = \frac{1}{(2\pi)^6}\int d^3x\, d^3k\, d^3k'\, e^{i(\mathbf{k}+\mathbf{k}')\cdot\mathbf{x}}\, e^{i\mathbf{k}'\cdot\mathbf{r}}\phi_{\mathbf{k}}\phi_{\mathbf{k}'}$$

$$\xi_\phi(\mathbf{r}) = \frac{1}{(2\pi)^3}\int d^3k\, e^{-i\mathbf{k}\cdot\mathbf{r}}\,|\phi_{\mathbf{k}}|^2, \tag{2.166}$$

where $\phi_{\mathbf{k}}$ is the Fourier transform of the the field $\phi(\mathbf{x},\tau)$. Performing the integration over the solid angle, assuming that $\phi_{\mathbf{k}} = \phi_k$ and setting $\mathbf{r} = 0$ we get

$$\xi_\phi(0) = \int d\ln k\, \mathcal{P}_\phi(k) \tag{2.167}$$

$$\mathcal{P}_\phi(k) = \frac{k^3}{2\pi^2}|\phi_k|^2. \tag{2.168}$$

For the two polarizations of the graviton, identifying $\phi_k = u_k$ using Eq. (2.135) and Eq. (2.136)

$$\langle h_{ij}(\mathbf{x},\tau)h^{ij}(\mathbf{x},\tau)\rangle = \frac{8\lambda_p^2}{a^2}\int d\ln k\, \mathcal{P}_u(k), \tag{2.169}$$

where we recall that the angular parenthesis represent the classical or quantum mechanical expectation value. The last equation immediately implies that

$$\mathcal{P}_h(k) = \frac{4\lambda_p^2}{a^2}\frac{k^3}{\pi^2}|v_k|^2. \tag{2.170}$$

This last quantity is usually referred as the *power spectrum*.
To evaluate the power spectrum, we have to solve the evolution equation Eq. (2.144) for the canonical variable. It can be seen that the evolution has two different regimes

1. The oscillatory sub-horizon regime ($k|\tau| \gg 1$):

$$v_k'' + k^2 v_k = 0 \tag{2.171}$$

$$v_k(\tau) = C_k e^{ik\tau} + D_k e^{-ik\tau} \tag{2.172}$$

2. The super-horizon regime ($k|\tau| \ll 1$) for $\tau_{ex} < \tau < 0$, where $k|\tau_{ex}| \approx 1$

$$v_k'' - \frac{\xi''}{\xi}v_k = 0, \tag{2.173}$$

$$v_k(\tau) = A_k\,\xi(\tau) + B_k\,\xi(\tau)\int^{\tau}\frac{1}{\xi^2(\tau')}d\tau' \Rightarrow$$

$$v_k(\tau) = A_k(-\tau)^{\alpha} + B_k(-\tau)^{1-\alpha}, \tag{2.174}$$

with $\alpha \neq \frac{1}{2}$, otherwise the second term has a logarithmic behavior. Care must be taken to interpret this result. Since the solution depends on α, we can distinguish 3 different behaviors

- If $\alpha < 0$, we have a Universe in accelerated expansion and the first term of Eq. (2.174) is always prevailing for $\tau \to 0^-$. In this regime the GW amplitude $h_k \sim \frac{v_k}{\xi(\tau)}$ approaches a constant value. Using Eqs. (2.138), (2.139) and (2.143) we obtain

  $$h_k(\tau) \sim A_k + B_k(-\tau)^{1-2\alpha}. \tag{2.175}$$

  It is clear that given this property, we are interested in the spectrum outside the horizon, because the super-horizon modes stay constant also after the subsequent phases of cosmological evolution until they re-enter.

- If $0 < \alpha < 1$, the background metric describes an accelerated contraction and as $\tau \to 0^-$ we have that the leading term of Eq. (2.174) is the first if $0 < \alpha < \frac{1}{2}$, while it is the second if $\frac{1}{2} < \alpha < 1$. In both cases the amplitude of v_k outside the horizon is decreasing but the density of the kinetic energy per mode k of the tensorial perturbation, namely ah' in the action Eq. (2.137) is increasing and grows like $(-\tau)^{-\alpha}$.

- If $\alpha > 1$ the metric describes an accelerated contraction as well, and the dominant term when $\tau \to 0^-$ is always the second. However both the canonical variable ($v_k \sim (-\tau)^{1-\alpha}$) and the density of the kinetic energy per mode k ($\xi h' \sim (-\tau)^{-\alpha}$) grow. This poses a serious problem because when the modes re-enter the horizon, they can have a great energy contribution causing the *back-reaction of the tensorial perturbations* to not be negligible and can be of the same order of the other gravitational sources. As a consequence these perturbations can disrupt the homogeneity and isotropy of the initial geometry. For this reason we will not consider this inflationary scenarios from now on.

However as we have already seen while discussing all the possible inflationary scenarios, the exponent of the scale factor can be in principle any power of the conformal time.

In the super-horizon regime the Hankel function in Eq. (2.165) can be approximated as follows

$$H_\nu^{(2)}(k\tau) \overset{k|\tau|\ll 1}{\sim} p_\nu^\star (k\tau)^\nu + i q_\nu (k\tau)^{-\nu}, \tag{2.176}$$

$$p_\nu^\star = i\frac{2^{-\nu}\cos(\pi\nu)\,\Gamma(-\nu)}{\pi} + \frac{2^{-\nu}}{\Gamma(\nu+1)}, \tag{2.177}$$

$$q_\nu = \frac{2^\nu \Gamma(\nu)}{\pi}. \tag{2.178}$$

For $\nu > 0$ ($\alpha < \frac{1}{2}$) and $k|\tau| \to 0$:

$$H_\nu^{(2)}(k\tau) \sim i q_\nu (k\tau)^{-\nu}, \tag{2.179}$$

where $\Gamma(\nu)$ is the Euler's gamma function. Inserting these relations in Eq. (2.165) and taking the squared modulus we arrive at

$$|v_k|^2 \sim \left(\frac{\pi\tau}{4}\right) |q_\nu|^2 (k\tau)^{-2\nu}. \tag{2.180}$$

Going back to Eq. (2.170) we get the pGW power spectrum

$$\mathcal{P}_h(k) = \frac{\lambda_p^2}{a^2}\frac{k^2}{\pi}|q_\nu|^2 (k\tau)^{1-2\nu}. \tag{2.181}$$

Defining the pivot wavenumber

$$k_I \equiv \frac{1}{\tau_I} \tag{2.182}$$

and substituting $a = \left(-\frac{\tau}{\tau_I}\right)^\alpha$, we finally arrive at

$$\mathcal{P}_h(k) = \frac{(\lambda_p k_I)^2 |q_\nu|^2}{\pi}\left(\frac{k}{k_I}\right)^{2\alpha+2} = A_T\left(\frac{k}{k_I}\right)^{2\alpha+2}. \tag{2.183}$$

Spectra that exhibit a decreasing behavior with the wavenumber are called red-tilted, and this is a general feature for all the inflationary models based on a power inflation scale factor $\alpha < -1$. On the other hand if the inflationary period is given

by an accelerated contraction or by a superinflationary behavior $\alpha > -1$, the spectrum is blue-tilted (increasing with the wavenumber).
It is important to remark that inflationary models with $\alpha = \frac{1}{2}$, naturally appear in string theory [58–60], in the so-called pre-Big Bang scenario which we will discuss in the next Chapter. In this limit case logarithmic corrections arise in Eq. (2.183) aside from the expected tensorial index $n_T = 3$, because the asymptotic expansion Eq. (2.176) has a logarithmic behavior for $\nu = 0$.

Chapter 3

String Theory and the Pre-Big Bang scenario

In this chapter we provide only a brief orientation to the basic ingredients of string theory and the pre–Big-Bang scenario. The discussion is neither self-contained nor comprehensive and does not aim at a theoretical minimum; it simply fixes notation and highlights the few elements needed for the subsequent chapters. A more thorough study of string theory can be found in the literature [61–67] and of the pre-Big Bang scenario in [20, 68, 69].

3.1 The Bosonic String

We start by writing the action of a string propagating in a D-dimensional manifold $\mathcal{M}$. In analogy to the point particle case, where the action is proportional to the line element spanned throughout the evolution (i.e. $S = -m \int ds$), in the case of a string, its action is proportional to the world-sheet Σ area. Introducing two coordinates ξ^a, $a = 0, 1$, with $\xi^0 = \tau$, with $-\infty < \tau < +\infty$ and $\xi^1 = \sigma$ with $0 \leq \sigma \leq \pi$, the induced metric on the world-sheet h_{ab}, we have the Nambu-Goto action

$$S = \frac{1}{2\pi\alpha'} \int_\Sigma d^2\xi \sqrt{-h}, \tag{3.1}$$

where $h_{ab} = \partial_a X^\mu(\xi) \partial_b X^\nu(\xi) \eta_{\mu\nu}$, where $\eta_{\mu\nu}$ is the Minkowski metric of the D-dimensional manifold $\mathcal{M}$, also known as the "Target Space", and $2\pi\alpha' = \lambda_s^2$.

This action can be brought into the Polyakov form, which is devoid of the square root, by introducing an auxiliary field γ_{ab} that represents the intrinsic metric of the 2-dimensional manifold Σ

$$S = \frac{1}{4\pi\alpha'} \int d^2\xi \sqrt{-\gamma}\gamma^{ab}\partial_a X^\mu \partial_b X^\nu \eta_{\mu\nu}. \tag{3.2}$$

The Polyakov action is manifestly invariant under conformal transformations of the intrinsic metric $\gamma_{ab} \to e^{\psi(\xi)}\gamma_{ab}$ that does not change the combination $\sqrt{-\gamma}\gamma^{ab}$, and under diffeomorphisms, hence one can use these two invariances to fix the intrinsic world-sheet metric to be flat, i.e. $\gamma_{ab} = \eta_{ab}$. This fixing procedure however must be performed after the E.O.M. for the intrinsic metric is evaluated, namely

$$T_{ab} = \frac{2}{\sqrt{-\gamma}} \frac{\delta(\sqrt{-\gamma}\mathcal{L})}{\delta\gamma^{ab}} = 0 \tag{3.3}$$

which leads to

$$T_{ab} = \partial_a X^\mu \partial_b X^\nu \eta_{\mu\nu} - \frac{1}{2}\gamma_{ab}\gamma^{ij}\partial_i X^\mu \partial_j X^\nu \eta_{\mu\nu} = 0, \tag{3.4}$$

while varying with respect to X^μ

$$\partial_a(\sqrt{-\gamma}\gamma^{ab}\partial_b X_\mu) = 0. \tag{3.5}$$

Fixing the intrinsic metric to be flat and denoting with a dot the derivative with respect to τ and a $'$ the derivative with respect to σ, we are left with

$$\ddot{X}_\mu - X''_\mu = 0 \tag{3.6}$$

and combining the Eqs. (3.4) we obtain the so-called *Virasoro constraints*

$$\begin{aligned} \frac{1}{2}\big(T_{00} + T_{10}\big) &= \frac{1}{4}\,\eta_{\mu\nu}\left(\dot{X}^\mu + X'^\mu\right)\left(\dot{X}^\nu + X'^\nu\right) = 0, \\ \frac{1}{2}\big(T_{00} - T_{10}\big) &= \frac{1}{4}\,\eta_{\mu\nu}\left(\dot{X}^\mu - X'^\mu\right)\left(\dot{X}^\nu - X'^\nu\right) = 0. \end{aligned} \tag{3.7}$$

Introducing the light-cone coordinates

$$\begin{aligned} \xi^\pm &= \tau \pm \sigma, \qquad & \partial_\pm &= \partial_\tau \pm \partial_\sigma, \\ \tau &= \frac{1}{2}(\xi^+ + \xi^-), & \sigma &= \frac{1}{2}(\xi^+ - \xi^-), \end{aligned} \tag{3.8}$$

we can rewrite the 2-dimensional wave equation and the Virasoro constraints as

$$\begin{aligned} \partial_+\partial_- X^\mu &= 0, \\ T_{++} = \partial_+ X^\mu \partial_+ X_\mu &= 0, \\ T_{--} = \partial_- X^\mu \partial_- X_\mu &= 0, \end{aligned} \tag{3.9}$$

where the solution to the wave equation can always be written as a sum of left-moving and right-moving waves,

$$X^\mu(\xi) = X^\mu_L(\xi^+) + X^\mu_R(\xi^-). \tag{3.10}$$

In this thesis we will focus on the closed string bosonic sector, so, to this aim, we are going to study strings subject to the following boundary condition $X^\mu(\tau, \sigma) = X^\mu(\tau, \sigma + \pi)$.

3.1.1 The closed Bosonic String quantization

The solution for the right moving and left moving waves with periodic boundary conditions expanded in Fourier modes is given by

$$\begin{aligned} X^\mu_R(\xi^-) &= \frac{x^\mu_0}{2} + \frac{\alpha'}{2}\, p^\mu\, \xi^- + i\sqrt{\frac{\alpha'}{2}} \sum_{n\neq 0} \frac{\alpha^\mu_n}{n}\, e^{-2in\xi^-}, \\ X^\mu_L(\xi^+) &= \frac{x^\mu_0}{2} + \frac{\alpha'}{2}\, p^\mu\, \xi^+ + i\sqrt{\frac{\alpha'}{2}} \sum_{n\neq 0} \frac{\tilde{\alpha}^\mu_n}{n}\, e^{-2in\xi^+}, \end{aligned} \tag{3.11}$$

where x^μ_0 and p^μ represents the initial position and the momentum, respectively, and $\alpha^\mu_{-n} = (\alpha^\mu_n)^\star$, $\tilde{\alpha}^\mu_{-n} = (\tilde{\alpha}^\mu_n)^\star$ for reality conditions of the coordinates X^μ. The general solution is thus given by the sum of the latter, namely

$$X^\mu(\tau, \sigma) = x^\mu_0 + \alpha' p^\mu \tau + i\sqrt{\frac{\alpha'}{2}} \sum_{n\neq 0} \frac{1}{n} (\alpha^\mu_n e^{2i\,n\sigma} + \tilde{\alpha}^\mu_n e^{-2i\,n\sigma}) e^{-2in\tau}. \tag{3.12}$$

Now we impose the Virasoro constraints and in order to do so we introduce the following functionals

$$\begin{aligned} L_m &= \frac{1}{4\pi\alpha'}\int_0^\pi d\sigma\, T_{--}\, e^{2im(\tau-\sigma)}, \\ \tilde{L}_m &= \frac{1}{4\pi\alpha'}\int_0^\pi d\sigma\, T_{++}\, e^{2im(\tau+\sigma)}, \end{aligned} \tag{3.13}$$

where again for reality conditions we have $L_m^\star = L_{-m}$ and $\tilde{L}_m^\star = \tilde{L}_{-m}$. Introducing $\alpha_0^\mu = p^\mu\sqrt{\alpha'/2}$ it easy to show using the orthonormality condition of the base $e^{2in\sigma}/\sqrt{\pi}$ in $L^2[0,\pi]$ that the Virasoro functionals take the following form

$$L_m = \frac{1}{2}\sum_{n=-\infty}^{n=+\infty}\alpha_{m-n}^\mu\alpha_{n\mu}, \qquad \tilde{L}_m = \frac{1}{2}\sum_{n=-\infty}^{n=+\infty}\tilde{\alpha}_{m-n}^\mu\tilde{\alpha}_{n\mu}, \tag{3.14}$$

with the Virasoro constraints imposed by the conditions $L_m = \tilde{L}_m = 0$.
We proceed now to present the results obtained in the canonical quantization scheme, however we mention that there are several ways to quantize the string (e.g. BRST, light-cone, covariant, ...). As usual the Fourier coefficients become creation and annihilation operators (or equivalently we impose the commutation relations at equal times for the fields X^μ and their conjugate momenta $\Pi^\mu = \dot{X}^\mu/(2\pi\alpha'))$, such that $[\Pi^\mu(\tau,\sigma'), X^\nu(\tau,\sigma),] = i\eta^{\mu\nu}\delta(\sigma-\sigma')$ and all other commutators are 0. Introducing the normalized operators $\alpha_m^\mu = \sqrt{m}a_m^\mu$, $\alpha_{-m}^\mu = (\alpha_m^\mu)^\dagger$, and the same for the tilde operators, we have

$$[\alpha_{-n}^\mu, \alpha_m^\nu] = [\tilde{\alpha}_{-n}^\mu, \tilde{\alpha}_m^\nu] = \sqrt{m}\eta^{\mu\nu}\delta_{n+m,0}, \qquad [a_n^{\mu\dagger}, a_m^\nu] = [\tilde{a}_n^{\mu\dagger}, \tilde{a}_m^\nu] = \eta^{\mu\nu}\delta_{nm},$$

$$[P_{\rm CM}^\mu, X_{\rm CM}^\mu] = i\eta^{\mu\nu}, \tag{3.15}$$

where $X_{\rm CM}^\mu = 1/\pi\int_0^\pi d\sigma X^\mu(\tau,\sigma)$ and the same for $P_{\rm CM}^\mu$. The vacuum state of the Fock space is defined as the eigenstate of the momentum operator $|0,p\rangle$ which is annihilated by all annihilation operators

$$\alpha_n^\mu|0,p\rangle = \tilde{\alpha}_n^\mu|0,p\rangle = 0, \qquad \forall n > 0, \tag{3.16}$$

while a generic state of the Fock space is generated by acting with creation operators

$$|n_1, m_1, \ldots, p\rangle = (\alpha_{-n}^\mu)^{n_1}(\alpha_{-m}^\mu)^{m_2}\ldots|0,p\rangle, \tag{3.17}$$

however, there are ghosts state such as $a_m^0|0,p\rangle$ that must be removed via the quantum Virasoro constraint, namely we consider only the subset of the Fock space such that $L_m|\Psi\rangle = \tilde{L}_m|\Psi\rangle = 0$. Using the usual normal ordering prescription, where the annihilation operators are moved to the right, $L_m = \frac{1}{2}\sum_n : \alpha^\mu_{m-n}\alpha_{n\mu} :$ we have that ordering ambiguities arise only for L_0 ($\tilde{L}_0$) because of the non-vanishing commutator, so we impose $(L_0 - \delta)|\Psi\rangle = (\tilde{L}_0 - \delta)|\Psi\rangle = 0$, where δ is determined by the normal ordering.

We assume the light-cone also in the target space manifold, $X^\mu = \{X^+, X^-, X^i\}$, with $i = 1, \ldots, D-2$ and $X^\pm = 1/\sqrt{2}(X^0 \pm X^{D-1})$. In this way the Virasoro constraints can be linearized and we use the residual conformal gauge to assume that the motion in the positive direction is translational, i.e. $X^+ = x_0^+ + 2\alpha' p^+ \tau$. In this way all the $a_m^+ = 0 = \tilde{a}_m^+$, $m \neq 0$ and from the Virasoro constraints we can express all the a_m^- ($\tilde{a}_m^-$) in terms of the spatial modes a_m^i ($\tilde{a}_m^i$). In this way we are left with $D-2$ transverse degrees of freedom.

Finally we note that the Hamiltonian is vanishing from the classical theory $H = \int_0^\pi d\sigma \dot{X}^\mu \Pi_\mu - L = 1/(2\pi\alpha') \int_0^\pi d\sigma \, (T_{++} + T_{--}) = 2(L_0 + \tilde{L}_0) = 0$, so we have to impose the Hamiltonian constraint $(L_0 + \tilde{L}_0)|\Psi\rangle = 0$ and $(L_0 - \tilde{L}_0)|\Psi\rangle = 0$. From Eq. (3.14), in the light-cone gauge and with the normal ordering, (we show the calculation only for the right moving modes)[1]

$$L_0 = \frac{1}{2}\left(\alpha_0^\mu \alpha_{0\mu} + \sum_{n\neq 0} : \alpha^\mu_{-n}\alpha_{n\mu} :\right) = \frac{\alpha'}{4} p_\mu p^\mu - N - \frac{D-2}{2}\sum_{n>0} n, \tag{3.18}$$

where we defined as usual the number operator as $N \equiv \sum_{n>0} \alpha_n^i \alpha^i_{-n}$, and the last term is given by the commutation relation of the annihilation and creation operators. We now use an exponential regulator to express the last term

$$\begin{aligned}
\lim_{\epsilon\to 0}\sum_{n>0} n e^{-\epsilon n} &= -\lim_{\epsilon\to 0}\left(\frac{d}{d\epsilon}\sum_{n>0} e^{-\epsilon n}\right) = -\lim_{\epsilon\to 0}\frac{d}{d\epsilon}\left(1 - e^{-\epsilon}\right)^{-1} \\
&= -\lim_{\epsilon\to 0}\frac{d}{d\epsilon}\frac{1}{\epsilon}\left(1 - \frac{\epsilon}{2} + \frac{\epsilon^2}{6} + \mathcal{O}(\epsilon^3)\right)^{-1} \\
&= -\lim_{\epsilon\to 0}\frac{d}{d\epsilon}\frac{1}{\epsilon}\left(1 + \frac{\epsilon}{2} + \frac{\epsilon^2}{12} + \mathcal{O}(\epsilon^3)\right) \\
&= \lim_{\epsilon\to 0}\left(\frac{1}{\epsilon^2} - \frac{1}{12} + \mathcal{O}(\epsilon)\right),
\end{aligned} \tag{3.19}$$

[1] Recall that in the light-cone gauge the line element is $ds^2 = dX^+ dX^- - dX^i dX^i$, hence $\alpha^\mu_{-n}\alpha_{n\mu} = \alpha^+_{-n}\alpha^-_n - \alpha^i_{-n}\alpha^i_n$.

hence by absorbing the infinite part in δ we have

$$\begin{aligned} L_0 &= \frac{\alpha'}{4} p_\mu p^\mu - \left(N - \frac{D-2}{24} \right), \\ \tilde{L}_0 &= \frac{\alpha'}{4} p_\mu p^\mu - \left(\tilde{N} - \frac{D-2}{24} \right), \end{aligned} \tag{3.20}$$

where $\tilde{N} \equiv \sum_{n>0} \tilde{\alpha}^i_n \tilde{\alpha}^i_{-n}$, and from $(L_0 - \tilde{L}_0)|\Psi\rangle = 0$ the level matching condition $N|\Psi\rangle = \tilde{N}|\Psi\rangle$. Hence we can write the Hamiltonian constraint ($p_\mu p^\mu = M^2$) as

$$H = 2(L_0 + \tilde{L}_0) = \frac{\alpha'}{2} M^2 - N - \tilde{N} + \frac{D-2}{12} = 0, \tag{3.21}$$

which leads to the mass spectrum of the theory

$$M^2 = \frac{2}{\alpha'} (N + \tilde{N} - \frac{D-2}{12}). \tag{3.22}$$

Since the number operator is semi positive, we have that the vacuum of the theory $|p, 0, \tilde{0}\rangle$ is tachyonic signaling quantum instabilities (although they are resolved in superstring theory) and the first excited state (taking into account the level matching condition) is $|p, 1, \tilde{1}\rangle = \alpha^\mu_{-1} \tilde{\alpha}^\nu_{-1} |p, 0, \tilde{0}\rangle$, hence a tensor state. Taking into account the Virasoro constraint generated by L_1 ($\tilde{L}_1$) and contracting with the polarization tensor $\epsilon_{\mu\nu}$ we have

$$\begin{aligned} 0 = L_1|p, 1, \tilde{1}\rangle &= \frac{1}{2} \epsilon_{\mu\nu} \sum_{n=-\infty}^{n=+\infty} : \alpha^\gamma_{1-n} \alpha_{n\gamma} : \, \alpha^\mu_{-1} \tilde{\alpha}^\nu_{-1} |p, 0, \tilde{0}\rangle \\ &= \tilde{\alpha}^\nu_{-1} \alpha^\gamma_0 \epsilon_{\mu\nu} \, \alpha_{1\gamma} \alpha^\mu_{-1} |p, 0, \tilde{0}\rangle = \tilde{\alpha}^\nu_{-1} \alpha^\gamma_0 \epsilon_{\mu\nu} [\alpha_{1\gamma}, \alpha^\mu_{-1}] |p, 0, \tilde{0}\rangle \\ &= \tilde{\alpha}^\nu_{-1} \alpha^\mu_0 \epsilon_{\mu\nu} |p, 0, \tilde{0}\rangle = \sqrt{\frac{\alpha'}{2}} \tilde{\alpha}^\nu_{-1} p^\mu \epsilon_{\mu\nu} |p, 0, \tilde{0}\rangle = 0, \end{aligned} \tag{3.23}$$

hence a transverse momentum to the polarization tensor $p_\mu \epsilon^{\mu\nu} = 0$. Since we have $D-2$ space-like degrees of freedom, this corresponds to a massless state in the tensor representation of the so-called *little group* of $SO(D-2)$. From the mass spectrum Eq. (3.22) (since $N = \tilde{N} = 1$) we must fix $D = D_c = 26$ (in superstring theory due to the introduction of world-sheet supersymmetry, this number is reduced to $D_c = 10$).

Finally the particle content of the theory can be extracted using standard irreducible representation of $SO(D-2)$

$$\epsilon_{ij} = h_{ij} + B_{ij} + \frac{\phi}{D-2} \delta_{ij}, \tag{3.24}$$

hence a traceless symmetric field $h_{\mu\nu}$, which is the graviton, an antisymmetric tensor field $B_{\mu\nu}$, which is the Kalb-Ramond and the trace part ϕ which is the Dilaton. Even though the result has been derived only in the bosonic string case, the closed string massless spectrum of all formulations of (super)-string theory contain this massless multiplet, which as we are going to see give rise to a modified theory of gravity.

3.2 Massless multiplet effective action

Let us consider a string propagating in a general background generated by the above mentioned fields, we have the following sigma model action

$$S = -\frac{1}{4\pi\alpha'}\int d^2\xi\sqrt{-\gamma}\Big(\gamma^{ab}\partial_a X^\mu \partial_b X^\nu g_{\mu\nu}(X) + \epsilon^{ab}\partial_a X^\mu \partial_b X^\nu B_{\mu\nu}(X) + \frac{\alpha'}{2}\,{}^{(2)}R\phi(X)\Big), \tag{3.25}$$

where γ^{ab} is the world sheet metric, ${}^{(2)}R$ is the 2-d Ricci scalar associated to the metric and ϵ^{ab} is the Levi-Civita symbol. Since the theory must retain the Weyl invariance as already noted before, we have to require the vanishing of the beta functions which fix the allowed backgrounds in which the conformal invariance is preserved[2], which at one-loop are [46]

$$\begin{aligned}
\beta_{\mu\nu}(g) &= \alpha' R_{\mu\nu} + \alpha'\nabla_\mu\nabla_\nu\phi - \frac{\alpha'}{4}H_{\mu\lambda\kappa}H_\nu{}^{\lambda\kappa} + \mathcal{O}(\alpha'^2) = 0,\\
\beta_{\mu\nu}(B) &= -\frac{\alpha'}{2}\nabla^\lambda\phi\, H_{\lambda\mu\nu} + \frac{\alpha'}{2}\nabla^\lambda H_{\lambda\mu\nu} + \mathcal{O}(\alpha'^2) = 0,\\
\beta(\phi) &= -\alpha' R - 2\alpha'\nabla^2\phi + \alpha'\nabla_\mu\phi\nabla^\mu\phi + \frac{\alpha'}{12}H_{\mu\nu\lambda}H^{\mu\nu\lambda} + \mathcal{O}(\alpha'^2) = c,
\end{aligned} \tag{3.26}$$

where $H_{\mu\nu\lambda} = 3\nabla_{[\mu}B_{\nu\lambda]}$ is the Kalb-Ramond field strength and $R_{\mu\nu}$ is the Ricci tensor associated to $g_{\mu\nu}$ and c is a constant ($c \sim (D - D_c)$) . These equations can be obtained by the following effective action which describes the evolution of the graviton, the dilaton and the Kalb-Ramond in the so-called string frame (S-frame), where the dilaton is not minimally coupled to the metric (assuming

[2]Conformal invariance fixes the background fields configuration

$D = D_c$)

$$S_{\text{eff}} = -\frac{1}{2\lambda_s^{D-2}} \int d^D x \sqrt{-g} e^{-\phi} (R + (\nabla\phi)^2 - \frac{1}{12} H_{\mu\nu\alpha} H^{\mu\nu\alpha}) + \mathcal{O}(\alpha'). \tag{3.27}$$

In the context of string theory we have two kinds of perturbative expansions, one is the higher-curvature expansion, namely α' expansion where additional terms arise from higher perturbation order in the bosonic string sigma model, (e.g. Eq. (8.1)), the other is in increasing complexity of the world-sheet topology, the so-called Genus expansion which is expressed in term of the string coupling $g_s^2 = e^{\langle\phi\rangle}$.
We conclude this section by remarking that upon a conformal rescaling of the metric $g^S_{\mu\nu} = g^E_{\mu\nu} \left(\frac{\lambda_s}{\lambda_p}\right)^2 e^{\frac{2}{D-2}\phi}$, the action takes the Einstein-frame form

$$S^E_{\text{eff}} = -\frac{1}{2\lambda_p^{D-2}} \int d^D x \sqrt{-g^E} \left(R^E - \frac{1}{D-2} (\nabla\phi)^2 - \frac{1}{12} e^{-\frac{4}{D-2}\phi} H_E^2 \right), \tag{3.28}$$

where we have defined $H^E_{\mu\nu\lambda} = \left(\frac{\lambda_p}{\lambda_s}\right)^2 H_{\mu\nu\lambda}$.

3.3 Compactification, Momentum Quantization, and T-Duality

As discussed in the previous section, quantum consistency of bosonic string theory requires a critical spacetime dimension. This raises the question of how extra spatial dimensions beyond those observed can be reconciled with phenomenology. A natural resolution is to assume that these extra dimensions are compact and small, such that they remain unobservable at accessible energy scales.

As a simple example, let us consider a target-space of the form $\mathcal{M}^{D-1} \times S^1$, that is, a $(D-1)$-dimensional Minkowski spacetime times a circle of radius R. Considering a closed bosonic string propagating along S^1, the momentum along the compact dimension is quantized as

$$p = \frac{n}{R}, \qquad n \in \mathbb{Z}.$$

In addition, the string can wrap the compact circle an integer number of times, characterized by the winding number $m \in \mathbb{Z}$. The general solution of the equations

of motion for the string coordinate Y along the compact direction is then

$$Y(\tau,\sigma) = y_0 + 2\alpha' \frac{n}{R}\,\tau + 2mR\,\sigma + i\sqrt{\frac{\alpha'}{2}} \sum_{n\neq 0} \frac{1}{n} \left(\alpha_n^\mu e^{2in\sigma} + \tilde{\alpha}_n^\mu e^{-2in\sigma}\right) e^{-2in\tau}. \quad (3.29)$$

It is convenient to introduce the left- and right-moving momenta

$$p_L = \frac{1}{2}\left(\frac{n}{R} + \frac{mR}{\alpha'}\right), \qquad p_R = \frac{1}{2}\left(\frac{n}{R} - \frac{mR}{\alpha'}\right), \quad (3.30)$$

so that the solution (3.29) can be recast in the form

$$Y(\tau,\sigma) = y_0 + 2\alpha' p_L(\tau+\sigma) + 2\alpha' p_R(\tau-\sigma) + \text{ oscillations}. \quad (3.31)$$

The Virasoro constraints in $D = 26$ dimensions, after separating the internal momenta p_L, p_R from the external momenta p_μ, read

$$L_0 = \frac{\alpha'}{4}M^2 - \alpha' p_R^2 - N + 1 = 0, \qquad \tilde{L}_0 = \frac{\alpha'}{4}M^2 - \alpha' p_L^2 - \tilde{N} + 1 = 0. \quad (3.32)$$

From their sum we obtain the generalized mass-shell condition

$$\frac{\alpha'}{2}M^2 = \frac{\alpha'}{2}\left(\frac{n^2}{R^2} + m^2\frac{R^2}{\alpha'^2}\right) + N + \tilde{N} - 2, \quad (3.33)$$

while from their difference we obtain the level-matching condition

$$N - \tilde{N} + nm = 0. \quad (3.34)$$

The resulting mass spectrum depends on the internal quantum numbers (n, m), and is manifestly invariant under the T-duality transformation

$$R \longleftrightarrow \frac{\alpha'}{R}, \qquad n \longleftrightarrow m. \quad (3.35)$$

This symmetry exchanges momentum and winding excitations, while leaving the physical mass spectrum unchanged.

This symmetry will be later discussed in cosmological backgrounds where it will be identified in the *Scale Factor Duality* (SFD) (Z_2^{D-1} symmetry of the scale factors) and to $O(d,d)$ symmetry in the presence of non-trivial Kalb-Ramond field.

As a final remark we notice that when $R/\alpha' \gg 1$ the winding modes become heavy

and hard to excite, while the opposite is true in the opposite limit $R/\alpha' \ll 1$, the momentum modes become irrelevant. The duality predicts the existence of a self-dual radius, namely $R \sim \sqrt{\alpha'}$ which is the minimum allowed extension for the compact dimension.

3.4 S-duality

In this section we will briefly mention S-duality which is a strong weak coupling duality that exchanges $g_s \to g_s^{-1}$. As a simple example we are going to consider the case of Heterotic superstrings in critical spatial dimensions $d = 9$. The effective action of the theory compactified on $\mathcal{M}_4 \times T^6$, with trivial moduli, Kaluza-Klein vectors and scalars arising from the metric, with a $4D$ Kalb-Ramond [3] and at zero order in the α' expansion (neglecting the gauge fields of $SO(32)$ or $E_8 \times E_8$) and in the Einstein-frame reads

$$S = -\frac{1}{2}\int d^4x\,\sqrt{-g}\Big[R - \frac{1}{2}(\nabla\phi)^2 - \frac{1}{12}e^{-2\phi}H_{\mu\nu\alpha}H^{\mu\nu\alpha}\Big]. \tag{3.36}$$

$H_{\mu\nu\alpha}$ can be expressed in the formalism of differential forms as $H = dB_2$, with the Bianchi identity $d^2B_2 = dH = 0$. We promote the dynamical field to be $H_{\mu\nu\alpha}$ and enforce the Bianchi identity

$$\frac{1}{3!}\eta^{\mu\nu\alpha\beta}\nabla_\mu H_{\nu\alpha\beta} = 0, \tag{3.37}$$

where $\eta^{\mu\nu\alpha\beta} = \frac{\epsilon^{\mu\nu\alpha\beta}}{\sqrt{-g}}$ is the Levi-Civita tensor, by introducing a lagrange multiplier σ, we can ensure that the Bianchi identity is fulfilled by adding to the lagrangian the term

$$\begin{aligned} S_\sigma &= -\frac{1}{2}\int d^4x\sqrt{-g}\sigma\Big[\frac{1}{3!}\eta^{\mu\nu\alpha\beta}\nabla_\mu H_{\nu\alpha\beta}\Big] \\ &= -\frac{1}{2}\int d^4x\sqrt{-g}\Big[-\frac{1}{3!}\eta^{\mu\nu\alpha\beta}H_{\nu\alpha\beta}\nabla_\mu\sigma\Big], \end{aligned} \tag{3.38}$$

where in the last line we used integration by parts. Varying with respect to $H_{\mu\nu\alpha}$ the action $S + S_\sigma$, we find $H_{\mu\nu\alpha} = -e^{2\phi}\eta_{\mu\nu\alpha\beta}\nabla^\beta\sigma$, where σ is the axionic dual of the Kalb-Ramond. Finally inserting this relation into the action $S + S_\sigma$ we find that

$$S = -\frac{1}{2}\int d^4x\,\sqrt{-g}\Big[R - \frac{1}{2}(\nabla\phi)^2 - \frac{1}{2}e^{2\phi}(\nabla\sigma)^2\Big]. \tag{3.39}$$

[3] Assuming a dependence for the K-R only on the "external coordinate" x, we are imposing triviality on 6 vectors $B_{\mu a}(x)$ with $a = 4\ldots9$ and 15 scalars $B_{ab}(x)$.

We notice that the action Eq (3.39) has an $SL(2,R)/U(1)$ structure, and so the two fields can be combined into a single complex degree of freedom $\lambda = \sigma + ie^{-\phi}$ with the $SL(2,R)$ ($SL(2,Z)$ quantum mechanically) symmetry acting like $\lambda \to \frac{a\lambda+b}{c\lambda+d}$ with $ad - bc = 1$. In this case the action takes the simpler form

$$S = -\frac{1}{2}\int d^4x\,\sqrt{-g}\Big[R - \frac{1}{2\mathrm{Im}(\lambda)^2}\nabla_\mu\lambda\nabla^\mu\bar{\lambda}\Big] \tag{3.40}$$

Starting with a configuration with constant axion $\sigma = \sigma_i$ this symmetry allows a weak-strong coupling duality for the peculiar values $\sigma_i = -d/c$, and $c^2 = 1$ with $e^\phi \to e^{-\phi}$. In general however we have that under the $SL(2,R)$ group a theory with small string coupling $e^\phi \ll 1$ can be transformed into a theory with large coupling $e^\phi \sim 1$.

3.5 The Pre-Big Bang scenario

As we have previously discussed the primordial cosmological problems may be solved by a period of *slow-roll* inflation, but we also have shown that other alternatives are possible with superinflation and accelerated contraction. There are different possible physical mechanisms able to produce periods of superinflation such as phantom scalar models ($w < -1$) in GR, and accelerated contraction driven by stiff fluids $w = 1$ or Ekpyrotic model. The pre-Big Bang model is able to bridge in some sense between those two pictures, since the primordial phase can be seen as a superinflationary model in the string frame (S-frame), and an accelerated contraction in the Einstein frame (E-frame).
The Pre Big-Bang scenario starts with the assumption that the universe emerges from the perturbative vacuum of string theory, hence with vanishing coupling $\phi \to -\infty$ and curvature. In this regime string theory predicts the existence of a massless multiplet of fields $g_{\mu\nu}$, $B_{\mu\nu}$, and the dilaton field. Moreover it assumes a trivial Kalb-Ramond field strength $H_{\mu\nu\alpha} = 0$, which in the case of the 4-D theory corresponds to a constant axion. In this context the action of the theory is simply given by the gravi-dilaton sector

$$S = -\frac{1}{2\lambda_s^{d-1}} \int d^{d+1}x\sqrt{-g}e^{-\phi}(R + (\nabla\phi)^2). \tag{3.41}$$

Assuming a Bianchi I background $g_{\mu\nu} = \mathrm{diag}(N^2, a_i^2\delta_{ij})$, where $N(t)$ is the lapse function, and we have a different scale factor $a_i(t)$ for every spatial dimension and there is no sum over the repeated indices. Introducing the shifted dilaton $\bar{\phi} = \phi - \sum_{i=1}^{d} \ln(a_i)$ we have that the evolution of the fields is governed by the following equations (the lapse being fixed to 1 by a gauge choice)

$$\dot{\bar{\phi}}^2 - \sum_i H_i^2 = 0, \tag{3.42}$$

$$\dot{H}_i - H_i\dot{\bar{\phi}} = 0, \tag{3.43}$$

$$2\ddot{\bar{\phi}} - \dot{\bar{\phi}}^2 - \sum_i H_i^2 = 0. \tag{3.44}$$

The theory possess a time reversal symmetry $t \to -t$ under which the equation of motion are invariant and an additional Z_2^d scale factor duality $H_i \to -H_i$ (or equivalently $a_i \to a_i^{-1}$) and $\bar{\phi} \to \bar{\phi}$ [70, 71]. This implies that given a solution

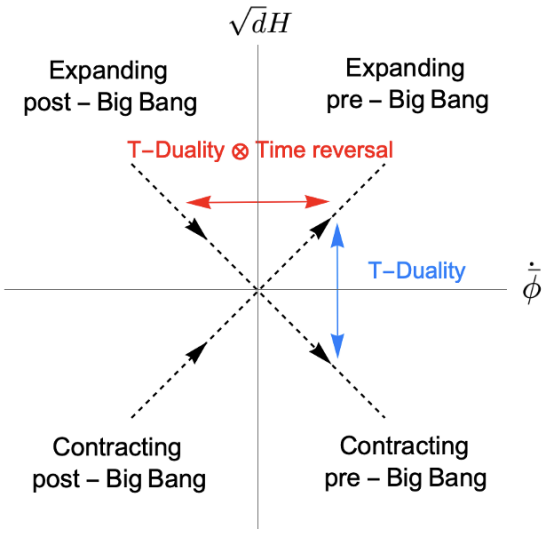

FIGURE 3.1: Graphical schematics of duality related solutions with d-isotropic spatial dimensions

$\{H_i(t), \dot{\bar{\phi}}(t)\}$ we have a family of 4 solutions related by the $Z_2^d \otimes$Time Reversal symmetry, namely under time reversal $\{-H_i(-t), -\dot{\bar{\phi}}(-t)\}$, under Z_2^d $\{-H_i(t), \bar{\phi}(t)\}$ and under the combination of the two $\{H_i(-t), -\dot{\bar{\phi}}(-t)\}$. This is a crucial difference between the string theory Gravi-Dilaton theory and GR, where the Z_2^d symmetry is absent. It is important to notice that in the expanding pre-Big Bang phase both the curvature and the dilaton grow, hence approaching a geometric singularity and the breakdown of the genus 0 approximation of the effective theory, hence higher-curvature corrections (α') and dilaton coupling must be included to correctly describe the transition between the first branch and its $Z_2^d \otimes$ Time Reversal counterpart that are disconnected at the tree-level.

To quantitatively illustrate the model we assume an FLRW geometry. In this case the solution to the Eqs. (3.42), (3.43) and (3.44) are (in the synchronous gauge)

$$\begin{aligned} a_\pm(t) &= t^{\pm\frac{1}{\sqrt{d}}}, \qquad H_\pm(t) = \pm\frac{1}{t\sqrt{d}} \qquad \bar{\phi}(t) = -\ln t, \qquad t > 0, \\ a_\pm(-t) &= (-t)^{\pm\frac{1}{\sqrt{d}}}, \quad H_\pm(t) = \pm\frac{1}{t\sqrt{d}} \quad \bar{\phi}(-t) = -\ln(-t), \qquad t < 0, \end{aligned} \tag{3.45}$$

and hence the dilaton is given by

$$\phi_\pm(\pm t) = \bar{\phi}(\pm t) + d\ln\big(a_\pm(\pm t)\big) = \big(\pm\sqrt{d} - 1\big)\ln(\pm t).$$

It can be easily seen that the asymptotic trivial string vacuum is reached in the asymptotic past $t \to -\infty$ by the solution $a_-(-t)$, which starts with vanishing

curvature $H \to 0$ and string curvature $e^{\phi} = g_s \to 0$ and they both grow until they reach a regime where non-perturbative effects become relevant both for the α' expansion and the coupling expansion. As we shall see in Chapter 4, the inclusion of a non-perturbative dilaton potential and all order α' correction is able to trigger a bouncing transition with a frozen dilaton and a constant (or decreasing) curvature. This primordial phase of evolution from the string perturbative vacuum is called Dilaton Driven Inflation phase (DDI) and may be followed as we are going to present in the following Chapters by an almost instant bouncing transition or by a period of constant curvature and linear dilaton called the String-phase. However this is a superinflationary solution in the S-frame but it corresponds to an accelerated contraction in the string frame , indeed by applying the conformal rescaling of the metric $g^S_{\mu\nu} = g^E_{\mu\nu} e^{\frac{2}{d-1}\phi}$, we have that the Einstein time is related to the string time by

$$N_E dt_E = N_S dt_S e^{-\frac{1}{d-1}\phi}, \tag{3.46}$$

hence in the synchronous gauge $t_S = t_E^{\frac{d-1}{d+\sqrt{d}}}$, while the scale factor becomes

$$a_E(t_E) = (-t_E)^{\frac{1}{d}}, \qquad H_E(t_E) = \frac{1}{d\, t_E}, \qquad \frac{d^2 a_E}{dt_E^2} < 0, \qquad t_E < 0, \tag{3.47}$$

thus an accelerated contraction.
We are now going to present the most general solution in a Bianchi I geometry with 3 isotropic expanding dimensions and n contracting ones, $g_{\mu\nu} = \mathrm{diag}(1, -a^2\delta_{ij}, -b_m^2\delta_{mn})$. Parametrizing the solution as $a(t) \sim (-t)^{\beta_0}$ and $b_i(t) \sim (-t)^{\beta_m}$ the solution is [68] (expressed in conformal time $dt = a d\tau$)

$$\begin{aligned} a &= \left(-\frac{\tau}{\tau_1}\right)^{\frac{\beta_0}{1-\beta_0}}, & b_m &= \left(-\frac{\tau}{\tau_1}\right)^{\frac{\beta_m}{1-\beta_0}}, \\ \phi &= \frac{\sum_m \beta_m + 3\beta_0 - 1}{1-\beta_0} \ln\left(-\frac{\tau}{\tau_1}\right), & 3\beta_0^2 &+ \sum_m \beta_m^2 = 1, \end{aligned} \tag{3.48}$$

where τ_1 is a reference time which may correspond to the end of the DDI phase.

3.5.1 Pre-Big Bang perturbation theory

We are now going to present the main results of perturbation theory in the pre-Big Bang string model. A preliminary remark is due, we have seen that the behavior of the background evolution depends on which frame one chooses to work with,

however observables are frame invariant, hence the spectrum of both tensor and scalar perturbations can be equivalently computed in both frames and they lead to the same result.

We start by computing tensor perturbations $h_{\mu\nu}$, assuming as in [68] that they are independent of the n internal coordinates. At linear order we have that the perturbations of the metric in the internal and external space, decouple, hence we can focus on the $1+3$ expanding subspace. The perturbed action after integrating out the internal dimensions $\int d^n y\sqrt{-g_n} = V_n \prod_m b_m$ is [68, 69, 72, 73]

$$\delta^{(2)}S = \frac{1}{2}\int d^3x d\tau a^2 \prod_m b_m e^{-\phi}(h'^2 + h\nabla^2 h). \tag{3.49}$$

From the standard theory of perturbations presented in the previous Chapter, we have that the pump-field is $\xi_h \sim a e^{-\phi/2}\prod_m b_m^{1/2}$, which is the same in both the S-frame and E-frame. We notice that the pump field can be expressed in a neat form as $\xi_h \sim a g_4^{-1}$, where $g_4 = e^{\bar{\phi}_4/2} = e^{1/2(\phi - \sum_m \ln b_m)}$ is the 4-dimensional string coupling. In the DDI phase the pump-field scales as a power of the conformal time hence the standard results can be readily applied. From Eqs. (3.48) we have that $\xi_h \sim (-\tau)^{\alpha_h}$ with

$$\alpha_h = \frac{1}{1-\beta_0}\Big[\beta_0 + \sum_i \frac{\beta_i}{2} - \frac{1}{2}(\sum_i \beta_i + 3\beta_0 - 1)\Big] = \frac{1}{2}, \tag{3.50}$$

regardless of the dynamics of the internal and external dimensions and of the dilaton. As a consequence the resulting power spectrum is (up to logarithmic corrections)

$$\mathcal{P}_h \sim \left(\frac{H_1}{M_p}\right)^2 \left(\frac{k}{k_1}\right)^3 \tag{3.51}$$

where $H_1 = k_1/a_1^E$. The same result applies also for the dilaton perturbations hence the dilaton cannot be responsible for the CMB anisotropies observed, both in amplitude and spectral index, which is $n_s \approx 0.9649$ [38].

However there is another field that is responsible for the CMB anisotropies in the PBB, the Kalb-Ramond axion. We have previosly seen that the Kalb-Ramond field has an axionic dual that in the string frame can be expressed as

$$H_{\mu\nu\alpha} = \frac{e^{\phi}}{\sqrt{-g}}\epsilon_{\mu\nu\alpha\beta}\nabla^\beta \sigma. \tag{3.52}$$

By perturbing the action up to the second order in $\delta\sigma = \chi$, integrating out the internal volume, and recalling that for our background $\sigma = \text{const}$, we have

$$\delta^{(2)} S_\sigma = \frac{1}{4} \int d^3x d\tau a^2 e^\phi \prod_m b_m^{-1} (\chi'^2 + \chi \nabla^2 \chi), \tag{3.53}$$

and the pump field is $\xi_\sigma \sim a e^{\phi/2} \prod_m b_m^{-1/2} \sim a g_4$. There is a duality relation between the behaviors of the two pump fields which is a consequence of S-duality symmetry, as a matter of fact the two differ from a weak-strong coupling inversion $g_4 \to 1/g_4$ [74]. Given the pump field, the pump field scales as $\xi_\sigma \sim (-\tau)^{\alpha_\sigma}$ where $\alpha_\sigma = \frac{5\beta_0 - 1}{2(1-\beta_0)}$ spectral index of the axion two point correlation function is given by

$$n_s = 3 + 2\alpha_\sigma = 2\frac{1+\beta_0}{1-\beta_0}, \tag{3.54}$$

so able to generate the desired observed spectrum. It is interesting to notice that assuming that the $n = 6$ internal dimensions are contracting with the duality relation $b_m = a^{-1}$, so $\beta_m \to -\beta_0$, we have that the Kasner-like condition Eqs. (3.48), gives $\beta_0 = -1/3$, hence $n_s = 1$, so a perfect Harrison–Zel'dovich flat spectrum.
In the context of CMB anisotropies, the axion spectrum is typically dominant and can act as a source of adiabatic curvature perturbations through the curvaton mechanism. After the bouncing transition, the axion field undergoes coherent oscillations around the minimum of its non-perturbative potential. These oscillations endow the axion with the role of a curvaton [75], transferring its isocurvature fluctuations into adiabatic curvature perturbations, while simultaneously acting as a reheating field by decaying into radiation. Consequently, an axion-dominated phase after the bounce provides a natural framework for the generation of the observed adiabatic CMB perturbations. In this context the curvature power spectrum is related to the axion spectrum via

$$\mathcal{P}_{\mathcal{R}_\sigma} = f^2(\sigma_i) \left(\frac{H_1}{M_P}\right)^2 \left(\frac{k}{k_1}\right)^{n_\sigma - 1}, \qquad k < k_1, \tag{3.55}$$

where

$$f(\sigma_i) = c_1 \frac{1}{\lambda_p \sigma_i} + c_2 + \lambda_p \sigma_i, \tag{3.56}$$

and σ_i is the non-trivial background value of the axion which emerged after the inflationary epoch from the (non-perturbative) potential. The constants are determined by numerical analysis [68] as $c_1 \sim 0.25$, $c_2 \sim -0.01$, $c_3 \sim 0.13$.

3.6 $O(d,d)$ invariance of Cosmological String Action to all orders α'

We conclude this Chapter by introducing the generalized version of the SFD in the presence of the Kalb-Ramond antisymmetric field. Hohm and Zwiebach [76] provided a framework in which all the α' corrections can be accounted for in string cosmological backgrounds.
Assuming a time dependent string background

$$g_{\mu\nu} = \begin{pmatrix} n^2(t) & 0 \\ 0 & -g_{ij}(t) \end{pmatrix}, \qquad B_{\mu\nu} = \begin{pmatrix} 0 & 0 \\ 0 & b_{ij}(t) \end{pmatrix}, \qquad \phi = \phi(t)\,, \tag{3.57}$$

and defining the following $2d \times 2d$ matrices

$$\mathcal{H} = \begin{pmatrix} g^{-1} & -g^{-1}b \\ bg^{-1} & g - bg^{-1}b \end{pmatrix}, \qquad \mathcal{D}_t \equiv \frac{1}{n}\partial_t, \qquad \bar{\phi} = \phi - \frac{1}{2}\ln(\det g),$$
$$\mathcal{S} = \eta\mathcal{H} = \begin{pmatrix} bg^{-1} & g - bg^{-1}b \\ g^{-1} & -g^{-1}b \end{pmatrix}, \quad \eta = \begin{pmatrix} 0 & 1 \\ 1 & 0 \end{pmatrix}, \tag{3.58}$$

the effective string action can be rewritten as (we are integrating the d-spatial dimensions)

$$S_0 = -\frac{\lambda_s}{2}\int dt\, n e^{-\bar{\phi}}\Big[(\mathcal{D}_t\bar{\phi})^2 + c_1 \mathrm{Tr}((\mathcal{D}_t\mathcal{S})^2)\Big], \tag{3.59}$$

where $c_1 = \frac{1}{8}$. The $O(d,d)$ group is defined as $\Omega \in O(d,d)$ if $\Omega^T\eta\Omega = \eta$, and from $\eta^2 = 1$ we have $\Omega^{-1} = \eta\Omega^T\eta$. It can checked that both $\mathcal{H}$ and $\eta \in O(d,d)$, and $\mathcal{S}^2 = 1$. The action Eq. (3.59) is invariant under the following transformation

$$\mathcal{H} \to \Omega^T\mathcal{H}\Omega, \qquad \bar{\phi} \to \bar{\phi}, \tag{3.60}$$

which in the case of $b_{ij} = 0$ and $\Omega = \eta$, maps $g \to g^{-1}$, hence to SFD.
Hohm and Zwiebach demonstrated that the most general action to all order α' preserving $O(d,d)$ invariance can be written as even powers of traces of $(\mathcal{D}_t\mathcal{S})^{2k}$,

namely

$$\begin{aligned} S \equiv S_0 + \int dt\, e^{-\bar{\phi}} \Bigg(& \alpha' \, c_{2,0} \operatorname{Tr}\big[(\mathcal{D}_t\mathcal{S})^4\big] + \alpha'^2 c_{3,0} \operatorname{Tr}\big[(\mathcal{D}_t\mathcal{S})^6\big] \\ & + \alpha'^3 \Big[c_{4,0} \operatorname{Tr}\big[(\mathcal{D}_t\mathcal{S})^8\big] + c_{4,1} \operatorname{Tr}\big[(\mathcal{D}_t\mathcal{S})^4\big] \operatorname{Tr}\big[(\mathcal{D}_t\mathcal{S})^4\big] \Big] \\ & + \alpha'^4 \Big[c_{5,0} \operatorname{Tr}\big[(\mathcal{D}_t\mathcal{S})^{10}\big] + c_{5,1} \operatorname{Tr}\big[(\mathcal{D}_t\mathcal{S})^6\big] \operatorname{Tr}\big[(\mathcal{D}_t\mathcal{S})^4\big] \Big] \\ & + \alpha'^5 \Big[c_{6,0} \operatorname{Tr}\big[(\mathcal{D}_t\mathcal{S})^{12}\big] + c_{6,1} \operatorname{Tr}\big[(\mathcal{D}_t\mathcal{S})^8\big] \operatorname{Tr}\big[(\mathcal{D}_t\mathcal{S})^4\big] \\ & \qquad + c_{6,2} \big(\operatorname{Tr}\big[(\mathcal{D}_t\mathcal{S})^6\big]\big)^2 + c_{6,3} \big(\operatorname{Tr}\big[(\mathcal{D}_t\mathcal{S})^4\big]\big)^3 \Big] + \cdots \Bigg). \end{aligned} \tag{3.61}$$

where the coefficients $c_{k.m}$ are prescribed by the string theory considered. In the simplest case of no multitrace terms the equations of motion read

$$\begin{aligned} (\mathcal{D}_t\bar{\phi})^2 - \sum_{k=1}^{\infty} \alpha'^{k-1} (2k-1) c_k \operatorname{Tr}\big[(\mathcal{D}_t\mathcal{S})^{2k}\big] = 0, \\ \mathcal{D}_t \left(e^{-\bar{\phi}} \sum_{k=1}^{\infty} \alpha'^{k-1} 4k \, c_k \, \mathcal{S} (\mathcal{D}_t\mathcal{S})^{2k-1} \right) = 0, \\ 2\mathcal{D}_t^2\bar{\phi} - (\mathcal{D}_t\bar{\phi})^2 - \sum_{k=1}^{\infty} \alpha'^{k-1} c_k \operatorname{Tr}\big[(\mathcal{D}_t\mathcal{S})^{2k}\big] = 0. \end{aligned} \tag{3.62}$$

We conclude by giving the equation of motion in the simple case of an FLRW metric $n(t) = 1$, $g_{ij} = a^2\delta_{ij}$, $b_{ij} = 0$, which reads

$$\dot{\bar{\phi}}^2 + HF'(H) - F(H) = 0, \tag{3.63}$$

$$\dot{H}F''(H) - \dot{\bar{\phi}}F'(H) = 0, \tag{6.78}$$

$$2\ddot{\bar{\phi}} - \dot{\bar{\phi}}^2 + F(H) = 0, \tag{3.64}$$

where the function $F(H)$ is defined as an infinite series of even powers of the Hubble parameter

$$F(H) = 2d \sum_{k=1}^{\infty} (-\alpha')^{k-1} c_k \, 2^{2k} H^{2k}, \tag{3.65}$$

with $(\cdots)'$ denoting derivation with respect to H, and the coefficients c_k are fixed by the string theory at hand.

Chapter 4

From the string vacuum to FLRW or de Sitter via α' corrections

4.1 Introduction

It is well-known [19, 70, 77] that the tree-level equations of string cosmology in d spatial dimensions, provided they possess d abelian isometries[1], are invariant under a continuous $O(d,d)$ group of transformations involving the spatial parts of the metric $g_{\mu\nu}$ and Kalb-Ramond tensor $B_{\mu\nu}$, as well as the dilaton ϕ. Such a symmetry has been argued to hold only at tree level in the string loop expansion but to all orders in the α' expansion [79], a property that has been explicitly checked up to $\mathcal{O}((\alpha')^3)$ [80–82]. In the particular case in which $B_{\mu\nu}$ is set to zero (to which we limit our considerations in this paper), such a symmetry reduces to a discrete Z_2^d scale-factor-duality (SFD) group together with time reversal T [71, 83]. In the strictly isotropic case the symmetry is further reduced to the four-dimensional group $Z_2^{SFD} \otimes Z_2^T$.

In a recent impressive paper, Hohm and Zwiebach (HZ) [76] have shown that, modulo field redefinitions and integrations by parts, the most general reduced (i.e. just time-dependent) cosmological action takes a particularly simple and manifestly $O(d,d)$-invariant form. For the case of an isotropic FLRW Universe

[1] The generalization to d' abelian isometries with $d' < d$ has been discussed in [78].

the HZ action depends on just a single even function $F(H)$ of the Hubble parameter $H(t)$. Further developments of the HZ approach have been given in several subsequent papers [84**?** –92].

In a very recent paper two of us [93] have reformulated in a Hamiltonian-like formalism (see Sect. 2 for more details) the HZ result, and have shown that this allows to characterise in a simple way the conditions[2] under which the field equations lead to regular cosmologies smoothly connecting an initial phase of low-energy pre-big bang evolution to its $SFD \otimes T$-related post-big bang configuration. Under these conditions, the solutions (that can be interpreted as a class of possible "string vacua") rather than breaking (say in the isotropic case) the original $Z_2^{SFD} \otimes Z_2^T$ symmetry down to nothing (which is the case at lowest order in α', whereby four distinct solutions are generated by the symmetry group [20]), are instead invariant under a diagonal Z_2 subgroup, connecting just pairs of duality-related solutions. As a very special case it was easy to recover the regular bouncing solution found by a trial and error procedure in [96, 97].

Resolving the curvature singularity separating the pre- and post-bounce phases would remove, of course, one of the most important obstacles facing the pre-big bang scenario. However, as widely discussed for instance in [21, 60], there are obvious theoretical and phenomenological shortcomings with a naive cosmology connecting the two $SFD \otimes T$-related solutions.

One of these is related to the choice of initial conditions: in a typical pre-bounce solution both curvature and string coupling ($g_s^2 = e^{\phi}$) grow. Let us recall, for instance, that in a d-dimensional isotropic cosmology the initial time evolution of the dilaton and of the Hubble parameter H is given by

$$\phi \sim -\left(1+\sqrt{d}\right)\ln(-t), \qquad H = \frac{1}{\sqrt{d}\,(-t)}\,, \qquad t \to -\infty\,, \quad (4.1)$$

so that both coupling and curvature go to zero in the far past ($t \to -\infty$). This led [98] to invoke a principle of *"Asymptotic Past Triviality"* governing the Universe's initial conditions. Indeed, it was argued in [98] (see also [99]) that generic (i.e. inhomogeneous and anisotropic) solutions becoming asymptotically trivial in

[2] These conditions include the requirement that the HZ function $F(H)$, describing the α'-corrected gravitational Lagrangian density, is non-analytic in the complex-H plane, as expected [94] from the known coupling between massless and massive string modes. The importance of a non-trivial branch-point structure in $F(H)$ has also been stressed in a recent application of this formalism to two-dimensional black holes [95].

the far past would be affected, as time grows, by gravitational instabilities leading, chaotically, to the formation of different trapped surfaces in different parts of the Universe, with a stochastic distribution of values for both curvature and string-coupling and a singularity in the future. Inside each trapped surface the geometry would become increasingly "velocity dominated" (i.e. with sub-dominant spatial gradients) as one approaches the singularity, and akin to the homogeneous solutions we have discussed above for the pre-bounce phase.

Thus, in different parts of the Universe, different realisations of the pre-big bang initial conditions will be effectively generated with a whole spectrum of small initial curvatures and couplings[3]. Regions with sufficiently small initial curvature and coupling would then lead to a long phase of dilaton-driven inflation, as described by Eq. (4.1). In other words, the principle of Asymptotic Past Triviality justifies our assumptions on the "initial" evolution of the homogeneous solutions, while allowing a whole spectrum of initial data (such a principle, by the way, is also needed for phenomenological reasons [100]). In this paper we will restrict our attention to cosmologies satisfying this "Asymptotic Past Triviality" requirement.

Turning now to the late time duality-related solution, however, this would pose serious problems if it could be trusted. In fact, at late times the dual solution to (4.1) is given by:

$$\phi \sim \left(\sqrt{d}-1\right)\ln(t), \qquad H=\frac{1}{\sqrt{d}\,t}\,, \qquad t\to+\infty\,, \tag{4.2}$$

so that the curvature goes to zero also in the far future but the coupling, instead, blows up. That means that, while we could trust the tree-level, low-curvature approximation in the far past, we cannot do the same in the future even if a regular bounce induced by the α' corrections copes with the high-curvature intermediate phase. Even if the coupling decreases during the short-lived bounce (as it indeed happens in the solutions discussed in [93]), eventually it will increase without limits implying that string loop corrections –and even non-pertubative effects– will eventually come into play (when exactly depends of course on the initial data).

[3]This is is due to the presence of two classical symmetries resulting in as many arbitrary integration constants [98].

These corrections break the duality symmetry, making the post-bounce evolution quite unlike its pre-bounce counterpart. Two important consequences come immediately to mind: *i*) the generation of a non-trivial dilaton potential, and *ii*) the turning on of cosmological perturbations and particle production. A third one, more typical of string theory, is the possible stabilization of the extra spatial dimensions (in which strings necessarily live) and the isotropisation of our three-dimensional space.

In this paper we move a first step in the direction of addressing these important problems by considering, on top of the α' corrections, the effects of a non-perturbative dilaton potential $V(\phi)$. We shall discuss, via both numerical and analytical methods, under which conditions these effects result in a stabilisation of the dilaton and in new kinds of interesting cosmologies at late times. It should be recalled, in this context, that the unavoidable presence of a non perturbative potential in a scenario with growing dilaton, and its possible stabilisation effects on both the curvature and the string coupling, were considered also in previous papers (see e.g. [101–104] and references therein). In that case, however, the higher order α' corrections were missing, and the conclusion was that there was no stable fixed point with frozen dilaton towards which a background starting from the string vacuum could be attracted. Here we will show how such a conclusion may change if we work with the HZ-modified string cosmology equations.

The rest of the paper is organized as follows: In Sect. 4.2 we generalize the approach of [93] by including a non vanishing dilaton potential. We will also make more precise the meaning of the "Hamiltonian" reformulation introduced in [93] by connecting it to the so-called Routhian approach to dynamical systems in classical mechanics [105]. In Sect. 4.3 we shall discuss, for the duality-invariant case with $V(\phi) = 0$, some general properties of regular isotropic bouncing solutions, extending the results of [93] to more complicated evolutions, and arguing that they all belong to the same topological class of background geometries. In Sect. 4.4, we will consider the effects of a dilaton potential in the isotropic case. We first discuss (Subsect. 4.4.1) the case of a potential with a local minimum $V_0 = 0$ and show that, under suitable initial conditions given in the regime of low-curvature pre-big bang inflation, there are regular solutions which, after the bounce, asymptotically approach a FLRW attractor of matter-dominated type with a stabilized dilaton. We then consider (Subsect. 4.4.2) the case of $V_0 > 0$, in which similar initial pre-big bang conditions lead again to late-time dilaton stabilisation, but

with an associated geometry describing a de Sitter inflationary phase (in both the String and Einstein frames because of dilaton's stabilization). In Sect. 4.4.3 we discuss the range of initial conditions compatible with these final attractors. In Sect. 4.5 we extend our considerations to the anisotropic case showing that late time attractors with a constant dilaton (and both $V_0 = 0$ and $V_0 > 0$), when they exist, must be isotropic. Sect. 4.6 summarizes our results and offers some concluding remarks. Finally, in Appendix A, we present an example of solution in which the initial perturbative evolution ends up, at late times, in its time-reversed counterpart.

4.2 Basic equations in a Routhian formalism

We shall write our equations in terms of the background fields defined in the so-called String frame (see e.g. [21]), in which the $O(d,d)$ symmetry is manifest. Limiting ourselves to the gravi-dilaton system with time-dependent field variables $\{\phi, g_{\mu\nu}\}$ and a d-dimensional spatially flat (but possibly anisotropic) spatial metric, we thus set $\phi = \phi(t)$, $g_{00} = N^2(t)$, $g_{ij} = -\delta_{ij}\, a_i^2(t)$, where $a_i = e^{\beta_i}$.

In such a case, by using the convenient "shifted dilaton" variable, defined by

$$\overline{\phi} = \phi - \sum_i \beta_i, \tag{4.3}$$

the effective action for the string cosmology equations, including higher-curvature string corrections to all orders in α', as well as a non-perturbative dilaton potential $V(\phi)$, can be written, slightly extending [76], as:

$$\begin{aligned} S &\equiv \int dt L = -\frac{1}{2}\int dt\, N e^{-\overline{\phi}} \left[N^{-2}\,\dot{\overline{\phi}}^{\,2} + F\left(N^{-1}\dot{\beta}_i\right) + 2\,(\alpha')^{(d-1)/2} V(\phi)\right], \\ F &= -N^{-2}\sum \dot{\beta}_i^2 + \mathcal{O}(\alpha') + \ldots, \end{aligned} \tag{4.4}$$

where the dot denotes time derivatives[4]. Here $N^{-1}\dot{\beta}_i = H_i$ is the ith-Hubble parameter, and the function $F(H_i)$ in the isotropic case reduces to the function introduced in [76]: it can be written as an infinite (and not necessarily convergent)

[4]Note that, besides the presence of V, there is also an overall factor $(-1/2)$ w.r.t. the action used in Ref. [93].

series of even powers of the Hubble parameter, and includes, in principle, the all-order α' corrections predicted by a given string model[5]. Note that, in order to keep the usual dimensions for V, and to make it appear in the action with the same dimensions as the kinetic terms, we have multiplied V by $(\alpha')^{(d-1)/2}$. In the following, when α' is not explicitly written, we shall be using units in which $\alpha' = 1$.

By varying the action (4.4) with respect to N, β_i and ϕ, and defining $f_i = \partial F/\partial H_i$, we obtain the following Euler-Lagrange equations in the cosmic-time gauge $N = 1$:

$$\dot{\overline{\phi}}^2 = F - \sum_i f_i H_i + 2V, \qquad \dot{f}_i = f_i \dot{\overline{\phi}} + 2\frac{\partial V}{\partial \phi}, \qquad 2\ddot{\overline{\phi}} = -\sum_i f_i H_i + 2\frac{\partial V}{\partial \phi}. \quad (4.5)$$

To zeroth order in α' one has $F = -\sum H_i^2$, and recovers the well known (see e.g. [20, 21]) tree-level low-curvature string cosmology equations.

In such a context, for any given function $F(H_i)$ we have a corresponding scenario of string cosmology evolution. However, as shown in [93], the models characterized by a regular bouncing transition, and describing a smooth evolution from the pre- to the post-big bang phase, must correspond to non-holomorphic functions $F(H_i)$ that satisfy, on top, quite complicated equations. To select such models it is better to work with the inverse functions $H_i(f_j)$, which gives the Hubble parameters H_i as a power series in $f_j = \partial F/\partial H_j$.

To this purpose, as shown in [93], one can conveniently adopt a "partial Hamiltonian" approach to the action (4.4) (also known as *Routhian* approach in a classical mechanics context, see e.g. [105]), and perform a Legendre transformation on just a subset of the original coordinates $N, \overline{\phi}, \beta_i$, in our case on just the latter d Lagrangian coordinates β_i. Denoting by π_i the momentum conjugate to β_i one defines:

$$\pi_i = \frac{\partial L}{\partial \dot{\beta}_i} = -\frac{1}{2}e^{-\overline{\phi}}\frac{\partial F}{\partial H_i} = -\frac{1}{2}e^{-\overline{\phi}} f_i \equiv e^{-\overline{\phi}} z_i, \quad (4.6)$$

where we have introduced, for later use, the more useful rescaled momenta $z_i = -f_i/2$. The associated Legendre transformation defines the so-called Routhian

[5] These are only known, unfortunately, at a relatively low order. In the spirit of the pre-big bang scenario we have not included a string-scale-size "cosmological constant" which arises in non critical dimensions (e.g. for $d \neq d_c = 9$ for the superstring) by simply assuming that $(d_c - d)$ compact dimensions are flat and frozen at the string length scale.

$\mathcal{R}(N, \overline{\phi}, \pi_i)$

$$\begin{aligned}
\mathcal{R}(N, \overline{\phi}, \pi_i) &= \sum_i \pi_i \, \dot{\beta}_i - L \\
&= N e^{-\overline{\phi}} \left[\frac{1}{2} N^{-2} \dot{\overline{\phi}}^2 + \frac{1}{2} \left(F - \sum_i \dot{\beta}_i \frac{\partial F}{\partial \dot{\beta}_i} \right) + V \left(\overline{\phi} + \sum_i \beta_i \right) \right], \\
\frac{\partial \mathcal{R}}{\partial \pi_i} &= \dot{\beta}_i \,, \qquad (4.7)
\end{aligned}$$

where the latter equation is to be used to express $\dot{\beta}_i$ in terms of the π_i. Introducing, as in [93], a reduced "Hamiltonian" $h(z_i)$, the above two equations can be rewritten as

$$\begin{aligned}
&\mathcal{R}(N, \overline{\phi}, \pi_i) = N e^{-\overline{\phi}} \left[\frac{1}{2} N^{-2} \dot{\overline{\phi}}^2 + h(z_i) + V \left(\overline{\phi} + \sum_i \beta_i \right) \right] \,, \\
&h(z_i) \equiv \frac{1}{2} \left(F - \sum_i \dot{\beta}_i \frac{\partial F}{\partial \dot{\beta}_i} \right) = \frac{1}{2} \sum z_i^2 + \mathcal{O}(\alpha') + \dots \,, \quad \frac{\partial h}{\partial z_i} = H_i \,. \qquad (4.8)
\end{aligned}$$

Note that the last equation for $H_i = N^{-1} \dot{\beta}_i$ basically inverts the functions $f_i = f_i(H_j)$, giving $H_i = H_i(z_j) = H_i(-\frac{1}{2} f_j)$.

Hence, in this new context, a given model is specified by the choice of $h(z_i)$ and of $V(\phi)$, and equations (4.5) can be rewritten in Routhian language as a combination of the Euler-Lagrange equations for N and $\overline{\phi}$ and the Hamilton equations for β_i, π_i, namely $\partial \mathcal{R} / \partial \pi_i = \dot{\beta}_i \,, \partial \mathcal{R} / \partial \beta_i = -\dot{\pi}_i$. Using (4.6), and after setting at the end $N = 1$, these equations can be finally rewritten in terms of z_i as:

$$\dot{\overline{\phi}}^2 = 2\, h(z_i) + 2V, \qquad \dot{z}_i = z_i \, \dot{\overline{\phi}} - \frac{\partial V}{\partial \phi}, \qquad \ddot{\overline{\phi}} = \sum_i z_i \, \frac{\partial h}{\partial z_i} + \frac{\partial V}{\partial \phi} \,, \qquad (4.9)$$

where, as usual, the first equation (the Hamiltonian constraint) together with the second set imply the last equation. These are the equivalent of equations (4.5) in the Routhian formalism.

Later in the paper we shall deal with cases in which some of the scale factors coincide. In these cases it is more convenient to deal with just the subset of distinct scale factors. Let us consider, as the simplest example, the fully isotropic case, $\beta_i = \beta$. We can easily go over from a given model specified by the function $F\left(N^{-1} \dot{\beta}_i\right)$ to the isotropic case by defining $F\left(N^{-1} \dot{\beta}\right) \equiv \; F\left(N^{-1} \dot{\beta}_i = N^{-1} \dot{\beta}\right)$.

Note, however, that when going to the Routhian written in terms of the momenta π congiugate to β, we get $\pi = \sum_{i=1}^{d} \pi_i \to d\pi_1$ (where we just picked one representative π_i). The relation:

$$H = \frac{\partial \mathcal{R}}{\partial \pi} \tag{4.10}$$

remains of course valid since it is an immediate consequence of the definition of $\mathcal{R}$. However, it is now more convenient (although not necessary) to define

$$z \equiv \frac{1}{d} e^{\bar{\phi}} \pi = -\frac{f}{2d}\,, \tag{4.11}$$

so that z and H coincide to leading order in the α' expansion Equation (4.10) thus becomes:

$$h(z) = \frac{d}{2} z^2 + \mathcal{O}(\alpha') + \dots \quad ; \quad H(z) = \frac{1}{d} \frac{\partial h(z)}{\partial z} = z + \mathcal{O}(\alpha') + \dots\,, \tag{4.12}$$

which can be used, if necessary, to reconstruct $h(z)$ from $H(z)$. For later use let us rewrite the Routhian equations (4.9) in the present case:

$$\dot{\bar{\phi}}^2 = 2\,h(z) + 2\,V, \qquad \dot{z} = z\,\dot{\bar{\phi}} - \frac{\partial V}{\partial \phi}, \qquad \ddot{\bar{\phi}} = z\,\frac{\partial h}{\partial z} + \frac{\partial V}{\partial \phi}\,. \tag{4.13}$$

Generalization of the above procedure to the case discussed in Sect. 4.5 in which $\beta_i = \beta$ for $i = 1, \dots, d$ and $\beta_i = \tilde{\beta}$ for $i = d+1, \dots, d+n$ is straightforward. The general equations (4.9), (4.13) will be the starting point of our subsequent discussion.

4.3 More on regular isotropic bouncing solutions with $V \equiv 0$

In this section we shall recall a few results concerning exact bouncing solutions of Eqs. (4.13) with α' corrections but without dilaton potential, and describing the smooth evolution of a $d+1$-dimensional isotropic background from the initial regime of Eq. (4.1) to the final, duality-related post-big bang regime of Eq. (4.2).

We will show, in particular, that the curvature bounce illustrated in [93] can be implemented also in a generalised (and highly non-trivial) way like, for instance,

through a phase of oscillating background curvature. However, all possible types of bouncing backgrounds obtained in this context, irrespectively of their (possibly) complicated kinematics, always belong to the same topological class in a sense defined below.

Let us first recall that, as discussed in [93] for the $V = 0$ case, the possible existence of regular bouncing solutions is controlled by the analytic properties of the function $h(z)$ and its associated "companion" in Eq. (4.12), $H(z) = -H(-z) = (1/d)(\partial h/\partial z)$. For a regular bounce to occur we must require that $h(z)$, which grows from zero to positive values for $z \ll 1$, exhibits a second zero at $z = z_2$ (and, of course, also at $z = -z_2$). Assuming $h(z)$ to be continuous and differentiable, this implies that $H(z)$ itself vanishes at (at least) one point $z_0 < z_2$ and to have local extrema at various points $(z_1, \dots)$ in that interval.

Simple examples satisfying such conditions (like, for instance, $h(z) \sim (1/2)z^2\,[1 - z^2/2]$) have been considered and discussed in [93]. There is also, however, the possibility of more complicated models[6] described by a function $H(z)$ which has several extrema (or zeros) in the range $\{0, |z_2|\}$. Consider, for instance, the model described by the following effective Hamiltonian:

$$\frac{h(z)}{d} = 1 - \cos z - \frac{2\,\epsilon}{9\,\pi^2}\left[1 + \left(\frac{z^2}{2} - 1\right)\cos z - z \sin z\right], \tag{4.14}$$

which gives, via (4.12)

$$H(z) = \sin\ z\left[1 + \epsilon\left(\frac{z}{3\pi}\right)^2\right]. \tag{4.15}$$

By assuming $\epsilon < 0$, and using the constraint $\dot{\bar{\phi}} = \pm\sqrt{2h}$ following from Eqs. (4.13) without dilaton potential, we can then obtain the corresponding model of regular bounce illustrated in the plane $\{\dot{\bar{\phi}}(z), \sqrt{d}H(z)\}$ by the parametric plot of Fig. 4.1.

The left panel of Fig. 4.1 is the plot of the curve $H(z)$. The zeros of H correspond to the values of z at which the curve intersects the horizontal axis, such as $\pm z_0$ positions of the points z_0, the extrema of H to maxima and minima such as $\pm z_1$. The shaded area subtended by the curve, for both the positive and the negative range of z, vanishes, such that the points $\pm z_2$ marking the end of the shaded

[6]Some of these models can be excluded a priori by being impossible to realise in string theory. These includes models in which, at intermediate times or near the bounce, the solution enters the perturbative region in a way incompatible with the known perturbative effective action.

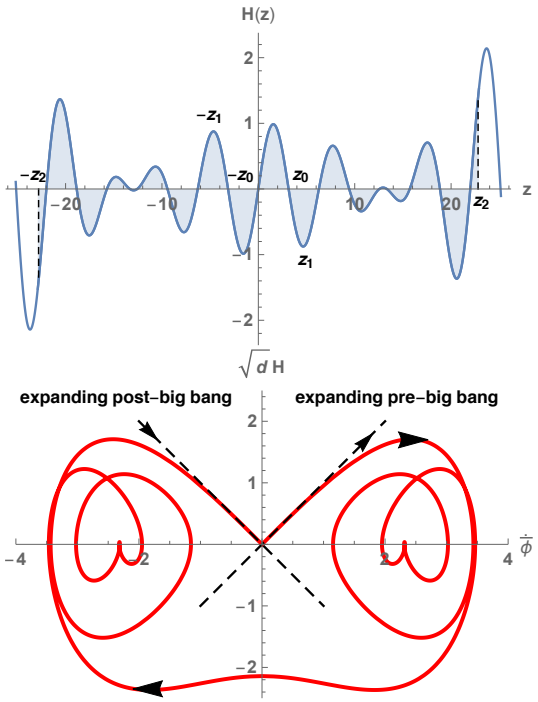

FIGURE 4.1: Left: the blue curve is the function $H(z)$ of Eq. (4.15) for $d = 3$ and $\epsilon = -0.5$. Along a given branch, positive or negative, the total shaded area subtended by the curve vanishes. Right: the red curve describes the parametric plot of a numerical solution of Eqs. (4.13) for the previous $H(z)$ and for $V(\phi) = 0$. The black dashed bisecting lines (satisfying the condition $\dot{\bar{\phi}} = \pm\sqrt{d}H$) represent the asymptotic regimes of initial low-energy expansion from the string vacuum, and final, post-big bang, decelerated expansion.

region correspond to the intersection of the curve with the vertical axis. Also, the contribution of ϵ introduces a modulation of the peaks which leads to a series of alternated local minima and maxima.

This last property is present also in the parametric plot of the right panel, producing a series of points where $|H|$ reaches a local maximum or a zero (corresponding to a transition from expansion to contraction or viceversa), even for $\dot{\bar{\phi}}$ non-vanishing. The existence of these peculiar points leads to the "vortex-like" red curve of Fig. 4.1. Note that the turning points of the parametric curves around $H = 0$ and $|\dot{\bar{\phi}}| \simeq 2.25$ are smooth, even though they might look cusps: this is only due to the overall size of the plot. It should be stressed, finally, that for $\epsilon \to 0$ the "bottom" of the red curve, corresponding to the point $\dot{\bar{\phi}} = 0$ which formally marks the transition from the pre- to the post-big bang regime (i.e. from the right to the left sector of the parametric plane), tends to approximate the origin from below, $H \to 0_-$. In that case one would just recover an example of the cases mentioned

in the previous footnote 6, as the solution would follow a low energy trajectory incompatible with the perturbative string cosmology equations.

The given example clearly displays the possibility of regular bouncing scenarios described by solutions which are always self-dual in the absence of a dilaton potential, but which may be characterised by a high-energy string phase with rapidly oscillating Hubble parameter, implying sudden (but smooth) transitions connecting expanding $\leftrightarrow$ contracting geometries.

Hence, in this general context, the word "bounce" in no way should be interpreted as meaning a localised transition from initial contraction to final expansion. More appropriately, with the word "bounce" we mainly refer in this paper to the absolute value of the curvature scale, occurring during a possibly extended (in string units) epoch needed to convert the initially accelerated, growing curvature expansion to the final decelerated, decreasing curvature expansion.

The class of solutions compatible with this scenario in principle is large, and controlled by the analytical properties of $h(z)$ (whose correct expression should be provided by string theory). However (in the absence of a dilaton potential), all such solutions are topologically equivalent with respect to the following geometric property of the curve describing the given solution in the parametric plot of Fig. 4.1: the vector connecting the origin to a point on the curve undergoes a clockwise rotation of $3\pi/2$ as one goes from the beginning to the end of the curve. The same is true for solutions smoothly connecting a contracting initial phase to the related final contracting one. The only difference is that the initial and final parts of the curve lay in the bottom-left and bottom-right sectors of the plane, respectively, and thus (as already noted in [93]) the rotation occurs in the anticlockwise direction.

4.4 Regular isotropic bouncing solutions and dilaton stabilisation with $V \neq 0$

As discussed in the introduction a tree-level string cosmology, even if it implements a regular bounce, cannot be realistic. As a first step towards making the model more realistic let us now include into the effective string cosmology equations the contributions of a non-perturbative dilaton potential $V(\phi)$, which goes to zero in

the small coupling limit $g_s^2 \to 0$ ($t \to -\infty$) with an instanton-like suppression of the type $V \sim e^{-\text{const}/g_s^2}$, and which becomes non-negligible in the opposite large time limit, thus breaking the duality symmetry and modifying the final, post-bounce asymptotic configuration. We may expect, in this way, not only a modified dilaton dynamics but also a modified final evolution of the cosmic geometry (no longer necessarily duality-related to that of the initial low-energy solution).

We are interested, in particular, in a "realistic" post-bounce scenario with the dilaton stabilized at a final constant value ϕ_0 such that $g_s^2(\phi_0) = e^{\phi_0}1$, and in which the asymptotic solution can approach the phase of standard cosmological evolution described by the Einstein gravitational dynamics (with no need of string loops and/or α' corrections). We shall thus consider an effective dilaton potential which has a local minimum $V = V_0$, needed to stabilise the dilaton, and which can be parametrised in a phenomenological way (and in units $\alpha' = 1$) as follows:

$$V(\phi) = A\, e^{-B(\phi)/\beta} \left[\left(c^2 - B(\phi)\right)^2 + \delta B(\phi) \right] \left[1 - q\, B^{-1}(\phi)\right], \tag{4.16}$$

where

$$B(\phi) = \frac{1 + \alpha\, g_s^2}{\alpha\, g_s^2} = \frac{1 + \alpha\, e^{\phi}}{\alpha\, e^{\phi}}, \tag{4.17}$$

and where A, c, α, β, δ and q are constant parameters controlling various features of V.

In particular, A (together with c) controls the overall magnitude of the potential; B is some kind of inverse 't Hooft coupling, λ_t^{-1}, in the weak coupling limit (with $\alpha \sim N_c$, the number of colors) while it approaches from above a finite value, here conventionally set to one, in the strong-bare-coupling limit[7].

In the presence of a local minimum of V at $\phi = \phi_m$, the parameter δ controls $V_0 \equiv V(\phi_m)$ i.e. V_0 is non-vanishing if and only if δ is non-vanishing (as illustrated in Fig. 4.2). The position ϕ_m of the local minimum, if present, is mainly controlled by c and α, while the parameter β mainly controls the height of the first potential peak. Also, the asymptotic behaviour of $V(\phi)$ at large positive values of ϕ depends

[7]This is the idea of the dilaton runaway scenario [106] (see also [107, 108] for its possible observable consequences) which is based on the assumption [109] that the limit $\phi \to +\infty$ is non singular and characterized by finite (and perhaps realistic) values for both the gauge and gravitational coupling (in string units). However, our simple description of that regime (through the relation between B and ϕ) is over-simplistic since it ignores the fact that loop corrections, besides generating a non trivial potential, will also modify the whole kinetic part of the action [106]. This, in turn, would make the passage from the S-frame to the E-frame more complicated than in the perturbative regime.

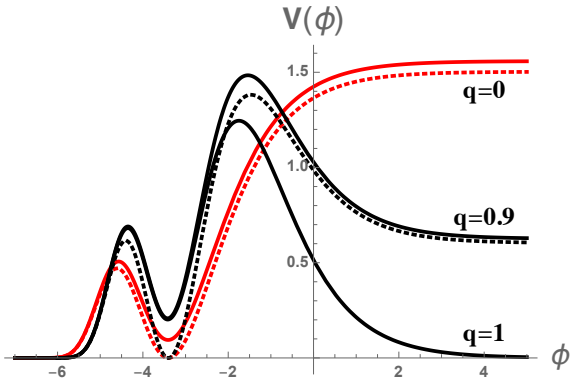

FIGURE 4.2: The red curves show an example of dilaton potential asymptotically approaching the maximum at large ϕ values, and obtained from (4.16) with $q = 0$. The black curves show an example of "runaway" potential, asymptotically going to zero for $q = 1$ and stabilising to a non-vanishing constant value for $0 < q < 1$. Solid curves are plotted with $\delta > 0$, and are characterised by a local minimum $V_0 > 0$. Dotted curves correspond to the same potential plotted however for $\delta = 0$, and with a local minimum $V_0 = 0$. All curves are plotted for $c = 2$, $\alpha = 10$. We have used $A = 0.22$, $\beta = 3.5$ for the red curves, and $A = 1$, $\beta = 2.5$ for the black curves.

on the parameter q: for $q \leq 0$ the potential approaches there its maximal constant value; for $0 < q < 1$ the potential approaches from above a non-vanishing positive constant[8]. Finally, for $q = 1$ the potential is asymptotically vanishing thereby realizing the so-called "dilaton runaway scenario" of [106] (see also [107, 108]). Fig. 4.2 gives a simple qualitative illustration of the various possible cases.

The specific "shape" and the amplitude of the potential strongly depend on the numerical values of the various phenomenological parameters, and the values used in Fig. 4.2 have been chosen mainly for the purpose of a clear graphical illustration of the possible differences. What is important to stress is that, depending on the values of such parameters (and on the initial conditions which identify the particular background whose evolution we are following from the asymptotic, low-energy regime), the potential may significantly affect the background evolution not only during the bounce, but also, and most important, in the final asymptotic post-bouncing regime. In addition, as we shall see below, the dilaton's evolution is best understood in the E-frame, in which it behaves like a minimally coupled scalar, while the potential in (4.16) refers to the S-frame. We stress again that the well known connection between the two frames in the perturbative regime can be

[8]Such a constant is negative if $q > 1$, but since in this paper we are mainly interested in a scenario where the dilaton growth is trapped by the potential (see below) without reaching the large ϕ regime, it will be enough to concentrate our discussion on the range $0 \leq q \leq 1$.

strongly modified at large positive ϕ in the runaway scenario of [106]. This being said we may expect, in general, three possible late-time dilaton evolutions.

The first case is the one in which the potential is unable to substantially modify the overall dilaton evolution: the dilaton keeps monotonically growing both before and after the bounce, and (with the appropriate model of α' corrections) we recover a regular transition from the expanding pre- to post-bang regime like in the cases with no potential (see [93] and Sect. 4.3). This will typically happen if the overall scale A of the potential is small enough as compared to the value of H and $\dot{\phi}$ when the dilaton is in the region of sizeable potential. Describing the late time physics corresponding to that case is not simple and will depend on whether the Einstein-frame potential falls asymptotically to zero, to a positive constant, or even grows indefinitely. Since the passage to the E-frame is not simple at large bare coupling, we shall postpone this case to some future work.

The second case is the one in which the potential is high enough to stop the growth of dilaton, and the dilaton bounces back towards the small coupling regime, monotonically approaching the asymptotic limit $\phi \to -\infty$: in that case the final background configuration after the bounce is exactly the time-reversed of the initial one, thus implementing a (new type of) regular bounce from expanding pre- to contracting post-bang regimes (see Appendix A).

Finally, the third (and phenomenologically most interesting) case is the one in which the dilaton gets trapped in the local minimum of the potential. The rest of this paper will be devoted to illustrate and discuss this last possibility, which has three important consequences. With an appropriate choice of the parameters of Eq. (4.16), the potential can produce *i*) the stabilisation of the dilaton at a final asymptotic value $\phi = \phi_0 = \text{const}$; *ii*) a final evolution of the metric of standard type, corresponding to a dust-dominated FLRW geometry if $V(\phi_0) = 0$ or to a de Sitter geometry if $V(\phi_0) > 0$; *iii*) the isotropisation of the final geometry if we start from anisotropic initial conditions. The first and second effects will be studied in this section, where we will concentrate on the case of an isotropic scenario. The isotropisation phenomenon will be discussed in Sect. 4.5.

4.4.1 FLRW attractors for a local minimum $V_0 = 0$

For a first illustration of the dilaton stabilisation mechanism we will start considering an initially expanding $(d+1)$-dimensional isotropic background geometry, asymptotically evolving from the string perturbative vacuum according to Eqs. (4.9), and a dilaton potential given by Eq. (4.16) with $\delta = 0$ (such that $V = 0$ at the local minimum $\phi = \phi_m$, see the dotted curves of Fig. 4.2).

Also, to stress the differences induced by the potential on the evolution of the background geometry, let us directly present a numerical integration for the same model of α' corrections producing the regular bounce first derived in [96]. As shown in [93], such a model provides a regular solution of the Lagrangian equations (4.5) corresponding to the inverse HZ function $H(f)$ given by

$$H(f) = -\frac{f}{2\,d} + \alpha' \left(\frac{f}{2\,d}\right)^3 . \tag{4.18}$$

Adopting the Hamiltonian formalism for isotropic backgrounds, and using in particular Eqs. (4.12) (recalling that in the isotropic case, $z = -(f/2d)$), we obtain that the above model is described by the effective Hamiltonian[9]

$$h(z) = \frac{d}{2}\left(z^2 - \alpha' \frac{z^4}{2}\right) , \tag{4.19}$$

where, unlike in the previous paper [93], we will use units in which $\alpha' = 1$.

Starting with this result, we can now easily provide a qualitative illustration of the dilaton stabilisation (and of the related effects) produced by the potential by performing a numerical integration of Eqs. (4.13), for any given model of potential specified by the parameters of Eq. (4.16). We shall consider, to this purpose, a simple example of runaway potential with $q = 1$, but the results we are presenting can be reproduced for other classes of potentials with $0 \leq q < 1$, and with different asymptotic behaviour (see Fig. 4.2). It should be stressed, however, that the value of q (and of other parameters) may be relevant to define the region of initial conditions compatible with the attraction to the final regime with stabilised dilaton, as we shall discuss in Sect. 4.4.3.

[9] The expression given in Eq. (4.19) matches, up to the first α' correction, the expression of $F(H)$ for the heterotic string [82].

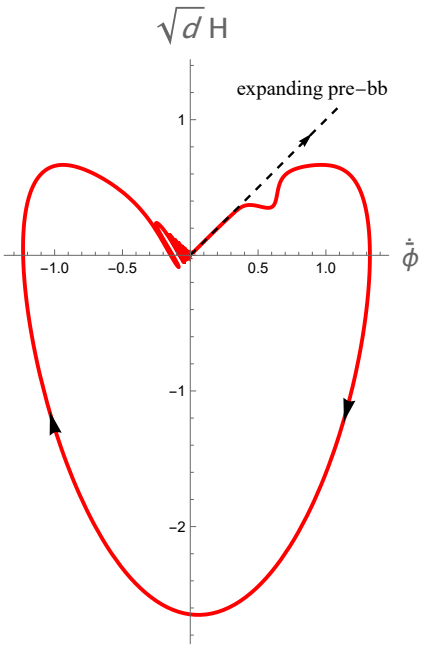

FIGURE 4.3: The red curve describes the parametric plot of a numerical solution of Eq. (4.9), with the potential (4.16) and the Hamiltonian (4.19). We have set $d = 3$ and $\alpha' = 1$ for the Hamiltonian, $A = 0.1$, $\alpha = 10$, $\beta = 3$, $c = 2$, $\delta = 0$, $q = 1$ for the potential, and $\phi = -3.5$, $z = 0.01$ for the initial conditions. The black dashed half-line corresponds to the initial trajectory evolving from the string perturbative vacuum and described by Eq. (4.1).

We shall impose on our initial conditions, fixed in the region where the dilaton potential (and the α' corrections) are still negligible, to satisfy the low energy pre-big bang equations $\dot{\phi} = \sqrt{d}H$. The numerical solution we obtain, with appropriate (small enough) values of the initial condition for ϕ and z, gives then the results illustrated by the parametric plot of Fig. 4.3. As already stressed we have chosen a potential with $\delta = 0$ and $q = 1$, and the numerical values of the other parameters are specified in the caption of the figure.

Note that we find again a regular bounce, described by a smooth curve turning clockwise in the plane of the figure (as repeatedly stressed in [93]). With respect to the case without potential, however, the curve describes a "deformed heart-like" path (no longer symmetric with respect to the vertical axes), and we have two types of deformations. A first deformation occurs in the pre-bounce regime (the upper right quadrant of the figure), where the effects of the potential first come into play (together with those of the α' corrections). The physically more significant deformation occurs however in the final, post-bounce regime (upper left quadrant), corresponding to a drastic change of the dilaton dynamics because of

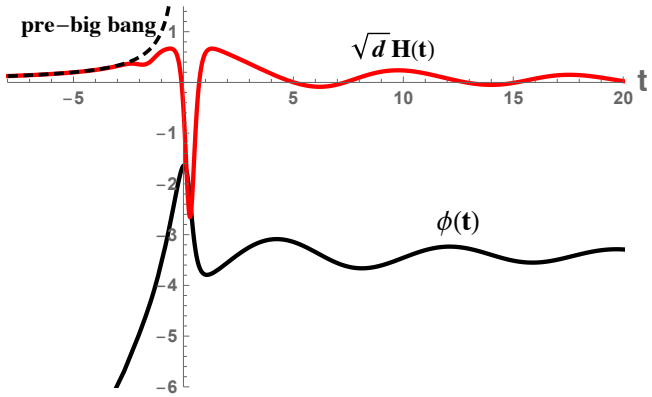

FIGURE 4.4: Time evolution of H (red curve) and ϕ (black curve) for the same numerical solution of Fig. 4.3. The black dashed curve describes the (unbounded) growth of the Hubble parameter for the low-energy pre-big bang solution of Eq. (4.1).

its trapping in the potential minimum. The produced result is an oscillating final regime, as shown in Fig. 4.3.

The final asymptotic effect of dilaton stabilisation and background oscillations can be explicitly illustrated also by plotting the time behaviour of the numerical solution for $H(t)$ and $\phi(t)$. The result, shown in Fig. 4.4, again emphasises the differences between the initial and final regimes which (because of the potential) are no longer duality related.

The dilaton stabilisation and oscillation effects are even more evident if we consider the parametric plot of $H = H(\phi)$, or its $3d$-version (i.e. the same parametric plot expanded as a function of time). Limiting our attention to the final, post-bounce regime we obtain the results shown, respectively, by the left and right sectors of Fig. 4.5. They clearly show that the oscillating background approaches an oscillating regime where the dilaton asymptotically reaches a final (constant, non vanishing) value $\phi_0 < 0$, and the Hubble parameter is asymptotically decreasing to zero.

To obtain a more precise information on the type of final geometry and show, in particular, that it describes a phase of standard (FLRW type) evolution (and not a post-big bang evolution of the string cosmology type), it is convenient to discuss the analytical solutions of Eq. (4.13) in the late-time regime where the final asymptotic value of the dilaton ϕ_0 coincides with the position of the local minimum $\phi_0 = \phi_m$, the trapped dilaton is oscillating around ϕ_m, and the potential

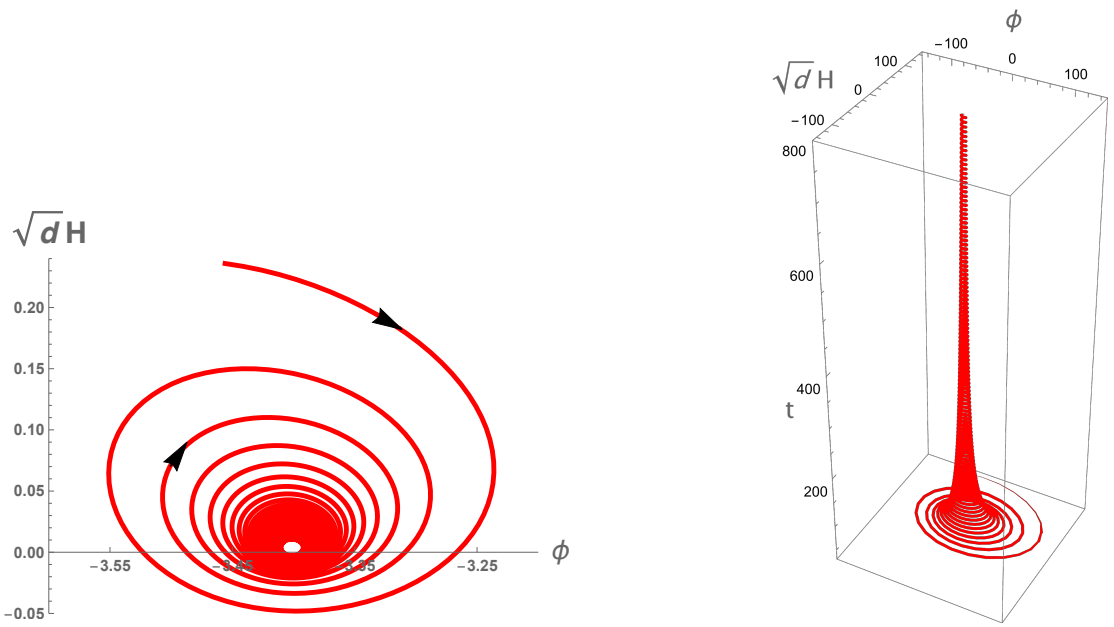

FIGURE 4.5: Left: two dimensional parametric plot of $H = H(\phi)$. Right: its three-dimensional version with explicit time evolution, $H(t) = H[\phi(t)]$, for the numerical solution of Fig. 4.3. In the three-dimensional plot the variables H and ϕ have been multiplied by 10^3 for a better graphic illustration of the damped oscillations regime.

can be approximated in functional form as:

$$V(\phi) \simeq \frac{1}{2} m^2 \left(\phi - \phi_m\right)^2 . \tag{4.20}$$

If the potential (4.16) has a local minimum, and if $\delta = 0$, then the minimum $V_0 = 0$ is located at $\phi_m = -\ln[\alpha(c^2 - 1)]$. In such a case, by expanding $V(\phi)$ up to second order around ϕ_m, we can also find the value of m^2 in terms of the other parameters, and we obtain $m^2 = (2A/c^2)(c^2 - q)(c^2 - 1)^2 \exp(-c^2/\beta)$.

We also note that, at late enough times (depending on the given initial conditions), the curvature scale is small enough (in units α') so that the higher order α' corrections can be neglected. With these approximations, the equations (4.13) can be rewritten as

$$\begin{aligned} \left(\dot{\phi} - d\,H\right)^2 &= d\,H^2 + m^2 \left(\phi - \phi_m\right)^2 , \\ \dot{H} &= H\left(\dot{\phi} - d\,H\right) - m^2 \left(\phi - \phi_m\right) , \\ \ddot{\phi} &= d\,\dot{H} + d\,H^2 + m^2 \left(\phi - \phi_m\right) . \end{aligned} \tag{4.21}$$

Looking for oscillating solutions, compatible with the asymptotic limit $\phi = \phi_0 = \phi_m$ and $H = 0$ for $t \to +\infty$, we set:

$$\phi(t) - \phi_0 \simeq \frac{M}{t^\gamma} \sin(\omega t + \theta) \tag{4.22}$$

(where θ is an arbitrary phase parameter), and we find that the above equations (4.21) are satisfied, to leading order in $1/t^\gamma$, provided that $\gamma = 1$, $\omega = m\sqrt{d-1}$, and

$$H(t) = \frac{1}{t} \frac{M\omega}{\sqrt{d}\,(d-1)} \left[1 + \sqrt{d}\,\cos(\omega t + \theta)\right]. \tag{4.23}$$

Finally, by expanding our solution for small values of M and $\dot{M}/M\omega$, we find at the first sub-leading order that $M\omega \simeq 2(d-1)/\sqrt{d}$, and that our asymptotic solution can be written as:

$$\begin{aligned} \phi(t) &= \phi_0 + \frac{2(d-1)}{t\,\omega\sqrt{d}} \sin(\omega t + \theta), \\ H(t) &= \frac{2}{t\,d} \left[1 + \sqrt{d}\cos(\omega t + \theta)\right]. \end{aligned} \tag{4.24}$$

We have checked that the percent difference between these analytical expressions and the previously presented numerical solutions is very small ($\lesssim 10^{-7}$) at large times.

Note that the time-averaged behaviour of the geometry gives $\langle H \rangle \simeq (2/d)t^{-1}$, corresponding to a scale factor $a(t) \sim t^{2/d}$, which exactly reproduces the time evolution of a standard, dust-dominated, FLRW cosmology. The role of the effective dust fluid, in this case, is played by the oscillating dilaton, which produces a phase of final post-bounce evolution very similar to the dust-like phase of post-big bang evolution dominated by the oscillations of the Kalb-Ramond axion (see e.g. [110, 111]).

What may look surprising, however, is that the oscillations in (4.24) have a large and constant amplitude (relative to the non-oscillating term) forcing $H(t)$ take both positive and negative values[10]. This is due to the fact that, as already mentioned, the dilaton does not behave in the string frame as a minimally coupled scalar. On the other hand, we might have expected that the stabilisation of the dilaton leads to the asymptotic identification of the S and E-frames.

[10]We are grateful to Robert Brandenberger and Jerome Quintin for having raised this point.

The computation of the E-frame Hubble parameter (see e.g. [60]) gives, from Eq. (4.24) (and in terms of the S-frame cosmic time t):

$$H_E(t) = e^{\phi/(d-1)} \left(H - \frac{\dot{\phi}}{d-1} \right) \equiv \frac{2}{t\,d}\, e^{\phi/(d-1)} \,. \tag{4.25}$$

We find again the dust-like behaviour, $H_E \sim (2/d)t^{-1}$, but this time with very small and damped oscillations due to the presence of $\phi(t)$ in the exponential factor. For $\phi \to$ const, the E-frame time coordinate is simply given by $t_E = t \exp[-\phi/(d-1)]$, and one exactly recovers dust dominated evolution $H_E = 2/(t_E\, d)$. In other words, even if the dilaton has damped oscillations, the passage to the Einstein frame is important for it to behave like a genuine minimally-coupled massive scalar.

Let us finally discuss, for the above given potential, the range of initial conditions compatible with the scenario we have discussed, i.e. the trapping of the dilaton in the $V_0 = 0$ minimum and the final associated regime of standard (dust-like) cosmic evolution. In particular, we would like to find out whether or not such initial conditions are highly fine-tuned.

In the isotropic case (see Sect. 4.5 for the extension to anisotropic cosmologies) the initial conditions consist of giving ϕ, $\dot{\phi}$ and H at some initial time t_0 in the far past. However, for any given model (i.e. for a given h and V) the Hamiltonian constraint (i.e. the first of Eqs. (4.13)) can be used to fix the initial value of $\dot{\phi}$ in terms of the other two. Furthermore, assuming that the evolution starts at sufficiently small coupling e^{ϕ}, where V is absolutely negligible, the second of Eqs. (4.13) implies the conservation law $e^{-\phi} z = \kappa^{-1}$, namely:

$$e^{\phi} = \kappa\, z(a^d) \sim \kappa z(\sqrt{d}\, H)^{\sqrt{d}} \sim \kappa\, (\sqrt{d}\, H)^{1+\sqrt{d}} \sim \kappa\, (\sqrt{d}\, z)^{1+\sqrt{d}} \,, \tag{4.26}$$

with κ a constant and the various approximate relations becoming exact in the $t \to -\infty$ limit. This means that changing κ does change the initial conditions. Instead, changing ϕ and H (or z) while keeping κ fixed, amounts physically to the same initial conditions simply referred to a shifted initial time. In other words, we expect the basin of attraction to the FLRW late time solution to be one-dimensional. It is given by some interval(s) in κ, a physical quantity given by a suitable combination of the coupling constant and curvature that remains constant during the very early time evolution. See in particular sect. 4.4.3 for a discussion

of the basin of attraction towards a final regime of stabilised dilaton, decreasing curvature and decelerated expansion illustrated in this subsection.

4.4.2 de Sitter attractors for a local minimum $V_0 > 0$

Another interesting cosmological scenario, still describing a regular bouncing evolution from the string perturbative vacuum but approaching a different final configuration, can be obtained with a slight modification of the dilaton potential used in the previous section.

Starting again with the general form (4.16) of $V(\phi)$, but including also the contribution of a (small) non-vanishing parameter δ, one finds that, in the presence of a local minimum, the latter is still approximately located for small δ at $\phi = \phi_m \simeq -\ln[\alpha(c^2-1)]$ (as illustrated in Fig. 4.2), but the associated potential energy is in general non-vanishing. In the limit $\delta \ll 1$, by computing the potential at the above minimum to first order in δ , we obtain in particular $V_0 = V(\phi_m) \simeq A\delta(c^2-q)\exp(-c^2/\beta)$.

Such a difference is important because the local minimum responsible for the dilaton stabilisation mechanism also controls the asymptotic value of the post-bounce Hubble parameter, and for $\delta > 0$, $V_0 > 0$ one finds that the background geometry approaches a final phase of standard de Sitter evolution. In that case, as we shall see, the final value ϕ_0 of the dilaton no longer coincides with the position of the local minimum, i.e. $\phi_0 \neq \phi_m$.

In order to illustrate the qualitative aspects of this modified scenario it may be appropriate to present, first of all, the results of a numerical integration of Eqs. (4.13) using for $h(z)$ exactly the same model of α' corrections as in the previous section 4.4.1, and specified by Eq. (4.19). In such a way all differences are only due to the modified potential, and in particular to the new contribution of a parameter $\delta \neq 0$.

We shall impose initial conditions satisfying as before the low-energy pre-big bang dynamics, specified (for $t \to -\infty$) by the constraint $\dot{\overline{\phi}} = \sqrt{d}H$. The numerical integration of Eqs. (4.13) with the particular value $\delta = 0.04$ then gives the result illustrated in Fig. 4.6. The left sector shows again a regular curvature bounce from the pre- to the post-big bang regime, similar to the case considered in the previous section and illustrated in Fig. 4.3. The differences from that case are all

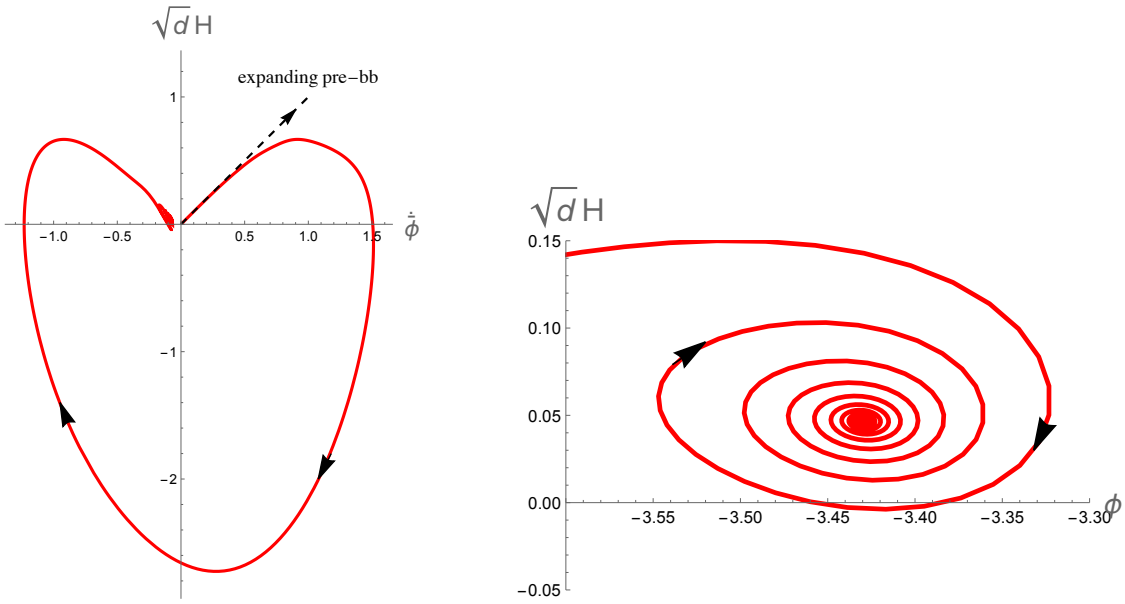

FIGURE 4.6: Left: the red curve describes the parametric plot of a numerical solution of Eq. (4.13), with the potential (4.16) and the Hamiltonian (4.19) (with $\alpha' = 1$ and $d = 3$). Differently from the previous figures we have set $\delta = 0.04 \neq 0$ to have a non-vanishing V_0 at the local minimum, and $\beta = 1$, $A = 1$ (to simplify the graphics). All the other parameters are the same as in the figures of Sect. 4.4.1: $\alpha = 10$, $c = 2$, $q = 1$, and the initial conditions are $z = 0.01$ and $\phi = -3.65$. The black dashed half line describes the initial trajectory evolving from the string perturbative vacuum, as in Fig. 4.3. Right: Parametric plot $H = H(\phi)$ for the same numerical solution, in the asymptotic range of large positive times.

concentrated in the final post-bounce regime (upper-left quadrant), showing that now the background oscillations due to the stabilisation of the trapped dilaton are no longer approaching the origin of the axes $\{\dot{\phi} = 0, H = 0\}$, but a new asymptotic (de Sitter) limit with $H = H_0 = \text{const}$, and $H_0 > 0$.

These oscillations around the new final attractor $\{\phi_0, H_0\}$ are more clearly shown if we concentrate our graphic analysis on the post-bounce region of large positive times, as illustrated by the parametric plot $H = H(\phi)$ presented in the right sector of Fig. 4.6, where we have used the previous numerical solution in the range $t > 0$. The final value of H_0 is controlled by the value of the parameter δ in the dilaton potential, and for $\delta \to 0$ one recovers the FLRW scenario with $H \to 0$ discussed in the previous section (see Fig. 4.5). For our illustrative purpose we have plotted a numerical solution with $\delta = 0.04$, but it should be stressed that, for small enough δ, the curvature scale H_0 of the final de Sitter regime can be fixed at values arbitrarily smaller than the string scale ($H_0 \ll \lambda_s^{-1}$), thus avoiding the need of

taking into account α' corrections for an analytical description of this regime[11].

Another important difference from the case with $\delta = 0$ (not so evident, even if we compare the right plot of Fig. 4.6 with the similar one of Fig. 4.5), is that the final value of the stabilised dilaton, $\phi = \phi_0$, no longer coincides with the minimum of the potential, $\phi = \phi_m = -\ln[\alpha(c^2 - 1)]$. A better illustration of this effect can be obtained by plotting the time evolution of $H(t)$ and $\phi(t)$, shown in Fig. 4.7. The first plot shows that the final value of H_0 is non-vanishing, while the second plot clearly shows the difference between the stabilised value ϕ_0 and the position of the local minimum ϕ_m.

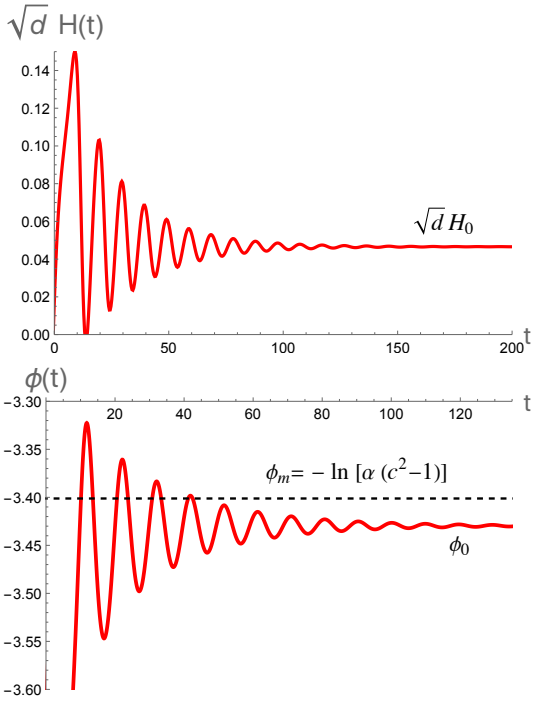

FIGURE 4.7: Time evolution of $H(t)$ and $\phi(t)$ for the same numerical solution of Fig. 4.6. The final asymptotic regime is characterised by a constant value of $H_0 > 0$ and a constant dilaton $\phi_0 \neq \phi_m$.

For an analytical discussion of this scenario in the final asymptotic regime and, in particular, for a physical interpretation of the difference between ϕ_0 and ϕ_m, let us now consider Eqs. (4.13) in the large time limit where we can neglect α' corrections. By evaluating such equations at the final attractor position, where $\phi = \phi_0$, $H = H_0$, $\dot{\phi} = 0 = \dot{H}$, we than obtain the conditions

$$d\, H_0^2 = -\left(\frac{\partial V}{\partial \phi}\right)_{\phi_0}, \qquad\qquad d\,(d-1) H_0^2 = 2\, V(\phi_0). \tag{4.27}$$

[11] In any case, the value of H_0, and then of δ, cannot be too high ($\delta \ll 1$), otherwise it is unlikely for the dilaton to be trapped in a final stabilised configuration.

They clearly show that *i*) for a non-vanishing value of H_0 the final stabilised dilaton ϕ_0 cannot be localised at the potential minimum ϕ_m (where $\partial V/\partial\phi = 0$); conversely, *ii*) if the final attractor coincides with the minimum position, $\phi_0 = \phi_m$, then we cannot avoid the final regime of standard evolution with decreasing curvature and a final value $H_0 = 0$ (consistently with the second equation (4.27) and with the fact that, as discussed in Sect. 4.4.1, in such a case the potential at the minimum is vanishing, $V_0 \equiv V(\phi_0) = V(\phi_m) = 0$).

Combining the two equations (4.27) we also obtain a condition on ϕ_0 which can be written as

$$\left[\frac{\partial}{\partial\phi}\left(Ve^{\frac{2\phi}{d-1}}\right)\right]_{\phi=\phi_0} = 0, \tag{4.28}$$

showing that the stabilised value ϕ_0 corresponds to the minimum of an "effective" potential $\widetilde{V} \sim V\exp\left[2\phi/(d-1)\right]$. Interestingly enough, and consistently with the scenario of a stabilised dilaton, $\widetilde{V}(\phi)$ is nothing else that the dilaton potential for the action (4.4) written in the E-frame (see e.g. [60]). This is, as in the case of $V_0 = 0$, a consequence of the dilaton being a minimally coupled scalar only in the E-frame. We stress that the above effective potential contains an explicit dependence on the number of spatial dimensions, and this, as already noticed, may affect the late-time post-bounce evolution of the gravi-dilaton background.

The difference between ϕ_0 and ϕ_m can be analytically estimated (again, in the asymptotic regime of low enough curvature scales corresponding to $V_0 \ll 1$, $\delta \ll 1$) by perturbatively expanding the potential around the minimum as

$$V(\phi) = V_0 + \frac{m^2}{2}\left(\phi - \phi_m\right)^2. \tag{4.29}$$

By inserting this expression into the condition (4.28), and solving for ϕ_0, we obtain (to first order in V_0/m^2)

$$\phi_0 \simeq \phi_m - \frac{2\,V_0}{m^2(d-1)} + \mathcal{O}\left(\frac{V_0^2}{m^4}\right). \tag{4.30}$$

On the other hand we recall that for our potential (4.16), and for small values of δ, we have $V_0 \simeq A\delta(c^2 - q)\exp(-c^2/\beta)$. By computing $m^2 = (\partial^2 V/\partial\phi^2)_{\phi=\phi_m}$, and expanding the ratio V_0/m^2 in powers of δ we obtain

$$\frac{V_0}{m^2} = \delta\,\frac{c^2}{2\left(c^2-1\right)^2} + \mathcal{O}(\delta^2), \tag{4.31}$$

so that for $\delta \ll 1$ we have also $V_0/m^2 \ll 1$. In this approximation we can then obtain an analytical estimate of the de Sitter curvature scale H_0 in terms of V_0 and we find, from Eqs. (4.27), (4.30):

$$H_0 \simeq \left[\frac{2\,V_0}{d\,(d-1)}\right]^{1/2}\left[1+\mathcal{O}\left(\frac{V_0}{m^2}\right)\right]. \tag{4.32}$$

The range of initial conditions compatible with a final attractor corresponding to a stabilised dilaton and a final de Sitter geometry will be discussed in Sect. 4.4.3. The only difference from the previous case is that $\delta \neq 0$ and $V_0 \neq 0$.

4.4.3 A numerical study of the initial conditions

Here we provide a numerical study of the initial conditions that are necessary for reaching a post-bounce phase with a stabilised dilaton. To this purpose we restrict ourselves to the approach presented at the end of Sect. 4.16 with the potential given in Eqs. (4.16) and (4.17) in which, we recall, we have set $\alpha' = 1$. We also limit the discussion to the case $d = 3$ although similar conclusions hold for generic d.

For the numerical code we set the initial conditions at $z_{in} = 0.01$ and have checked that, as long as $z_{in} \ll 1$, the results are independent of z_{in} provided we keep κ fixed. We will then discuss how the allowed range of κ compatible with a stabilised dilaton varies as a function of A, β and q while keeping fixed values for the other parameters i.e. $\alpha = 10$, $c = 2$ and $\delta = 0.01$. Concerning this last choice, we anticipate that the attraction basins do not appreciably change if $\delta = 0$, so that the same discussion can be applied also to the case $V_0 = 0$, corresponding to the FLRW post-bouncing phase of Sect. 4.4.1. On the other hand, if δ is so large that the local minimum has a height comparable to the peaks of V, the basin of attraction can be considerably reduced.

Our first results are shown in Fig. 4.8, where we have considered the runaway potential with $q = 1$ and varied β and A. The range of κ leading to a stabilised dilaton is illustrated by the blue regions reported in the figure, showing that the lower the magnitude of the potential, the larger is the basin of attraction.

In particular, for $A = 0.01$, κ may vary of about two orders of magnitude when $\beta = 3$. This roughly corresponds to an initial amplitude of the dilaton in the

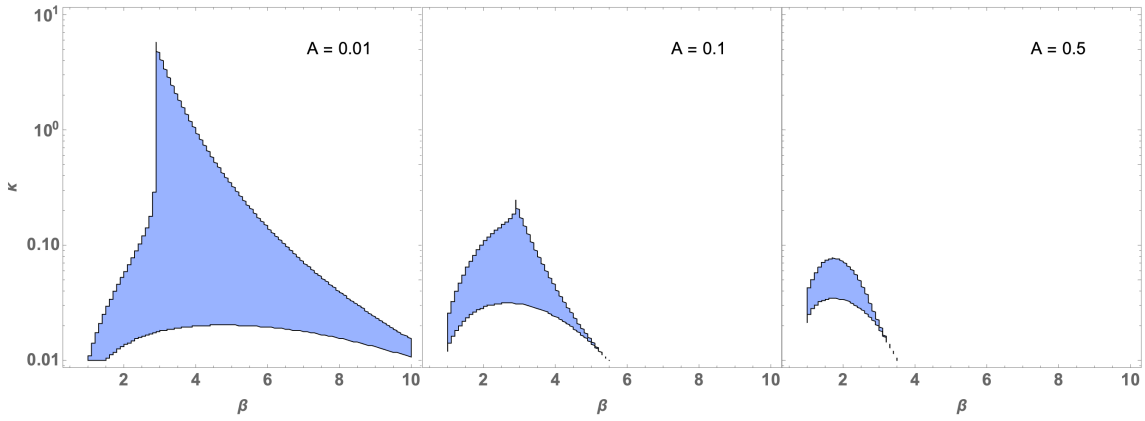

FIGURE 4.8: The blue regions represent the basins of attraction for a post-bounce phase with stabilised dilaton, with the initial condition $z = 0.01$ and κ ranging as a function of β. We have adopted a dilaton potential (4.16) with $V_0 > 0$ and fixed the parameters of the potential to be $\alpha = 10$, $c = 2$, $\delta = 0.01$ and $q = 1$. The magnitude of the potential, controlled by A, varies from smaller (left) to higher (right) values.

range $\phi \in [-15, -9.5]$. This range drops dramatically to $\phi \in [-14.6, -13.6]$ when A increases to 0.5. This case also exhibits a shift of the peak value of β to the lower value $\beta = 2$.

To give an alternative discussion, in Fig. 4.9 we have set $\beta = 3$ and varied κ as a function of A and q, exploring then the basin of attraction for different behaviours of the potential in the limit $\phi \to +\infty$. Independently of the value of A, the general trend is that a larger range of κ is achieved when the runaway potential tends to vanish at $\phi = +\infty$. On the contrary, the range of κ is suppressed when the potential in the same limit reaches its maximum.

Let us finally note that, for $d = 3$, if the initial value of κ is outside the allowed range of Fig. 4.9 then the dilaton cannot be stabilised, it "bounces back" to $-\infty$, and the final background evolution asymptotically corresponds to the time reversed of the initial one (i.e. to the second one of the three cases mentioned in Sect. 4.4, and illustrated in more detail in Appendix A). This happens because for $d = 3$ the (naively computed) effective potential in the E-frame never goes to zero as $\phi \to +\infty$. However, for higher values of d, or for different choices of the potential, the situation can be different and there are two possibilities for a non-stabilized dilaton: the dilaton runaway scenario (with growing dilaton both before and after the bounce) corresponding to the first case of Sect. 4.4, and the previous case of a bouncing dilaton.

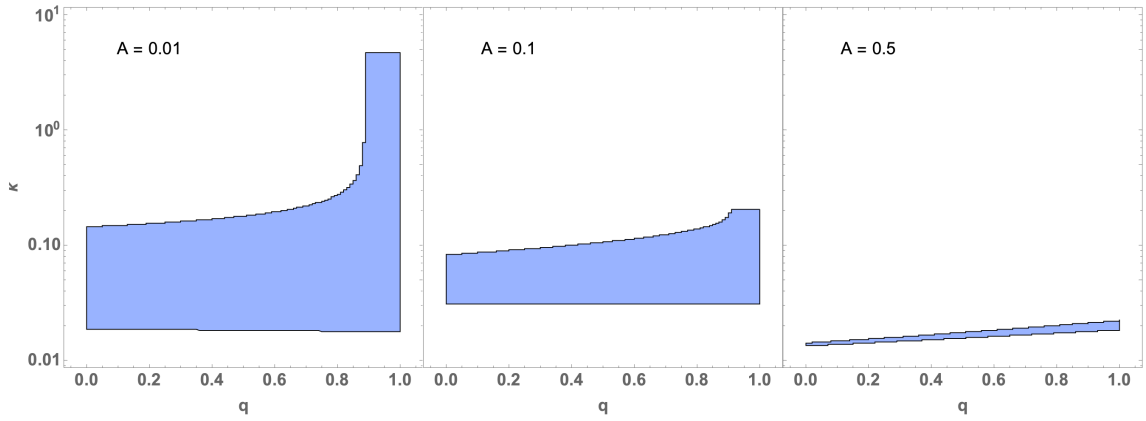

FIGURE 4.9: The blue regions represent the basins of attraction of the post-bounce phase with a stabilised dilaton with initial condition $z = 0.01$ and κ ranging as a function of q. We have adopted the dilaton potential (4.16) with $V_0 > 0$ and fixed the parameters of the potential to be $\alpha = 10$, $c = 2$, $\delta = 0.01$ and $\beta = 3$. The magnitude of the potential controlled by A varies from smaller (left) to higher (right) values.

This is illustrated in Fig. 4.10, where we have varied the number of spatial dimensions keeping fixed $A = 0.1$ and with all other parameters fixed at the same values as in Fig. 4.9. The red regions, appearing for $d > 3$ and lying outside the attraction basin, correspond to initial conditions leading to a final unbounded growth of the dilaton.

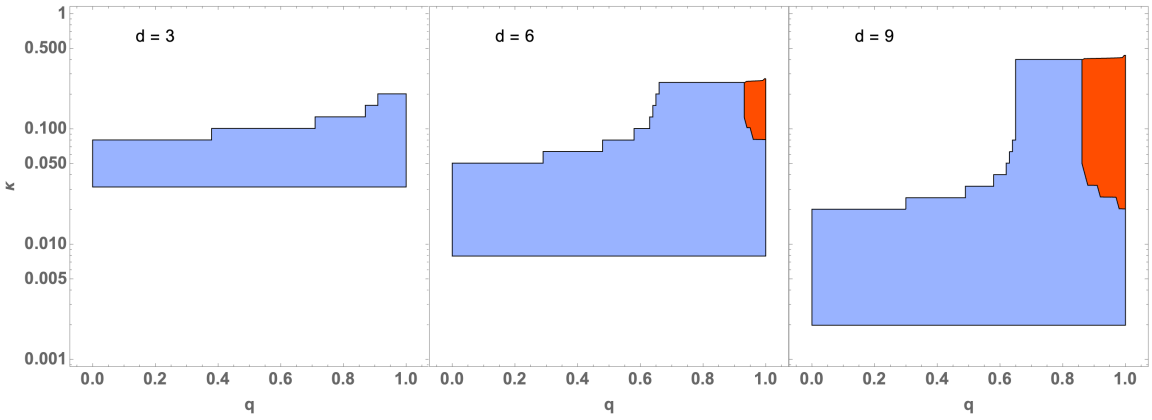

FIGURE 4.10: The same as Fig. 4.9, but we have fixed $A = 0.1$ and varied the number of spatial dimensions. The blue regions represent the basins of attraction of the post-bounce phase with a stabilised dilaton. The red regions correspond to initial conditions leading to a post bounce phase with unbounded growth of the dilaton. In the white regions, the final post bounce phase corresponds to the time reversal of the initial one.

4.5 Dilaton stabilisation and isotropisation by α' corrections and $V \neq 0$

In this Section we consider the case of a generically anisotropic initial (pre-bouncing) cosmology described by a Bianchi-I type metric, and address the question of whether, in the presence of a potential, it can also admit late time attractors with a stabilised dilaton. Furthermore, we can ask whether such attractors, when they exist, are isotropic. This is, of course, an important question since we do not want to fine-tune the initial conditions to be isotropic: like in the standard inflationary scenario we would like initial anisotropy to be washed out at late times. We remind the reader that the low-curvature Kasner-like solutions of string cosmology do not have such a property: the ratio between the initial shear and the volume-expansion rate remains essentially constant in the lowest-order solutions [112].

Taking into account α' corrections and a dilaton potential the situation can change. We know that, in principle, there are multi-trace terms in the original HZ action (and consequently in our "Hamiltonian" $h(z_i)$). Such terms, by coupling different H_i's can mimic effective "viscosity terms", which are known to be able to wash out (or limit the growth of) the initial anisotropies (see e.g. [113] and references therein). However, we have not made yet a systematic study of this possibility, also because such multi-trace terms are supposed to emerge only at order α'^4 (or higher) in the curvature expansion [76]. Fortunately, late-time isotropisation of an initial anisotropic metric can also occur as a result of the presence of $V(\phi)$ alone, which induces a non-linear dependence upon $\sum \beta_i$.

It is known, in fact, that the presence of homogeneous and isotropic sources (like, for instance, the effective radiation fluid describing the back-reaction of the amplified perturbations) may lead to a final asymptotic regime of isotropic expansion even starting from an initial regime with both expanding and contracting dimensions (see e.g. [114]). In our context the role of the homogeneous source can be played by the potential energy of the stabilised dilaton, and the implementation of such an isotropisation mechanism only requires starting from initial conditions compatible with the final stabilising attractor (see the discussion at the end of this section). In particular, the following simple result can be obtained from the relevant equations (4.9):

Whenever there is a late-time attractor with constant ϕ and z_i the attractor must be isotropic, i.e $z_i = z = z_0$, and consequently $H_i = H = H_0$.

The proof is simple: If $\phi = \phi_0 = \text{const}$ then $\dot{\overline{\phi}} = -\sum_i H_i$ and the last two Eqs. (4.9) become, in the attractor limit,

$$\left(\sum_j H_j\right) z_i + \frac{\partial V}{\partial \phi} = 0 \ ; \qquad \sum_i z_i H_i + \frac{\partial V}{\partial \phi} = 0 \, . \tag{4.33}$$

The first set of equations tells us already that z_i, at the attractor, is independent of i, which is consistent with the last equation and gives

$$d\, z_0\, H_0 = -\left(\frac{\partial V}{\partial \phi}\right)_{\phi=\phi_0} . \tag{4.34}$$

Then the first of Eqs. (4.9) gives the further constraint:

$$d^2 H_0^2 = 2\,(h)_{z_i=z_0} + 2\,V(\phi_0). \tag{4.35}$$

The system of equations (4.34), (4.35) (equivalent to the previous Eqs. (4.27) if the attraction point is located in the low-energy regime) is not over-constrained, and typically admits a finite number of solutions for ϕ_0 and z_0, and thus for H_0, once $h(z_i)$ is given.

The existence of such attractors is confirmed by a numerical study of Eqs. (4.9). Under a suitable choice of the potential and of the initial conditions one can find indeed regular solutions described, in the parametric plane $\{\dot{\overline{\phi}}, H_i\}$, by smooth curves (like those of Figures 4.3, 4.6), connecting the initial anisotropic configuration to the same final fixed point attractor. Let us give immediately an explicit example for an anisotropic, Bianchi-I type gravi-dilaton background whose dynamical evolution is controlled by this simple, α'-corrected, effective Hamiltonian:

$$h(z_i) = \frac{1}{2}\sum_i z_i^2 - c_2 \frac{\alpha'}{8} \sum_i z_i^4 . \tag{4.36}$$

For $c_2 = 2$, and in the isotropic d-dimensional limit, we recover the Hamiltonian (4.19) used in the numerical examples of the previous sections. We also note that (after taking into account the overall factor $-1/2$ of difference in the definition of h) this model of Hamiltonian exactly coincides with the model of anisotropic α'

corrections presented in Ref.[93] but *without* the multi-trace term considered in that paper.

For a better graphical illustration of the numerical solution it is convenient to consider a potential with a non-vanishing local minimum $V_0 > 0$, so that the final isotropic attraction point in the $\{\dot{\overline{\phi}}, H\}$ plane is different from the origin. We will thus consider a potential of the "runaway" type with $\delta = 0.01$, and with all the the same values of the other parameters as those used in the plot of Fig. 4.6 (except for the numerical values $A = 0.1$ and $\beta = 3$). Also, we shall work with a $d+n$-dimensional space, where d dimensions are expanding with scale factor a_1 and n dimensions are expanding with scale factor a_2, imposing, as initial conditions at $t \to -\infty$, $H_i \to 0$, that the solution satisfies the low-energy pre-big bang equation $dH_1^2 + nH_2^2 = \dot{\overline{\phi}}^2$, with $H_1 \neq H_2$ and $H_1 > 0$, $H_2 > 0$. In this limit, the solution can be explicitly written as [**?**]

$$a_i \sim (-t)^{-\gamma_i}, \qquad \gamma_i > 0, \qquad \sum \gamma_i^2 = 1, \qquad H_i = \frac{\gamma_i}{t}, \qquad \phi \sim -\left(\sum \gamma_i + 1\right) \ln(-t), \tag{4.37}$$

and we can define a constant κ, as in Sect. 4.4.1, which controls the initial conditions and is determined by the initial values of ϕ, H_1 and H_2 as follows:

$$\kappa = e^{\phi} \left[\frac{d\, H_1 + n\, H_2}{\sqrt{d+n}}\right]^{-(1+d\,\gamma_1 + n\,\gamma_2)} \sim e^{\phi} \left[\frac{d\, z_1 + n\, z_2}{\sqrt{d+n}}\right]^{-(1+d\,\gamma_1 + n\,\gamma_2)}, \tag{4.38}$$

where the last equality holds in the limit $t \to -\infty$, in analogy with what discussed in the isotropic case. The initial anisotropy is imposed by choosing $\gamma_1 = \sqrt{(1 - n\,\epsilon)/(d+n)}$ and $\gamma_2 = \sqrt{(1 + d\,\epsilon)/(d+n)}$, satisfying, for any ϵ, the Kasner condition of (4.37) i.e. $d\gamma_1^2 + n\gamma_2^2 = 1$.

The numerical results are illustrated in Fig. 4.11 for $d = 1$ and $n = 2$ (however, the results is qualitatively the same for different choices of d and n, for instance $d = 3$ and $n = 6$). As clearly shown in the figure, in spite of the very different (largely anisotropic) behaviour of the d and n spatial dimensions both before and during the bounce, after the bounce they all converge (after an oscillating epoch) to the same attraction point, controlled by the dilaton trapped in the potential minimum. Note that the two parametric curves for H_1 and H_2 plotted in the left sector of Fig. 4.11 are not topologically equivalent in the sense explained at the end of Sect. 4.3, as one is turning clockwise, the other anti-clockwise, in the

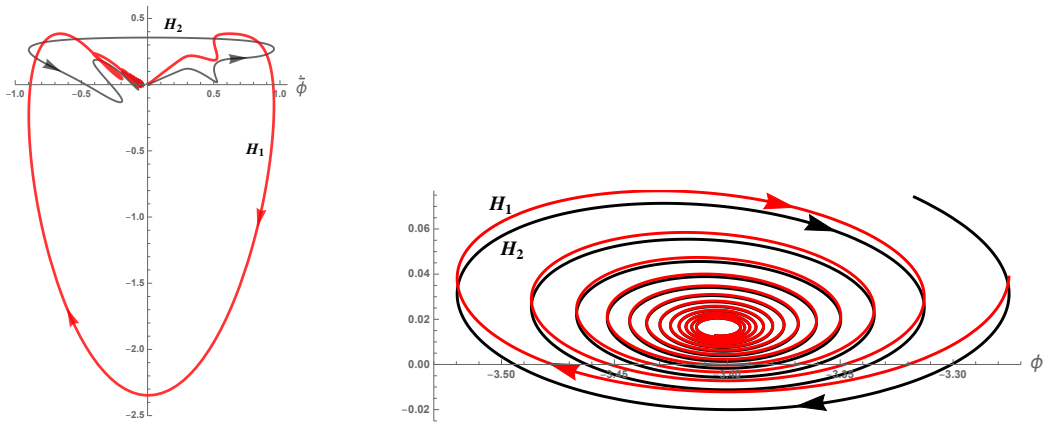

FIGURE 4.11: Left: parametric plot of a numerical solution of Eqs. (4.9) with the potential (4.16) and the Hamiltonian (4.36), written for $c_2 = 2$, $\alpha' = 1$. We have assumed an anisotropic configuration with d coordinates with momentum z_1 and n coordinates with momentum z_2. The red curve describes the evolution of the d Hubble parameters H_1, the black curve of the n Hubble parameters H_2. The initial anisotropy is specified by $\epsilon = 0.3$ and we have chosen an initial parameter (see Eq. (4.38)) $\kappa = 0.073$. Finally, we have set $d = 1$, $n = 2$, and used the following numerical values for the potential: $A = 0.1$, $\alpha = 10$, $\beta = 3$, $c = 2$, $\delta = 0.01$, $q = 1$. Right: parametric plot of $H_1(\phi)$ (red curve) and $H_2(\phi)$ (black curve) for the same numerical solution, in the asymptotic range of large positive times. The attraction point is localized at $H_0 \simeq 0.016$, $\phi_0 \simeq -3.4$, according to Eqs. (4.30)–(4.32).

parametric plane $\{\dot{\phi}, H\}$. This difference from the solutions of Sect. 4.3 is due to the presence of the dilaton potential.

The final oscillations, as well as the isotropic convergence towards the same final attractor $\{\phi_0, H_0\}$, are clearly displayed if we restrict the parametric plots to the large time limit, obtaining the behaviour of $H_1(\phi)$ and $H_2(\phi)$ illustrated in the right sector of Fig. 4.11. Given the numerical values of the potential parameters, and using Eqs. (4.30)–(4.32), we can easily compute the coordinates ϕ_0, H_0 of the attraction point, and check that they coincide with the result shown in the figure.

Let us now discuss the basin of attraction for this class of anisotropic backgrounds following the same discussion presented in Sect. 4.4.3. To this purpose we will use of the definition of κ of Eq. (4.38) to study the initial conditions in the parametric plane $\{\epsilon, \kappa\}$. For what concerns the potential, following the results obtained in the isotropic case, we will consider the illustrative example with $A = 0.01$, $\alpha = 10$, $\beta = 3$, $c = 2$ and $\delta = 0.01$, choosing $d = 1$ and $n = 2$ for the geometrical shear. This limit ϵ to range from 0 (isotropic limit) to 0.5 (highest anisotropy) in order

for the γ_i's to be real. The results we obtain are shown in Fig. 4.12 for the cases $q = 0$ and $q = 1$.

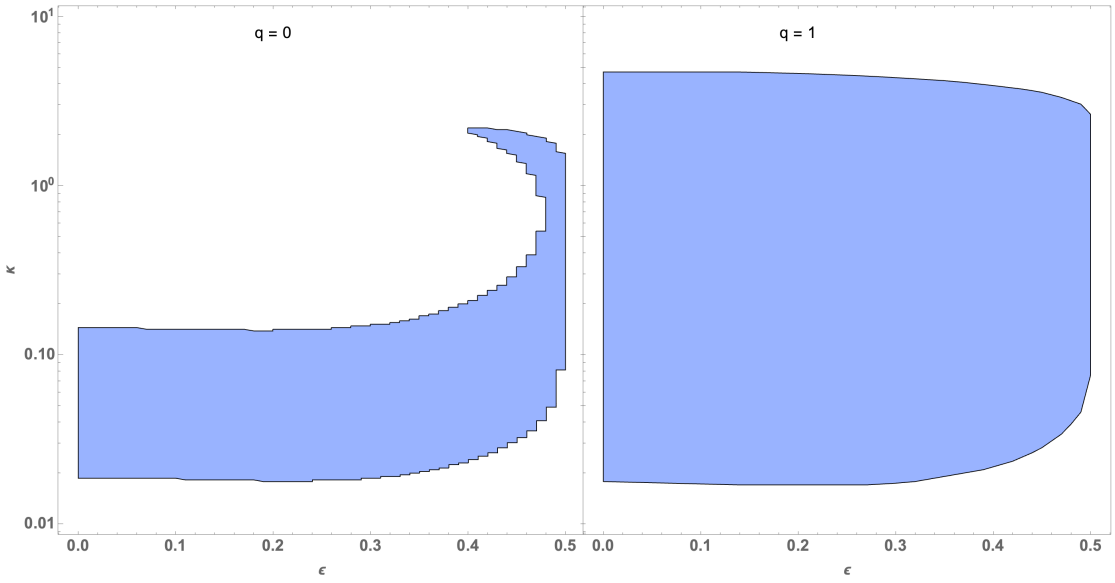

FIGURE 4.12: The blue regions represent the basins of attraction of the post-bounce phase with a stabilised dilaton and spatial isotropisation in the parametric plane $\{\epsilon, \kappa\}$ in $1+2$ dimensions. Here we have adopted the dilaton potential (4.16) with $V_0 > 0$ and fixed the parameters of the potential to be $A = 0.01$, $\alpha = 10$, $c = 2$, $\delta = 0.01$ and $\beta = 3$. We show the separate results for $q = 0$ (left) and $q = 1$ (right).

In both cases the basin of attraction remains quite stable, regardless of the amplitude of the initial geometrical shear. The case of a potential reaching its maximum at $\phi = +\infty$ ($q = 0$) looks quite intriguing, since in this case a shift towards slightly higher and multi-valued regions of κ emerges. However, the overall permitted amplitude of κ is quite insensitive to the degree of initial anisotropy: hence, the mechanism proposed to get a suitable post-bounce phase with a stabilised dilation looks pretty robust to guarantee also a final isotropisation, regardless of the amplitude of the anisotropy in the pre-bounce perturbative vacuum.

4.6 Summary and outlook

Let us start by summarizing the main results of this paper. We started by making more precise and general the reformulation given in [93] of the Hohm-Zwiebach approach to "classical" (i.e at lowest order in the string loop expansion but at all

orders in α') string cosmology. We did this by appealing to the Routhian formulation of dynamical systems in which part of the degrees of freedom are treated in a Hamiltonian approach (through the standard Legendre transform) while the rest of the variables is kept at the Lagrangian level. This approach is known to be most useful when some of the former degrees of freedom are cyclic variables leading to corresponding conservation laws. This is precisely the situation for the d scale-factors of a Bianchi I cosmology to which the HZ treatments applies. We have also stressed that, in this case, when the Hamiltonian of the system obeys the conditions spelled out in [93], the regular bouncing solutions preserve a subgroup of the $SFD \otimes T$ global symmetry, unlike the lowest-order singular ones that break it spontaneously. These regular solutions can be classified as being "self-dual".

We have then added to the Lagrangian a non-perturbative, local dilaton potential. In this case, having assumed the principle of "Asymptotic Past Triviality" formulated in [98], the above-mentioned conservation laws are still valid in the asymptotic past but are explicitly broken as soon as the potential starts to be felt. As a result we are still able to give the initial data in terms of the asymptotically conserved quantities.

After having specified the potential in terms of a few parameters we have studied numerically, and in certain simple situations analytically, the evolution of the system at late times. The main results of this analysis can be summarized as follows:

- The presence of the potential (always taken not exceeding V of order one in string units) does not seem to affect the existence or non-existence of regular bounces: this seems to depend essentially only on the form of the kinetic part of the Hamiltonian as discussed in [93]. Nonetheless, the potential can affect the cosmological evolution both during and, even more dramatically, after the bounce.

- For choices of the Hamiltonian leading to a regular bounce, the late-time cosmology is determined by the shape of the potential and by the initial conditions. Several cases are possible, not all equally interesting for physics.

- In the isotropic case we have seen three possible behaviors at late time: *i*) the dilaton can go through the potential barriers and ends up again in the same dual asymptotic solution as the one encoutered in the $V = 0$ case; *ii*)

it can be "reflected" by the potential and go back to $-\infty$ (see Appendix A for details), in which case the final cosmology is just the time-reversal of the initial one; *iii*) finally, and most interesting, the dilaton can be stabilized at the minimum of an effective potential $\widetilde{V}$ (not necessarily identical to the given V) and the late time evolution is either a matter-dominated FLRW decelerating cosmology, or a de-Sitter like accelerated expansion, depending on the value of the potential at the minimum.

- For anisotropic initial conditions the situation is similar with an extra welcome feature: whenever the dilaton is stabilized at late times, the attractor is isotropic so that the regular bounce, with the help of the potential, washes out any initial anisotropy.

For the future, several interesting questions remain to be addressed:

- To implement in these scenarios a stabilizing mechanism for the internal compact dimensions (assumed to satisfy the usual T-duality symmetries).
- To add the Kalb-Ramond $B_{\mu\nu}$ field (possibly in its axionic dual form) in order to exploit the full $O(d,d)$ symmetry of the HZ action. We recall that the axion plays an important role in the traditional pre-big bang scenario via the curvaton mechanism [110, 111]. It is not clear whether, in this new context, such a mechanism is still needed (see below).
- Computing perturbations in these new scenarios is an important but non trivial problem since it requires to break the abelian isometries of the homogeneous solutions. On the other hand, bouncing scenarios, unlike ordinary inflation, do not suffer from a transplanckian problem (see e.g. [115]) so that initial conditions can be given in the perturbative, asymptotically trivial, regime. In particular, if the final attractor is de-Sitter-like (as in Sect. (4.4.2)), we may expect various branches in the spectrum of abiabatic scalar and tensor perturbation (neglecting the isocurvature axionic perturbations discussed in [110, 111]): perturbations going out of the horizon during the initial perturbative phase of dilaton-driven inflation (leading to a steep blue spectrum [21]), those coming from the (relatively short) high curvature bounce and, finally, perturbations generated by the final frozen dilaton de Sitter phase and expected to be nearly scale-invariant.

At a more conceptual level we wish to emphasize again the two most important open issues:

1. Can the Lagrangians, Hamiltonians, or Routhians that implement a regular bounce correspond to the dimensional reduction of some general covariant action to the case of an homogeneous background with d abelian isometries? Constructing such an action, at least perturbatively in the spatial gradients, would be also most important phenomenologically, in particular for the study of perturbations.

2. This whole approach is deeply routed in the duality symmetries of string theory but we are still lacking tools for finding out whether the particular duality-invariant models that looks phenomenologically promising do follow from any specific consistent string theory.

Chapter 5

pGW Spectrum from a minimal pre-Big Bang scenario

This Chapter reports the result we obtained in [4], not including other primordial scenarios which are not discussed in this thesis.

5.1 Introduction

Gravitational waves (GWs) are one of the newest and most exciting windows into the workings of gravity. Thanks to the observation of GWs from binary systems by the LIGO-Virgo-KAGRA (LVK) network of ground-based interferometers [116, 117], and of a gravitational-wave background (GWB) $\Omega_{\rm GW}(f) \sim f^{2/3}$ of possibly astrophysical origin in the International Pulsar Timing Array (IPTA) [30, 32, 35, 36, 118–120], we have acquired a better understanding of the physics of neutron stars and black-hole binaries, as well as of the behavior of the gravitational force near these compact objects and of its propagation across cosmological distances. Both LVK and third-generation instruments such as the Laser Interferometer Space Antenna (LISA) [22–24, 121], Einstein Telescope (ET) [25, 26] and DECIGO [27–29] will be able to further probe Einstein's theory and its extensions to modified gravity and quantum gravity [122–138].

The detection of a relic primordial GWB [139–141] would be a momentous opportunity to look into the early universe and the gravitational interaction in extreme curvature or energy regimes. At the level of fundamental physics it is not easy to

construct robust cosmological models embedded in realistic scenarios of modified or quantum gravity, and even less so to obtain one such model predicting an observable signal without invoking an *ad hoc* matter field dynamics. With a first, rapid scan of the literature we may find five candidates attempting to fulfill these characteristics, heterogeneous in terms of robustness and predictive power [133]: nonlocal Starobinsky inflation [142, 143], Brandenberger–Ho non-commutative inflation [144, 145], the S-brane ekpyrotic universe [146–148], string-gas cosmology [87, 149–153] and multi-fractional inflation [154]. However, only the last four are possibly able to produce a detectable signal and only crossing the DECIGO sensitivity curve in the most optimistic cases. A sixth model of quantum gravity, nonlocal and non-minimally coupled with radiation, appeared afterwards with similar characteristics [136]. Recently, however, a more detailed exploration of the landscape of quantum and string cosmologies [24] singled out a model with a signal potentially reaching LISA and the Einstein Telescope, the pre-Big Bng scenario. The pre-Big Bang model evolving from the string perturbative vacuum, proposed long ago [20, 21, 69, 155] on the grounds of the string cosmological equations, which enjoy T-duality [71] and may be characterized by a non-singular bounce thanks to all-orders (higher-curvature) α' corrections [5, 93]. This model is based on the modified gravitational dynamics uniquely fixed, in principle, by the string unification of all fundamental interactions, at all energy scales including their quantum limit; however, it also contains phenomenological aspects concerning the (presently unknown) details of the dilaton dynamics in the strong coupling regime. In any case, the model above is one among the very few in quantum gravity possibly able to produce a GWB, arising from the vacuum fluctuations of the metric tensor, with high enough amplitude in the frequency range of third-generation detectors. The model is characterized by an initial phase of growing curvature scale (described by a contracting kinematics with the metric of the Einstein frame), preceding the final decelerated expansion and passing through a non-singular bounce of spacetime curvature. The presence of accelerated contraction ($\dot{a} < 0$, $\ddot{a} < 0$, $\dot{H} < 0$) or of super-inflationary expansion ($\dot{a} > 0$, $\ddot{a} > 0$, $\dot{H} > 0$) in different metric frames is responsible for a strong blue tilt in the primordial tensor spectrum (i.e., growing with the frequency).

For the model an approximate GWB profile is known (first computed in [72, 73, 156, 157] and recently discussed in [155]). The GWB , however, has not been studied systematically so far, and the question of whether its signal can reach LISA, ET or DECIGO remains open. It is the purpose of this Chapter to give an

answer to these questions and to complement the analysis of [133] done for other models of quantum gravity with a blue primordial tensor spectrum.
We find that within the theoretically allowed parameter space, the GWB of the pre-Big Bang model reaches the LISA and ET observational window while respecting present bounds. In all plots, we use the latest ET sensitivity curve for a single 10 km triangular interferometer with a signal-to-noise ratio 1 and a one-year observation run [26, 158]. To the best of our knowledge, the pre Big-Bang model and those studied in [133] are the only ones motivated by quantum gravity and generating a detectable GWB directly from the primordial tensor sector. Recently, another bouncing model was proposed where curvature perturbations evolving through a bounce can trigger the formation of primordial black holes and also induce a GWB signal with high amplitude crossing also the LISA and ET windows [159]. However, we do not consider scalar-induced GWBs here.

5.1.1 Basic formulæ

Primordial GWs can be described by a small set of quantities and observables, independently of the underlying model. We denote the primordial tensor and scalar spectra as, respectively, $\mathcal{P}_{\rm t}(k)$ and $\mathcal{P}_{\rm s}(k)$, where k is the comoving wavenumber. From here, one calculates the tensor-to-scalar ratio at any given pivot scale $k = k_*$,

$$r \coloneqq \frac{\mathcal{P}_{\rm t}}{\mathcal{P}_{\rm s}}\,, \tag{5.1}$$

as well as the tensor and scalar spectral indices

$$n_{\rm t} \coloneqq \frac{d\ln\mathcal{P}_{\rm t}(k)}{d\ln k}\,, \qquad n_{\rm s} - 1 \coloneqq \frac{d\ln\mathcal{P}_{\rm s}(k)}{d\ln k}\,. \tag{5.2}$$

The current estimate for the scalar amplitude is $\mathcal{P}_{\rm s}(k_*) \approx 2.1\times10^{-9}$ at the cosmic microwave background (CMB) scale $k_* = 0.05\,\mathrm{Mpc}^{-1}$ [160], while $n_{\rm s} = 0.9649 \pm 0.0042$ at 68% confidence level at the same pivot scale, assuming $dn_{\rm s}/d\ln k = 0$ [161, 162]. The upper bound on (5.1) is $r(k_*) < 0.036$ at the same scale at 95% confidence level [163].

In general, the amplitude of the GWB is defined as

$$\Omega_{\rm GW}(k,\tau_0) = \frac{1}{\rho_{\rm crit}(\tau_0)}\frac{d\rho_k(\tau_0)}{d\ln k}\,, \tag{5.3}$$

where τ_0 is the present value of the conformal time τ, defined in terms of the cosmic time t as $\tau \coloneqq \int dt/a(t)$, where $a(t)$ is the scale factor, $\rho_{\rm crit} = 3M_{\rm Pl}^2 H^2$ is the critical density, $M_{\rm Pl}^2 = (8\pi G)^{-1}$ is the reduced Planck mass and $\rho_k(\tau_0)$ is the energy density of the k-th Fourier mode of tensor perturbations amplified by the given model of the early universe and evaluated at the present time τ_0. For GWs generated by tensor perturbations, the GWB spectral shape can be recast as

$$\Omega_{\rm GW}(f) = \frac{k^2}{12 a_0^2 H_0^2} \mathcal{P}_{\rm t}(k)\, \mathcal{T}^2(k, \tau_0)\Big|_{k=2\pi f}, \tag{5.4}$$

where $f = k/(2\pi)$ is the GW frequency measured in Hz, a_0 is the scale factor today ($a_0 = 1$), H_0 is the value of the Hubble parameter today and $\mathcal{T}(k, \tau_0)$ is the transfer function encoding how the primordial spectrum evolved after horizon crossing until today [164–166]. The expressions below are valid for any model where observable perturbations have re-entered the horizon in the past, either because they were originally generated inside the horizon and were later expelled out (e.g., by inflation), or because they were generated outside the horizon in the first place.

5.2 Minimal pre-Big Bang pGW spectrum

A possible example of primordial tensor perturbations peaked at high frequencies, with a strongly blue-tilted low-frequency regime of spectrum, is provided by the so-called Pre-Big-Bang (PBB) scenario [20, 21], based on the scale-factor duality of the string cosmology equations [71]. Such symmetry is a peculiar property of string theory, and is a crucial ingredient not only to fix the slope of the primordial spectrum [72, 156, 157] but also, as confirmed by recent results [5, 93], to implement a smooth transition from the initial growing curvature (PBB) regime to the standard regime of decreasing curvature evolution. According to this model, the evolution of our Universe, characterized by decelerated expansion (at intermediate times), decreasing temperature and curvature, weak gravitational coupling, should be preceded in time by an almost specularly symmetric phase of accelerated expansion, increasing curvature, increasing density and temperature and growing coupling. Such a dual counterpart of the present one describes a "pre-big-bang" evolution from a flat, cold, empty initial state with negligible interactions to a final high-curvature, high-energy, explosive bounce, marking the transition to

the more standard cosmological regime (see, e.g., [167] for a recent non-technical introduction, and [60] for a more detailed and complete discussion).

Here we recall the derivation of the associated GWB in a self-contained way. We shall introduce the spectral energy density of the relic GW radiation present today inside our cosmic horizon, and produced by a simple model of PBB scenario which satisfies all present observational constraints and depends on four constant parameters (see also [155]). Two of these parameters control the inflationary growth of the scale factor and of the string coupling in the high-energy regime preceding the bounce; the other ones control the beginning and the end of the axion-dominated phase occurring after the curvature bounce. We recall that the presence of a dust-like phase dominated by the oscillations of the Kalb–Ramond axion is in general needed in the PBB scenario to obtain (via the curvaton mechanism) a flat spectrum of scalar metric perturbations [110, 111].

At present, the first two parameters are largely arbitrary, while the other two may vary in a rather small range of values. We stress, however, that the dependence of the amplitude of the GWB on the full set of the above four parameters is given and discussed, for the first time, in this paper. We have neglected a possible further parameter, the effective propagation speed of tensor perturbations during the high curvature string phase, as it seems to have small effects on the energy density of the GW spectrum.[1]

Let us now compute the spectral energy density in critical units of the GWB, eq. (5.3) with $k_0 \leqslant k \leqslant k_1$, in such a way that all modes k of eq. (5.3) satisfy the condition $k\tau_0 \gtrsim 1$ (i.e., they are all inside our present Hubble horizon, $k \gtrsim k_0 = \tau_0^{-1}$). The highest mode $k_1 = \tau_1^{-1}$ is the maximum amplified frequency crossing the horizon just at the end of the phase of PBB inflation. Higher frequency modes ($k \gg k_1$) can, in principle, be included into Eq. (5.3), but their amplitude is exponentially suppressed [169–171] and their contribution to $\Omega_{\rm GW}$ is negligible. For the explicit computation of $\Omega_{\rm GW}$, two comments must be made.

The first is that, even if we are working in general with a higher-dimensional space-time manifold (an unavoidable choice in the string theory context), we are mainly interested in the tensor perturbations of the four-dimensional metric, $\delta g_{\mu\nu} = h_{\mu\nu}$, assuming that the extra spatial dimensions are today compactified with frozen

[1] On the contrary, the effective sound speed of scalar curvature perturbations and of axion perturbations is important for the production of primordial black holes, as discussed, e.g., in [168] for the PBB scenario.

dynamics. However, this does not mean that we are neglecting the possible effects of the higher-dimensional geometry during its initial, non-trivial evolution: indeed, all such higher-dimensional contributions will be included into the canonical equation which controls the dynamics of $h_{\mu\nu}$ [21, 60, 155].

The second point is that, as usual, we are interested in the contributions to $\Omega_{\rm GW}$ arising from the cosmological amplification of the quantum vacuum fluctuations of the metric tensor. This implies that we can describe the amplification of tensor perturbations as a quantum (or semi-classical) field-theory process of production of pairs of gravitons from the initial vacuum state (see, e.g., [60]) and we can write, for each mode k, the differential energy density of the amplified perturbations as follows:

$$d\rho_k(\tau_0) = 2k\,\langle n_k(\tau_0)\rangle\,\frac{d^3\boldsymbol{k}}{(2\pi)^3} = \frac{k^4}{\pi^2}\,\langle n_k(\tau_0)\rangle\,d\ln k\,, \tag{5.5}$$

where 2 is the number of polarization states and $\langle n_k(\tau_0)\rangle$ the number density of produced gravitons at the final epoch τ_0. The last equality follows from assuming an isotropic final distribution.

To obtain $\langle n_k\rangle$ and then $\Omega_{\rm GW}$, we need now to solve the evolution equation for the Fourier component of the (Mukhanov-Sasaki) canonical variable, $v_k(\tau)$, defined by putting in canonical form the quadratic action for the tensor fluctuation mode h_k [12]:

$$v_k'' + \left(k^2 - \frac{\xi''}{\xi}\right) v_k = 0\,. \tag{5.6}$$

Here a prime denotes differentiation with respect to the conformal time, $v_k = \xi h_k$ and $\xi(\tau)$ is the so-called "pump field" which controls, according to the above equation, the dynamics of the perturbation modes in the given background.

In the model we are considering, the background may be approximated as a sequence of various cosmic phases, and in each of them the pump field ξ is characterized by a simple power-law behavior. In particular, in the initial PBB regime $-\infty < \tau \leqslant -\tau_1$, starting asymptotically from the string perturbative vacuum and approaching the curvature bounce at $\tau = -\tau_1$, we have two different phases with the following (canonically normalized) pump field behavior [155]:

$$\xi \sim \frac{M_{\rm Pl}}{\sqrt{2}}(-\tau)^{1/2}, \qquad \tau < -\tau_s\ ; \qquad\qquad \xi \sim \frac{M_{\rm Pl}}{\sqrt{2}}(-\tau)^{\beta-1}, \qquad -\tau_s < \tau < -\tau_1\,. \tag{5.7}$$

The parameter β describes the high-energy growth of the dilaton and the dynamics of the internal dimensions, while the time scale τ_s is a free parameter which marks the transition from the low-energy initial phase to a possible late-time attractor, where spacetime curvature stays frozen at the value controlled by the fundamental string mass scale [172]. In both phases, the evolution of the pump field takes into account not only, as usual, the inflationary growth of the scale factor but also the additional string-theory effects [21, 60], such as the dynamics of the extra dimensions and the growth of the string coupling controlled by the scalar dilaton field (see also [73, 172]).

In the subsequent post-bouncing regime $-\tau_1 < \tau \leqslant \tau_0$, the cosmic evolution is decelerated and we may have in principle three phases with the following pump-field behavior [155]:

$$\xi \sim \frac{M_{\rm Pl}}{\sqrt{2}}\,\tau, \quad -\tau_1 < \tau < \tau_\sigma; \quad \xi \sim \frac{M_{\rm Pl}}{\sqrt{2}}\,\tau^2, \quad \tau_\sigma < \tau < \tau_d; \quad \xi \sim \frac{M_{\rm Pl}}{\sqrt{2}}\,\tau, \quad \tau_d < \tau < \tau_{\rm eq}. \tag{5.8}$$

Here we are assuming that the extra-dimensional geometry and the string coupling (i.e., the dilaton) are frozen after the bounce, so that the pump field simply coincides with the scale factor. Here, again, we have two free parameters: the time scale τ_σ, marking the beginning of the dust-like phase dominated by the axion oscillations, and the time scale τ_d, marking the epoch of axion decay associated with the conventional reheating (source of the CMB radiation that we are presently observing) and corresponding to the beginning of the standard post-big-bang evolution[2].

As discussed in previous papers [110, 111, 155], instead of τ_σ and τ_d we can conveniently use as parameters the corresponding curvature scales $H_\sigma \coloneqq H(\tau_\sigma)$ and $H_d \coloneqq H(\tau_d)$ which can be expressed in terms of the (unknown) mass m of the Kalb–Ramond axion and of its initial amplitude σ_i after the bounce:

$$H_\sigma \simeq m\left(\frac{\sigma_i}{M_{\rm Pl}}\right)^4, \qquad\qquad H_d \simeq m\left(\frac{m}{M_{\rm Pl}}\right)^2. \tag{5.9}$$

For a consistent model, the allowed values of the parameters m and σ_i must satisfy the scale hierarchy $M_{\rm Pl} \gtrsim H_1 \gtrsim H_\sigma \gtrsim H_d$. In addition, we have the obvious

[2]There is also the final matter-dominated phase completing the cosmic evolution from the equality epoch $\tau_{\rm eq}$ down to the present epoch τ_0. However, such a phase only affects the very low frequency modes $k < k_{\rm eq} = \tau_{\rm eq}^{-1}$, whose amplitude is so small (because of the strongly blue-tilted spectrum) to be fully negligible for this thesis.

condition $H_d > H_N$, where $H_N \sim (1\,\mathrm{Mev})^2/M_{\rm Pl}$ is the nucleosynthesis scale of the standard cosmological scenario.

Given the full model of background evolution from the initial state at $\tau \to -\infty$ down to the present epoch τ_0, and given the power-law behavior of ξ in the various phases, we can now work in the so-called "sudden approximation" [170] by imposing on the pump field to be continuous at the transitions scales, and solving, in each phase, the canonical equation (5.6). We recall that, in general, for a pump field given by $\xi = (M_{\rm Pl}/\sqrt{2})|\tau/\tau_1|^\alpha$, the exact solution for h_k obtained from (5.6) can be written in terms of the first- and second-kind Hankel functions, $H_\nu^{(1)}$, $H_\nu^{(2)}$, as

$$h_k(\tau) = \frac{v_k}{\xi} = \left(\frac{2\tau_1}{M_{\rm Pl}^2}\right)^{\frac{1}{2}} \left|\frac{\tau}{\tau_1}\right|^\nu \left[A_+(k) H_\nu^{(2)}(k\tau) + A_-(k) H_\nu^{(1)}(k\tau)\right], \tag{5.10}$$

where $\nu = -\alpha + 1/2$. The complete solution for $h_k(\tau)$, describing its evolution from $-\infty$ to τ_0, is then obtained by solving the canonical equation in the various phases and matching h_k and h_k' at the transition scales.

In our model, in particular, we have four transitions (at τ_s, τ_1, τ_σ, τ_d), which means five different phases of background evolution (see eqs. (5.7) and (5.8)), which implies five different solutions like (5.10), and thus ten different coefficients $A_\pm(k)$ to be determined at the various epochs. The continuity of h_k and h_k' only gives eight conditions. The two remaining conditions are obtained by imposing on the canonical variable to initially describe a positive-frequency mode normalized to the quantum fluctuations of the Bunch–Davies vacuum, namely, by imposing $v_k = (1/\sqrt{2k})\exp(-ik\tau)$ for $\tau \to -\infty$: this implies (using the large-argument limit of the Hankel functions [60]) $A_- = 0$ and $A_+ = \sqrt{\pi/4}$ for the solution describing perturbations in the initial regime $\tau \to -\infty$.

With such a canonical normalization, the sought value of the number density $\langle n_k(\tau_0)\rangle$ of produced gravitons is then automatically obtained from the coefficient $A_-(k)$ of the first-kind Hankel function describing the perturbation mode $h_k(\tau)$ in the final regime $\tau \to +\infty$ (actually, for our purpose, in the limit $\tau \to \tau_0$). More precisely, one finds (see, e.g., [60])

$$\langle n_k(\tau_0)\rangle = \frac{4}{\pi}\,|A_-(k)|_{\tau=\tau_0}\,. \tag{5.11}$$

By performing the above computation and varying k in the allowed frequency range we find that there are, in principle, four different branches of the energy density spectrum (5.3), (5.5), depending on the epochs of horizon crossing of the various modes. Noting that the axion-dominated phase is expected to occur soon after the bounce, in order to have a short duration with respect to the preceding high-curvature string phase (namely, $\tau_d/\tau_\sigma \ll \tau_1/\tau_s$) we may consistently assume that all modes re-entering the horizon before, during, or soon after the axion phase are amplified modes leaving the horizon during the high-curvature string phase. This means, in other words, that we can work with the following hierarchy of wave-number scales: $k_1 \geqslant k_\sigma \geqslant k_d > k_s$, where $k_i \coloneqq \tau_i^{-1}$ is the limiting frequency of a mode crossing the horizon at the transition epoch τ_i.

To obtain the explicit (parameter-dependent) form of the GWB, it is useful to first compute the frequency ratios of the four scales k_i. We note that in our model there are two phases of radiation-dominated evolution (i.e., $a \sim \tau \sim H^{-1/2}$) for $-\tau_1 < \tau < \tau_\sigma$ and for $\tau > \tau_d$, one phase of matter-dominated evolution (i.e., $a \sim \tau^2 \sim H^{-2/3}$) for $\tau_\sigma < \tau < \tau_d$, and one phase where the string frame scale factor undergoes a de Sitter-like evolution (i.e., $a \sim |\tau|^{-1}$) for $-\tau_s < \tau < -\tau_1$. By defining the convenient parameters

$$z_s \coloneqq \frac{\tau_s}{\tau_1} = \frac{k_1}{k_s}, \qquad z_\sigma \coloneqq \frac{\tau_\sigma}{\tau_1} = \frac{k_1}{k_\sigma}, \qquad z_d \coloneqq \frac{\tau_d}{\tau_1} = \frac{k_1}{k_d}, \tag{5.12}$$

controlling the time extension of the pre-bouncing high curvature regime and of the two post-bouncing, non-standard phases, we find[3] (using eq. (5.9))

$$\begin{aligned}
z_\sigma &= \frac{k_1}{k_\sigma} = \frac{H_1 a_1}{H_\sigma a_\sigma} = \left(\frac{H_1}{H_\sigma}\right)^{\frac{1}{2}} \simeq \left(\frac{H_1}{M_{\rm Pl}}\right)^{\frac{1}{2}} \left(\frac{m}{M_{\rm Pl}}\right)^{-\frac{1}{2}} \left(\frac{\sigma_i}{M_{\rm Pl}}\right)^{-2}, \\
\frac{z_d}{z_\sigma} &= \frac{k_\sigma}{k_d} = \frac{H_\sigma a_\sigma}{H_d a_d} = \left(\frac{H_\sigma}{H_d}\right)^{\frac{1}{3}} \simeq \left(\frac{m}{M_{\rm Pl}}\right)^{-\frac{2}{3}} \left(\frac{\sigma_i}{M_{\rm Pl}}\right)^{\frac{4}{3}}, \\
\frac{z_s}{z_d} &= \frac{k_d}{k_s} = \frac{k_d}{k_1}\frac{k_1}{k_s} = z_s \frac{H_d}{H_1}\frac{a_d}{a_\sigma}\frac{a_\sigma}{a_1} \simeq z_s \left(\frac{H_1}{M_{\rm Pl}}\right)^{-\frac{1}{2}} \left(\frac{m}{M_{\rm Pl}}\right)^{\frac{7}{6}} \left(\frac{\sigma_i}{M_{\rm Pl}}\right)^{\frac{2}{3}}.
\end{aligned} \tag{5.13}$$

[3]Conventions: we denote with ω the usual (time-dependent) proper frequency evolving in time like the inverse scale factor, $\omega(t) \equiv k/a(t)$. Hence, the proper frequency crossing the horizon at the given time t_1, $\omega_1 = H_1 = H(t_1)$, and evaluated at a general time t, is given by $\omega_1(t) = H(t_1)a(t_1)/a(t) \equiv H_1 a_1/a$. The time-dependent scale factor obviously disappears in the ratios of two frequency scales so that, for instance, $\omega_1/\omega_\sigma = H_1 a_1/H_\sigma a_\sigma = k_1/k_\sigma$.

By inverting the above relations we can also express σ_i and m in terms of H_1 and of the parameters z_s, z_σ and z_d as follows:

$$\frac{\sigma_i}{M_{\rm Pl}} \simeq \left(\frac{H_1}{M_{\rm Pl}}\right)^{\frac{1}{6}} z_d^{\frac{1}{4}} z_\sigma^{-\frac{7}{12}}\,, \qquad\qquad \frac{m}{M_{\rm Pl}} \simeq \left(\frac{H_1}{M_{\rm Pl}}\right)^{\frac{1}{3}} z_d^{-1} z_\sigma^{\frac{1}{3}}. \tag{5.14}$$

Let us now give an example of full computation of the spectral distribution (5.3) for the highest frequency branch of the spectrum ($k_\sigma < k < k_1$) and for a generic epoch τ (late enough, however, to have all such modes inside the horizon, $k\tau \gg 1$). To this purpose, let us express the energy density of the perturbations in terms of their (time-dependent) proper frequency ω scaling in time like the inverse scale factor, $\omega(\tau) = k/a(\tau)$. From eqs. (5.3) and (5.5), we obtain

$$\Omega_{\rm GW}(k,\tau) = \frac{\omega^4}{\pi^2 \rho_{\rm crit}(\tau)} \langle n_\omega(\tau)\rangle\,, \qquad\qquad k_\sigma < k < k_1. \tag{5.15}$$

The modes we are considering are amplified by the pump field (5.7) of the high-curvature string phase, and the canonical equations (5.10), (5.11) then give [60]

$$\langle n_\omega(\tau)\rangle \simeq \left(\frac{\omega}{\omega_1}\right)^{-1-|3-2\beta|} = \left(\frac{k}{k_1}\right)^{-1-|3-2\beta|}. \tag{5.16}$$

Also, it is convenient to express the critical density $\rho_{\rm crit}$ in terms of the critical fraction of radiation energy density, $\Omega_{\rm r} = \rho_r/\rho_{\rm crit}$, so that, referring to radiation produced at the axion-decay scale, we have

$$\rho_{\rm crit}(\tau) = \frac{\rho_r(\tau)}{\Omega_{\rm r}(\tau)} = \frac{3M_{\rm Pl}^2 H_d}{\Omega_{\rm r}(\tau)} \left(\frac{a_d}{a}\right)^4. \tag{5.17}$$

Finally, for each mode of proper frequency $\omega(\tau)$ we can express its ω^4 contribution to eq. (5.15) as

$$\omega^4 = \left(\frac{k}{a}\right)^4 = \left(\frac{k}{k_1}\right)^4 \left(\frac{H_1 a_1}{a}\right)^4. \tag{5.18}$$

Combining all these results and using eq. (5.9) we then find, for the considered band of frequency,

$$\Omega_{\rm GW}(k,\tau) = \frac{\Omega_{\rm r}(\tau)}{\Omega_{\rm r0}}\,\Omega_{\rm PBB} \left(\frac{k}{k_1}\right)^{3-|3-2\beta|}, \qquad\qquad k_\sigma < k < k_1, \quad \tau > \tau_d, \tag{5.19}$$

where $\Omega_{\rm r0} \equiv \Omega_{\rm r}(\tau_0) \approx 4.15 \times 10^{-5} h^{-2}$ is the present critical fraction of radiation energy density (including neutrinos) and we have defined the constant (parameter

dependent) dimensionless amplitude

$$\Omega_{\rm PBB} \coloneqq \Omega_{\rm r0}\left(\frac{H_1}{M_{\rm Pl}}\right)^2\left(\frac{mM_{\rm Pl}}{\sigma_i^2}\right)^{4/3} = \Omega_{\rm r0}\left(\frac{H_1}{M_{\rm Pl}}\right)^2\left(\frac{z_\sigma}{z_d}\right)^2 . \tag{5.20}$$

For simplicity we have absorbed all numerical factors of order of unity into the unknown scale H_1. Obviously, the result (5.19) is also valid if applied in particular to the present epoch $\tau = \tau_0$, with $\Omega_{\rm r}(\tau) = \Omega_{\rm r0}$.

By following the same procedure for the other (lower frequency) branches of the spectrum, and turning to the more conventional frequency variable[4] $f = k/(2\pi)$, we obtain that the full GWB can be written synthetically as

$$\Omega_{\rm GW}(f) = \begin{cases} \Omega_{\rm PBB}\left(\dfrac{f}{f_1}\right)^{3-|3-2\beta|}, & f_\sigma \lesssim f \lesssim f_1 \\ \Omega_{\rm GW}(f_1)\left(\dfrac{f_\sigma}{f_1}\right)^{3-|3-2\beta|}\left(\dfrac{f}{f_\sigma}\right)^{1-|3-2\beta|}, & f_d \lesssim f \lesssim f_\sigma \\ \Omega_{\rm GW}(f_\sigma)\left(\dfrac{f_d}{f_\sigma}\right)^{1-|3-2\beta|}\left(\dfrac{f}{f_d}\right)^{3-|3-2\beta|}, & f_s \lesssim f \lesssim f_d \\ \Omega_{\rm GW}(f_d)\left(\dfrac{f_s}{f_d}\right)^{3-|3-2\beta|}\left(\dfrac{f}{f_s}\right)^{3}, & f \lesssim f_s \end{cases} \tag{5.21}$$

where the three ratios of frequency scales f_σ/f_1, f_d/f_σ, f_s/f_d can be expressed in terms of the parameters z_s, z_σ, z_d (or m, σ_i, H_1) according to eq. (5.13). We may note, for a better explanation of the above spectrum, that the higher frequency regime with interval $f\,\epsilon\,[f_\sigma, f_1]$ concerns modes which exit the horizon in the string phase and re-enter in an early radiation-dominated phase, while modes with $f\,\epsilon\,[f_d, f_\sigma]$ exit in the string phase but re-enter in a matter-dominated phase: hence the transfer function is different and yields the additional f^{-2} spectral factor for $\beta \approx 0$. Also, modes with $f\,\epsilon\,[f_s, f_d]$ exit the horizon in the same phase as before and re-enter in the standard big-bang radiation phase. Finally, the lowest frequency modes $f < f_s$ with the strongly blue spectrum $\Omega \sim f^3$ exit the horizon in a low-energy phase which is stiff and contracting in the Einstein frame, with pump field $\xi(\tau) \sim (-\tau)^{1/2}$. Very simple plots for the time evolution of the effective

[4]Note that the initial normalisation of the spectrum to the quantum fluctuations of the vacuum, leading to the results (5.11), (5.15), is performed as usual in units $\hbar = 1$. Hence, $\omega = 2\pi f$.

horizon, illustrating how modes belonging to different spectral regimes may cross (in and out) the horizon, can be found, for instance, in [58, 60].

It is also important to note that, for $f > f_1$, the spectrum is exponentially suppressed as $\Omega_{\rm GW}(f) = \Omega_{\rm PBB}\exp\{[-(f-f_1)/f_1\}]$, so that a smooth interpolation of all the branches can be given by the following expression proven in Appendix B:

$$\begin{aligned}\Omega_{\rm GW}(f) &= \Omega_{\rm PBB}\, f^3 \left(f^2+f_s^2\right)^{-\frac{|3-2\beta|}{2}} \left(f^2+f_d^2\right)^{-1} \left(f^2+f_\sigma^2\right) \left(f^2+f_1^2\right)^{\frac{|3-2\beta|-3}{2}} \\ &\quad \times \exp\left\{\left(-\frac{f}{f_1}+\arctan\frac{f}{f_1}\right)\right\}. \end{aligned} \tag{5.22}$$

The smoothing of the piecewise profile (5.21) does not change the underlying scenario because the transition epochs from one phase to another are of very short, negligible duration compared with the time extension of such phases.

There are now two important points to be stressed. The first is that the overall GWB, and in particular the peak amplitude, is controlled not only by the bouncing curvature scale H_1 but also by the parameters m and σ_i and, thus, by the details of the post-bounce evolution. This implies, in particular, that the amplitude may result strongly suppressed with respect to the natural value fixed by the fundamental string mass scale $M_{\rm s}$, even for the highest frequency modes crossing the horizon at such scale.

The second point concerns the number of parameters controlling the shape of the spectrum. There are four time (or curvature) scales and one dimensionless number, the power β of the pump field in the string phase; see (5.7). However, these five parameters must satisfy an important phenomenological condition. The PBB scenario we are considering, in fact, besides producing relic GW radiation must also produce a suitable large-scale background of scalar curvature perturbations with a nearly flat spectrum, in order to be compatible with CMB observations.

This is known to be possible via the curvaton mechanism [75, 173, 174] triggered by the Kalb–Ramond axion [110, 111], but this imposes constraints on the previous spectral parameters [155]. In particular, the primordial scalar amplitude $\mathcal{P}_{\rm s}(k_*)$ and spectral index $n_{\rm s}$ must be in agreement with the observational results reported below (5.2). By imposing such conditions on the scalar perturbations produced by the PBB model we are considering, whose spectrum is controlled by the same set of parameters as the GWB of (5.21) or its smooth version (5.22), we can then eliminate one of the previous five parameters and fix, for instance, the transition

scale H_1 as a function of z_s, β, m, σ_i and of the two observables $\mathcal{P}_{\rm s}(k_*)$ and $n_{\rm s}$. This is done in Appendix C.1, where we conclude that the parameter space of the model is

$$\{\beta, z_s, z_d, z_\sigma\}\,. \tag{5.23}$$

Without assuming any prior on these parameters, one can plot (5.22) and find some general trends. For instance, the larger β, the smaller the amplitude, so that, in practice, only values of β near zero generate a detectable signal. Also, as the parameter z_d increases, the spectral shape is squeezed and the peak becomes narrower but neither its frequency nor its amplitude vary appreciably. On the other hand, the parameter z_σ changes the shape but not much the frequency peak or the amplitude, while the parameter z_s which affects both the range and the amplitude of the intermediate plateau or slope.

However, the four parameters (5.23) do obey a non-trivial set of theoretical priors determined in Appendix C.2. Within this space, in Appendix C.2.1 we circumscribe the region in the parameter space where the peak amplitude of the GWB is maximized. This happens for $\beta = 0$, $\sigma_i = M_{\rm Pl}$, z_σ determined by eq. (C.13) and the values of z_s and z_d shown in Fig. 5.1.

Any given set of parameters z_s, z_d, z_σ satisfying eq. (C.13) together with all other constraints, and implementing the additional limiting condition $\log_{10}(H_1/M_{\rm Pl}) \approx -3.29$, produces a GWB with a peak of maximum intensity $\Omega_{\rm GW}^{\rm max} \sim 10^{-11} - 10^{-10}$ (eq. (C.15)). For phenomenological reasons, however, we are interested not only in the maximal amplitude but also in the maximal extension in frequency (in particular, towards small frequencies) of the allowed spectral region. This last property can be easily obtained by choosing, among all possible combinations of parameters producing the maximal amplitude, the combination selecting the maximal allowed value of z_s (i.e., $z_s \approx 10^{22.3}$), together with the corresponding minimal value of z_d (i.e., $z_d \approx 10^{2.19}$), together with the associated minimal value of z_σ (i.e., $z_\sigma \approx 1$, according to eq. (C.13)).

The GWB (5.22) with the above numerical values of the parameters (satisfying $\sigma_i = M_{\rm Pl}$) and with $\beta = 0$ provides the border of the shaded area in Fig. 5.2 within which the primordial GWB of pre-big-bang cosmology with maximal peak amplitude falls. Such region respects known constraints obtained from the observations of millisecond pulsars [175], which imply $\Omega_{\rm GW} \lesssim 10^{-8}$ at a frequency scale $f \sim 10^{-8}$ Hz. It is also consistent with large-scale CMB constraints on the

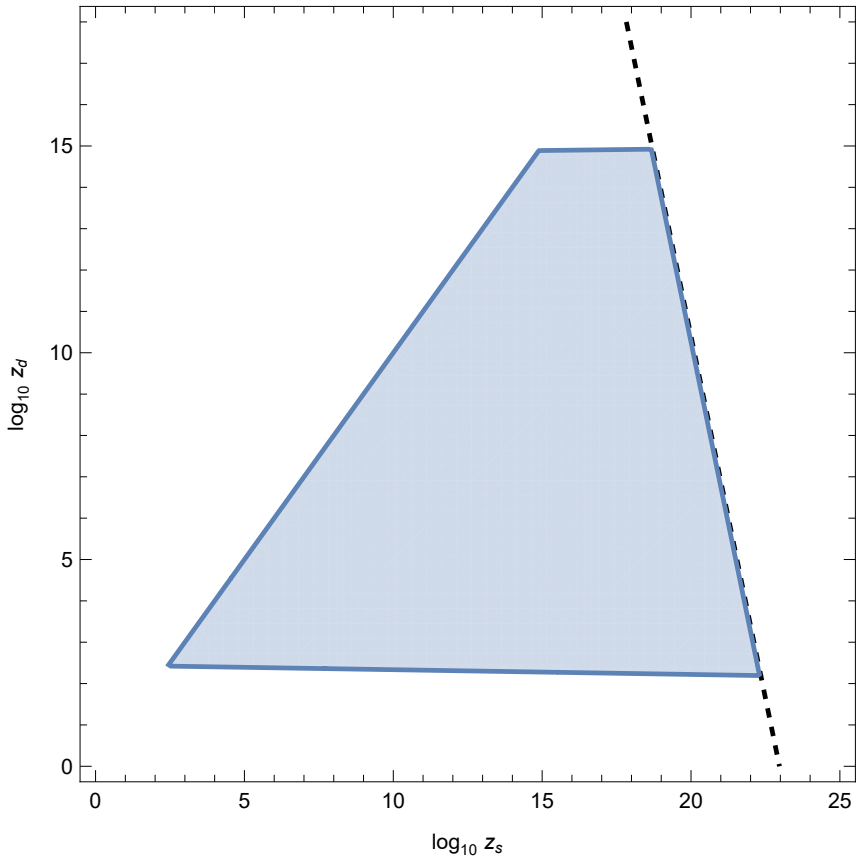

FIGURE 5.1: The shaded area shows the allowed region in the $(\log_{10} z_s, \log_{10} z_d)$ plane for the limiting case $\beta = 0$ and $\sigma_i = M_{\rm Pl}$, which maximizes the peak amplitude of the primordial GWB. The maximal allowed intensity is reached for parameter values lying on the dashed straight line marking the right border of the region, corresponding to $\log_{10}(H_1/M_{\rm Pl}) \approx -3.29$, as explained in Appendix C.2.1.

tensor spectrum. In the frequency range of IPTA, the maximal GWB amplitude is smaller than the signal detected [30, 32, 35, 36, 119] and is therefore consistent with those observations.

For an illustrative purpose, in Fig. 5.2 we have also plotted a few examples of GWBs produced by different sets of parameters satisfying all required constraints. The plotted spectra maximize neither the peak amplitude nor the extension in frequency but they are well inside the border of the allowed region and they can still produce a detectable signal within the LISA and the ET frequency range.

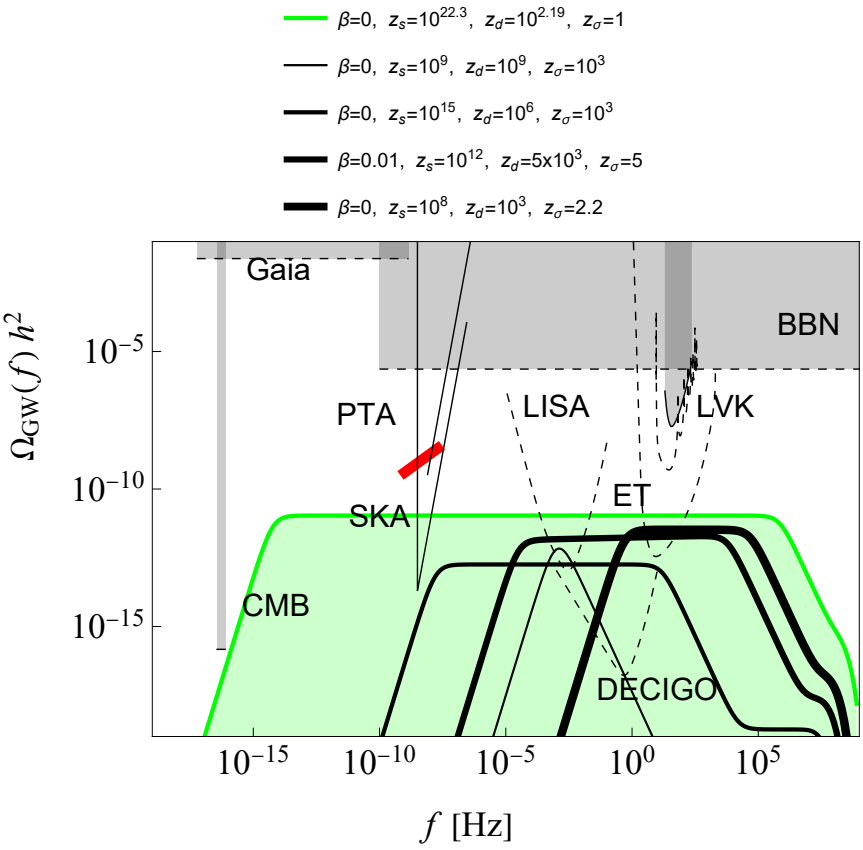

FIGURE 5.2: The shaded area is the maximal allowed region for the GWB (5.22) extended in the low-frequency range, with all its parameters satisfying the self-consistency constraints (C.7)–(C.11). We have also plotted four possible spectra corresponding to different sets of parameters giving rise to different kinematic details of the phases of earlier, non-standard cosmic evolution, preceding and following the curvature bounce.

5.3 Discussion

In this Chapter, we have studied the tensor-produced primordial GWB in the pre-Big Bang scenario [20, 21, 69, 155]. The model strikes a balance between observability in the high-frequency range and observational. We found that its primordial GWB has a convex shape with an intermediate flat plateau. The parameter space of the model is tightly constrained theoretically but it still gives enough phenomenological freedom, to the point that this GWB can comfortably fall within the sensitivity window of both LISA and ET. When the parameter β is close to zero, in this range of frequencies the GWB of this model is a single power law

$$\Omega_{\rm GW}(f) \sim f^{n_{\rm GW}}\,, \qquad n_{\rm GW} = 2 + n_{\rm t} \simeq 3 - |3 - 2\beta| \approx 0\,. \tag{5.24}$$

When z_d grows, the signal becomes a broken power law,

$$\Omega_{\rm GW}(f) \sim \begin{cases} f^{n_{\rm GW,1}}, & f \ll \bar{f} \\ f^{n_{\rm GW,2}}, & f \gg \bar{f} \end{cases}, \tag{5.25}$$

where the slopes depend on where the transition scale $\bar{f}$ lies in the model's scales hierarchy and on whether the intermediate plateau is extended enough:

$$\begin{aligned} &\bar{f} = f_d \ : && n_{\rm GW,1} \simeq 3 - |3 - 2\beta| \approx 0\,, && n_{\rm GW,2} \simeq 1 - |3 - 2\beta| \approx -2\,, \\ &\bar{f} = f_s \ : && n_{\rm GW,1} \approx 3\,, && n_{\rm GW,2} \simeq 3 - |3 - 2\beta| \approx 0\,, \\ &\bar{f} = f_s \simeq f_d \ : && n_{\rm GW,1} \approx 3\,, && n_{\rm GW,2} \simeq 1 - |3 - 2\beta| \approx -2\,. \end{aligned} \tag{5.26}$$

Both the single- and the broken-power-law shapes (5.24) and (5.26) fit the two simplest templates commonly used for inflationary models [176] and they could be submitted to the same type of analysis performed in [177] as well as to a discussion on degeneracies and model selection when compared with alternative candidates with similar spectral shapes.

In general, the higher the signal-to-noise ratio, the smaller the error on the parameters of the spectral shape, as has been verified for a variety of cases [138, 176, 177]. Thus, for the PBB model one would be able to identify the corner of the parameter space such that the tilt or tilts of the GWB (and, thus, β) would be determined with an accuracy of, say, 1% by LISA and ET in their respective observability window.

In the case of the broken power law, the sharper the transition from one slope to the other with respect to the sensitivity curve the more difficult the determination of the parameters, due to the fact that the binning of the data introduces a certain level of coarse graining of short-range features [178]. We do not expect to have this problem for the PBB model, since the aforementioned transition is gentle enough (Fig. 5.2). These and other aspects of the PBB model (like, for instance, the possible contributions of shear and bulk viscosity arising at high-energies which will be accounted for in Chapter VIII.

Chapter 6

Constraints on the Pre-Big Bang scenario from a cosmological interpretation of the NANOGrav data

6.1 Introduction

There is an exciting possibility that the signal observed by multiple Pulsar Timing Array (IPTA) collaborations, including NANOGrav [30, 31], the Parkes PTA (PPTA) [32, 33], the European PTA (EPTA) in partnership with the Indian PTA (InPTA) [34, 35], and the Chinese PTA (CPTA)[36], can be interpreted as the first detection of a cosmological stochastic gravity-wave (GW) background.

In particular, in a very recent paper [179] the NANOGrav 15-year data set has been compared with the possible amplitude and frequency scale of the relic GW spectrum predicted long ago in the context of the pre-big bang (PBB) scenario [20, 21, 180, 181], and thus used to constrain the related string cosmology parameters[1].

[1]We recall that the PBB scenario is deeply rooted in the duality symmetries of the tree-level cosmological string equations [19, 70, 71, 74, 77, 79], which also constrain theoretically its parameters.

The results presented in [179] are certainly interesting, but they seem to disagree with another recent analysis of the primordial spectrum of relic pre-big bang gravitons [4]. In fact, let us recall that the data fit presented in [179] is based on a string cosmology GW spectrum $\Omega_{\rm GW}(f)$ with two different frequency branches. In the low-frequency branch, $\Omega_{\rm GW}$ scales as f^3 up to a transition frequency f_s, characteristic of string theory and marking the onset of the high-curvature regime. Beyond f_s, the spectrum retains a power-law form but with a different exponent: specifically, $\Omega_{\rm GW} \sim f^\alpha$, where $\alpha < 3$.

The data fit presented in [179] indicates that, for frequencies $f_s \lesssim f \lesssim 10^{-6}$ Hz, the high frequency spectrum is nearly flat or slightly decreasing and that the spectral amplitude satisfies

$$\Omega_{\rm GW}(f_s) \simeq 2.9^{+5.4}_{-2.3} \times 10^{-8}, \qquad f_s \simeq (1.2 \pm 0.6) \times 10^{-8}\text{Hz}. \tag{6.1}$$

Such a spectral amplitude is *outside* the allowed region of the plane $\{f, \Omega_{\rm GW}\}$, determined in [4] on the grounds of a phenomenologically complete model of pre-big bang evolution.

The main purpose of this paper is twofold. First of all we will explain in Sect. 6.2 why the two discussions of the pre-big bang spectrum presented in [179] and [4] lead to different results, even if both are correct within their own assumptions. Second, we will suggest in Sect. 6.3 how the minimal scenario used in [4] could be generalized to accommodate the production of a relic signal that is also consistent with the data fit presented in (6.1). Finally, Sect. 6.4 will be devoted to some concluding remarks.

6.2 A phenomenologically viable minimal Pre-Big Bang scenario

The first point to be stressed is that the relic GW spectrum discussed in [179] refers to a preliminary and very simple example of pre-big bang spectrum presented in various old papers [59, 72, 156, 157]. Such a spectrum, however, may be regarded as incomplete as it does not include all frequency branches arising in a realistic and phenomenologically viable string model of the early Universe.

A viable inflationary scenario must indeed predict, besides the relic GW background, also a related spectrum of adiabatic scalar curvature perturbations able to explain the observed large scale anisotropy. This has been shown to be possible [74, 110, 111] (see also [60] for a more complete review) thanks to the contribution of the string Kalb-Ramond axion field acting as a curvaton [75, 174], and producing a cosmic phase of axion dominated oscillations. The inclusion of this important aspect in the scenario modifies however the standard post-bouncing evolution and this, in its turn, may affect the sub-horizon propagation of tensor perturbation modes after their re-entry, thus producing additional frequency branches with different spectral indices in today's observed GW spectrum (see e.g. [4, 155, 168] for recent quantitative discussions of such an effect).

The pre-big bang model used in [179] does not take into account this crucial ingredient determining the final observed GW spectrum, and thus neglects the important associated constraints. Such an ingredient, on the contrary, is properly accounted for in the spectrum analyzed in [4]. As a result, the corresponding, more tightly constrained spectral region does not overlap with the region of the IPTA signal (see, in particular, Fig. 4 of [4]). It should be stressed, however, that the spectral model considered in [4] is based on a complete but "minimal" example of pre-big bang scenario. It corresponds to the simplest description of a complete bouncing evolution from the string perturbative vacuum down to the present epoch, in agreement with all string theory constraints (see e.g. [5] for an exact string model of bounce), but is also based on ad hoc assumptions chosen to minimise the number of unknown parameters. It may be useful to recall here, in view of its generalisation to be presented in the next section, the basic aspects of such a minimal scenario.

First of all it must include, for its completeness, at least two different pre-bouncing phases as well as other two post-bouncing phases, occurring before the reheating epoch marking the beginning of standard cosmology. Starting from initial conditions asymptotically approaching the flat perturbative vacuum with vanishing Hubble parameter, $H \to 0$, such a scenario is thus characterized by four different Hubble scales: H_s, marking the beginning of the string high-curvature regime; H_1, corresponding to the bouncing from accelerated to decelerated, decreasing curvature expansion; H_σ, marking the beginning of the dust-like phase dominated by the oscillating axion; and H_d, associated to the axion decay that triggers the

reheating and the beginning of the standard radiation-dominated era. Obviously,

$$H_s \lesssim H_1 \lesssim M_{\rm Pl}, \qquad\qquad H_1 \gtrsim H_\sigma > H_d \gtrsim H_N, \tag{6.2}$$

where $H_N \simeq (1\text{MeV})^2/M_{\rm Pl}$ is the scale of standard nucleosynthesis, and $M_{\rm Pl} \equiv (8\pi G)^{-\frac{1}{2}} \simeq 2 \times 10^{18}$ GeV is the (reduced) Planck mass scale. We also recall, for later use, that H_σ and H_d can be expressed in terms of the axion mass m and of the initial, post-bouncing axion amplitude σ_i as follows [60, 110, 111]:

$$H_\sigma \simeq m \left(\frac{\sigma_i}{M_{\rm Pl}}\right)^4, \qquad\qquad H_d \simeq m \left(\frac{m}{M_{\rm Pl}}\right)^2. \tag{6.3}$$

The axion field starts oscillating at a scale $H \simeq m$, hence the condition that the axion is oscillating when it becomes dominant (required for the curvaton mechanism to be efficient) implies $m \gtrsim H_\sigma$, namely[2] $\sigma_i \lesssim M_{\rm Pl}$.

The amplification of metric perturbations, in this scenario, is thus characterised by four typical frequency scales: f_s, f_1, f_σ, f_d, where f_s is the proper frequency of a mode crossing the horizon at the beginning of the string phase, f_1 is the maximal amplified frequency, while f_σ and f_d are the frequency of modes re-entering the horizon, respectively, at the beginning and conclusion of the axion-dominated era. It follows, automatically, that $f_1 \gtrsim f_\sigma > f_d$, while f_s satisfies $f_s \lesssim f_1$, but its particular value is free, in principle, with respect to the values of f_σ and f_d. We shall assume here, as in [4, 155, 168, 182], that f_s is smaller than the other frequencies typical of the pre-big bang scenario, but larger than the frequencies constrained by the CMB data, i.e. the pivot frequency scale $f_* \simeq 0.05\,\text{Mpc}^{-1}$, and the typical frequency of Large Scale Structure (LSS) observations, $f_{\rm LSS} \simeq 60\, f_*$. Hence, the model we shall consider here will be characterised by the following hierarchy of frequency scales:

$$f_* < f_{\rm LSS} \lesssim f_s \lesssim f_d < f_\sigma \lesssim f_1. \tag{6.4}$$

Given an inflationary scenario with four typical frequency scales, the amplified spectrum of Fourier modes of tensor perturbations, h_k, will be characterised in general by four different spectral branches to be computed by solving, for each

[2] This is effectively the case if, as expected, the axion potential is periodic with a periodicity smaller than $M_{\rm Pl}$.

mode k, the canonical perturbation equation

$$v_k'' + \left(k^2 - \frac{\xi_h''}{\xi_h}\right) v_k = 0. \tag{6.5}$$

Here $v_k = \xi_h(\tau) h_k$ is the (Mukhanov-Sasaki) variable [12] for which the effective action for the tensor field h_k takes the standard canonical form, the (background dependent) variable $\xi_h(\tau)$ is the so-called pump field controlling the GW dynamics in the various cosmic phases, and a prime denotes differentiation with respect to the conformal time τ. It should be recalled that the Fourier parameter k for a mode re-entering the horizon at a given time t in the post-bouncing epochs described by a standard FLRW metric background, is related to the proper frequency of that mode observed at the present time t_0, i.e. $f(t_0)$, by $f(t_0) = \omega(t_0)/2\pi$, where $\omega(t_0) = k/a(t_0) = H(t)a(t)/a(t_0)$.

In order to solve Eq. (6.5) and obtain the GW spectrum, we need the explicit behaviour of the pump field for tensor perturbations in the various cosmic phases. The answer is simple for the low-curvature (low energy) regimes, where we can use the tree-level string cosmology equations. Assuming, as in [4, 155, 168, 182], to start with a ten-dimensional gravi-dilaton string background with 3 expanding dimensions with scale factor a, and 6 contracting spatial dimensions with scale factors b_i, which asymptotically evolves from the perturbative vacuum at $\tau \to -\infty$ up to the string scale (i.e. for $0 \leqslant H \leqslant H_s$), we then find for the tensor pump field the simple form

$$\xi_h(\tau) \sim a g_4^{-1} = a \left(\prod_{i=1}^{6} b_i\right)^{1/2} e^{-\phi/2}, \tag{6.6}$$

where ϕ is the dilaton and g_4 is the effective (time-dependent) 4-dimensional string coupling. It is well known [183, 184] that this uniquely fixes the power law behaviour of ξ to be $\xi_h(\tau) \sim (-\tau)^{1/2}$.

The answer is simple also in the post-bouncing regime if we assume that in our minimal scenario, at all epochs from H_1 down to the present epoch H_0, the internal dimensions as well as the dilaton, controlling the string coupling, are already stabilised at the string scale. In that case the tensor pump field simply coincides with the scale factor $a(\tau)$ describing decelerated, decreasing curvature expansion. In the radiation-dominated phases, occurring from H_1 to H_σ and for $H_d \geqslant H \geqslant H_{\rm eq}$, where $H_{\rm eq}$ is the equality scale, the pump field is then given by $\xi_h(\tau) \sim \tau$,

while for the dust-like phases, i.e. for $H_\sigma > H > H_d$ and $H < H_{\rm eq}$ we have, as usual, $\xi_h(\tau) \sim \tau^2$.

Finally, for the pump field of the high-curvature string phase, i.e. for H ranging from H_s to H_1, we can still use a parametrization based on a power-law behaviour, but we have to take into account the effects of higher order string α' corrections, as well as other possible high energy effects typical of string theory. In the minimal scenario considered in [4, 155, 168, 182] it has been assumed $\xi_h(\tau) \sim (-\tau)^{-1+\beta}$, where the factor $(-\tau)^{-1}$ corresponds to having frozen the string-frame curvature at the string scale[3] and, β is a positive parameter describing the rate of growth of the four-dimensional string coupling g_4 (a combined effect of the dilaton and internal volume time-dependence, see Eq. (6.6)) according to:

$$\beta \equiv \frac{d\log g_4}{d\log a}\ ; \qquad\qquad 0 \lesssim \beta < 3. \tag{6.7}$$

Here the lower limit is required for a monotonically growing coupling, while the upper limit is to avoid quantum background instabilities [185]. The idea of the scenario is that g_4 starts very small at the beginning of the string phase and becomes of $\mathcal{O}(1)$ at its end.

It is important to stress that the same parameter β, in this scenario, also appears (with the opposite sign) in the axion pump field ξ_σ governing the amplification of the axion fluctuation during the string phase, which takes in fact the form $\xi_\sigma(\tau) \sim (-\tau)^{-1-\beta}$, according to the S-duality symmetry of string theory [74]. Hence, the same parameter β appears in the primordial spectrum $P_s(f)$ of scalar curvature perturbations produced via the curvaton mechanism, and thus contributes to the important constraint following from the standard normalisation of the scalar spectrum at the CMB pivot scale (see e.g. [162]), which implies [4, 155, 168, 182]

$$P_s(f_*) \equiv 2.1\times 10^{-9} \simeq \frac{T^2(\sigma_i)}{2\pi^2}\left(\frac{H_1}{M_{\rm Pl}}\right)^2\left(\frac{f_s}{f_1}\right)^{3-|3+2\beta|}\left(\frac{f_*}{f_s}\right)^{n_s-1}, \tag{6.8}$$

and which provides a stringent constraint on all the parameters. Here $n_s \simeq 0.965$ is the scalar spectral index, and $T(\sigma_i)$ is the transfer function connecting the amplitude of axion and scalar curvature perturbations, which can be written (according

[3] Attractors of this type have been discussed in [172].

to a numerical integration of the perturbation equations [111]) as

$$T(\sigma_i) \simeq 0.13 \left(\frac{\sigma_i}{M_{\rm Pl}}\right) + 0.25 \left(\frac{M_{\rm Pl}}{\sigma_i}\right) - 0.01. \tag{6.9}$$

Summing up and imposing all above mentioned constraints (given by Eqs. (6.7), (6.8), plus the hierarchy of scales (6.4), plus the condition $\sigma_i \leqslant M_{\rm Pl}$), it turns out that the allowed amplitude of the relic GW spectrum for this minimal scenario (see [4]) cannot reproduce the results (6.1) obtained with the fit of the NANOGrav data set (unless we allow $\beta < 0$, which is however inconsistent with the physical interpretation of this parameter, see Eq. (6.7)). We have checked that the same result is obtained even if we assume higher (and in principle allowed) values of the frequency f_s, changing the hierarchy of Eq. (6.4) and choosing, for instance, $f_d \lesssim f_s < f_\sigma$, or $f_\sigma \lesssim f_s \lesssim f_1$.

6.3 A non-minimal Pre-Big Bang scenario

6.3.1 Parametrization of the non-minimal model and related constraints

The minimal scenario of the previous section takes into account two typical effects of the high-curvature string phase: the late-time attractor and the growth of the dilaton. But there are in principle other possible high-energy string theory effects like, for instance, the production of a dense gas of primordial, string-size, black holes or "string holes" [186–188]. Such effects can modify not only the background evolution but also, and in a different way, the propagation of different types of perturbations like tensor-metric [6] and axion-field perturbations.

It seems appropriate, therefore, to consider also a more general, non-minimal phenomenological scenario where, during the high-curvature string phase, the tensor and axion pump fields (ξ_h and ξ_σ) can still be described by a power-law behaviour but with two new parameters, in principle unrelated to β and also to each other

(in case S-duality is broken). We can parametrize them as follows:

$$\begin{aligned} \xi_h &\sim (-\tau)^{-1+\beta+\gamma} \equiv (-\tau)^{-1+\beta_h}\,; \\ \xi_\sigma &\sim (-\tau)^{-1-\beta+\delta} \equiv (-\tau)^{-1+\beta_\sigma}\,; \\ \beta_\sigma &= -\beta_h + \epsilon, \qquad \epsilon \equiv \delta + \gamma\,. \end{aligned} \tag{6.10}$$

We have $\epsilon = 0$ if the S-duality assumed in the minimal scenario is still valid, while we recover the previous scenario if both γ and δ are vanishing. Let us then present the modified spectrum, and the related constraints, for the non-minimal case with $\gamma \neq 0$ and $\delta \neq 0$.

Assuming the same hierarchy of frequency scales as before (given by Eq. (6.4)), solving Eq. (6.5) in the various phases (with the new tensor pump field), matching the solutions, and computing the final, presently observed GW spectral energy density expressed in units of critical density ρ_c, i.e. $\Omega_{\rm GW}(k,t_0) = \rho_c^{-1}(t_0) d\rho_k(t_0)/d\ln k$, we obtain (besides a negligible contribution for $f > f_1$):

$$\frac{\Omega_{\rm GW}(f,t_0)}{\Omega_{\rm GW}(f_1,t_0)} = \begin{cases} \left(\dfrac{f}{f_1}\right)^{3-|3-2\beta_h|}, & f_\sigma \lesssim f \lesssim f_1 \\ \left(\dfrac{f_\sigma}{f_1}\right)^{3-|3-2\beta_h|} \left(\dfrac{f}{f_\sigma}\right)^{1-|3-2\beta_h|}, & f_d \lesssim f \lesssim f_\sigma \\ \left(\dfrac{f_\sigma}{f_1}\right)^{3-|3-2\beta_h|} \left(\dfrac{f_d}{f_\sigma}\right)^{1-|3-2\beta_h|} \left(\dfrac{f}{f_d}\right)^{3-|3-2\beta_h|}, & f_s \lesssim f \lesssim f_d \\ \left(\dfrac{f_\sigma}{f_1}\right)^{3-|3-2\beta_h|} \left(\dfrac{f_d}{f_\sigma}\right)^{1-|3-2\beta_h|} \left(\dfrac{f_s}{f_d}\right)^{3-|3-2\beta_h|} \left(\dfrac{f}{f_s}\right)^{3}, & f \lesssim f_s\,. \end{cases} \tag{6.11}$$

Note the difference from the results of [4] due to the new parameter γ (or rather β_h).

In order to discuss the various phenomenological constraints it is useful to work, as in [4], with the following frequency ratios

$$z_s = \frac{f_1}{f_s}, \qquad z_d = \frac{f_1}{f_d}, \qquad z_\sigma = \frac{f_1}{f_\sigma}, \qquad z_s \gtrsim z_d > z_\sigma \gtrsim 1. \tag{6.12}$$

In terms of such variables, the end-point amplitude of the spectrum is given by [4]:

$$\Omega_{\rm GW}(f_1,t_0)=\Omega_r(t_0)\left(\frac{H_1}{M_{\rm Pl}}\right)^2\left(\frac{z_\sigma}{z_d}\right)^2, \tag{6.13}$$

where $\Omega_r(t_0)\sim 10^{-4}$ is the present critical fraction of radiation energy density (including neutrinos), and we have neglected a possible suppression of $\Omega_{\rm GW}(f_1,t_0)$ due to significant late entropy production [157]. Also, the typical axion parameters σ_i and m, controlling the post-bouncing scales H_σ and H_d according to Eq. (6.3), can be written as:

$$\frac{m}{M_{\rm Pl}}\simeq\left(\frac{H_1}{M_{\rm Pl}}\right)^{1/3} z_d^{-1}z_\sigma^{1/3}, \qquad \frac{\sigma_i}{M_{\rm Pl}}\simeq\left(\frac{H_1}{M_{\rm Pl}}\right)^{1/6} z_d^{1/4}z_\sigma^{-7/12}. \tag{6.14}$$

The constraints to be imposed on this scenario can now be explicitly written (in base 10 logarithmic form, useful for later applications) as follows. The condition $\sigma_i\lesssim M_{\rm Pl}$ becomes:

$$\log\left(\frac{H_1}{M_{\rm Pl}}\right)+\frac{3}{2}\log z_d\lesssim\frac{7}{2}\log z_\sigma. \tag{6.15}$$

The condition $H_d\gtrsim H_N$ becomes:

$$\log\left(\frac{H_1}{M_{\rm Pl}}\right)-3\log z_d+\log z_\sigma\gtrsim\ \log\left(\frac{H_N}{M_{\rm Pl}}\right)\approx -42-\log 4\,. \tag{6.16}$$

The condition $f_{\rm LSS}<f_s$ (see Appendix B.2 of [4]) becomes:

$$\log z_s\lesssim 26-\log 9+\frac{1}{2}\log\left(\frac{H_1}{M_{\rm Pl}}\right)+\frac{1}{2}\left(\log z_\sigma-\log z_d\right)\,. \tag{6.17}$$

The phenomenological normalization (6.8), generalized to the non-minimal scenario, leads to a condition which also include the new parameter δ (or ϵ, see Eq. (6.10)):

$$\begin{aligned}\log\left(\frac{H_1}{M_{\rm Pl}}\right)=\frac{2}{5-n_{\rm s}}\Big\{&\log\left[\frac{4.2\pi^2}{T^2(\sigma_i)}\right]-9+(1-n_{\rm s})(\log 1.5-27)\\&+(4-n_{\rm s}-|3+2(\beta_h-\epsilon)|)\log z_s\\&+\frac{n_{\rm s}-1}{2}\left(\log z_\sigma-\log z_d\right)\Big\}\lesssim 0,\end{aligned} \tag{6.18}$$

where the inequality on the right hand side has been imposed according to Eq. (6.2).

All the constraints listed up to now are to be always applied, in general, for the internal as well as for the phenomenological consistency of the non-minimal scenario that we are considering. But let us now introduce a further, more constraining ingredient, by imposing on the lowest energy branch of our non-minimal spectrum (6.11) to exactly satisfy the numerical values of Eq. (6.1), to be in agreement with the data fit of [179]. From the first condition of Eq. (6.1) we then obtain

$$2\log\left(\frac{H_1}{M_{\rm Pl}}\right) \simeq -4 + \log 2.9 + (3 - |3 - 2\beta_h|)\log z_s, \tag{6.19}$$

while the second condition of Eq. (6.1) gives

$$\frac{1}{2}\log\left(\frac{H_1}{M_{\rm Pl}}\right) \simeq -19 + \log 1.93 + \log z_s + \frac{1}{2}\left(\log z_d - \log z_\sigma\right), \tag{6.20}$$

that makes the inequality of Eq. (6.17) automatically satisfied. In such a context one should note that the amplitude $\Omega_{\rm GW}(f_s)$ of Eq. (6.1), reached by the spectrum at a relatively low frequency scale $f_s \sim 10^{-8}$ Hz, is quite close to the experimental upper bound recently imposed by the data of the LIGO-Virgo-KAGRA (LVK) network [116], which provides the condition:

$$\Omega_{\rm GW}(f_{\rm LVK}) < 4.12 \times 10^{-8}, \qquad\qquad f_{\rm LVK} \simeq 35.4\,{\rm Hz}\,. \tag{6.21}$$

Taking into account that our spectrum (6.11) may be flat, or even increasing, for $f > f_s$, it follows that we should add to the list of our constraints also the above condition, suitably imposed on the whole range of spectral frequencies larger than f_s.

In addition, since the string phase should be characterized by a curvature scale of order the string mass scale $M_{\rm S}$, we should in principle restrict the ratio $(H_1/M_{\rm Pl})$ to lie in the canonical range $10^{-2} - 10^{-1}$. Nonetheless, in order to consider also some more exotic possibilities and/or to consistently take into account the approximate definition of some of our parameters, we will enlarge our parameter space to include the wider range:

$$-3 \lesssim \log\left(\frac{H_1}{M_{\rm Pl}}\right) \lesssim -1. \tag{6.22}$$

Finally, we should also take into account the possibility that, in the non-minimal scenario we are considering, the modified axion parameter β_σ is small enough but positive, thus describing a spectrum of induced scalar-curvature perturbations which is growing at high frequency. In that case the lowest frequency branch

$f \lesssim f_s$ of the scalar spectrum has then the same behaviour reported in Eq. (6.8) (with β obviously replaced by $-\beta_\sigma$), while for $f \gtrsim f_s$ we find [110, 111]

$$P_s(f) \simeq \frac{T^2(\sigma_i)}{2\pi^2}\left(\frac{H_1}{M_{\rm Pl}}\right)^2\left(\frac{f}{f_1}\right)^{3-|3-2\beta_\sigma|}, \qquad f_s \lesssim f \lesssim f_1. \tag{6.23}$$

In such a case we have to impose a further constraint, needed for the self-consistency of our scenario: the condition of negligible backreaction of the produced perturbations on the assumed model of background evolution, $P_s(f) \lesssim 1$,which, imposed at the peak values of the scalar spectrum, gives the condition:

$$\log\frac{T(\sigma_i)}{\sqrt{2\pi^2}} + \log\left(\frac{H_1}{M_{\rm Pl}}\right) \lesssim 0. \tag{6.24}$$

By using our previous result $\sigma_i \lesssim M_{\rm Pl}$ we can also rewrite the above condition in simplified form as $H_1 \lesssim \sigma_i$.

The question is now: is it possible to find a set of parameters $\{\beta_h, \beta_\sigma, z_s, z_d, z_\sigma, \sigma_i, m, H_1\}$ satisfying all physical and model-dependent constraints of the non-minimal scenario, Eqs. (6.7), (6.12), (6.15), (6.16), (6.17), (6.18), (6.21), and compatible with the two conditions (6.19), (6.20) obtained from the analysis of the NANOGrav data, plus the additional conditions (6.22), (6.24)?

6.3.2 Allowed region in parameter space

The total number of parameters of our non-minimal (yet simple) model is quite large. The whole set consists of $H_1, m, \sigma_i, z_s, z_d, z_\sigma$ and the two spectral parameters β_h and β_σ. However, they are not all independent. After several attempts, we have found the best way to present our results to be as follows.

We first choose a value for σ_i. Recalling that, before a non-perturbative axion potential is generated, any value of σ_i (modulo its periodicity $\mathcal{O}(M_{\rm Pl})$) is equally probable, we could sample, for instance, the values $\sigma_i/M_{\rm Pl} = 1, 0.5, 0.1$. Although much smaller values of σ_i may correspond to considerable fine-tuning of initial conditions, we will allow for the more generous range:

$$10^{-3/2} \lesssim \frac{\sigma_i}{M_{\rm Pl}} \lesssim 1. \tag{6.25}$$

In any case, as we shall see, an order-of-magnitude change in σ_i has only a modest effect on the allowed ranges for the other parameters.

Once σ_i is given, there are enough equations (i.e. (6.14), (6.18), (6.19), (6.20)) to determine all the remaining physical parameters in terms of the two spectral ones, β_h and β_σ. Therefore, the constraints (6.22),(6.25), (6.15), (6.16),(6.17) define a (hopefully non empty) region in an easily plotted $\{\beta_h, \beta_\sigma\}$ plane, that will be illustrated in Fig. 6.1.

The two missing constraints are the ones given by LVK bound (6.21) and by the absence of strong back-reaction effects (6.24). It is easy to check that this latter constraint is automatically satisfied in the region already defined (indeed, for $H_1/M_{\rm Pl} \lesssim 0.1$, it only requires $\sigma_i/M_{\rm Pl} > 0.01$). On the other hand, the LVK bound can be non trivial (depending on the sign of β_h), and cuts off some corner of parameter space as we shall discuss in a moment. Within the resulting allowed region, each point represents a consistent spectrum of gravitational and scalar perturbations that can be readily drawn as we shall see in the next subsection. Inside the allowed region we can draw contour lines along which each of the remaining parameters $(H_1, m, z_s, z_d, z_\sigma)$ takes constant values (so-called level curves). Luckily, one finds that z_s (the total duration of the string phase in red-shift space) is only a function of the combination $\beta_\sigma - \beta_h$. This explains why it is convenient to plot our parameter space in the two-dimensional plane spanned by the coordinates $\{\beta_h, \beta_\sigma - \beta_h\}$, as we have done in Fig. 6.1.

Two further simplifications occur when solving our equations, at least for $3-2\beta_\sigma > 0$ (which turns out to be largely satisfied by our constraints). These are apparent in the explicit solutions given in Eqs. (D.1) in the Appendix D. The first is that the level-curves of H_1/M_p are straight lines coming from the origin $\beta_\sigma = \beta_h = 0$. The second is that the level curves of $m/M_{\rm Pl}$, z_s/z_d, z_s/z_σ are all the same (they are given by the straight lines originating from the point $\beta_\sigma = \beta_h = 2$). That also means that, for a given $\sigma_i/M_{\rm Pl}$ and $m/M_{\rm Pl}$, the two ratios z_s/z_d and z_s/z_{sg} can be determined. For the convenience of the reader we also give in the Appendix D these explicit relations.

After the above discussion it is now straightforward to describe the properties the allowed region of parameter space shown in the four panels of Fig. 6.1, corresponding to the four choices $\log(\sigma_i/M_{\rm Pl}) = 0, -1/2, -1, -3/2$. We stress immediately that the region has a trapezoidal shape except for a small "tooth" on the lower

right side. This is precisely the extra constraint due to the LVK bound on $\Omega_{\rm GW}$, physically due to the fact that the value of $\Omega_{\rm GW}(f_s)$ imposed to fit the NANOGrav data is close to the upper limit of LVK; thus, for a positive β_h, it is not trivial to avoid a clash between the two constraints.

In each panel the σ_i-dependent correspondence between $\beta_\sigma - \beta_h$ and z_s is clearly displaced. The level curves for $\log(H_1/M_{\rm Pl}) = -1, -2, -3$ are the nearly vertical straight lines. To these we add the line (dotted in red) representing the condition $\epsilon = 0$, i.e. $\beta_\sigma = -\beta_h$, and corresponding to models satisfying the S-duality symmetry. In the duality-symmetric case the corresponding value of $\log(H_1/M_{\rm Pl})$ is a mildly varying function of σ_i and is indicated in the accompanying Table. It varies between -2.60 and -3.20 for our chosen interval of σ_i and is within the allowed region for $\sigma_i/M_{\rm Pl} > 0.1$, a value with 90% probability of being realized assuming uniform priors for the parameters distribution.

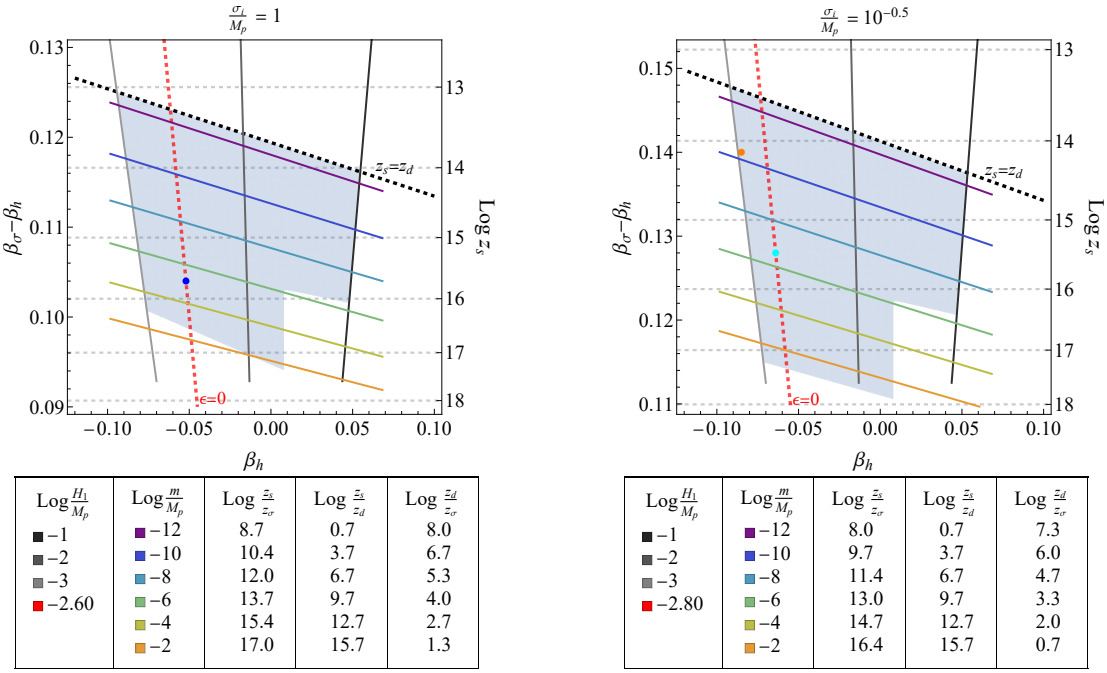

Log $\frac{H_1}{M_p}$	Log $\frac{m}{M_p}$	Log $\frac{z_s}{z_\sigma}$	Log $\frac{z_s}{z_d}$	Log $\frac{z_d}{z_\sigma}$
−1	−12	8.7	0.7	8.0
−2	−10	10.4	3.7	6.7
−3	−8	12.0	6.7	5.3
−2.60	−6	13.7	9.7	4.0
	−4	15.4	12.7	2.7
	−2	17.0	15.7	1.3

(A)

Log $\frac{H_1}{M_p}$	Log $\frac{m}{M_p}$	Log $\frac{z_s}{z_\sigma}$	Log $\frac{z_s}{z_d}$	Log $\frac{z_d}{z_\sigma}$
−1	−12	8.0	0.7	7.3
−2	−10	9.7	3.7	6.0
−3	−8	11.4	6.7	4.7
−2.80	−6	13.0	9.7	3.3
	−4	14.7	12.7	2.0
	−2	16.4	15.7	0.7

(B)

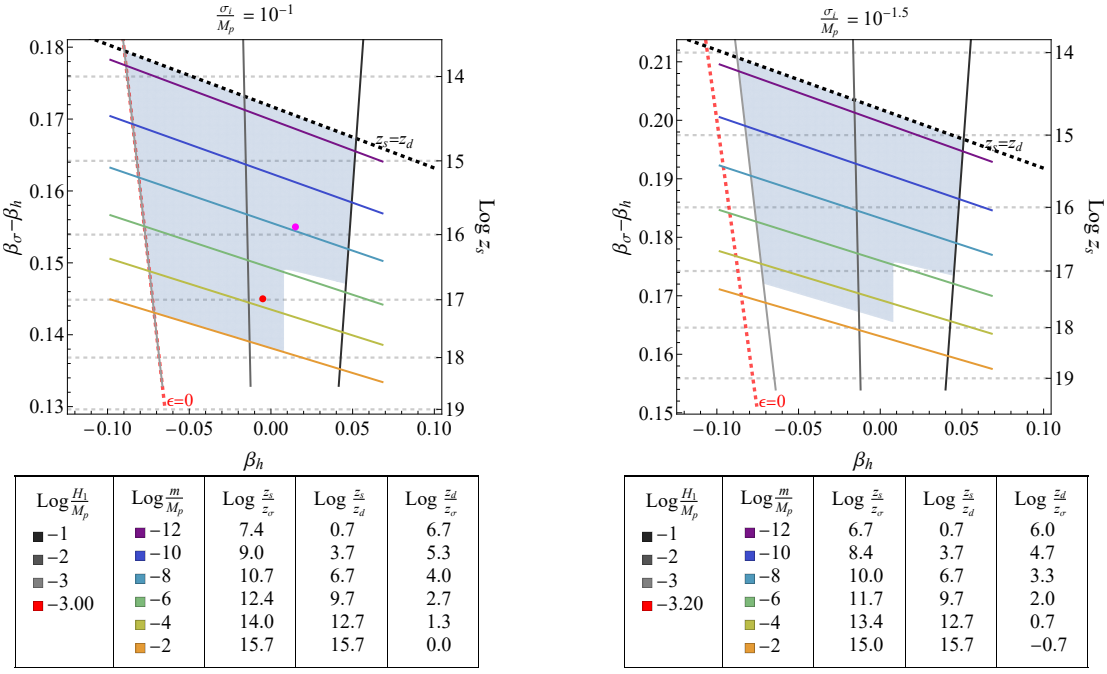

Log $\frac{H_1}{M_p}$	Log $\frac{m}{M_p}$	Log $\frac{z_s}{z_\sigma}$	Log $\frac{z_s}{z_d}$	Log $\frac{z_d}{z_\sigma}$
−1	−12	7.4	0.7	6.7
−2	−10	9.0	3.7	5.3
−3	−8	10.7	6.7	4.0
−3.00	−6	12.4	9.7	2.7
	−4	14.0	12.7	1.3
	−2	15.7	15.7	0.0

(C)

Log $\frac{H_1}{M_p}$	Log $\frac{m}{M_p}$	Log $\frac{z_s}{z_\sigma}$	Log $\frac{z_s}{z_d}$	Log $\frac{z_d}{z_\sigma}$
−1	−12	6.7	0.7	6.0
−2	−10	8.4	3.7	4.7
−3	−8	10.0	6.7	3.3
−3.20	−6	11.7	9.7	2.0
	−4	13.4	12.7	0.7
	−2	15.0	15.7	−0.7

(D)

FIGURE 6.1: The shaded blue region represents the allowed parameter space. The condition $\epsilon = 0$ (red dashed line) defines the duality region, where $\beta_h = -\beta_\sigma$. Vertical black lines correspond to variations in the parameter $\log(H_1/M_p)$, while horizontal dashed gray lines represent the parameter $\log z_S$. The dashed black lines, marking the curve $z_s = z_d$, delineate the upper boundary of the allowed region. Oblique curves illustrate variations in $\log(m/M_p)$, $\log(z_s/z_d)$, $\log(z_s/z_\sigma)$, and $\log(z_d/z_\sigma)$, as explained in the legend. The colored dots correspond to the GW spectra reported in Fig. 6.2.

Finally, the nearly horizontal lines are the common level curves for the remaining quantities $m/M_{\rm Pl}, z_s/z_d, z_s/z_\sigma$ whose corresponding values are also given again in each Table (together with their trivial combination z_d/z_σ). It may be useful to note, also, that relaxing the lower limit (6.22) of H_1 has the effect of allowing higher and higher values of β_σ, as well as lower and lower (negative) values of β_h. The same effect on the parameter β_σ is obtained if we relax the lower limit (6.25) on the axion amplitude σ_i; in that case, however, the related effects on β_h are much smaller and, in any case, the allowed range of β_h does not increase, but it tends to sligthly decrease.

Such properties are important to understand the variation in shape of the GW spectrum under a given variation of its parameters, to be illustrated in the next Sect. 6.3.3 where we will present some examples of GW spectra coming from the various regions of Fig. 6.1. In the final subsection 6.3.4 we will also present, for completeness, the associated power spectra of induced scalar curvature perturbations, leaving to future works the study of their possible implications .

6.3.3 Typical spectra for non-minimal models consistent with a fit of the NANOGrav data

Given the allowed values of the parameters defined in the previous subsection, we can now easily illustrate the possible spectral distribution of the relic GW background (6.11) in the various frequency branches. In spite of the rather small and compact size of the allowed region of parameter space there is a wide range of possible spectra that, we have illustrated in Fig. 6.2 in order to compare their shape with the expected sensitivity of present and near future GW detectors. We have plotted the spectra using a smooth interpolation between the various branches[4], following the method previously introduced in [4] (in particular, in Appendix B).

For our illustrative purpose we have plotted in the $\{f, \Omega_{\rm GW}\}$ plane a few spectra which are all compatible with the bounds of Fig. 6.1 but which describe distinct physical configurations, such as different extensions of a large spectral amplitude towards the high frequency range (the red and orange curves), or the possibility of

[4]The smoothing of the piecewise profile (6.11) does not change the underlying scenario because the transition epochs from one phase to another are of negligible duration compared with the time extension of such phases.

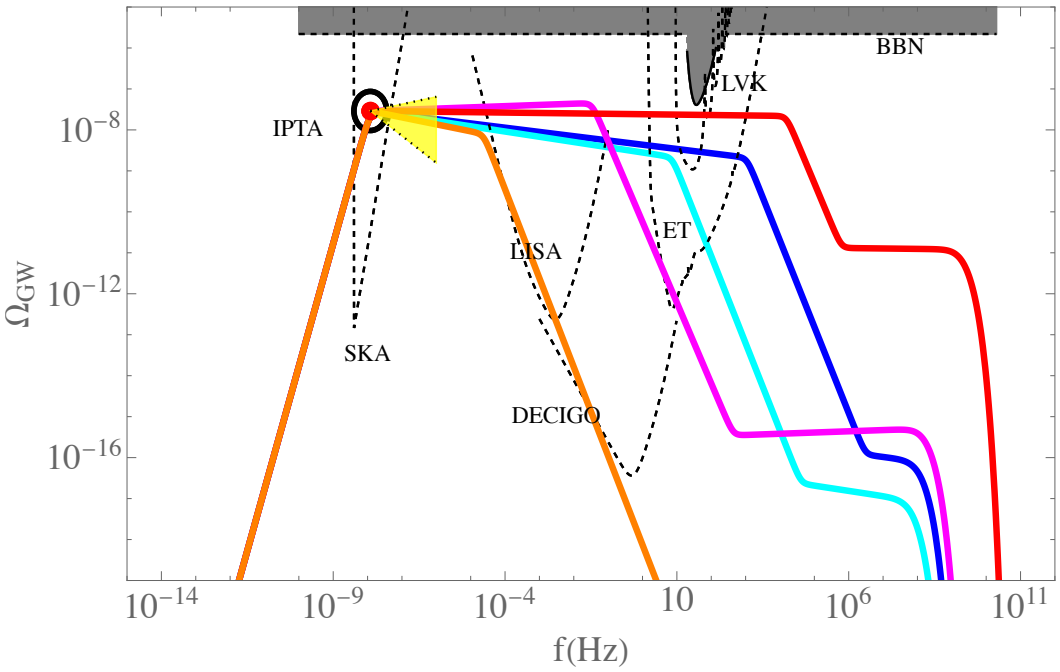

FIGURE 6.2: Possible examples of relic primordial GW spectrum produced in the context of a non-minimal model of pre-big bang evolution satisfying all present phenomenological constraints, and consistent with the data fit reported in Eq. (6.1) (the red dot localised inside the black circle). The corresponding values of their parameters are shown in Table 6.1. Also shown are the expected sensitivity of SKA, LISA, ET, DECIGO (the regions inside the dashed curves), and the upper bounds (the grey shaded areas) imposed by the present results of the LVK network and by the standard nucleosynthesis. The blue and cyan curves are example of spectra compatible with S-duality symmetry, while the red, magenta and orange curves are obtained if such a symmetry is violated in the high-curvature string phase. The yellow shaded region describes the allowed spectral region for $f_s < f < 10^{-6}$ Hz suggested by the results of [179].

a growing behaviour for modes with $f > f_s$, amplified during the high-curvature string phase (the magenta curve).

We have also included, for comparison, examples with a similar spectral behaviour but produced by models preserving the S-duality symmetry, and thus characterised by a parameter $\epsilon = 0$ (the blue and cyan curves). It may be interesting to note that, for all duality invariant models, the high-frequency spectral branches with $f > f_s$ must be characterised by a decreasing behaviour, given the negative allowed range of $\beta_h < 0$ along the red dotted lines $\epsilon = 0$ (see Fig. 6.1). The precise numerical values of all the parameters for the five plotted spectra are listed in Table 6.1.

In any case, it should be noted that all spectra have their lowest-frequency branch well inside the expected sensitivity of the Square Kilometer Array (SKA) [189]

collaboration and that, for most of the spectra, the peak value turns out to be localised just in correspondence of the value reported in Eq. (6.1) and obtained from International Pulsar Timing Array (IPTA) collaboration (IPTA) [119], as illustrated in the figure. Note also that the high-frequency behaviour of the spectrum may by compatible (in agreement with the results of [4]) with the expected sensitivity range of near-future detectors, represented by the regions inside the dashed curves of Fig. 6.2: in particular those of LISA [24], ET [26], DECIGO [29] and SKA [189]. Marginally, also with the expected sensitivity of Advanced LIGO [117]. In addition, all the plotted spectra are automatically compatible with the well known bound on the standard big bang nucleosinthesys (BBN) [157], which requires $\Omega_{\rm GW} < 2.2 \times 10^{-6}$ in a very wide frequency range $f \gtrsim 10^{-8}$ Hz, and which is illustrated by the shaded grey area of Fig. 6.2.

	$\log z_s$	$\log z_d$	$\log z_\sigma$	ϵ	β_h	$\log \frac{\sigma_i}{M_{\rm P}}$	$\log \frac{H_1}{M_{\rm P}}$	$\log \frac{m}{M_{\rm P}}$
	15.89	9.44	5.32	0.19	0.02	−1.00	−1.53	−8.18
	16.98	4.88	3.28	0.14	−0.01	−1.00	−1.85	−4.41
	14.14	10.48	4.65	−0.03	−0.08	−0.50	−2.97	−10.30
	15.70	4.74	1.29	0	−0.05	0.00	−2.60	−10.40
	15.46	6.68	2.93	0	−0.06	−0.50	−2.80	−9.10

TABLE 6.1: Numerical values of the parameters for the spectra plotted in Fig. 6.2

Finally, it may be interesting to check that the allowed spectra of our non-minimal model are compatible not only with the normalisation (6.1) of the spectral amplitude, but also with the power-law behaviour f^α suggested at the 90% confidence level by the data fit of [179] in the frequency range $f_s \lesssim f \lesssim 10^{-6}$ Hz, with a power roughly given by $-0.66 \lesssim \alpha \lesssim 0.18$. The corresponding allowed region for the spectrum is illustrated by the yellow shaded area of Fig. 6.2, well consistent with the allowed spectra of the non-minimal models both with and without S-duality symmetry.

6.3.4 Remarks on the spectrum of scalar curvature perturbations

To complete our presentation of the main physical aspects of the non-minimal scenario, introduced in order to support a possible cosmological interpretation of the IPTA signal, it may be useful to briefly illustrate also the properties of the

primordial spectrum of adiabatic scalar curvature perturbations produced by the axion through the curvaton mechanism [75, 110, 111, 174], and associated to the relic GW spectrum discussed before.

Let us recall, to this purpose, that in the minimal pre-big bang scenario the (superhorizon) scalar spectrum of metric perturbations $P_s(f)$ at the axion decay time τ_d is simply proportional to the primordial axion perturbation spectrum $P_\sigma(f)$ at all perturbation scales, i.e. $P_s \sim T^2 P_\sigma$, where T is given by Eq. (6.9). Also, in the minimal scenario, the low frequency branch of the scalar spectrum ($f < f_s$) has a slightly decreasing power-law behaviour in agreement with the observed CMB anisotropy, i.e. $P_s(f) \sim f^{n_s-1}$. For the high frequency modes, leaving the horizon during the high energy string phase ($f_s < f < f_1$), the power-law behaviour is determined by the same parameter β (but with the opposite sign) controlling the growth of tensor perturbations, so that $P_s(f) \sim f^{-2\beta}$. Since $\beta > 0$ it turns out, for the minimal scenario, that the intensity of the scalar spectrum is always decreasing with frequency, and it becomes fully negligible in the high frequency limit.

In the context of the non-minimal scenario that we are considering here the situation is quite similar, but with only one (crucial) difference: the two parameters controlling the pump field evolution and the spectral distribution, in the case of tensor perturbations (β_h) and of axion/scalar perturbations (β_σ), are in general different and in principle unrelated, $\beta_\sigma = -\beta_h + \epsilon$, see Eq. (6.10). However, they are strongly constrained by the whole set of theoretical as well as phenomenological conditions discussed in Sects. 3.1, 3.2. It turns out, in particular, that the allowed values of β_σ are always positive, and small enough so that the high frequency branch of the scalar perturbation spectrum, according to Eq. (6.22), is always growing in frequency as $P_s(f) \sim f^{2\beta_\sigma}$, $\beta_\sigma > 0$.

Note that, unlike the GW spectrum, the axion and (as a consequence) the curvature power spectrum do not have breaks in the slope at f_d and f_σ. This is because axion perturbations re-entering the horizon during the axion-dominated phase are already non relativistic (since $f/(2\pi) \sim H < m$) as discussed in detail in Appendix A of [111].

This important physical difference between the minimal and non-minimal scenario is emphasized in Fig. 6.3. We have plotted, for the non-minimal scenario, the primordial spectra of scalar perturbations exactly corresponding to the GW spectra

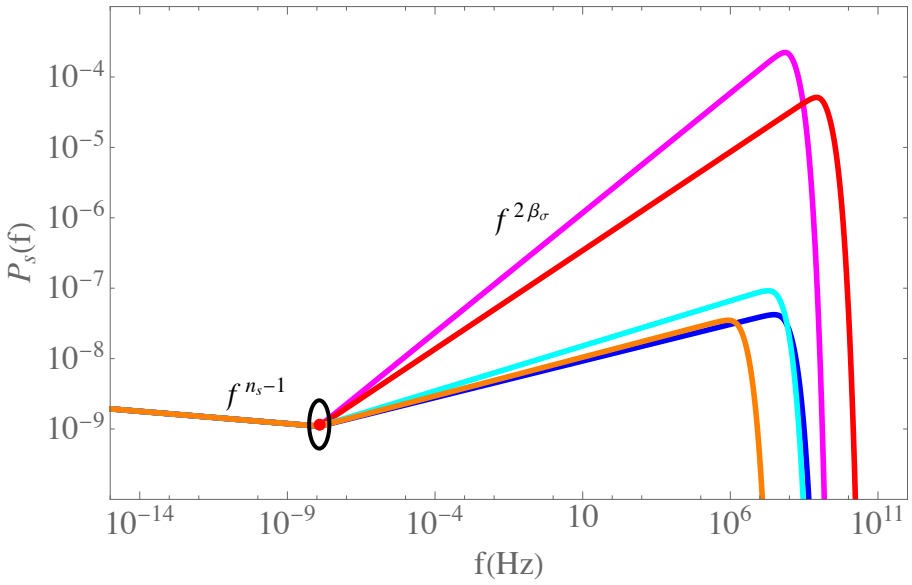

FIGURE 6.3: The five spectra of scalar perturbations associated with the five GW spectra of the non-minimal models illustrated in Fig. 6.2 and Table 6.1 (with the same colors).The change of slope correspond to the frequency f_s obtained from the fit of the NANOGrav data. Note that, contrary to the case of the GW spectrum, the scalar spectrum is always growing for $f > f_s$.

illustrated in Fig. 6.2, and with the colors exactly corresponding to the list of five different models reported in Table 6.1. Note that the change of slope, for all spectra, obviously correspond to the frequency f_s reported in Eq. (6.1) and obtained with the fit of the NANOGrav data (the corresponding spectral amplitude is different, of course, as it describes primordial scalar perturbations).

It should be stressed, finally, that such a class of scalar spectra is well compatible with present phenomenological bounds (see e.g. [190], [191]), and may have interesting applications on the possible production of primordial black holes (PBH), as we are planning to discuss in a future paper.

6.4 Outlook

The conclusion of this paper is that the interpretation of the IPTA signal [30–33, 35, 36] as due to a stochastic background of relic gravitons produced in a string model of pre-big bang evolution, as suggested in [179] on the ground of a simple but phenomenologically incomplete GW spectrum, and referred in particular to a fit of the NANOGrav 15-year data set, may still be valid, and consistent with all

constraints, if based on GW spectra obtained from more general, "non-minimal" string cosmology scenarios.

In this paper we have followed the results of [179], and we assumed ab initio that the frequency obtained with the fit of the NANOGrav data can be identified with the frequency f_s of the transition from the dilaton to the string-curvature phase (see Eq. (6.1)). One could ask what happens if f_s is left as another parameter of the model to be best-fitted to the data. While we are convinced that choosing $f_s \gg f_{\rm PTA} \approx 1.2 \times 10^{-8}$Hz would not be able to reproduce observations (because of the fast drop of the spectrum below f_s) it is not clear to what extent the case $f_s < f_{\rm PTA}$ can be ruled out. We could ask, also, to what extent the results of this paper may change if, instead of starting from the fit of Eq. (6.1), one would attempt a global fit of the complete set of IPTA data. Answering these questions would amount to finding out to what extent our non-minimal model is fine-tuned.

We will give a possible string-theoretical interpretation of the approximately flat GW spectra which seems to be needed just above f_s, if we want to attribute the IPTA signal to a cosmological scenario of this type in Chapter 8.

Chapter 7

Viscosity in Isotropic Cosmological Backgrounds in General Relativity and Scalar-Tensor Gravity

In this Chapter I will present some of the results obtained in [1] which are functional to the analysis of Gravitational Wave propagation in the presence of shear viscous fluids during the string phase in the pre-Big Bang scenario. In particular I will show that in a general class of homogeneous but not isotropic space-time (which includes the FLRW case), comoving shear viscous fluids do not alter the background geometry evolution. This result is valid both in the Einstein frame and in the Jordan frame and some useful transformations will be derived for the dissipative coefficients of a viscous fluid when changing frame.

7.1 Introduction

In the last years the study of the gravitational and electromagnetic luminosity distance has been considered, because it is an excellent test for general relativity, in which the two distances are equal in Friedmann-Lamaître-Robertson-Walker (FLRW) backgrounds [127, 192–205]. In relation to this topic, in a recent paper

[206], the authors expand on our previous results [6, 8, 207] on the ratio between the gravitational wave luminosity distance and electromagnetic luminosity distance in a viscous dark matter cosmological model in Einstein and Starobinsky gravity [208–211]. They claim that the presence of shear viscous fluids in Starobinsky gravity is able to change the electromagnetic luminosity distance $d_L^{\rm EM}$, and they perform cosmological parameter estimation using Supernova Ia, Cosmic Chronometers and Gamma Ray Bursts with two types of evolution for the shear viscosity η_V.
However we find that the very first assumption on the influence of the shear viscosity on the background evolution contradicts our previous results obtained in [8], where we claimed that in a standard FLRW cosmology, shear viscosity does not modify the Friedmann equations and, leads to a luminosity distance for electromagnetic waves unaltered by its presence. This feature is preserved also in modified gravity theories, such as $F(R)$ gravity and in the Gravi-Dilaton sector coming from String Theory.

The motivation for this Chapter is to point out from general geometrical arguments that the time component of the divergence of the stress-energy tensor $\nabla_\mu T^{\mu\nu}$, regardless of the gravitational theory under exam, cannot be affected by the presence of anisotropic stresses (that is the case for comoving viscous fluids), for a larger class of isotropic but non-homogeneous space-time that includes the FLRW case (Sect. 7.2), both in the Einstein Frame and in the Jordan Frame (Sect. 7.3) [212–215], where we show how viscous coefficients and the continuity equation transform under conformal rescaling. These results are useful for a comprehensive understanding of the final Chapter 8.

7.2 The continuity equation in a class of isotropic geometries

In this section we demonstrate that regardless of the gravitational theory under study, the covariant derivative of the stress-energy tensor for a comoving dissipative fluid, in a particular class of isotropic, but non-homogeneous space-time is independent from the shear viscosity. We work in the Eckart reference frame,

where the 4-velocity is taken to be parallel to the particle flux and heat transfer is manifest. The 4-velocity can be expressed as $u^\mu(x)$ and it is a time-like vector $u_\mu u^\mu = 1$. We can decompose the energy-momentum tensor in terms of projections parallel and perpendicular to u^μ by defining the following projector $h_{\mu\nu} = g_{\mu\nu} - u_\mu u_\nu$, with the properties $h_{\mu\nu}h^{\mu\nu} = 3$, $h_{\mu\alpha}h^{\alpha\nu} = \delta^\nu_\mu$ and orthogonal to the 4-velocity, $h_{\mu\nu}u^\nu = 0$. In this frame we identify the energy density ρ, the pressure p, the bulk pressure Π, the heat flux q_μ and the anisotropic stress $\pi_{\mu\nu}$ (which is related to the shear viscosity), as follows [216]

$$\begin{aligned} \rho &= T_{\mu\nu}u^\mu u^\nu, \\ p + \Pi &= -\frac{1}{3}T_{\mu\nu}h^{\mu\nu}, \\ q_\mu &= h_\mu{}^\lambda u^\nu T_{\nu\lambda}, \\ \pi_{\mu\nu} &= T_{\langle\mu\nu\rangle}, \end{aligned} \tag{7.1}$$

where the angular parenthesis denote symmetric and traceless part of the tensor projected on the space-like sub-space orthogonal to u_μ, namely

$$A_{\langle\mu\nu\rangle} = \left(h_\mu{}^{(\alpha|}h_\nu{}^{|\beta)} - \frac{1}{3}h_{\mu\nu}h^{\alpha\beta}\right)A_{\alpha\beta}, \tag{7.2}$$

where we denote the usual symmetrization in round brackets $B_{(\mu\nu)} \equiv \frac{1}{2}\left(B_{\mu\nu} + B_{\nu\mu}\right)$. With this typical conventions, the stress-energy tensor can be written as

$$T_{\mu\nu} = \rho u_\mu u_\nu - (p + \Pi)h_{\mu\nu} + 2u_{(\mu}q_{\nu)} + \pi_{\mu\nu}. \tag{7.3}$$

The geometrical meaning of each term is now manifest, every term in the stress-energy tensor is decomposed in the basis defined by the projector tensor $h_{\mu\nu}$, the 4-velocity $u_\mu u_\nu$ and the vectorial part obtained by projecting the stress-energy tensor on $h_\mu{}^\lambda u^\alpha$. Most importantly the anisotropic stress is the part of the stress-energy tensor, orthogonal to u_μ and traceless, so $u^\mu\pi_{\mu\nu} = 0 = h^{\mu\nu}\pi_{\mu\nu}$ and for this reason it is the source of the modification in the evolution equation of transverse and traceless tensor perturbations [6].

We also recall that the bulk pressure Π and the anisotropic stress $\pi_{\mu\nu}$ are related via the bulk ($\zeta \geqslant 0$) and shear ($\eta_V \geqslant 0$) viscosity to the expansion rate Θ and shear tensor $\sigma_{\mu\nu}$ respectively, by the following relations

$$\begin{aligned} \Pi &\equiv -\zeta\Theta = -\zeta h^\alpha_\mu \nabla_\alpha u^\mu = -\zeta\nabla_\alpha u^\alpha, \\ \pi_{\mu\nu} &\equiv 2\eta_V\sigma_{\mu\nu} = 2\eta_V h^\alpha_{\langle\mu|}\nabla_\alpha u_{|\nu\rangle} = 2\eta_V\nabla_{\langle\mu|}u_{|\nu\rangle}, \end{aligned} \tag{7.4}$$

where in the last two equalities we used $u_\mu \nabla_\nu u^\mu = 0$ and, the last term in the previous expression is the traceless and orthogonal to u^μ part of the strain-rate tensor $\nabla_\mu u_\nu$. After some algebraic manipulation the stress-energy tensor can be expressed as

$$\begin{aligned} T_{\mu\nu} =& \rho u_\mu u_\nu - (p - \zeta \nabla_\alpha u^\alpha) h_{\mu\nu} + 2u_{(\mu} q_{\nu)} \\ & - \eta_V \big(u_\mu u^\alpha \nabla_\alpha u_\nu + u_\nu u^\alpha \nabla_\alpha u_\mu - \nabla_\mu u_\nu - \nabla_\nu u_\mu + \frac{2}{3} h_{\mu\nu} \nabla_\alpha u^\alpha \big), \end{aligned} \tag{7.5}$$

in concordance with [6, 8, 206]. Now we are going to compute the divergence of Eq. (7.5). In order to have the energy continuity equation, we evaluate the projection of the divergence of the stress-energy tensor on the 4-velocity, $u_\mu \nabla_\nu T^{\mu\nu}$. Using the following identities

$$u_\mu q^\mu = 0, \qquad \nabla_\mu h^{\mu\nu} = -u^\nu \Theta, \qquad u_\mu \nabla_\nu q^\mu = -q^\mu \nabla_\nu u_\mu, \tag{7.6}$$

and the orthogonality relations, we have

$$\begin{aligned} u_\mu \nabla_\nu (\rho u^\mu u^\nu) &= u^\nu \nabla_\nu \rho + \rho \Theta, \\ u_\mu \nabla_\nu [(p + \Pi) h^{\mu\nu}] &= -(p + \Pi)\Theta, \\ u_\mu \nabla_\nu (2 q^{(\mu} u^{\nu)}) &= \nabla_\nu q^\nu - u^\nu q^\mu \nabla_\nu u_\mu, \\ u_\mu \nabla_\nu \pi^{\mu\nu} &= \eta_V \big[- (\nabla_\nu u^\alpha)(\nabla_\alpha u^\nu) - (\nabla^\alpha u_\nu)(\nabla_\alpha u^\nu) \\ &\quad + u^\nu u^\alpha (\nabla_\nu u_\mu)(\nabla_\alpha u^\mu) + \frac{2}{3}\Theta^2 \big] \\ &= -2\eta_V \sigma^2, \end{aligned} \tag{7.7}$$

where in the last equality we have defined $\sigma^2 \equiv \sigma_{\mu\nu}\sigma^{\mu\nu}$. Finally using Eqs. (7.7) we find

$$u_\mu \nabla_\nu T^{\mu\nu} = u^\nu \nabla_\nu \rho + (\rho + p + \Pi)\Theta + \nabla_\nu q^\nu - u^\nu q^\mu \nabla_\nu u_\mu - 2\eta_V \sigma^2. \tag{7.8}$$

The question whether or not the shear viscosity can enter the energy equation is now a matter of evaluating the shear tensor for a given geodesic in a given space-time.

For the sake of generality we do not assume homogeneity for our background geometry, namely we use a rotationally invariant (isotropic) metric in the synchronous gauge, with line element given by:

$$ds^2 = dt^2 - e^{2\lambda(t,r)} \left(A(r)^2 dr^2 + B(r)^2 d\Omega_2^2 \right), \tag{7.9}$$

with $d\Omega_2^2 = d\theta^2 + \sin^2(\theta)d\phi^2$. The reason behind this choice is to prove, as long as the fluid is comoving, that shear viscosity cannot enter into the expression $u_\mu \nabla_\nu T^{\mu\nu}$ in more generic space-time that are isotropic but not homogeneous. We would also like to stress, that for the metric given in Eq. (7.9), a comoving observer, $u^\mu = (1, 0, 0, 0)$ is also geodesic, $u^\mu \nabla_\mu u^\nu = \Gamma_{00}{}^{\nu} = 0$, so we will assume that our fluid is comoving with the geometry itself.

Under the assumption of comoving fluid it is straightforward to evaluate the shear tensor

$$\begin{aligned} \sigma_{\mu\nu} &= \nabla_{(\mu} u_{\nu)} - u_{(\mu|} u^\alpha \nabla_\alpha u_{|\nu)} - \frac{1}{3} h_{\mu\nu} \nabla_\lambda u^\lambda \\ &= \nabla_{(\mu} u_{\nu)} - \frac{1}{3} h_{\mu\nu} \nabla_\lambda u^\lambda, \end{aligned} \tag{7.10}$$

where in the last line we used the geodesic equations. The $0 - \mu$ component of Eq. (7.10) is vanishing because of the orthogonality conditions $\sigma_{\mu 0} = u^\nu \sigma_{\mu\nu} = 0$, while the $i - j$ components are given by

$$\sigma_{ij} = -\Gamma_{ij}{}^{0} - \frac{1}{3} g_{ij} \Gamma_{\lambda 0}{}^{\lambda}. \tag{7.11}$$

Defining $\partial_0 \lambda(t, r) \equiv H(t, r)$, we have $\Gamma_{ij}{}^{0} = -H(t, r) g_{ij}$ and $\Gamma_{\lambda 0}{}^{\lambda} = 3H(t, r)$, so $\sigma_{ij} = 0$ and we conclude that the shear tensor is vanishing and so $\sigma^2 = 0$. We generically proved that the gravitational equations of a yet to be specified gravitational theory, cannot be affected by the presence of a shear viscous contribution, as long as the background fluid source is comoving.[1]. As a consequence the background evolution is not affected by its presence and, so are null geodesics, implying that also the luminosity distance is independent on the shear viscosity. It is easy to check that upon the following identifications, $e^{2\lambda(t,r)} \to a^2(t)$, $A(r)^2 \to \frac{1}{1-kr^2}$ and $B(r)^2 \to r^2$, the line element Eq. (7.9) is the standard FLRW one. The immediate consequence is that no shear contribution can be present in the energy equation, nor in the background evolution equations, hence it cannot affect the background geometry evolution.

For completeness we evaluate Eq. (7.8) for a comoving fluid in the space-time given by Eq. (7.9), including possible heat flux, $q^\mu \neq 0$. Due to the choice of the metric and the comoving fluid, the only component of the heat flux that is non trivial is q^1. This statement can be understood using the orthogonality $q^\mu u_\mu = 0$, which implies $q^0 = 0$ and, the Einstein ($F(R)$) equations. Assuming $F(R) = R + \alpha f(R)$,

[1] Assuming that the gravitational equations are in the form $L_{\mu\nu} = \lambda_p^2 T_{\mu\nu}$, where the tensor $L_{\mu\nu}$ is intended to be containing the geometrical information of the theory (e.g. $L_{\mu\nu} = G_{\mu\nu}$ in General Relativity)

denoting with $f_R \equiv \frac{df(R)}{dR}$ and defining

$$\mathcal{A}_{\mu\nu} \equiv f_R\, R_{\mu\nu} + g_{\mu\nu}\big(\nabla^2 f_R - \frac{1}{2} f\big) - \nabla_\mu \nabla_\nu f_R, \tag{7.12}$$

we can write the Einstein ($F(R)$) equations as

$$G_{\mu\nu} + \alpha \mathcal{A}_{\mu\nu} = \lambda_p^2 T_{\mu\nu}, \tag{7.13}$$

where $G_{\mu\nu}$ is the Einstein tensor $G_{\mu\nu} \equiv R_{\mu\nu} - \frac{1}{2} g_{\mu\nu} R$ and α is a constant. The only off diagonal terms in these equations are the one given by the $0-1$ component and they can be sourced only by the term $q_1 u_0$ in the stress-energy tensor. The other off-diagonal terms are vanishing on the left hand side of Eq. (7.13) and enforce $q_\mu = (0, q_1, 0, 0)$[2]. Denoting with a dot the derivative with respect to t and with a $'$ the derivative with respect to r, we find that Eq. (7.8) reduces to

$$\begin{aligned} u_\mu \nabla_\nu T^{\mu\nu} = {} & \dot{\rho} + q'^1 + 3H(t,r)\left[\rho + p - 3\zeta H(t,r)\right] \\ & + 3\lambda'(t,r) q^1 + \big(\frac{A'(r)}{A(r)} + 2\frac{B'(r)}{B(r)}\big) q^1. \end{aligned} \tag{7.14}$$

Assuming, $\zeta = 0$, $q^\mu = 0$, a dust dark matter $p = 0$, and an FLRW geometry, namely $H(t,r) = H(t)$, recalling that as consequence of the Bianchi identities, both in Einstein and Starobinsky theories the divergence of the left hand side of Eq. (7.13) is vanishing [207], we recover from Eq. (7.14) the standard continuity equation

$$u_\mu \nabla_\nu T^{\mu\nu} = \dot{\rho} + 3H(t)(\rho + p) = 0. \tag{7.15}$$

We emphasize that no shear viscous contributions are present. However, if we allow the presence of a non trivial bulk viscosity $\zeta \neq 0$, but retaining the FLRW geometry we find from Eq. (7.14) the well known result

$$u_\mu \nabla_\nu T^{\mu\nu} = \dot{\rho} + 3H(t)\big[\rho + p - 3\zeta H(t)\big] = 0. \tag{7.16}$$

We note that the analysis has been carried out without assuming any specific gravitational theory, and as a general feature, even for the broader class of isotropic geometries considered in Eq. (7.9), the covariant divergence of the stress-energy tensor projected along the comoving 4-velocity does not include contributions from

[2]The presence in General Relativity ($\alpha = 0$) of a trivial heat flux $q^\mu = 0$, would imply $G_{01} = -2\partial_r H(t,r) = 0$, and would enforce the separability $e^{\lambda(t,r)} = a(t)C(r)$. The factor $C(r)$ can be absorbed by a redefinition of the functions $A(r)$ and $B(r)$ leading to a more restricted space-time than the one in Eq. (7.9).

anisotropic stress.

In $F(R)$ and String gravity, this conclusion remains valid even when reformulating the theory in the so-called Einstein frame: no shear contributions appear in the continuity equation. However, additional terms can arise on the right-hand side of Eq. (7.15) due to the conformal rescaling of the metric $g^J_{\mu\nu} = e^{\psi} g^E_{\mu\nu}$. These include terms like $2\rho\dot{\psi}$ in the Jordan frame or $\frac{\dot{\psi}}{2}(\rho - 3p)$ in the Einstein frame, depending on the comoving frame adopted. While these terms may resemble the structure of viscous contributions, their form is not arbitrary: they must be consistent with the Friedmann equations and the dynamics of a minimally coupled scalar field with potential $\tilde{V}(\psi) = \frac{RF'(R) - F(R)}{F'(R)^2}$ and $\psi = -\ln F'$. In the next section, we will derive the continuity equation for a dissipative fluid in both frames for the general isotropic space-time given in Eq. (7.9).

7.3 Conformal rescaling and the continuity equation: absence of shear viscous contributions in general isotropic space-time

In this section, we provide a detailed derivation to support our claim that the modification of the continuity equation under conformal rescaling is not associated with shear viscosity effects. Although modifications of the continuity equation arise naturally in the Einstein frame (EF) when matter is non-minimally coupled via the conformal factor, they cannot be interpreted as contributions from shear viscosity. This holds regardless of the specific gravitational theory considered, as long as the Einstein frame exists. One can foresee without any explicit computation that based solely on geometrical arguments, a conformal rescaling can alter "volume changing" terms, but not deformation terms such as the shear tensor for the very nature of conformal transformations, since they are volume changing and angle preserving. It is worth noting that in the Jordan frame, where conformal rescaling is not active, such modifications do not occur. Even going from the Jordan frame (JF) to the Einstein frame (EF), shear viscosity only couples to the shear tensor, that is vanishing in both frames when an FLRW space-time is assumed, or the more general class considered in Eq. (7.9). In the following we are going to give a detailed analysis of this statement.

Starting with a minimally coupled dissipative fluid in the JF we perform a conformal transformation in the form $g^J_{\mu\nu} \to e^{\psi} g^E_{\mu\nu}$, without specifying the gravitational theory under exam. For instance the conformal factor ψ can be identified as the dilaton field ϕ when going from the so called String frame to the Einstein frame while dealing with the effective tree-level action of the bosonic massless multiplet of string theory in 4-dimensions

$$S^S_{\rm string} \sim -\int d^4x\sqrt{-g^S}e^{-\phi}(R^S + (\nabla\phi)^2 - \frac{1}{12}H_{\mu\nu\alpha}H^{\mu\nu\alpha}) + S^S_m(g^S_{\mu\nu}, ...), \quad (7.17)$$

that after conformal rescaling $g^S_{\mu\nu} \to e^{\phi} g^E_{\mu\nu}$ becomes

$$S^E_{\rm string} \sim -\int d^4x\sqrt{-g^E}(R^E - \frac{1}{2}(\nabla\phi)^2 - \frac{1}{12}e^{-2\phi}H_{\mu\nu\alpha}H^{\mu\nu\alpha}) + S^E_m(g^E_{\mu\nu}e^{\phi}, ...). \quad (7.18)$$

In $F(R)$ gravity the action can be recasted in a scalar-tensor form via the introduction of a Lagrange mulptiplier $\chi = F'(R)$

$$S^J = -\frac{1}{2\lambda_P^2}\int d^4x\sqrt{-g^J}(\chi R - V(\chi)) + S_m(g^J_{\mu\nu}, ...), \quad (7.19)$$

where $V(\chi) = RF'(R) - F(R)$. A conformal rescaling of the metric and neglecting total derivatives leads to

$$S^E = -\frac{1}{2\lambda_P^2}\int d^4x\sqrt{-g^E}e^{2\psi}\Big[e^{-\psi}\chi(R^E - \frac{3}{2}(\nabla\psi)^2) - V(\chi)\Big] + S_m(g^E_{\mu\nu}e^{\psi}, ...). \quad (7.20)$$

Fixing $\psi = -\ln\chi$ we end up with the following action

$$S^E = -\frac{1}{2\lambda_P^2}\int d^4x\sqrt{-g^E}(R^E - \frac{3}{2}(\nabla\psi)^2 - \tilde{V}(\psi)\Big] + S_m(g^E_{\mu\nu}e^{\psi}, ...), \quad (7.21)$$

where $\tilde{V}(\psi) = \frac{RF'(R) - F(R)}{F'(R)^2}$. We emphasize that an exponential pre-factor arise in the matter lagrangian which couples non trivially the new scalar degree of freedom ψ to matter, namely

$$S^E_m \sim \int d^4x\sqrt{-g^E}e^{2\psi}\mathcal{L}^J(g^E_{\mu\nu}e^{\psi}, ...). \quad (7.22)$$

This is the starting point of our analysis. We start with a minimally coupled fluid in the JF and under conformal rescaling we will derive the continuity equation in the EF, without specifying the particular theory under exam, (as long as a conformal rescaling can bring the original theory action to an Einsteinian form).

We will show that also in this case, even if additional terms arise in the case of Starobinsky gravity, they do not couple to the shear tensor in the isotropic metric considered in Eq. (7.9), hence in the FLRW case.
The general transformation for the energy-momentum tensor can be evaluated by varying the matter action in the JF with respect to its metric and applying the conformal transformation (we evaluate the transformation in general $d+1$ dimensions)

$$\begin{aligned}\delta_{g^J} S_m &\equiv \frac{1}{2}\int d^{d+1}x\sqrt{|g^J|}T^J_{\mu\nu}\delta g^{\mu\nu}_J = \frac{1}{2}\int d^{d+1}x\sqrt{|g^E|}e^{\frac{d-1}{2}\psi}T^J_{\mu\nu}\delta g^{\mu\nu}_E\,,\\ \delta_{g^E} S_m &\equiv \frac{1}{2}\int d^{d+1}x\sqrt{|g^E|}T^E_{\mu\nu}\delta g^{\mu\nu}_E\,,\end{aligned} \tag{7.23}$$

so by comparing the last two lines we get

$$T^J_{\mu\nu} = e^{-\frac{d-1}{2}\psi}\,T^E_{\mu\nu}. \tag{7.24}$$

In the following we are going to assume that, as in $F(R)$ theories, the stress-energy tensor is conserved in the JF [3], and we are going to evaluate the divergence on both sides. We recall that the Christoffel connection transforms as follows

$$\Gamma^J_{\mu\nu}{}^{\alpha} = \Gamma^E_{\mu\nu}{}^{\alpha} + \mathcal{C}_{\mu\nu}{}^{\alpha}, \qquad \mathcal{C}_{\mu\nu}{}^{\alpha} \equiv \frac{1}{2}\big(\delta^\alpha_\nu\partial_\mu\psi + \delta^\alpha_\mu\partial_\nu\psi - g^E_{\mu\nu}g^{\alpha\rho}_E\partial_\rho\psi\big). \tag{7.25}$$

Using the continuity equation in the JF we obtain the following identity in the EF

$$0 = \nabla_\mu T^{\mu\nu}_J = \nabla^E_\mu\big(e^{-\frac{d+3}{2}\psi}T^{\mu\nu}_E\big) + \mathcal{C}_{\mu\alpha}{}^{\mu}e^{-\frac{d+3}{2}\psi}T^{\alpha\nu}_E + \mathcal{C}_{\mu\alpha}{}^{\nu}e^{-\frac{d+3}{2}\psi}T^{\mu\alpha}_E, \tag{7.26}$$

where we defined $\nabla^E_\mu A^{\alpha\nu\cdots} \equiv \partial_\mu A^{\alpha\nu\cdots} + \Gamma^E_{\mu\rho}{}^{\mu}A^{\rho\nu\cdots} + \dots$. A straight forward evaluation leads using Eqs. (7.25) to the conservation equation in the EF as

$$\nabla^E_\mu\, T^{\mu\nu}_E = \frac{T_E}{2}\partial^\nu\psi, \tag{7.27}$$

where $T_E = g^E_{\mu\nu}T^{\mu\nu}_E$ is the trace of the stress-energy tensor in the Einstein frame. Following the geometrical definitions given in Eqs. (7.1) and demanding that $u^J_\mu u^\mu_J = 1 = u^E_\mu u^\mu_E$, so that $u^\mu_J = e^{-\frac{\psi}{2}}u^\mu_E$, $h^J_{\mu\nu} = g^J_{\mu\nu} - u^J_\mu u^J_\nu = e^\psi h^E_{\mu\nu}$ we find

$$\Pi^J = e^{-\frac{\psi}{2}}\Pi^E, \qquad \Pi^E \equiv -\zeta^J\big(\Theta^E + \frac{d}{2}u^\mu_E\partial_\mu\psi\big), \qquad \Theta^E \equiv \nabla^E_\mu u^\mu_E, \tag{7.28}$$

[3] this is not the case for the effective theory coming from string theory when there is a dilatonic charge $\delta_\phi S_m = -\frac{1}{2}\int d^{d+1}x\sqrt{|g|}\sigma\delta\phi \neq 0$.

and recalling the definition of the angular parenthesis given in Eq. (7.2) (in d dimensions)

$$A_{\langle\mu\nu\rangle} = \left(h_\mu{}^{(\alpha|}h_\nu{}^{|\beta)} - \frac{1}{d}h_{\mu\nu}h^{\alpha\beta}\right)A_{\alpha\beta}, \tag{7.29}$$

we find for the anisotropic stress

$$\begin{aligned} \pi^J_{\mu\nu} &= 2\eta^J_V\sigma^J_{\mu\nu} = 2\eta^J_V e^{\frac{\psi}{2}}\sigma^E_{\mu\nu} \\ \sigma^E_{\mu\nu} &\equiv \nabla^E_{\langle\mu}u^E_{\nu\rangle}, \end{aligned} \tag{7.30}$$

and finally $q^J_\mu = q^E_\mu e^{-\frac{d}{2}\psi}$. Using Eq. (7.3) we are now able to evaluate the stress-energy tensor in the E-frame using Eqs. (7.28) and (7.30) and inverting the relation (7.24)

$$T^E_{\mu\nu} = \rho^E u^E_\mu u^E_\nu - \left[p^E - \zeta^E\left(\Theta^E + \frac{d}{2}u^\mu_E\partial_\mu\psi\right)\right]h^E_{\mu\nu} + 2u^E_{(\mu}q^E_{\nu)} + 2\eta^E_V\sigma^E_{\mu\nu} \tag{7.31}$$

where we defined the following transformations laws from the JF to the EF

$$\rho^E \equiv e^{\frac{d+1}{2}\psi}\rho^J, \qquad p^E \equiv e^{\frac{d+1}{2}\psi}p^J, \qquad \zeta^E \equiv e^{\frac{d}{2}\psi}\zeta^J, \qquad \eta^E_V \equiv e^{\frac{d}{2}\psi}\eta^J_V. \tag{7.32}$$

The divergence in the EF of the stress-energy tensor follows the same relations of Eqs. (7.7)

$$\begin{aligned} u^E_\mu\nabla^E_\nu(\rho^E u^\mu_E u^\nu_E) &= u^\nu_E\nabla^E_\nu\rho^E + \rho^E\Theta^E, \\ u^E_\mu\nabla^E_\nu[(p^E + \Pi^E)h^{\mu\nu}_E] &= -(p^E + \Pi^E)\Theta^E, \\ u^E_\mu\nabla^E_\nu(2q^{(\mu}_E u^{\nu)}_E) &= \nabla^E_\nu q^\nu_E - u^\nu_E q^\mu_E\nabla^E_\nu u^E_\mu, \\ u^E_\mu\nabla^E_\nu\pi^{\mu\nu}_E &= -2\eta^E_V\sigma^2_E, \end{aligned} \tag{7.33}$$

and the trace of Eq. (7.31) reads

$$T^E = \rho^E - d(p^E + \Pi^E) = \rho^E - dp^E + d\zeta^E\Theta^E + \frac{d^2}{2}u^\mu_E\partial_\mu\psi. \tag{7.34}$$

Projecting on the four velocity the right hand side of Eq. (7.27) we finally obtain the continuity equation in the EF

$$\begin{aligned} &u^\nu_E\nabla^E_\nu\rho^E + (\rho^E + p^E + \Pi^E)\Theta^E - \frac{u^\mu_E\partial_\mu\psi}{2}\left[\rho^E - d(p^E + \Pi^E)\right] \\ &+ \nabla^E_\nu q^\nu_E - u^\nu_E q^\mu_E\nabla^E_\nu u^E_\mu - 2\eta^E_V\sigma^2_E = 0. \end{aligned} \tag{7.35}$$

This equation justifies the expectations we exposed at the beginning, the conformal rescaling cannot affect the shear part of the stress-energy tensor if the stress

tensor is vanishing in one frame, due to Eq. (7.30). To fully conclude our argument we have to specify a background metric and the motion of our background fluid. Two possibilities now arise, the fluid is geodesic in the EF, or the fluid is geodesic in the JF. It is widely known that a geodesic fluid in the JF, under conformal rescaling is not geodesic in the EF in general and vice versa, and only a radiation fluid stays geodesics (i.e. conformal transformations preserve the light-like geodesics), so we are going to analyze both cases. As will become evident, modifications of the continuity equation consistent with shear viscosity do not naturally arise from the conformal structure, regardless of the frame considered.

7.3.1 Geodesic fluid in the Jordan Frame

Although one can go through an explicit derivation of the shear tensor in the EF, this is not necessary, since we have already proven that for the general class of space-time Eq. (7.9), $0 = \pi^J_{\mu\nu} = 2\eta^J_V \sigma^J_{\mu\nu}$, but making use of the transformations in Eqs. (7.30), also $\sigma^E_{\mu\nu} = 0$, hence $\sigma^2_E = 0$ and no shear viscous contributions are present in the continuity equation (7.35) also in the EF. Being valid for the general case of Eq. (7.9), it still holds for the particular case of FLRW. This result says that even from a phenomenological standpoint, the correction to the conservation equation due to the conformal rescaling, does not involve shear viscosity. We recall that physical observables such as the luminosity distance are frame independent [217–219], so no matter the frame, the observed luminosity distance is not affected by which frame one decide to work with. From the geodesic condition in the JF $u^\nu_J \nabla^J_\nu (u^\mu_J) = 0$ we have that $u^\nu_E \nabla^E_\nu (u^\mu_E) = \frac{1}{2}(\partial^\mu \psi - u^\mu_E u^\nu_E \partial_\nu \psi)$ and from the comoving condition in the Jordan frame (we are fixing $d = 3$ from now on), we have $u^\mu_E = e^{\frac{\psi}{2}}(1,0,0,0)$. From $q^E_\mu u^\mu_E = 0$ we have $q^E_0 = 0$, and moreover we know that the Einstein equations can be written as $G_{\mu\nu} = \lambda^2_P T^{tot}_{\mu\nu}$, where $T^{tot}_{\mu\nu} = T^{\psi}_{\mu\nu} + T^{fluid}_{\mu\nu}$, where the stress-energy tensor for ψ corresponds to the one of a scalar field with potential $\tilde{V}(\psi)$. From the symmetries of the metric under study, we know that also in the EF, where the metric is $g^E_{\mu\nu} = e^{-\psi} g^J_{\mu\nu}$, the only off-diagonal non-vanishing components of the Einstein tensor are the $0-1$, hence $q^\mu_E = (0, q^1_E, 0, 0)$ and $\psi = \psi(t, r)$. Using for the JF metric the one given in Eq. (7.9), we get the

continuity equation as

$$\begin{aligned}&\dot{\rho}^E + 3H(t,r)(\rho^E + p^E - 3\zeta^E H(t,r)e^{-\psi}) \\ &- 2\rho^E\dot{\psi} + e^{-\frac{\psi}{2}}\left[q_E'^1 + q_E^1\left(\frac{A'}{A} + 2\frac{B'}{B} + 3\lambda' - \frac{3}{2}\psi'\right)\right] = 0.\end{aligned} \tag{7.36}$$

In the FLRW limit for dust fluid, where $\psi = \psi(t)$ and with vanishing bulk viscosity we get

$$\dot{\rho}^E + 3H(\rho^E + p^E) - 2\rho^E\dot{\psi} = 0. \tag{7.37}$$

This confirms our initial statement: in the Einstein frame, corrections induced by conformal transformations are constrained and cannot reintroduce shear contributions.

7.3.2 Geodesic fluid in the Einstein Frame

For this case we assume that the line element in the Einstein frame is the one given by Eq. (7.9) and that the fluid is comoving $u_E^\mu = (1,0,0,0)$, hence geodesic in the EF. For the same reasons given in the previous subsection, also in this case, the shear tensor vanishes identically, ruling out any shear-viscous contribution to the conservation equation. In this case the continuity equation reads

$$\begin{aligned}&\dot{\rho}^E + 3H(t,r)\left[\rho^E + p^E - 3H(t,r)e^{-\frac{3}{2}\psi}\zeta^E\right] \\ &- \frac{\dot{\psi}}{2}\left(\rho^E - 3p^E - \frac{3}{2}e^{-\frac{3}{2}\psi}\zeta^E\dot{\psi}\right) + q_E^1\left(\frac{A'}{A} + 2\frac{B'}{B} + 3\lambda'\right) = 0,\end{aligned} \tag{7.38}$$

and finally in the FLRW limit and for vanishing bulk viscosity we recover

$$\dot{\rho}^E + 3H\left(\rho^E + p^E\right) - \frac{\dot{\psi}}{2}\left(\rho^E - 3p^E\right) = 0. \tag{7.39}$$

The same conclusions as in the case of a fluid comoving in the JF can be drawn also in this case.

7.4 Outlook

In this Chapter, we have shown that shear viscosity does not influence the background dynamics of isotropic cosmological models, as long as the fluid is comoving and geodesic. Our analysis relies on general geometric arguments valid for a broad class of isotropic (but not necessarily homogeneous) metrics, and the result holds independently of the gravitational theory under consideration. In particular, we verified that in both General Relativity and $F(R)$ gravity including Starobinsky model the shear tensor vanishes identically for comoving fluids in these backgrounds, implying that anisotropic stresses do not enter the continuity equation.

We extended this result to both Jordan and Einstein frames, showing that conformal transformations do not introduce shear-dependent terms into the divergence of the stress-energy tensorwhen starting from a shear-free configuration. This supports the conclusion that shear viscosity cannot alter the evolution of the Hubble parameter, and thus cannot affect the electromagnetic luminosity distance in FLRW, which depends only on the background geometry via the Hubble parameter.

Overall, while our results do not exclude the possibility that shear viscosity plays a role in more complex or perturbed settings (e.g. tensor modes as we are going to discuss in the next Chapter), they suggest that constraints on shear viscosity cannot be reliably extracted from background observables.

Chapter 8

A simple example of "non-minimal" Pre-Big Bang scenario

8.1 Introduction

In a recent paper [3] we have discussed the possible interpretation of the signal detected by the multiple Pulsar Timing Array (IPTA) collaborations, including NANOGrav [30, 31], the Parkes PTA (PPTA) [32, 33], the European PTA (EPTA) in partnership with the Indian PTA (InPTA) [34, 35], and the Chinese PTA (CPTA)[36], as due to a stochastic background of relic primordial gravity-wave (GW) radiation produced in the context of the Pre-Big Bang (PBB) scenario [20, 21, 180, 181, 220], based on the duality symmetries of the string cosmology equations [19, 70, 71, 77, 79].

Such an interpretation, as discussed in [3], is impossible for the GW spectrum produced by the so-called "minimal" version of such a scenario (see e.g. [4, 155]), as it requires appropriate modification of the GW spectrum amplified during the high-curvature string phase. The aim of this paper is to provide a simple but physically motivated example of how such modifications could be implemented in the context of a "non-minimal" model of PBB evolution still described by the standard string cosmology equations.

Let us start by recalling the basic elements of the minimal PBB scenario [20, 85, 220]: the cosmological evolution starts asymptotically from the string perturbative vacuum and, after a low-energy phase of growing curvature and growing dilaton, reaches a high-energy phase with string-scale curvature, preceding the bounce and the beginning of the standard, decreasing curvature, frozen dilaton, post-big bang evolution. The high-energy string phase of the minimal scenario, in particular, is described by an epoch in which the curvature of the internal and external dimensions is nearly constant at the string scale, and the effective string coupling, controlling the string loop corrections, is growing (according to the explicit model first discussed in [172]).

Let us try to preserve the above-mentioned properties of the string phase also in the modified version of the non-minimal scenario. To this purpose we recall that the string phase of the minimal scenario is described by a fixed-point solution of the *vacuum* gravi-dilaton equations, including higher-curvature corrections to first order in the string α' expansion [172]. Therefore, we will modify such a scenario by only adding to the background dynamics the contribution of non trivial (high-energy) effective matter sources; and we will ask whether, depending on the properties of these sources, the amplified tensor and axion perturbations may be characterized by spectral powers different from those of the minimal model, so as to satisfy the constraints discussed in [3] needed to produce the signal detected by the IPTA collaboration. Finally, we will describe the matter sources as a higher-dimensional fluid (as usual in the context of homogeneous cosmologies), with possibly anisotropic pressure (in case of a different dynamics for internal and external spatial dimensions), and with possibly intrinsic shear viscosity (to produce a scenario with broken S-duality symmetry [74]).

We have found, with explicit calculations, that there are various models of sources able to produce the required scenario. For the illustrative purpose of this paper, and for the sake of brevity, we shall mainly concentrate our discussion on three cases: *i*) radiation, described by fluid sources with traceless stress tensor; *ii*) gas of primordial unstable strings [221, 222], described by fluid sources with equation of state, in an isotropic D-dimensional geometry, given by $p/\rho = -1/(D-1)$; *iii*) gas of string holes (i.e. string-size black holes) [186–188, 223, 224], described by fluid sources whose pressure p is related to the dilaton charge σ, in the string frame (S-frame), by $p = \sigma/2$. We have chosen these three examples because we

may naturally expect the presence of these type of sources in the high-curvature regime of the string phase.

Finally, let us anticipate here a result which, in our opinion, is probably one of the most interesting ones of this paper: the new allowed background solutions describing the string phase, and satisfying the required constrains needed for a successful non-minimal scenario, may be characterized by spatial dimensions evolving with an effective Hubble parameter of opposite sign to that of the initial asymptotic regime. For instance, by an external space which is contracting at constant curvature (or even flat), instead of being expanding. Note that this is not an unphysical result (as it might seem at first glance) but, on the contrary, an interesting (and in principle expected) result, since it describes just the same type of kinematics of the high-curvature phase obtained in the context of regular and self-dual string models of bounces (see e.g. [5, 93, 96]).

The paper is organised as follows. In Sect. 8.2 we introduce the background dynamics and its perturbations for our model of high-curvature, non-vacuum string phase. In Sect. 8.3 we present and discuss, for the chosen examples of fluid sources, their effects on the dynamics of the string phase, the resulting modification of the perturbation spectra,and their behaviour in the spectral plane to be compatible with the PTA signal. We also consider examples of viscous sources, producing non-minimal models with broken S-duality symmetry [74]. Sec. 8.4 is devoted to our concluding remarks. The explicit form of the modified background equations is reported in App. E, and the canonical evolution of axion perturbations, including first-order, higher-curvature corrections, is presented in App. E.1. The main details of the non-minimal GW spectrum, and the theoretical, phenomenological and self-consistency constraints to be imposed for its compatibility with the detected PTA signal, are finally summarised in App. E.2.

8.2 A non-vacuum string phase: background and perturbation equations

Let us start with the S-frame action used to describe the string phase in the context of the minimal PBB scenario [172], and obtained to first order in α' from the two-loop sigma model through a field redefinition (see e.g. [50]) which gives an action without higher-than-second derivatives in the corresponding equations of

motion. By including the string antisymmetric tensor[1] $B_{\mu\nu} = -B_{\nu\mu}$, and adding the source contribution described by the matter action S_m, the total action, in a general D-dimensional space-time geometry, is then given by

$$\begin{aligned} S = \quad & S_m - \frac{1}{2\lambda_{\rm s}^{D-2}} \int d^D x \sqrt{-g} e^{-\phi} \left[R + \partial\phi^2 - \frac{1}{12} H^2_{ABC} - \alpha' \alpha_0 \left(R^2_{GB} - \nabla\phi^4 \right) \right. \\ & - \alpha' a_0 H^2_{ABC} \left(\frac{1}{12} g^{MN} R_{MN} + \frac{5}{4} \nabla\phi^2 \right) - \alpha' a_0 H^{MAB} H_{NAB} \left(R_M{}^N - \nabla_M \phi \nabla^N \phi \right) \\ & - \alpha' a_0 \left(\frac{1}{24} H_{MNL} H^N{}_{RA} H_S{}^{MA} H^{RSL} - \frac{1}{8} H_{MRL} H_N{}^{RL} H^{MSA} H^N{}_{SA} \right) \\ & \left. + \frac{1}{2} \alpha' a_0 R_{ABCD} H^{ABM} H^{CD}{}_M \right] . \end{aligned} \tag{8.1}$$

Here $\lambda_{\rm s}^2 \equiv 2\pi\alpha'$ is the string length parameter, ϕ is the dilaton, $H_{ABC} = \partial_A B_{BC} + \partial_B B_{CA} + \partial_C B_{AB}$, where B is the NS-NS two-form (related in four dimension to the so-called Kalb-Ramond axion), and a_0 is a numerical parameter depending on the given type of string model: in particular, $a_0 = 1/4$ for the bosonic string, and $a_0 = 1/8$ for the heterotic superstring. Finally, R^2_{GB} is the Gauss-Bonnet quadratic curvature invariant, and capital latin indices run from 0 to $D-1$.

8.2.1 Background dynamics of the string phase

Consider a higher-dimensional geometry of Bianchi-I type, describing the product of two isotropic subspaces with $d = 3$ (external) and n (internal) dimensions, represented (using the cosmic time t) by the metric

$$\begin{aligned} & g_{AB} = {\rm diag}\,(g_{\mu\nu}, \gamma_{mn}) = {\rm diag}\,(1, -a^2\delta_{ij}, -b^2\delta_{mn}), \\ & a = e^{\beta(t)}, \qquad\qquad b = e^{\gamma(t)}, \end{aligned} \tag{8.2}$$

where Greek indices run from 0 to 3, Latin indices i, j from 1 to 3, Latin indices m, n from 4 to $4+n$, capital Latin indices from 0 to $D-1 = 3+n$.

By assuming that the background value of the Kalb-Ramond strength tensor is vanishing ($H_{ABC} = 0$) we find, for the given class of geometric backgrounds, that the action (8.1) reduces to the following effective action for the variables

[1] This background field is an essential ingredient for a phenomenologically complete scenario able to produce the today observed spectrum of scalar metric perturbations [74].

$\{N, \phi, \beta, \gamma\}$:

$$S = S_m - \frac{1}{2\lambda_s^{D-1}} \int \frac{dt}{N} e^{3\beta+n\gamma-\phi} \left\{ \left[\dot{\phi}^2 + 6\dot{\beta}^2 + n(n-1)\dot{\gamma}^2 + 6n\dot{\beta}\dot{\gamma} - 6\dot{\beta}\dot{\phi} - 2n\dot{\gamma}\dot{\phi} \right] - \frac{\alpha' a_0}{N^3} \left[c_2\dot{\gamma}^4 + c_3\dot{\phi}\dot{\beta}^3 + c_4\dot{\gamma}^3(\dot{\phi} - 3\dot{\beta}) - \dot{\phi}^4 + c_5\dot{\beta}\dot{\gamma}^2(\dot{\phi} - \dot{\beta}) + c_3 n\dot{\gamma}\dot{\beta}^2(3\dot{\phi} - \dot{\beta}) \right] \right\}, \tag{8.3}$$

where $N^2 = g_{00}$ is the so-called lapse function, and where:

$$c_2 = -\frac{n}{3}(n-1)(n-2)(n-3), \qquad c_4 = \frac{4n}{3}(n-1)(n-2), \qquad c_5 = 12n(n-1) \tag{8.4}$$

(we are using the same notations as in [172]).

As already mentioned we shall use a fluid model of sources, possibly coupled to the dilaton, with possibly different external (p) and internal (q) pressure (in agreement with the spatial anisotropy of the metric (8.2)), and with the possible presence of intrinsic shear viscosity η_V. The variation of the matter action with respect to the metric and to the dilaton then gives the so-called dilaton charge σ and the canonical stress tensor, defined as usual by

$$\frac{\sigma}{2} = -\frac{1}{\sqrt{-g}} \frac{\delta S_m}{\delta \phi}, \qquad T^{AB} = -\frac{2}{\sqrt{-g}} \frac{\delta S_m}{\delta g_{AB}}. \tag{8.5}$$

The stress tensor, taking into account the particular spatial structure of the metric (8.2) describing the direct product of 3-d and n-d isotropic subspaces, and including (in the standard form) the shear viscosity contribution, can be written covariantly as follows:

$$T_{AB} = (\rho + \widetilde{p})\, u_A u_B - \widetilde{p} g_{AB} + (\widetilde{q} - \widetilde{p})\, v_A v_B - \eta_V \left[u_{(A|} u^M \nabla_M u_{|B)} - \nabla_{(A} u_{B)} \right] \tag{8.6}$$

(round brackets denote symmetrisation). Here u^A and v^A are, respectively, time-like and space-like vectors satisfying the conditions $u_A u^A = 1$, $v_A v^A = -n$ (see e.g. [225, 226] for the formal description of anisotropic fluid sources in the special case of $D = 1 + 3$ dimensions). Finally, the tilde symbol over the internal and external pressures denotes as usual the possible presence of the shear viscosity contribution η_V as follows:

$$\widetilde{p} = p + \frac{2}{3+n} \eta_V \nabla_A u^A, \qquad \widetilde{q} = q + \frac{2}{3+n} \eta_V \nabla_A u^A. \tag{8.7}$$

An explicit computation for the background metric of Eq. (8.2), performed in

the comoving gauge where $u_A u^B = \delta^0_A\,\delta^B_0$ and $v_A v^B = -\delta^m_A\,\delta^B_n\,\delta^n_m$, then gives the following modified components of the source stress tensor:

$$T^0_0 = \rho, \quad T^j_i = -\delta^j_i\left[p + \frac{2\eta_V}{3+n} n(\dot\gamma - \dot\beta)\right], \quad T^n_m = -\delta^n_m\left[q + \frac{2\eta_V}{3+n} 3(\dot\beta - \dot\gamma)\right] \tag{8.8}$$

(note that in the limit of an isotropic geometry, $\dot\beta = \dot\gamma$, there are no contributions of the shear viscosity to the stress tensor and to the background equations, as expected [6]). We shall assume, in the following, that the non-viscous components of the source satisfy the perfect fluid equation of state, namely namely:

$$p = w_1\rho, \qquad q = w_2\rho, \qquad \frac{\sigma}{2} = w_3\rho, \tag{8.9}$$

with $w_i = \text{const}$.

The explicit equations governing the dynamics of the string phase are now obtained by varying the gravi-dilaton part of the action (8.3) with respect N, β, γ, ϕ, and by adding the associated contribution of the fluid sources. After the variation we set $N = 1$ (cosmic time gauge), and we look, as in the minimal model, for background solutions with constant curvature and with a dilaton which is linearly evolving with respect to the cosmic time coordinate. Namely, we impose $\dot a/a = \dot\beta = \text{const}$, $\dot b/b = \dot\gamma = \text{const}$, $\dot\phi = \text{const}$, where the dot denotes cosmic time derivative. The explicit form of the resulting equations, including the fluid source contribution parametrised as in Eqs. (8.8), (8.9), is reported in Appendix E. It can be easily checked that the sources, to be consistent with the given type of background solutions, must satisfy the conditions

$$\lambda_s^{D-1} e^\phi \rho \equiv C = \text{const}, \qquad \lambda_s^{D-2}\eta_V\, e^\phi \equiv H_V = \text{cost}. \tag{8.10}$$

(see Eqs. (E.1)–(E.4)).

The equations reported in Appendix E are a system of four algebraic equations for the unknown constants $\dot\beta, \dot\gamma, \dot\phi, C, H_V, w_1, w_2, w_3$, and we shall look for non trivial solutions for appropriate fluid models. In the absence of sources only three of the above equations are independent and, in the particular limit of an isotropic geometry, $\dot\beta = \dot\gamma$, one can recover the known solutions of the minimal model presented in [172]. In that case, however, we cannot satisfy the conditions required to produce a GW spectrum compatible with the PTA signal.

For an explicit formulation of the required conditions let us now introduce a few details on the evolution of axion and tensor perturbations in the chosen model of string-phase background.

8.2.2 Axion perturbations with α' corrections

Let us report here the basic results needed to compute the axion spectrum (which is a crucial ingredient, for the PPB scenario, to produce the today observed background of isocurvature scalar metric perturbations via the curvaton mechanism [60, 74, 110, 111]).

We will assume that the matter sources are not directly coupled to the Kalb-Ramond field, so that the resulting axion-perturbation equation will be exactly the same as that of the minimal scenario. However, we will explicitly take into account the possible contribution of the α' corrections typical of the string phase[2], and present indeed in the action (8.1).

Let us start with the action (8.1), consider the first order perturbations of the Kalb-Ramond field strength, $H_{ABC} \to H_{ABC} + \delta H_{ABC}$, assume that the zeroth-order background contribution is vanishing, $H_{ABC} = 0$, and compute from (8.1) the effective action quadratic in the perturbation δH_{ABC}. We are interested, in particular, in the dynamics of the pseudo-scalar Kalb-Ramond axion field χ, i.e. the spacetime dual of the four-dimensional component of the Kalb-Ramond perturbations. It is defined by

$$\delta H^{\mu\nu\alpha} = \frac{e^{\phi}}{\sqrt{|\gamma|}} \frac{\epsilon^{\mu\nu\alpha\beta}}{\sqrt{-g}} \nabla_{\beta}\chi \equiv e^{\overline{\phi}} \eta^{\mu\nu\alpha\beta} \partial_{\beta}\chi, \tag{8.11}$$

where $\mu, \nu, ... = 0, 1, 2, 3$, $\eta^{\mu\nu\alpha\beta}$ is the four-dimensional totally antisymmetric tensor, and $e^{\overline{\phi}} = e^{\phi}/\sqrt{|\gamma|} = e^{\phi}/b^n \equiv g_4^2$ is the square of the effective four-dimensional string coupling.

We shall now perturb the action (8.1) according to Eq. (8.11) up to terms of quadratic order $(\partial\chi)^2$ and, by taking into account that $\chi = \chi(t, x_i)$, we shall use the Fourier component of the axion perturbation χ_k, such that $\nabla^2\chi_k = \partial_i\partial^i\chi_k = -k^2\chi_k$. By introducing the conformal-time coordinate τ such that $dt = ad\tau$, and

[2]This is a point which, to the best of our knowledge, has never been taken into account for the axion in previous papers.

factorising the volume integral $\int d^n y$ over the internal spatial dimensions, we then obtain the following quadratic perturbed action for χ_k:

$$\delta_H S = -\frac{1}{2\lambda_s^2} \int d\tau \left[z^2(\tau) \chi_k'^2 - k^2 \chi_k^2 y^2(\tau) \right]. \tag{8.12}$$

Here a prime denotes differentiation with respect to the conformal time, and z and y are functions of time depending on the background fields (see Appendix E.1 for an explicit computation and a general definition of these functions). From the action (8.12) we can immediately obtain the equation of motion for the axion perturbation χ_k:

$$\chi'' + 2\frac{z'}{z}\chi' + k^2 \frac{y^2}{z^2}\chi = 0, \tag{8.13}$$

and the corresponding evolution equation for the canonical variable $v_k = z\chi_k$ which diagonalises the kinetic term of the action (8.12):

$$v_k'' + k^2 v_k - V_k(\tau) v_k = 0, \qquad V_k(\tau) = \frac{z''}{z} - \frac{k^2}{z^2}\left(y^2 - z^2\right). \tag{8.14}$$

Let us now take into account that our background describing the string phase is characterized by constant values of the parameters $\dot{\beta}, \dot{\gamma}, \dot{\phi}$ controlling the curvature and the dilaton dynamics. In such a case it turns out that the two functions z and y are proportional (see their explicit expression in Appendix E.1), and are given by

$$z = \alpha_1 \xi_\sigma, \qquad y = \alpha_2 \xi_\sigma, \qquad \xi_\sigma = a\, b^{-n/2} e^{\phi/2}, \tag{8.15}$$

where α_1, α_2 are numerical constants of order one. The canonical equation (8.14) determining the axion spectrum thus reduces to

$$v_k'' + \left(k^2 c_s^2 - \frac{\xi_\sigma''}{\xi_\sigma} \right) v_k = 0, \tag{8.16}$$

where ξ_σ is the so-called axion pump field, and $c_s = \alpha_2/\alpha_1 \sim 1$ is the effective "sound velocity" of the axion fluctuations (see e.g. [168, 182] for the possible physical consequences of a speed $c_s \neq 1$).

The primordial axion spectrum amplified by this model of string phase has thus a

spectral index determined (according to standard cosmological perturbation theory [12, 60]) by the power-law evolution of the pump field ξ_σ, expressed in conformal time. For the background we are considering we have, in cosmic time,

$$\xi_\sigma = a\, b^{-n/2} e^{\phi/2} \sim e^{\dot\beta t}\, e^{-n\dot\gamma t/2}\, e^{\dot\phi t/2}, \tag{8.17}$$

for $-\infty < t < +\infty$. Hence, in conformal time where $a \sim (-\dot\beta\tau)^{-1}$,

$$\xi_\sigma \sim (-\dot\beta\tau)^{-1+\beta_\sigma}, \qquad \beta_\sigma = \frac{1}{2\dot\beta}\left(n\dot\gamma - \dot\phi\right), \tag{8.18}$$

where $\tau < 0$ for $\dot\beta > 0$ and $\tau > 0$ for $\dot\beta < 0$.

It should be noted that the canonical equation (8.16) determining the axion spectrum only contains second derivatives with respect to the conformal time, and is invariant with respect to the change of coordinates $\tau \to -\tau$. The definition of the pump field parameter β_σ is thus valid quite independently of the sign of $\dot\beta$, controlling the external-space kinematics (i.e. constant-curvature expansion for $\dot\beta > 0$, constant-curvature contraction for $\dot\beta < 0$).

8.2.3 Tensor perturbations including viscosity

For tensor metric perturbations the procedure is the same as the previous one used for axion perturbations. We start with the action (8.1) and consider the first order perturbation $\delta g_{AB} = h_{AB}$ of the metric tensor, expanding the metric as $g_{AB} \to g_{AB} + \delta g_{AB}$, and computing the perturbed action up to terms of order h^2. Assuming as before that the background value of the Kalb-Ramond strength tensor is vanishing ($H_{ABC} = 0$), we shall concentrate on perturbations propagating in the $d = 3$ external space, $h_{ij} = h_{ij}(t, x_i)$, and satisfying the usual transverse-traceless (TT) condition: $\partial_j h_i{}^j = 0 = h_i{}^i$. Let us first assume that there is no shear viscosity in the matters sources. The only contributions to the perturbed action come then from the gravi-dilaton part of the action, and in particular from the terms of Eq. (8.1) not containing the Kalb-Ramond field: the results are known, as already computed in previous papers [73].

For the purpose of this paper it will be enough to recall that the quadratic perturbed action for the Fourier components of tensor perturbations, h_k, is formally of the same type as in the axion case, Eq. (8.12), and that we obtain exactly the

same type of Eqs. (8.13), (8.14) for the propagation of h_k and of its corresponding canonical variable, $v_k = z h_k$. The only difference is that the effective pump fields z and y, for the tensor modes, are different functions of the background variables a, b, ϕ (see e.g. [73]).

However, in the special case of a background with constant values of $\dot{\beta}, \dot{\gamma}, \dot{\phi}$ it turns out again that the two functions z and y are proportional, and thus define a unique pump field ξ_h for tensor perturbations, in a way similar to Eq. (8.15). One obtains, in particular:

$$z \sim y \sim \xi_h \sim a\, b^{n/2} e^{-\phi/2}. \tag{8.19}$$

The canonical equation, determining the tensor propagation spectrum, then takes the form

$$v_k'' + \left(k^2 c_s^2 - \frac{\xi_h''}{\xi_h}\right) v_k = 0 \tag{8.20}$$

(where again $c_s \sim 1$, but its precise value is in general different from that of the corresponding parameter of axion perturbations).

Like in the axion case, we can express the tensor pump field in conformal time, and we obtain:

$$\xi_h \sim e^{\dot{\beta} t}\, e^{n\dot{\gamma} t/2}\, e^{-\dot{\phi} t/2} \sim (-\tau)^{-1+\beta_h}, \qquad \beta_h = \frac{1}{2\dot{\beta}}\left(\dot{\phi} - n\dot{\gamma}\right) = -\beta_\sigma, \tag{8.21}$$

valid as before for both expanding space, $\dot{\beta} > 0$ with $\tau < 0$, and contracting space, $\dot{\beta} < 0$ with $\tau > 0$. We note that the obtained relation $\beta_h = -\beta_\sigma$ is an expected consequence of the S-duality symmetry [74] satisfied by the model of string phase that we are considering.

The S-duality symmetry could be broken, however, if we would like to consider a fluid source with non-vanishing shear viscosity. Such an additional "non-minimal" ingredient is not necessarily required, as we shall see, to obtain a scenario compatible with the fit of the PTA data; however, it may be interesting (and useful) to sketch here the basic effects of shear viscosity on tensor perturbations, also in view of the possibility that future detections of relic GW backgrounds, corresponding to unexpected amplitude in unexpected frequency ranges, might be better explained by a spectrum produced in the context of models with broken S-duality symmetry.

Indeed, let us recall that the shear viscosity of the sources, unlike bulk viscosity, directly affects the propagation of tensor perturbations, and can thus induce significant modifications of their spectrum. We refer to [6] for an introduction to this effect, and for its detailed discussion. Here we only report the modified form of the evolution equation for the Fourier components of the 3-d tensor perturbation modes h_k, in the TT gauge, explicitly written in the same string phase as before (we put for simplicity $c_s = 1$), and modified by the presence of a non-vanishing shear viscosity:

$$h_k'' + 2\left(\frac{\xi_h'}{\xi_h} + aH_V\right) h_k' + k^2 h_k = 0. \tag{8.22}$$

Here ξ_h is the tensor pump field of Eqs. (8.19), (8.21), and H_V is the parameter depending on the shear viscosity and on the dilaton already defined in Eq. (8.10). Note that the explicit form of Eq. (8.22) and, in particular, the presence of the dilaton in the viscosity contribution represented by H_V, is due to the direct rescaling of the tensor perturbation equation with viscosity from the Einstein frame used in [6] to the String frame, used in this paper (see e.g. [60**?**] for the details of the transformations between the two frames, in an arbitrary number of dimensions). It should be stressed, finally, that for the constant-curvature background that we are considering, the parameter H_V is constant (see instead [8] for an example of time-dependent H_V in more general background geometries).

According to Eq. (8.22), the presence of shear viscosity defines a new effective tensor pump field $\widetilde{\xi}_h$ such that

$$\frac{\widetilde{\xi}_h'}{\widetilde{\xi}_h} = \frac{\xi_h'}{\xi_h} + a\, H_V, \tag{8.23}$$

and a new "viscous" canonical variable $v = \widetilde{\xi}_h h_k$. satisfying the generalised equation

$$v_k'' + \left(k^2 - \frac{\widetilde{\xi}_h''}{\widetilde{\xi}_h}\right) v_k = 0. \tag{8.24}$$

We can easily find the power-law behaviour of the new, viscous pump field $\widetilde{\xi}_h$ in conformal time from Eq. (8.23). Putting $\widetilde{\xi}_h \sim (-\dot{\beta}\tau)^K$, and solving for K, we obtain

$$\widetilde{\xi}_h(\tau) \sim (-\dot{\beta}\tau)^{-1+\widetilde{\beta}_h}, \qquad \widetilde{\beta}_h = \frac{1}{2\dot{\beta}}\left(\dot{\phi} - n\dot{\gamma} - 2H_V\right) = -\beta_\sigma - \frac{H_V}{\dot{\beta}}. \tag{8.25}$$

As before, the above result for $\widetilde{\xi}_h$ is valid for both expanding ($\dot{\beta} > 0, \tau < 0$) or contracting ($\dot{\beta} < 0, \tau > 0$) external 3-d space.

We note, finally that S-duality is explicitly broken ($\widetilde{\beta}_h \neq -\beta_\sigma$, compare with Eq. (8.21)), because shear viscosity affects the tensor pump field and the tensor perturbation spectrum, but not the corresponding parameters of axion perturbations, which are left unchanged. It follows that the phenomenological parameter controlling the S-duality violation, defined as $\epsilon \equiv \beta_\sigma + \widetilde{\beta}_h$ in our previous paper [3], turns out to be directly related to the viscosity of the sources as $\epsilon = -H_V/\dot{\beta}$.

8.3 Examples of physical models compatible with the PTA signal

Looking at the allowed region of the spectral parameter space presented in [3] it should be noted, first of all, that the conditions to be satisfied by the variables $\dot{\beta}, \dot{\gamma}, \dot{\phi}, H_V, \ldots$, characterising the chosen background model, are significantly affected by the presence or absence of the S-duality symmetry.

Let us recall, in fact, that the overall shape of the today-observed relic GW spectrum is determined not only by the spectral tilt (controlled by β_h) of the modes amplified during the string phase, but also by many other model-dependent details such as the duration of the pre-bouncing evolution, the bouncing energy scale, the durations of the post-bouncing axion-dominated regime and so on (see Appendix E.2). Hence, for any given couple of values of β_h, β_σ, their localisation inside or outside the allowed region of a PTA-compatible spectrum also depends on the variation range of all the other parameters (as illustrated in particular by Fig. 1 of ref. [3])). The overall allowed region must of course satisfy, in addition, all existing phenomenological constraints such as the bounds imposed by Big Bang nucleosynthesis [157], by the CMB observations [162], by the present data of the LKV network [116] and so on. All such conditions have been summarised in Appendix E.2, but see [3] for an explicit and detailed discussion.

It follows, in particular, that when the two pump-field parameters β_h, β_σ are directly related by S-duality, and if we apply on one of them the needed constraints, the other one is also automatically constrained. Conversely, when duality is broken and the two parameters are independent, there is no automatic transmission

of constraints, and the allowed range of the two parameters is larger. In the first (S-dual) case where $\beta_h = -\beta_\sigma$ it turns out, from the results of [3], that the GW spectral parameter for a scenario compatible with the PTA signal must be confined inside the (rather small) range

$$-0.09 \lesssim \beta_h \lesssim -0.05. \tag{8.26}$$

In the second (S-duality broken) case, like for instance the viscous model of the previous section (with $\widetilde{\beta}_h \neq -\beta_\sigma$) one finds instead that the spectral parameters must satisfy two independent conditions:

$$-0.08 \lesssim \widetilde{\beta}_h \lesssim 0.05, \qquad\qquad 0.10 \lesssim \beta_\sigma - \widetilde{\beta}_h \lesssim 0.21. \tag{8.27}$$

In spite of these rather strong conditions, we have found various possible examples of fluid sources, with and without dilatonic charge, with and without viscosity, producing a spectrum of tensor and axion perturbations determined by the pump field parameters satisfying the conditions (8.26) or (8.27). In the following subsections we shall present a detailed illustration of simple and physically motivated models of fluid sources compatible with the mentioned constraints, and useful to illustrate the typical properties of the non-minimal scenario.

Let us notice, to this purpose, that the above conditions (8.26), (8.27) provide constraints on the values of $\dot{\beta}, \dot{\gamma}, \dot{\phi}$ (and possibly H_V) obtained by solving the background equations (E.1)–(E.4), and describing a particular example of string phase kinematics. The string phase describes an epoch of pre-bouncing evolution, and thus it is naturally associated to a growing string loop parameter, $\dot{\phi} > 0$. In such a context, it would seem natural to expect also an expanding external space with $\dot{\beta} > 0$, and contracting (or frozen) internal dimensions with $\dot{\gamma} \leqslant 0$.

As already mentioned, however, this is not necessarily the case, as explicitly shown by the regular, exact (to all orders in α') and self-dual models of bounce [5, 93, 96]. In that case, indeed, the high curvature regime tends to be characterized by a sign of the effective Hubble parameter which is exactly the opposite of the sign typical of the asymptotic (initial or final) regimes: namely, a sign which corresponds to a contracting (or even flat) external space, $\dot{\beta} \leqslant 0$, and/or to an expanding internal space, $\dot{\gamma} > 0$. In the same way, those models also suggests the possibility of a high-curvature pre-bouncing regime with decreasing dilaton $\dot{\phi} < 0$: in such a

case, however, the self-consistency of the PBB scenario requires a growth of the effective four-dimensional string coupling $g_4 \sim e^{\phi/2} b^{-n/2}$, namely $\dot{g}_4 > 0$, which implies $\dot{\phi} > n\dot{\gamma}$.

In the following subsections we will thus consider examples of background solutions satisfying the conditions (8.26) or (8.27) without imposing constraints, a priori, on the sign of $\dot{\beta}, \dot{\gamma}, \dot{\phi}$.

8.3.1 Anisotropic fluid sources without viscosity: S-dual GW spectrum

The simplest and most natural example of source physically compatible with the high-energy string phase is probably that of radiation, represented by a perfect fluid with traceless stress tensor, i.e. satisfying the condition $3w_1 + nw_2 = 1$ (see Eqs. (8.8), (8.9)). It might represent the possible effects of the backreaction due to the amplified perturbations, and it could even correspond to an isotropic spatial distribution throughout the entire (external and internal) space, with equation of state $p = \rho/(3+n)$, namely with $w_1 = w_2 = 1/(3+n)$. Assuming that there is no viscosity we have no breaking of the S-duality for the GW spectrum, and we may look for solutions of the background equations (E.1)–(E.4) (with $\eta_V = 0$) satisfying the stronger condition (8.26), where β_h is defined by Eq. (8.21).

In the isotropic case we have checked that there are solution with β_h varying in the whole allowed range (8.26). However, they need a non-vanishing dilaton charge, and are characterized by numerical values of the parameter w_3 which do not seem to have any clear interpretation in terms of physical models of sources.

To this purpose, let us briefly discuss how the dilaton charge density σ could be physically introduced for the (possibly anisotropic) fluid model of source that we are considering. First of all we note that the the canonical stress tensor (8.6), without viscosity, can be easily derived from the following effective action,

$$S_m = -\frac{1}{2}\int d^{4+n}x\sqrt{-g}\left[((\rho+p)\, g_{AB}\, u^A u^B + (q-p)\, g_{AB}\, v^A v^B - (\rho+3p) - n(p-q)\right], \tag{8.28}$$

which generalises to our higher-dimensional metric (8.2) the action for an isotropic fluid given in [227]. By applying the canonical definition (8.5) and specifying, after

the variation, the vectors u^A and v^A in the comoving gauge, we obtain indeed the previous results (8.8), (8.9) with $\eta_V = 0$.

Suppose now we introduce for this model of fluid the coupling to the dilaton, according to the standard string coupling expansion: namely by multiplying the Lagrangian of the action (8.28) by $e^{k\phi}$, where $k = -1$ for the small coupling limit of the tree-level contribution, $k = 0$ for the one-loop contribution, and so on. We then obtain a dilaton-dependent action $S_m(\phi)$ with the same form of Eq. (8.28), but with rescaled fluid variables:

$$\rho \to \rho(\phi) = e^{k\phi}\rho, \qquad p \to p(\phi) = e^{k\phi}p, \qquad q \to q(\phi) = e^{k\phi}q. \tag{8.29}$$

In that case, the canonical definition of the dilaton charge (see Eq. (8.5)) immediately gives

$$\frac{\sigma}{2} = -kp = -kw_1\rho \equiv w_3\rho. \tag{8.30}$$

At the tree-level, in particular, we have $w_3 = w_1$. We shall now consider three simple examples of sources.

- **Radiation-like sources**

Coming back to our radiation-like model of source, and considering the anisotropic case which satisfies the condition $3w_1 + nw_2 = 1$, we are now physically motivated to look for solutions with no dilaton charge, $w_3 = 0$, or with tree-level charge, $w_3 = w_1$. In both cases we find that there are non-trivial solutions to Eqs. (E.1)–(E.4), for the four variables $C, \dot{\beta}, \dot{\gamma}, \dot{\phi}$, and with $C > 0$, for any given value of β_h in the range (8.26).

If we assume $w_3 = 0$ we find that the solutions are characterized by opposite values of the sign of $\dot{\beta}$ and $\dot{\gamma}$. However, if we want to obtain a growing dilaton and 4-dimensional string coupling, $\dot{\phi} > 0$, $\dot{g}_4 > 0$, then we are left with the case $\dot{\beta} < 0$ and $\dot{\gamma} > 0$, namely (as anticipated) with a solution describing contracting external space and expanding internal space, just in agreement with the high-curvature kinematics of the previously mentioned regular bouncing scenarios [5, 93, 96]. We have checked that the above properties hold for arbitrary numbers n of internal dimensions. If we choose, for instance, the typical superstring value $n = 6$, and

the particular (allowed) value $\beta_h = -0.06$ for the spectral parameter, we obtain

$$\beta_h = -0.06, \qquad C \simeq 2.20, \qquad \dot{\beta} \simeq -0.063, \qquad \dot{\gamma} \simeq 0.30, \qquad \dot{\phi} \simeq 1.80, \qquad \dot{g}_4 > 0. \tag{8.31}$$

If we assume instead $w_3 = w_1$ (tree-level dilaton charge), we find for the allowed solutions that $\dot{\beta}$ and $\dot{\gamma}$ must have the same sign, while $\dot{\phi}$ and $\dot{g}_4$ the opposite one: and if we choose, in particular, a growing dilaton, $\dot{\phi} > 0$, we obtain that the external and internal space must be expanding, $\dot{\beta} > 0, \dot{\gamma} > 0$, while $\dot{g}_4 < 0$. The opposite is true if we choose $\dot{\phi} < 0$. For the typical value $n = 6$, and, again, for $\beta_h = -0.06$, we obtain, for instance:

$$\beta_h = -0.06, \qquad C \simeq 0.020, \qquad \dot{\beta} \simeq 0.037, \qquad \dot{\gamma} \simeq 0.23, \qquad \dot{\phi} \simeq 1.39, \qquad \dot{g}_4 < 0. \tag{8.32}$$

- **Unstable strings**

Another possible example of source, also typical of the high-curvature string phase, may correspond to the presence of a stochastic distribution of primordial unstable strings [221, 222], described by a gas which in the isotropic D-dimensional case is characterized by the averaged equation of state $p = -\rho/(D-1)$, i.e. by $w_1 = w_2 = -1/(3+n)$. In such a case we can find background solutions compatible with the condition (8.26) but, like in the case of isotropic radiation, the needed value of the dilaton charge seems to have no direct physical interpretation. In particular, there are no solutions with a value of w_3 which is nonvanishing and compatible with the model of coupling described by Eq. (8.30).

However, for an anisotropic distribution of unstable strings (without viscosity) whose stress tensor, of the type (8.9), satisfies the generalised condition $3w_1 + nw_2 = -1$, the results are different. There are indeed background solutions compatible with the range of Eq. (8.26), and sourced by anisotropic unstable strings with tree-level dilaton charge: namely by a fluid with $w_2 = -(1+3w_1)/n$ and $w_3 = w_1$. The properties of such solutions are very similar to those of the previously obtained solutions sourced by a charged radiation fluid: indeed, we have again $\dot{\beta} > 0$, $\dot{\gamma} > 0$, $\dot{\phi} > 0$, $\dot{g}_4 < 0$ (like in Eq. (8.32)). Interestingly enough, we recall that the presence of a fully expanding (external and internal) space, in this case, is not an optional (or casual) property of the obtained geometry, but an unavoidable result needed for the consistency of the unstable-string model

[221, 222]. To give here an example of explicit solution we can choose, as before, $n = 6$, $\beta_h = -0.06$, and we find

$$\beta_h = -0.06, \qquad C \simeq 0.017, \qquad \dot{\beta} \simeq 0.036, \qquad \dot{\gamma} \simeq 0.23, \qquad \dot{\phi} \simeq 1.37, \qquad \dot{g}_4 < 0. \tag{8.33}$$

- **String-hole gas**

Let us finally consider a third example of fluid source, which is probably the most natural and physically motivated one possibly present in the string phase: the so-called string holes gas (SHG), namely a spatially isotropic distribution of high-energy, string-size black holes, typically formed when the curvature reaches the string scale (see eg. [186, 187, 223]). The isotropy gives $p = q$, and the string hole condition implies, in the String frame, $p = \sigma/2$. Hence $w_1 = w_2 = w_3$.

We can then consider the particular case $w_i = -1$, which also corresponds to a very simple (and possibly interesting) physical interpretation of the source in terms of an exponential dilaton potential. Indeed, let us start with the following matter action S_m,

$$S_m = -\int d^D x\sqrt{-g}\, V_0 e^{-\phi}, \qquad\qquad V_0 = \text{const}, \tag{8.34}$$

and apply the previous canonical definitions of the stress tensor and of the dilatonic charge. We immediately obtain

$$T_A{}^B = \delta_A^B\, V_0\, e^{-\phi}, \qquad\qquad \frac{\sigma}{2} = -V_0\, e^{-\phi}, \tag{8.35}$$

which implies, using the fluid model of Eq. (8.9), $w_1 = w_2 = w_3 = -1$.

Quite independently of its possible interpretation, even in this case we obtain non-trivial solutions of Eqs. (E.1)–(E.4), with $\eta_V = 0$, for any value of β_h compatible with Eq. (8.26), and for arbitrary values of n. Again we find that a growing dilaton, $\dot\phi > 0$, must be associated to an expanding (internal and external) geometry, $\dot\beta > 0, \dot\gamma > 0$, but, in this case, even the four-dimension string coupling turns out to be growing, $\dot g_4 > 0$. For the case $n = 6$ and $\beta_h = -0.06$ we obtain, for instance,

$$\beta_h = -0.06, \qquad C \simeq 0.009, \qquad \dot\beta \simeq 0.035, \qquad \dot\gamma \simeq 0.22, \qquad \dot\phi \simeq 1.33, \qquad \dot g_4 > 0. \tag{8.36}$$

All the previous examples of backgrounds, sourced by isotropic or anisotropic high-energy fluids, with or without dilaton charge, and without viscosity, are able to produce a GW spectrum (and an associated, $S-$duality-related axion spectrum) which, in the frequency band amplified by the string phase, has a spectral power controlled by the parameter β_h satisfying the condition (8.26). See Appendix E.2 for the explicit form of the spectral energy density $\Omega_{GW}(f)$ written in terms of

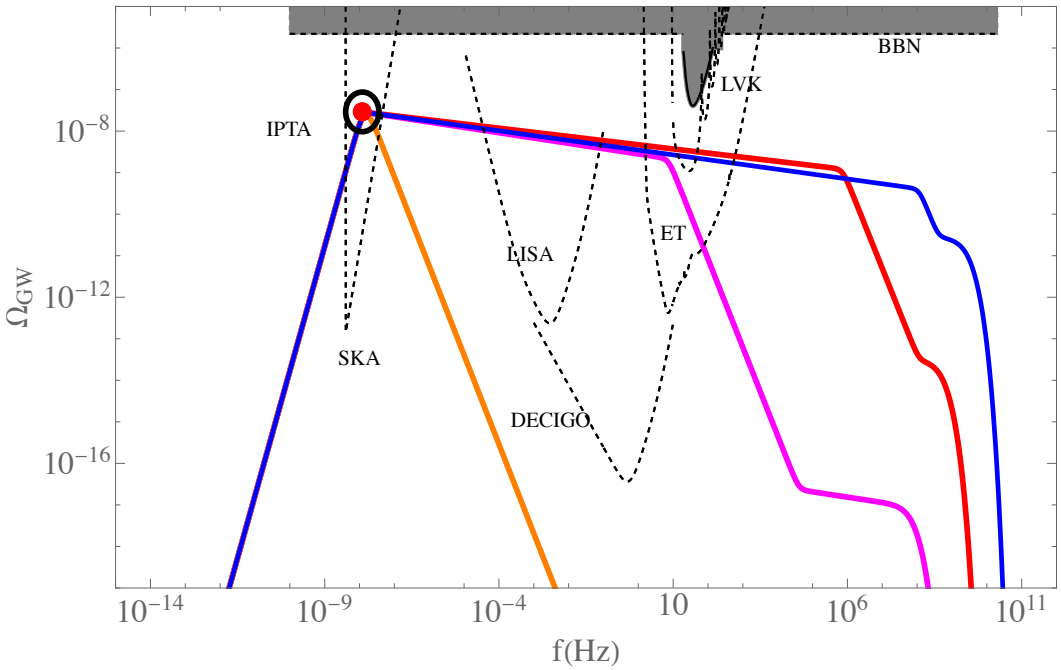

FIGURE 8.1: Examples of GW spectra produced by non-minimal but still S-dual models, with a string phase described by the background solutions of Sect. 8.3.1. All plotted spectra satisfy the constraints of Appendix E.2, but with different values of β_h and $\sigma_i/M_{\rm Pl}$. In particular: the red spectrum corresponds to $\beta_h = -0.05$ and $\sigma_i/M_{\rm Pl} = 1$; the blue spectrum corresponds to $\beta_h = -0.058$ and $\log(\sigma_i/M_{\rm Pl}) = -1/2$; the orange spectrum corresponds to $\beta_h = -0.073$ and $\log(\sigma_i/M_{\rm Pl}) = -1/2$. Also shown is a typical S-dual spectrum with $\beta_h = -0.064$ and $\log(\sigma_i/M_{\rm Pl}) = -1/2$ (the magenta plotted curve), providing an explicit example of how this class of models, beside explaining the already detected signal, could also produce signals in the sensitivity range of future detectors such as LISA, ET and DECIGO.

β_h and of the other parameters. Of course, as previously mentioned, the today observed GW spectrum, and in particular a spectrum responsible of the detected PTA signal, must satisfy many other phenomenological and model-dependent constraints reported in Appendix E.2 and discussed in details in [3]. We have shown in Fig. 8.1 a few example of such spectra compatible with all the imposed constraints, and chosen in such a way as to qualitatively represent the possibly allowed larger amplitude (the red plotted curve), the possibly allowed higher frequency extension (the blue plotted curve), and the limiting case in which the string phase ends with a bouncing transition just after the horizon-exit of the modes producing the PTA signal (the orange plotted curve).

In that figure $\Omega_{GW} = f d\rho_{GW}/(\rho_c df)$ is the spectral energy density in units of critical energy density ρ_c, f is the today observed proper frequency of the wave modes, and the IPTA signal (with $\Omega_{GW} \simeq 2.9\times10^{-8}$, $f \simeq 1.2\times10^{-8}$Hz) is denoted

by the red dot localised inside the black circle. The low-energy spectrum amplified before the beginning of the string phase ($f < f_s$) has a steep power-law growth, $\Omega_{GW} \sim f^3$, represented by the steep solid line (common to all the plotted spectra) reaching the red dot at $f = f_s$.

We have also inserted into the figure the expected sensitivities of near-future GW detectors like SKA [189], LISA [24], ET [26], DECIGO [29] (corresponding to the regions of the spectral plane inside the black dashed curves). It may be interesting to note that the spectra predicted by these examples of non-minimal models are possibly well inside the expected experimental sensitivities. Finally, the grey-shaded area describes the upper bounds presently imposed by the LKV network [116] and by Big Bang nucleosynthesis [157]

8.3.2 Viscosity and broken S-duality

To give an example of non-minimal pre-big bang scenario with broken S-duality symmetry we shall now assume that the fluid source contributing to the dynamics of the high-curvature string phase has a non-vanishing shear viscosity, $\eta_V \neq 0$, as explicitly taken into account in Sect. 8.2.1 (see in particular Eqs. (8.6), (8.8)). This may typically happen at high curvature, and has been recently discussed, in particular, for the SHG case [113] (but the presence of viscosity can affect, of course, also other models of sources). In such a case the slope of the high-frequency GW spectrum, controlled by $\widetilde{\beta}_h$, would be modified as discussed in Sect. 8.2.3, while the slope of the associated axion spectrum, controlled by β_σ, would keep unchanged: one would then obtain $\widetilde{\beta}_h \neq -\beta_\sigma$ and $\epsilon = \beta_\sigma + \widetilde{\beta}_h \neq 0$, according to Eq. (8.25). We have, in particular, two possibilities.

The first one is a string phase with an isotropic geometry, $\dot{\beta} = \dot{\gamma}$. In that case the shear viscosity does not contribute to the background solution [6] (see Eq. (8.8)) but only to the evolution of tensor perturbations. Hence, the shear parameter H_V is in principle free, and can be modeled *ad hoc* to try to satisfy the two conditions (8.27), once the background values of $\dot{\beta} = \dot{\gamma}$, $\dot{\phi}$ and C are given.

The second one refers, as before, to an anisotropic geometry, $\dot{\beta} \neq \dot{\gamma}$. In that case the viscosity explicitly appears in the stress tensor (see again Eq. (8.8)), hence it also contributes to the background equations of motion, and it is no longer a free parameter but it turns out to be fixed by the given chosen solution.

Considering the second, more general possibility we have explicitly checked that allowed S-duality breaking solutions, giving a non-minimal spectrum compatible with all constraints, can be obtained by adding the shear-viscosity contribution to any one of the three types of fluid sources considered in the previous section (radiation, unstable strings, SHG). However, the corresponding allowed values of β_σ, $\widetilde{\beta}_h$ do not necessarily cover the whole range of values defined by Eqs. (8.27) for all types of sources.

For brevity, we present here a single, straightforward example involving a fluid source that describes anisotropic radiation with shear viscosity and no dilaton charge: a fluid source with equation of state $3w_1 + nw_2 = 1$, and $w_3 = 0$. We choose this model, in particular, to emphasise the main possible difference with the $S-$dual examples of the previous section: namely, a GW spectrum with a blue (i.e. growing) spectral behaviour in the string phase, which requires $\widetilde{\beta}_h > 0$ (see the spectral distribution (E.11)). Indeed, for the other two previous examples (string holes and unstable strings) there are no allowed background solutions with this property, even assuming that their viscosity is non-vanishing.

Assuming as before $n = 6$ we can take, for instance, $\widetilde{\beta}_h = 0.01$, $\beta_\sigma - \widetilde{\beta}_h = 0.14$, just to use values located around the middle of the allowed region (8.27), and we then obtain

$$\begin{aligned} &\tilde{\beta}_h = 0.01, \qquad \beta_\sigma - \tilde{\beta}_h = 0.14, \quad C \simeq 2.20, \quad H_V \simeq 0.009, \\ &\dot{\beta} \simeq -0.06, \qquad\qquad \dot{\gamma} \simeq 0.30, \quad \dot{\phi} \simeq 1.81. \end{aligned} \tag{8.37}$$

It should be noted that for such solution (but also for solutions corresponding to different values of the spectral parameters) the dilaton is growing (as expected), and, just like in the previous examples without viscosity, the solutions again describe a string phase with contracting external space and expanding internal space ($\dot{\beta} < 0$, $\dot{\gamma} > 0$), just as predicted by the high-curvature kinematics of the regular bouncing scenarios [5, 93, 96].

Given the above values of the spectral parameters, and taking into account all spectral constraints reported in Appendix E.2, we are only left (as in the previous duality-invariant case) with the freedom of shifting the value of the axion-parameter $\sigma_i/M_{\rm Pl}$ using, for instance, the allowed variation range assumed in [3]. We obtain in this way a corresponding allowed region for the GW spectrum of this non-minimal, non-dual model illustrated by the pink shaded area of Fig. 8.2,

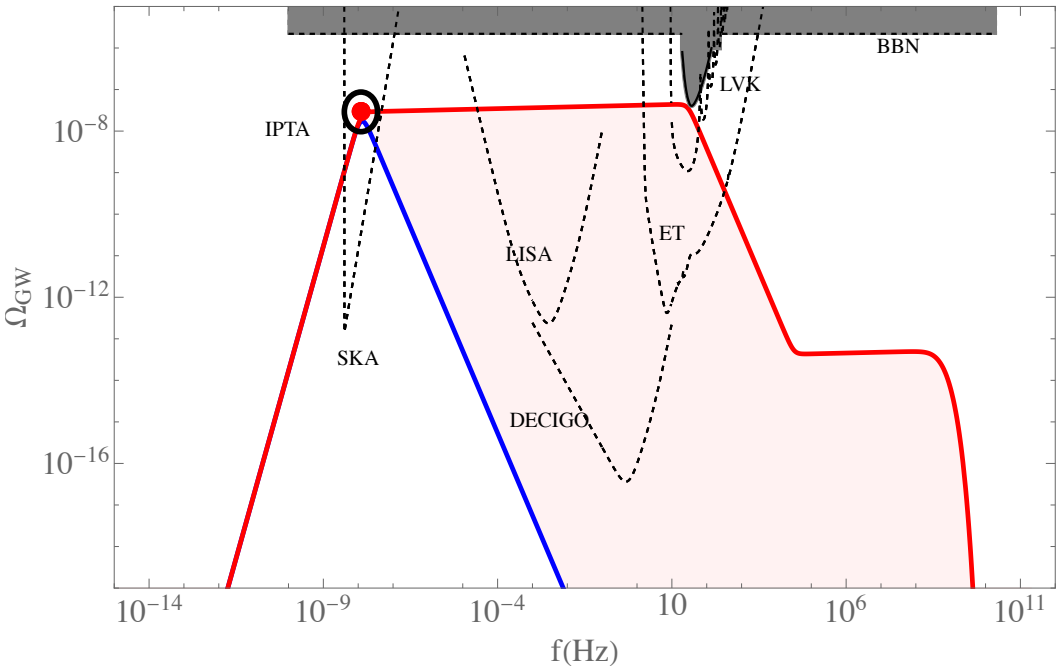

FIGURE 8.2: The allowed region (the pink shaded area) spanned by the GW spectra produced by a string phase described by the solution (8.37). The two limiting GW spectra, represented by the red and blue curves, are both violating the standard $S-$duality symmetry with the same symmetry breaking parameter, $\epsilon = 0.16$. However, the red curve corresponds to $\log(\sigma_i/M_{\rm Pl}) = -0.81$, the blue one corresponds to $\log(\sigma_i/M_{\rm Pl}) = -0.49$.

and limited by the spectrum with minimal (the blue curve) and maximal (the red curve) extension of a string phase producing a slightly growing spectrum with spectral parameter $\widetilde{\beta}_h = 0.01$.

It should be stressed, finally, that the plotted spectra and the corresponding allowed region are only a very simple example of a non-dual and non-minimal model based on high-curvature background equations modified by the presence of viscous, anisotropic, radiation-like sources. By no means they are to be regarded as describing the general predictions of a non-minimal scenario with duality-broken symmetry. Such a general discussion is outside the object of this short paper, and will be possibly discussed in future works.

8.4 Outlook

In this paper we have presented, for the first time (we believe) in the literature of theoretical cosmology, two new results: *i*) the explicit computation of the perturbation equation for the Kalb-Ramond axion field including higher-curvature corrections to first order in α'; and *ii*) the explicit contribution of shear viscosity to the tensor metric perturbations of the gravi-dilaton equations written in the String frame.

We have used such results to discuss examples of high-curvature, non-vacuum, non-minimal pre-big bang models giving a spectral distribution of relic stochastic gravitons, $\Omega_{GW}(f)$, which may be the source of the signal recently detected by the IPTA collaboration. We have shown, also, that the GW distribution of the considered models, in the spectral plane $\{f, \Omega_{GW}(f)\}$, may have an intensity possibly detectable even in the higher-frequency sensitivity window of the so-called third generation GW antennas, such as LISA, ET and DECIGO.

Finally, we have presented a mechanism able to break the string theory S-duality relating the primordial graviton and axion spectra. The breaking may be induced by the intrinsic presence of shear viscosity in the fluid sources contributing to the dynamics of the high-curvature string phase, and it could be important to interpret (and explain) possible future signals of relic GW backgrounds detected with unexpected amplitude in atypical (high-energy) frequency ranges.

Conclusions

In this thesis we have investigated the dynamics and observational consequences of pre–Big Bang (PBB) cosmology, a string motivated alternative to inflation. The central aim was to understand how higher-curvature corrections and string dualities affect the possibility of obtaining a smooth cosmological bounce and of generating a primordial gravitational wave background that can be confronted with present and future observations.

At the theoretical level, we have worked within the Hohm–Zwiebach framework, which incorporates the gravi–dilaton system to all orders in α' at tree level in the string coupling. By reformulating the dynamics in terms of the Routhian and focusing on homogeneous Bianchi-I configurations, we showed that this effective action admits non-singular, "self-dual" bouncing solutions. These solutions evade the curvature singularity that appears at lowest order, and in particular they connect pre-bounce and post-bounce branches in a way consistent with scale factor duality. The result provides a realization of the bounce in string cosmology.

We then explored how the addition of a non-perturbative dilaton potential modifies this picture. Importantly, the existence of regular bounces is controlled mainly by the reduced hamiltonian, but the late-time fate of the dilaton may differ according to the initial conditions. Depending on the shape of the potential and on initial conditions, the system can rejoin the dual of the vacuum branch, reflecting back to weak coupling, or stabilize at a finite value, thereby leading either to decelerated FLRW expansion or to an accelerated phase reminiscent of de Sitter space. Moreover, we found that isotropization is a robust feature: even starting from anisotropic initial conditions, the evolution drives the system toward isotropy.

On the phenomenological side, we considered the production of primordial gravitational waves in minimal PBB model that includes the axion curvaton mechanism

required to generate adiabatic scalar perturbations and a constant curvature linear dilaton string phase. Once the post-bounce axion-dominated phase is properly taken into account, the resulting amplitude in the nanohertz range falls short of explaining the signal suggested by NANOGrav and the IPTA. This mismatch demonstrates that the minimal, S-duality-symmetric PBB scenario cannot reproduce the PTA data. Nonetheless, this minimal setup is far from unobservable: it still predicts detectable pGW signals well within the forecasted sensitivities of LISA, DECIGO, and ET. This shows that even the most conservative version of PBB cosmology offers falsifiable predictions for the next generation of detectors.

The situation changes if one allows for a non-minimal high-curvature string phase that breaks S-duality. In particular, we considered the effect of anisotropic sources and viscous stresses, which provide a concrete way of breaking S-duality. While in isotropic cosmologies shear viscosity does not affect the background dynamics we have shown that it contributes to the propagation of tensor modes. This makes it a natural mechanism to decouple the axion and graviton spectra and to enlarge the range of viable predictions. Within this generalized framework, it is possible to reconcile the PBB scenario with the PTA signal while remaining consistent with all the cosmological bounds.

From an observational perspective, the non-minimal PBB scenarios explored here is testable. Not only it can account for the nanohertz-band hints reported by PTA collaborations, but is also generically predict an excess of gravitational wave power in the milli- and deca-hertz ranges, which fall within the reach of forthcoming detectors such as LISA, the Einstein Telescope, and DECIGO. This multi-band signature provides a criterion to test string cosmology.

In conclusion, this work has shown that the pre–Big Bang scenario, with and without modest departures from exact dualities, can not only achieve a smooth non-singular bounce but also yield a spectrum of primordial gravitational waves that is both compatible with present PTA hints and testable by the next generation of detectors. The near future of gravitational wave cosmology thus holds the potential to confirm or exclude concrete realizations of string-motivated early-universe dynamics.

Appendix A

From expanding pre-big bang to contracting post-big bang

As discussed in Sect. 4.4, one of the possible effects of the potential (4.16) is that of producing an effective potential barrier which stops the growth of the dilaton and "reflects back" the dilaton towards the large negative values of the perturbative string vacuum.

Such an effect, combined with the curvature regularisation due to the α' corrections, leads to a new interesting type of bouncing scenario where the final background is no longer described by the duality-transformed initial solution (indeed, duality is broken by the presence of the potential), but it nevertheless corresponds to the time-reversed version of the initial solution. Hence, if we start with an initial (isotropic, $(d+1)$-dimensional) pre-big bang configuration describing growing dilaton, growing curvature, and accelerated expansion ($\dot{a} > 0$, $\ddot{a} > 0$, $t \to -\infty$,):

$$a \sim (-t)^{-1/\sqrt{d}}, \quad H = \frac{1}{\sqrt{d}\,(-t)} > 0, \quad \phi \sim -\left(1+\sqrt{d}\right)\ln(-t), \quad \dot{\bar{\phi}} = \sqrt{d}\,H > 0, \tag{A.1}$$

(see also Eq. (4.1)), we end up with a post-bounce configuration asymptotically describing decreasing dilaton, decreasing curvature, and decelerated contraction ($\dot{a} < 0$, $\ddot{a} > 0$, $t \to +\infty$):

$$a \sim (t)^{-1/\sqrt{d}}, \quad H = -\frac{1}{\sqrt{d}\,(t)} < 0, \quad \phi \sim -\left(1+\sqrt{d}\right)\ln(t), \quad \dot{\bar{\phi}} = \sqrt{d}\,H < 0, . \tag{A.2}$$

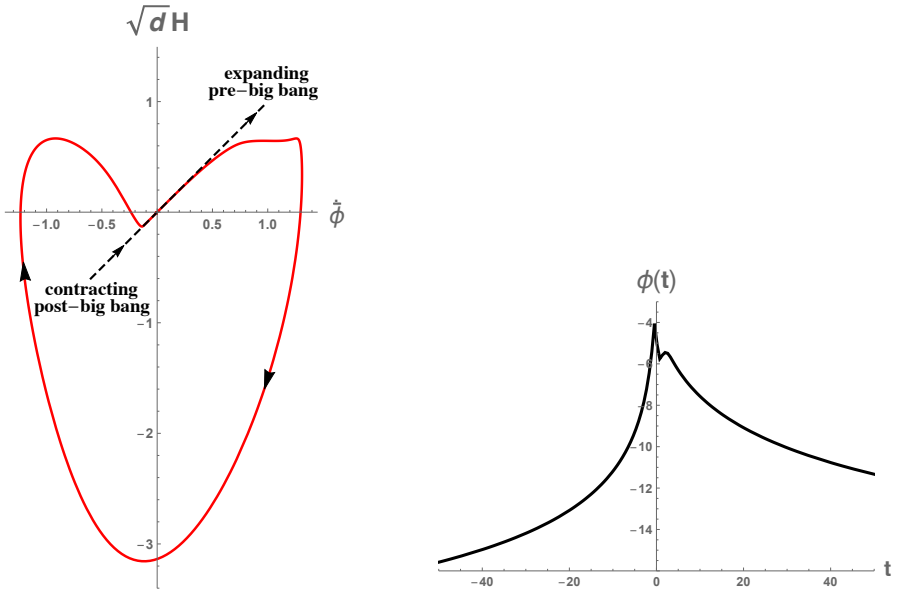

FIGURE A.1: Left: parametric plot obtained with a numerical solution of Eq. (4.13) with the potential (4.16) and the Hamiltonian (4.19). We have set $d = 3$, $\alpha' = 1$ for the Hamiltonian, $A = 1/3$, $\alpha = 10$, $\beta = 3$, $c = 2$, $\delta = 0.01$, $q = 1$ for the potential, and $\kappa = 0.0075$ for the initial conditions at $t = -200$. The black dashed bisecting line describes the initial evolution (A.1) expanding from the perturbative regime (upper-right quadrant), and the final time-reversed contracting evolution (A.2) (lower-left quadrant). Right: time evolution of the dilaton according to a numerical integration of (4.13) performed with the same parameters and the same initial conditions.

A simple illustration of this scenario can be provided by a numerical integration of Eqs. (4.13) with appropriate values of the initial conditions, which in our case are controlled by the parameter κ of Eq. (4.26), defined at large negative times by $\kappa = e^{\phi}\left(\sqrt{d}\,H\right)^{-(1+\sqrt{d})}$. According to Eq. (A.1) this parameter goes to a constant for $t \to -\infty$. Such a constant depends on the initial value of the dilaton and, as discussed in Sect. 4.4.1, it is equivalent (but more convenient) to specify initially the value κ rather than that of ϕ. For initial values of κ small enough with respect to the parameters controlling the height of the potential, the numerical integration gives the results reported in Fig. A.1 (see the caption for the used numerical values).

In the left panel we have the parametric plot describing a smooth, regular transition from the initial configuration (A.1) to the final configuration (A.2). The corresponding evolution of the dilaton, which reaches a maximum and then bounces back to the asymptotically perturbative regime, is shown in the right panel of the figure. Note that the red curve describing the parametric evolution of $H(\dot{\bar{\phi}})$ starts and ends at the origin, is still turning clockwise in the parametric plane,

but it is not topologically equivalent to the curves given in the plots of Sect. 4.3 and Sect. 4.4.1, (always associated with a final expanding regime). Indeed, in the parametric plot of of Fig. A.1 the vector connecting the origin to a point on the red curve undergoes a clockwise rotation of π (and not $3\pi/2$) as one goes from the beginning to the end of the curve.

Appendix B

Smooth interpolation of a broken power law

Suppose we have a piecewise continuous function $f(x) : \mathbb{R}^+ \to \mathbb{R}^+$ such that, in each interval, its behaviour is given by a power law $f(x) \sim x^m$. Then, we can define a sequence of exponents $m_1, m_2, \ldots$ and interval extrema $x_{1,2}, x_{2,3}, \ldots$ such that $x_{i,i+1} < x_{i+1,i+2}$. The derivative of the logarithm of the function with respect to the logarithm of its argument is simply given by

$$\frac{d\ln f(x)}{d\ln x} = m_1 + (m_2 - m_1)\Theta(\ln x - \ln x_{1,2}) + (m_3 - m_2)\Theta(\ln x - \ln x_{2,3}) + \ldots, \quad \text{(B.1)}$$

where Θ is the Heaviside step function: $\Theta(y) = 1$ for $y \geqslant 0$ and $\Theta(y) = 0$ otherwise. Let us approximate the Heaviside function with a logistic function:

$$\Theta(y - y_0) \simeq \frac{1}{1 + e^{-l(y-y_0)}}, \quad \text{(B.2)}$$

where l is a positive constant and the greater l the better the approximation. Substituting the latter into (B.1) and defining a different l for each Θ, we have in compact form

$$\frac{d\ln f(x)}{d\ln x} = m_1 + \sum_{i=1}^{N-1} \frac{m_{i+1} - m_i}{1 + (\frac{x}{x_{i,i+1}})^{-l_{i+1}}}\,. \quad \text{(B.3)}$$

We can moreover rewrite the last equality with respect to the x-derivative as

$$\frac{d\ln f(x)}{dx} = \frac{m_1}{x} + \sum_{i=1}^{N-1} \frac{m_{i+1}-m_i}{x} \frac{1}{1+(\frac{x}{x_{i,i+1}})^{-l_{i+1}}}\,. \tag{B.4}$$

Integrating the last expression, we obtain

$$\ln f(x) = \ln A + \ln(x^{m_1}) + \sum_{i=1}^{N-1} \ln\Big(x^{l_{i+1}} + x_{i,i+1}^{l_{i+1}}\Big)^{(m_{i+1}-m_i)/l_{i+1}}\,,$$

where A is a constant, and finally

$$\begin{aligned} f(x) &= A\,x^{m_1} \prod_{i=1}^{N-1} \Big(x^{l_{i+1}} + x_{i,i+1}^{l_{i+1}}\Big)^{(m_{i+1}-m_i)/l_{i+1}} \\ &= A\,x^{m_1} \left(x^{l_2} + x_{1,2}^{l_2}\right)^{(m_2-m_1)/l_2} \left(x^{l_3} + x_{2,3}^{l_3}\right)^{(m_3-m_2)/l_3} \times \ldots\,. \end{aligned} \tag{B.5}$$

If we wish to introduce an exponential cut-off for $x > x_{N,N+1}$ such that $f(x) \sim \exp[-(x - x_{N,N+1})/x_{N,N+1}]$, then we have to add to (B.1) an additional contribution given by $(-x/x_{N,N+1} - m_{N+1})\Theta(\ln x - \ln x_{N,N+1})$. Let us denote $x_{N,N+1} \equiv x_M$ and $l_{N+1} \equiv l$. Following the same steps as before, one finds upon integration and exponentiation that

$$\begin{aligned} f(x) &= A\,x^{m_1} \prod_{i=1}^{N-1} \Big(x^{l_{i+1}} + x_{i,i+1}^{l_{i+1}}\Big)^{(m_{i+1}-m_i)/l_{i+1}} \left(x^l + x_M^l\right)^{-m_{N+1}/l} \\ &\quad \times \exp\left[-\frac{(x/x_M)^{1+l}\,{}_2F_1(1,\,1+1/l,\,2+1/l,\,-(x/x_M)^l)}{1+l}\right], \end{aligned} \tag{B.6}$$

where ${}_2F_1(a,b,c,z)$ is the Gauss hypergeometric function. Translating into the general language we introduced before for the power spectrum of (5.21), we have $m_1 = 3$, $m_2 = 3 - |3-2\beta|$, $m_3 = 1 - |3-2\beta|$, $m_4 = 3 - |3-2\beta|$, $x_{1,2} = f_s$, $x_{2,3} = f_d$ and $x_{3,4} = f_\sigma$ and $x_M = f_1$, so that (setting $l_i = l$ for all i)

$$\begin{aligned} \Omega_{\rm GW}^{\rm smooth}(f) &= A\,f^3 \left(f^l + f_s^l\right)^{-\frac{|3-2\beta|}{l}} \left(f^l + f_d^l\right)^{-\frac{2}{l}} \left(f^l + f_\sigma^l\right)^{\frac{2}{l}} \\ &\quad \times \left(f^l + f_1^l\right)^{\frac{|3-2\beta|-3}{l}} \mathcal{F}(f, f_1, l)\,, \end{aligned} \tag{B.7}$$

where we defined the function $\mathcal{F}(f, f_1, l)$ as the exponential cutoff appearing in the last line of (B.6). Setting $l = 2$, we obtain (5.22):

$$\begin{aligned}\Omega_{\rm GW}^{\rm smooth}(f) &= A\, f^3 \left(f^2 + f_s^2\right)^{-\frac{|3-2\beta|}{2}} \left(f^2 + f_d^2\right)^{-1} \left(f^2 + f_\sigma^2\right) \left(f^2 + f_1^2\right)^{\frac{|3-2\beta|-3}{2}} \\ &\quad \times \exp\left\{\left(-\frac{f}{f_1} + \arctan\frac{f}{f_1}\right)\right\}. \end{aligned} \tag{B.8}$$

The integration constant A is fixed to match the asymptotic behaviour in the limit $f \to 0$ with the explicit formula given in (5.21),

$$\Omega_{\rm GW}(f) \overset{f\to 0}{\simeq} \Omega_{\rm PBB}\, (f_\sigma)^2 (f_d)^{-2} (f_s)^{-|3-2\beta|} (f_1)^{|3-2\beta|-3} f^3, \tag{B.9}$$

while for the smooth interpolation (B.8)

$$\Omega_{\rm GW}^{\rm smooth}(f) \overset{f\to 0}{\simeq} A\, (f_\sigma)^2 (f_d)^{-2} (f_s)^{-|3-2\beta|} (f_1)^{|3-2\beta|-3} f^3, \tag{B.10}$$

which yields $A = \Omega_{\rm PBB}$.

Appendix C

Parameter space of the PBB model

In this appendix, we show that the parameter space of the PBB model is $\{\beta, z_s, z_d, z_\sigma\}$ (section C.1) and we discuss the theoretical priors on these parameters (section C.2). We also determine the region in parameter space for which the promordial GWB amplitude is maximized (section C.2.1). In view of a numerical implementation of these conditions and to emphasize orders of magnitude, it may be useful to work with base-10 logarithmic expressions.

C.1 Reducing the number of parameters

First, we show that the transition scale H_1 is not independent and can be fixed by the other parameters,

$$H_1 = H_1(\beta, z_s, z_d, z_\sigma)\,. \tag{C.1}$$

By using previous results [74, 155], obtained under the natural assumption that the pivot scale belongs to the low-frequency band of the scalar spectrum (i.e., $k_* < k_s$), the condition on H_1 following from the normalization of the scalar spectrum can be written as

$$\begin{aligned}\left(\frac{H_1}{M_{\rm Pl}}\right)^{\frac{5-n_{\rm S}}{2}} &= \frac{2\pi^2}{\mathcal{T}^2(\sigma_i)}\mathcal{P}_{\rm S}(k_*)\, z_s^{1-n_{\rm S}-2\beta}\left[\left(\frac{H_*}{M_{\rm Pl}}\right)^{-\frac{1}{2}}\left(\frac{mM_{\rm Pl}}{\sigma_i^2}\right)^{\frac{1}{3}}\right]^{n_{\rm S}-1} \\ &= \frac{2\pi^2}{\mathcal{T}^2(\sigma_i)}\mathcal{P}_{\rm S}(k_*)\, z_s^{1-n_{\rm S}-2\beta}\left(\frac{H_*}{M_{\rm Pl}}\frac{z_d}{z_\sigma}\right)^{-\frac{n_{\rm S}-1}{2}}\,,\end{aligned} \tag{C.2}$$

where we have recast m and σ_i according to (5.14), H_* is the curvature scale at the epoch in which the pivot mode k_* re-enters the horizon and $\mathcal{T}(\sigma_i)$ is the transfer function connecting the amplitude of the primordial axion fluctuations to the final amplitude of the scalar curvature modes of metric perturbations. A numerical integration of the scalar perturbation equations gives the simple result [59]

$$\mathcal{T}(\sigma_i) \simeq 0.13\,\frac{\sigma_i}{M_{\rm Pl}} + 0.25\,\frac{M_{\rm Pl}}{\sigma_i} - 0.01\,, \tag{C.3}$$

where σ_i can be expressed in terms of the z parameters as in (5.14). To obtain H_*, we can conveniently refer to the equilibrium scale by noting that $k_* \simeq 5k_{\rm eq}$. This implies $H_*^{1/2} \simeq 5H_{\rm eq}^{1/2}$. On the other hand, it is known that the Hubble parameter at radiation-matter equality is given by $H_{\rm eq} \simeq 1.6\times 10^5 H_0 \approx 9.5\times 10^{-56} M_{\rm Pl}$. We thus obtain

$$\left(\frac{H_*}{M_{\rm Pl}}\right)^{1/2} \approx 1.5\times 10^{-27}\,. \tag{C.4}$$

Now we can then express the normalization (C.2) in terms of the four parameters $\{\beta, z_s, z_d, z_\sigma\}$ (and of known experimental numbers) as follows:

$$\begin{aligned}\log_{10}\left(\frac{H_1}{M_{\rm Pl}}\right) \;=\; & \frac{2}{5-n_{\rm s}}\left\{\log_{10}\left[\frac{4.2\pi^2}{\mathcal{T}^2(\sigma_i)}\right] - 9 + (1-n_{\rm s})(\log_{10}1.5 - 27)\right. \\ & \left. + (1-n_{\rm s}-2\beta)\log_{10} z_s + \frac{n_{\rm s}-1}{2}\left(\log_{10} z_\sigma - \log_{10} z_d\right)\right\}\end{aligned} \tag{C.5}$$

where we have used $\mathcal{P}_{\rm s}(k_*) = 2.1\times 10^{-9}$. It should be noted that $\mathcal{T}^2(\sigma_i)$ also contains H_1 through (5.14) but the solution for H_1 can always be numerically obtained, in general, for any given set of values of the four independent parameters.

Finally, the other important quantity appearing in the GWB (5.21) is today's value of the highest amplified frequency mode f_1, which is given by

$$\begin{aligned} f_1 \;=\; & \frac{\omega_1(\tau_0)}{2\pi} = \frac{H_1 a_1}{2\pi a_0} = \frac{H_1}{2\pi}\frac{a_1}{a_\sigma}\frac{a_\sigma}{a_d}\frac{a_d}{a_{\rm eq}}\frac{a_{\rm eq}}{a_0} \simeq \frac{H_1}{2\pi}\left(\frac{H_\sigma}{H_1}\right)^{\frac{1}{2}}\left(\frac{H_d}{H_\sigma}\right)^{\frac{2}{3}}\left(\frac{H_{\rm eq}}{H_d}\right)^{\frac{1}{2}}\left(\frac{H_0}{H_{\rm eq}}\right)^{\frac{2}{3}} = \\ =\; & \frac{H_1^{\frac{1}{2}}}{2\pi}\left(\frac{z_\sigma}{z_d}\right)^{\frac{1}{2}}\frac{H_0^{\frac{2}{3}}}{H_{\rm eq}^{\frac{1}{6}}} \simeq \frac{3.9\times 10^{11}}{2\pi}\left(\frac{H_1}{M_{\rm Pl}}\right)^{\frac{1}{2}}\left(\frac{z_\sigma}{z_d}\right)^{\frac{1}{2}}\,{\rm Hz}\,. \end{aligned} \tag{C.6}$$

C.2 Theoretical priors

Having thus determined that the parameter space is $\{\beta, z_s, z_d, z_\sigma\}$, let us now turn to the priors we can impose on it theoretically.

A first condition concerns the parameter β controlling the power-law behaviour of the primordial GW spectrum at high frequencies, which is constrained to be in the range

$$0 \leqslant \beta < 3\,. \tag{C.7}$$

The lower limit is due to the assumption of growing string coupling (needed to implement a smooth bouncing transition [5, 93, 172]), while the upper limit has to be imposed to avoid background instabilities [185].

We have then a number of constraints following from the (already mentioned) hierarchy of the transition frequency scales, which must satisfy the conditions $f_1 \gtrsim f_\sigma > f_d > f_s$. They imply

$$1 \lesssim z_\sigma < z_d < z_s\,. \tag{C.8}$$

In addition, for an efficient implementation of the curvaton mechanism based on the oscillations of the Kalb–Ramond axion, the axion background field must be oscillating when it becomes dominant (at the curvature scale H_σ). From the axion dynamical equations, one finds [110, 111] that the oscillating regime starts at the scale $H_m \simeq m$. This leads to the condition $H_m \geqslant H_\sigma$, which implies $\sigma_i \leqslant M_{\rm Pl}$ and which, by using Eq. (5.14), can be written in logarithmic form as

$$\log_{10}\left(\frac{H_1}{M_{\rm Pl}}\right) + \frac{3}{2}\log_{10} z_d - \frac{7}{2}\log_{10} z_\sigma \leqslant 0\,. \tag{C.9}$$

Also, to be consistent with the established results of the post-inflationary scenario, we may expect that the reheating produced by the axion decay at the scale H_d, and marking the beginning of the standard cosmological evolution, occurs before the BBN scale, $H_{\rm BBN} \simeq (1\,{\rm MeV})^2/M_{\rm Pl}$. This implies $H_d > H_{\rm BBN}$ from which, using eqs. (5.9) and (5.14), we have the constraint

$$\log_{10}\left(\frac{H_1}{M_{\rm Pl}}\right) - 3\log_{10} z_d + \log_{10} z_\sigma > -42 - \log_{10} 4\,, \tag{C.10}$$

where we have used $M_{\rm Pl} \approx 2 \times 10^{18}$ GeV.

Finally, the conditions concerning the scalar perturbation spectrum must be imposed not only at the pivot frequency scale k_* but also, in principle, to all frequency scales included into the multipole expansion of the CMB anisotropy, and constrained by observational data. This means, in other words, that also the highest frequency modes $k_{\rm LSS}$ presently constrained by large scale structure (LSS) observations must be below the lowest frequency branch of the axion perturbation spectrum [74, 155], and this implies $k_{\rm LSS} < k_s$, where $k_{\rm LSS} \sim 3\,{\rm Mpc}^{-1} \approx 60\,k_*$, namely $H_{\rm LSS}^{1/2} \simeq 60\,H_*^{1/2}$. The condition $k_{\rm LSS}/k_s = (k_{\rm LSS}/k_1)z_s < 1$ then leads to yet another constraint that can be written as follows. Since

$$\begin{aligned}\frac{k_1}{k_{\rm LSS}} &= \frac{H_1 a_1}{H_{\rm LSS}a_{\rm LSS}} = \frac{H_1}{H_{\rm LSS}}\frac{a_1}{a_\sigma}\frac{a_\sigma}{a_d}\frac{a_d}{a_{\rm LSS}} \simeq \frac{H_1}{H_{\rm LSS}}\left(\frac{H_\sigma}{H_1}\right)^{\frac{1}{2}}\left(\frac{H_d}{H_\sigma}\right)^{\frac{2}{3}}\left(\frac{H_{\rm LSS}}{H_d}\right)^{\frac{1}{2}} \\ &= \left(\frac{H_1}{M_{\rm Pl}}\right)^{\frac{1}{2}}\left(\frac{H_*}{M_{\rm Pl}}\right)^{-\frac{1}{2}}\left(\frac{H_*}{H_{\rm LSS}}\right)^{\frac{1}{2}}\left(\frac{H_\sigma}{H_d}\right)^{-\frac{1}{6}},\end{aligned}$$

from eqs. (5.9) and (5.14) we get $H_\sigma/H_d = (z_d/z_\sigma)^3$ and from (C.4) we obtain

$$\log_{10} z_s < 26 - \log_{10} 9 + \frac{1}{2}\log_{10}\left(\frac{H_1}{M_{\rm Pl}}\right) + \frac{1}{2}\left(\log_{10} z_\sigma - \log_{10} z_d\right) . \qquad \text{(C.11)}$$

C.2.1 Maximizing the signal

Given the condition (C.5) on $H_1/M_{\rm Pl}$, the amplitude and the frequency distribution of the GWB (5.21) or (5.22) are fully determined by $\beta, z_s, z_d, z_\sigma$. These four parameters are not completely free, as they must satisfy a non-trivial set of self-consistency conditions (Appendix C.2). Taking into account these constraints on the parameters, we can determine the maximal allowed region for the PBB signal in the spectral plane $(\Omega_{\rm GW}, f)$. Let us first notice that, thanks to the condition (C.7), the GWB (5.22) may be possibly decreasing only in the frequency branch $f_d \leqslant f \leqslant f_\sigma$. The peak of the spectrum may thus be located either at f_1 or at f_d, with corresponding amplitudes

$$\Omega_{\rm GW}(f_1) = \Omega_{\rm r0}\left(\frac{H_1}{M_{\rm Pl}}\right)^2\left(\frac{z_\sigma}{z_d}\right)^2, \qquad \Omega_{\rm GW}(f_d) = \Omega_{\rm r0}\left(\frac{H_1}{M_{\rm Pl}}\right)^2 z_d^{|3-2\beta|-3}. \qquad \text{(C.12)}$$

In the first case, given the constraints (C.8), the maximal amplitude can be reached for the limiting values $z_d \simeq z_\sigma$, which imply however $H_d \simeq H_\sigma$: hence, in that case, the axion starts decaying as soon as it becomes dominant, and there is not enough time for an efficient curvaton mechanism. Also, in that case, the maximal

amplitude would correspond to a frequency range $f \sim f_1$, in general too high for the sensitivity of present detectors.

In the second case with the peak at f_d, given again the constraints (C.7) and (C.8), the maximal amplitude can be obtained either in the limit $z_d \simeq z_\sigma \to 1$ or in the limit $\beta \to 0$. Discarding the first possibility (for the same reasons as before), in order to find the allowed region for the GW signal of maximal intensity we will thus concentrate on the limiting case $\beta = 0$ which, as we will see, automatically leads to a peak located in frequency ranges possibly accessible to third-generation detectors.

It should be noted, in addition, that the limiting amplitude reached at f_d for $\beta = 0$ is only controlled by the ratio $H_1/M_{\rm Pl}$, whose maximal allowed value is bounded by the constraints (C.9): hence, the amplitude of the GWB approaches its allowed maximum in the limit in which the condition (C.9) is saturated by the equality

$$\log_{10} z_\sigma = \frac{2}{7} \log_{10} \left(\frac{H_1}{M_{\rm Pl}} \right) + \frac{3}{7} \log_{10} z_d \,. \tag{C.13}$$

This result has two important consequences.

First of all, by using eq. (5.14), we can check that the above condition is equivalent to the condition $\sigma_i = M_{\rm Pl}$, and this uniquely fixes the transfer function (C.3) leading to the constant numerical value $\mathcal{T}^2 \approx 0.137$. Second, by inserting into the above condition the general expression (C.5) for H_1, and solving for the variable $\log_{10} z_\sigma$, we can eliminate z_σ everywhere and confine our discussion of the maximum allowed spectrum to a two-dimensional parameter space spanned by the variables $\{\log_{10} z_s, \log_{10} z_d\}$, with $\beta = 0$, z_σ given by eq. (C.13) and H_1 given by

$$\begin{aligned} \log_{10} \left(\frac{H_1}{M_{\rm Pl}} \right) \;\simeq\; & \frac{14}{37 - 9 n_{\rm s}} \left[\log_{10} \left(\frac{4.2 \pi^2}{0.137} \right) - 9 + (1 - n_{\rm s})(\log_{10} 1.5 - 27) \right. \\ & \left. + (1 - n_{\rm s}) \log_{10} z_s + \frac{2}{7} (1 - n_{\rm s}) \log_{10} z_d \right] . \end{aligned} \tag{C.14}$$

We can now easily impose all constraints (C.8)–(C.11) and evaluate, in such a context, both the allowed region of parameter space and the maximal allowed value of the peak amplitude. It turns out (see Fig. 5.1), that the maximal value of eq. (C.14) compatible with the given constraints corresponds to $\log_{10}(H_1/M_{\rm Pl}) \approx -3.29$, so that the expected maximum intensity of the primordial GWB is given

by

$$\Omega_{\rm GW}^{\rm max} = \Omega_{\rm r0} \left(\frac{H_1}{M_{\rm Pl}} \right)^2 \approx 10^{-10.6} \,. \tag{C.15}$$

The allowed values of the parameters compatible with this maximal intensity (and with the imposed constraints) are in the range $18.7 \lesssim \log_{10} z_s \lesssim 22.3$ and $2.19 \lesssim \log_{10} z_d \lesssim 14.9$, as shown in Fig. 5.1. The corresponding value of z_σ is given by eq. (C.13) and lies in the range $0 \lesssim \log_{10} z_\sigma \lesssim 5.5$.

Appendix D

Appendix D

In this appendix we provide some useful explicit relations that can be found by solving the set of equations (6.14), (6.18), (6.19), (6.20).

The first set of relations (6.14), (6.18) gives the five quantities $H_1, m, z_s, z_d, z_\sigma$ in terms of $\sigma_i/M_{\rm Pl}$, β_h and β_σ:

$$\begin{aligned}
\log z_s =& -\frac{K}{(\beta_\sigma-\beta_h)};\\
\log\frac{H_1}{M_{\rm Pl}} =& \frac{C}{2}-\frac{K\beta_h}{(\beta_\sigma-\beta_h)};\\
\log\frac{z_s}{z_\sigma} =& \frac{3}{2}B-\frac{5}{8}C+3\log\left(\frac{\sigma_i}{M_{\rm Pl}}\right)-\frac{5}{4}\frac{K(2-\beta_h)}{(\beta_\sigma-\beta_h)};\\
\log\frac{z_d}{z_\sigma} =& -2B+\frac{1}{2}C+\frac{K(2-\beta_h)}{(\beta_\sigma-\beta_h)};\\
\log\frac{m}{M_{\rm Pl}} =& 3B-\frac{3}{4}C+2\log\left(\frac{\sigma_i}{M_{\rm Pl}}\right)-\frac{3}{2}\frac{K(2-\beta_h)}{(\beta_\sigma-\beta_h)},
\end{aligned} \tag{D.1}$$

where we have defined the following (in general $\sigma_i/M_{\rm Pl}$-dependent) quantities:

$$\begin{aligned}
K\left(\frac{\sigma_i}{M_{\rm Pl}}\right) &= \frac{1}{2}\left[A\left(\frac{\sigma_i}{M_{\rm Pl}}\right)-C+(n_s-1)B\right]\ ,\\
A &= \log\left(\frac{4.2\pi^2}{T^2(\sigma_i)}\right)-9+(1-n_s)(\log 1.5-27)\ ,
\end{aligned}$$

$$B = \log\left(\frac{2\pi f_s}{H_0^{\frac{1}{2}} M_{\rm Pl}^{\frac{1}{2}}}\right) - \frac{1}{6}\log\left(\frac{H_0}{H_{\rm eq}}\right) = \log\left(\frac{2\pi f_s}{3.9\times 10^{11}}\right) \ ,$$
$$C = \log\frac{\Omega_{\rm GW}(f_s)}{\Omega_r(t_0)} = -4 + \log 2.9 \ . \tag{D.2}$$

Eqs. (D.1) show that the two ratios z_s/z_σ, z_s/z_d (and therefore also z_d/z_σ) can be expressed in terms of $\sigma_i/M_{\rm Pl}$, $m/M_{\rm Pl}$, and other known constants. More explicitly we find:

$$\begin{aligned}\log\left(\frac{z_s}{z_d}\right) &= \frac{3}{2}\log\left(\frac{m}{M_{\rm Pl}}\right) + \frac{1}{6}\log\left(\frac{H_0}{H_{\rm eq}}\right) + \log\left(\frac{H_0^{\frac{1}{2}} M_{\rm Pl}^{\frac{1}{2}}}{2\pi f_s}\right) \\ &= \frac{3}{2}\log\left(\frac{m}{M_{\rm Pl}}\right) + \log\left(\frac{3.9\times 10^{11}}{2\pi f_s}\right) \ ,\end{aligned} \tag{D.3}$$

$$\begin{aligned}\log\left(\frac{z_s}{z_\sigma}\right) &= \frac{5}{6}\log\left(\frac{m}{M_{\rm Pl}}\right) + \frac{4}{3}\log\left(\frac{\sigma_i}{M_{\rm Pl}}\right) + \frac{1}{6}\log\left(\frac{H_0}{H_{\rm eq}}\right) + \log\left(\frac{H_0^{\frac{1}{2}} M_{\rm Pl}^{\frac{1}{2}}}{2\pi f_s}\right) \\ &= \frac{5}{6}\log\left(\frac{m}{M_{\rm Pl}}\right) + \frac{4}{3}\log\left(\frac{\sigma_i}{M_{\rm Pl}}\right) + \log\left(\frac{3.9\times 10^{11}}{2\pi f_s}\right) \ ,\end{aligned} \tag{D.4}$$

$$\log\left(\frac{z_d}{z_\sigma}\right) = \frac{4}{3}\log\left(\frac{\sigma_i}{M_{\rm Pl}}\right) - \frac{2}{3}\log\left(\frac{m}{M_{\rm Pl}}\right), \tag{D.5}$$

where $H_{\rm eq} = 1.6\times 10^5 H_0 = 9.5\times 10^{-56} M_{\rm Pl}$ and $M_{\rm Pl} \approx 2\times 10^{18}\,\text{GeV}$.

Appendix E

Field equations for the non-minimal, non-vacuum string phase

Here we give explicitly the equations controlling the time evolution of the string phase background, describing the chosen model of non-minimal PBB scenario.

Let us start with the action (8.3), and with the sources described by Eqs. (8.5)–(8.9). We vary the action with respect to N, β, γ, ϕ and, after the variation, we put $N = 1$ (cosmic time gauge), and $\ddot{\beta} = 0$, $\ddot{\gamma} = 0$, $\ddot{\phi} = 0$ (to obtain a constant spacetime curvature and a linearly evolving dilaton, as in the minimal case). We then obtain, respectively, the following four algebraic equations:

$$\begin{aligned}
&\dot{\phi}^2 + 6\dot{\beta}^2 + n(n-1)\dot{\gamma}^2 + 6n\dot{\beta}\dot{\gamma} - 6\dot{\beta}\dot{\phi} - 2n\dot{\gamma}\dot{\phi} - \\
&-3\alpha' a_0 \left[c_2\dot{\gamma}^4 + 8\dot{\phi}\dot{\beta}^3 + c_4\dot{\gamma}^3(\dot{\phi} - 3\dot{\beta}) - \dot{\phi}^4 + c_5\dot{\beta}\dot{\gamma}^2(\dot{\phi} - \dot{\beta}) + 8n\dot{\gamma}\dot{\beta}^2(3\dot{\phi} - \dot{\beta})\right] = \\
&= 2\lambda_{\rm s}^{D-1} e^{\phi}\rho, \qquad \text{(E.1)}
\end{aligned}$$

$$\begin{aligned}
&-\dot{\phi}^2 - 6\dot{\beta}^2 + 4\dot{\beta}\dot{\phi} + 2n\dot{\gamma}(\dot{\phi} - 2\dot{\beta}) - n(n+1)\dot{\gamma}^2 \\
&-\alpha' a_0 \left[8\dot{\phi}^2\dot{\beta}^2 - 16\dot{\phi}\dot{\beta}^3 - \dot{\phi}^4\right] - \alpha' a_0\dot{\gamma}^4(c_2 + nc_4) + \frac{n}{3}c_5\alpha' a_0\dot{\gamma}^3(\dot{\phi} - 2\dot{\beta}) \\
&+\alpha' a_0\dot{\gamma}^2\left[-\dot{\beta}^2(c_5 + 8n^2) + \dot{\beta}\dot{\phi}\left(\frac{2}{3}c_5 + 16n^2\right) - \frac{c_5}{3}\dot{\phi}^2\right] + 8n\alpha' a_0\dot{\gamma}\left[5\dot{\beta}^2\dot{\phi} - 2\dot{\beta}^3 - 2\dot{\beta}\dot{\phi}^2\right] = \\
&= 2\lambda_{\rm s}^{D-1} e^{\phi}\left[w_1\rho + \frac{2\eta_V}{3+n}\frac{n}{\lambda_{\rm s}}(\dot{\gamma} - \dot{\beta})\right], \qquad \text{(E.2)}
\end{aligned}$$

$$
\begin{aligned}
&-n^2(n-1)\dot\gamma^2 - 6n(n-1)\dot\gamma\dot\beta + 2n(n-1)\dot\gamma\dot\phi + 6n\dot\beta\dot\phi - n\dot\phi^2 - 12n\dot\beta^2 \\
&+\alpha' a_0 3nc_2\dot\gamma^4 + \alpha' a_0 2\dot\gamma^3(\dot\phi - 3\dot\beta)(nc_4 - 2c_2) + \alpha' a_0\dot\gamma^2\left[nc_5\dot\beta(\dot\phi-\dot\beta) - 3c_4(\dot\phi - 3\dot\beta)^2\right] \\
&+\alpha' a_0\dot\gamma\left[c_5(\dot\phi-\dot\beta)(6\dot\beta^2 - 2\dot\phi\dot\beta)\right] - \alpha' a_0 n\left[-72\dot\phi\dot\beta^3 - \dot\phi^4 + 24\dot\beta^2(\dot\phi^2+\dot\beta^2)\right] = \\
&= 2n\lambda_{\rm s}^{D-1}e^{\phi}\left[w_2\rho + \frac{2\eta_V}{3+n}\frac{3}{\lambda_{\rm s}}(\dot\beta - \dot\gamma)\right],
\end{aligned}
\tag{E.3}
$$

$$
\begin{aligned}
&\dot\phi^2 + 12\dot\beta^2 - 6\dot\beta\dot\phi + n(n+1)\dot\gamma^2 + 2n\dot\gamma(3\dot\beta - \dot\phi) + \alpha' a_0\left[24\dot\beta^4 + 3\dot\phi^4 - 12\dot\beta\dot\phi^3\right] \\
&+\alpha' a_0\left[\dot\gamma^4(c_2 + nc_4) + \dot\gamma^3 nc_5\dot\beta + \dot\gamma^2\dot\beta^2(2c_5 + 24n^2) + n\dot\gamma(72\dot\beta^3 - 4\dot\phi^3)\right] = \\
&= -2w_3\lambda_{\rm s}^{D-1}e^{\phi}\rho.
\end{aligned}
\tag{E.4}
$$

For all the applications of this paper we shall use the convention $\alpha' a_0 = 1/4$ (bosonic string model in units $\alpha' = 1$ and heterotic superstrings in units $\alpha' = 2$), and we shall define the constants C and H_V, related to the energy density and viscosity of the matter sources as well as to the dilaton, as specified in Eq. (8.10).

E.1 Axion perturbations in the string phase background

Let us start with the α'-corrected action (8.1), and perturb the NS-NS two-form B by putting $H_{ABC} \to H_{ABC} + \delta H_{ABC}$, where δH is defined in terms of the Kalb-Ramond axion χ according to Eq. (8.11). Let us assume that $\chi = \chi(t, x_i)$, that the zeroth-order Kalb-Ramond background is vanishing ($H_{ABC} = 0$), and that the matter action S_m is decoupled from B. Working with the explicit form (8.2) of the metric tensor, but using the convenient conformal time coordinate τ defined by $dt = a d\tau$, we then obtain the following quadratic perturbed action

$$
\delta_H S = -\frac{1}{2\lambda_{\rm s}^2}\int d\tau\, a^2 b^{-n} e^{\phi}\left[A(\tau)\partial_\mu\chi\partial^\mu\chi + B^{\mu\nu}(\tau)\partial_\mu\chi\partial_\nu\chi\right],
\tag{E.5}
$$

where

$$
\begin{aligned}
A &= \frac{1}{2}\left[1 + \alpha'\alpha_0\left(g^{MN}R_{AMN}{}^{A} + 4g^{\mu\nu}R_{A\mu\nu}{}^{A} + 2g^{\mu\nu}R_{\alpha\mu\nu}{}^{\alpha} + 11\nabla\phi^2\right)\right], \\
B_{\mu\nu} &= 2\alpha' a_0\left(\partial_\mu\phi\partial_\nu\phi - R_{A\mu\nu}{}^{A} - R_{\alpha\mu\nu}{}^{\alpha}\right).
\end{aligned}
\tag{E.6}
$$

Note that in the above equations we have explicitly written the coefficients $\alpha' a_0$ for a clear identification of the high-curvature α' contributions. We also recall that capital Latin indices run from 0 to $D-1$, Greek indices from 0 to 3. Finally, it should be noted that the three Ricci tensors $R_{AMN}{}^{A}$, $R_{A\mu\nu}{}^{A}$ and $R_{\alpha\mu\nu}{}^{\alpha}$, appearing in Eq. (E.6), are in general all different, as they contain different contributions of the internal and external geometry. We have, for our metric (8.2):

$$\begin{aligned} R_{\alpha 00}{}^{\alpha} &= -3(\ddot{\beta}+\dot{\beta}^2), & R_{\alpha ij}{}^{\alpha} &= -g_{ij}(\ddot{\beta}+3\dot{\beta}^2), \\ R_{A00}{}^{A} &= -3(\ddot{\beta}+\dot{\beta}^2)-n(\ddot{\gamma}+\dot{\gamma}^2), & R_{Aij}{}^{A} &= -g_{ij}(\ddot{\beta}+3\dot{\beta}^2+n\dot{\gamma}\dot{\beta}), \\ R_{Amn}{}^{A} &= -g_{mn}(\ddot{\gamma}+n\dot{\gamma}^2+3\dot{\beta}\dot{\gamma}). \end{aligned} \tag{E.7}$$

For a more explicit form of the action (E.5) controlling the axion dynamics we need, in particular, the functions A, B_{00}, B_{ij}. By using Eqs. (E.6), (E.7) we find that the effective action for the Fourier components χ_k of the axion perturbations can be put in the form of Eq. (8.12) with

$$z^2(\tau) = a^2 b^{-n} e^{\phi} f_1(\tau), \qquad y^2(\tau) = a^2 b^{-n} e^{\phi} f_2(\tau), \tag{E.8}$$

where

$$\begin{aligned} f_1(\tau) &= \frac{1}{2}\left[\frac{15}{2}\dot{\phi}^2 - 9\ddot{\beta} - n\ddot{\gamma} - 30\dot{\beta}^2 - \frac{n}{2}(n+1)\dot{\gamma}^2 - 9n\dot{\gamma}\dot{\beta}\right], \\ f_2(\tau) &= \frac{1}{2}\left[\frac{11}{2}\dot{\phi}^2 - 17\ddot{\beta} - 3n\ddot{\gamma} - 30\dot{\beta}^2 - \frac{n}{2}(n+5)\dot{\gamma}^2 - 7n\dot{\gamma}\dot{\beta}\right]. \end{aligned} \tag{E.9}$$

Finally, for the particular background we are considering, we have to impose $\ddot{\beta} = 0 = \ddot{\gamma}$. In this limit f_1 and f_2 are constant ($f_1 = \alpha_1^2$, $f_2 = \alpha_2^2$), the two pump fields z and y become proportional as anticipated in Eqs. (8.15), and the final canonical equation for the axion perturbations takes the form (8.16), with

$$c_s^2 = \left(\frac{\alpha_1}{\alpha_2}\right)^2 = 1 + \frac{2}{\alpha_2^2}\left(\dot{\phi}^2 + n\dot{\gamma}^2 - 2n\dot{\gamma}\dot{\beta}\right). \tag{E.10}$$

E.2 The non-minimal relic GW spectrum and the associated constraints

We briefly report here, for the reader's convenience, the explicit form of the relic GW spectrum obtained in the context of a non-minimal pre-big bang scenario, and the phenomenological and theoretical constraints to be imposed for the consistent interpretation of such a spectrum as a possible source of the observed PTA signal.

The today observable energy density of this spectrum $\Omega_{GW}(f,t_0)=\rho_c(t_0)^{-1}d\rho_{GW}(t_0)/(d\ln f)$, given in units of critical energy density $\rho_c(t_0)$, has in general four high-frequency branches corresponding to modes living the horizon in the initial dilaton-driven phase or in the string phase, and re-entering the horizon in the dust-like phase dominated by the oscillations of the axion background or in the standard radiation era. It can be parametrised as follows [4, 155, 179]:

$$\frac{\Omega_{\rm GW}(f,t_0)}{\Omega_{\rm GW}(f_1,t_0)}=\begin{cases}\left(\dfrac{f}{f_1}\right)^{3-|3-2\beta_h|}, & f_\sigma\lesssim f\lesssim f_1\\[2ex] \left(\dfrac{f_\sigma}{f_1}\right)^{3-|3-2\beta_h|}\left(\dfrac{f}{f_\sigma}\right)^{1-|3-2\beta_h|}, & f_d\lesssim f\lesssim f_\sigma\\[2ex] \left(\dfrac{f_\sigma}{f_1}\right)^{3-|3-2\beta_h|}\left(\dfrac{f_d}{f_\sigma}\right)^{1-|3-2\beta_h|}\left(\dfrac{f}{f_d}\right)^{3-|3-2\beta_h|}, & f_s\lesssim f\lesssim f_d\\[2ex] \left(\dfrac{f_\sigma}{f_1}\right)^{3-|3-2\beta_h|}\left(\dfrac{f_d}{f_\sigma}\right)^{1-|3-2\beta_h|}\left(\dfrac{f_s}{f_d}\right)^{3-|3-2\beta_h|}\left(\dfrac{f}{f_s}\right)^{3}, & f\lesssim f_s\,.\end{cases} \tag{E.11}$$

Here

$$\Omega_{\rm GW}(f_1,t_0)=\Omega_r(t_0)\left(\frac{H_1}{M_{\rm Pl}}\right)^2\left(\frac{f_d}{f_\sigma}\right)^2, \tag{E.12}$$

where $\Omega_r(t_0)\sim 10^{-4}$ is the present critical fraction of radiation energy density (including neutrinos), and H_1 (in units of Planck mass $M_{\rm Pl}$) is the curvature "bouncing scale" marking the transition to the decelerated post-inflationary evolution. The spectral parameter β_h is the same as given in Eq. (8.21); obviously, in the presence of viscosity ($H_V\neq 0$), it has to be replaced by the generalised parameter $\widetilde{\beta}_h$ of Eq. (8.25). Finally, f_s, f_1, f_σ, f_d are transition frequency scales marking, respectively, the beginning and the end of the string phase, and the beginning and

the end of the post-bouncing, axion-dominated regime. They are related to the physical parameters represented the bouncing scale H_1, the initial value σ_i of the post-bouncing axion background, and the mass m of the oscillating axion, and can be conveniently expressed in terms of the dimensionless parameters z_s, z_d, z_σ as follows:

$$z_s = \frac{f_1}{f_s}, \qquad z_d = \frac{f_1}{f_d}, \qquad z_\sigma = \frac{f_1}{f_\sigma}, \qquad\qquad z_s \gtrsim z_d > z_\sigma \gtrsim 1. \tag{E.13}$$

Let us now give the full list of constraints to be imposed on the spectral distribution (E.11) and on its parameters.

First of all, in order to reproduce the PTA signal, we shall assume that [179]

$$\Omega_{\rm GW}(f_s, t_0) \simeq 2.9 \times 10^{-8}, \qquad\qquad f_s \simeq 1.2 \times 10^{-8}{\rm Hz}. \tag{E.14}$$

Since the (non-dual) spectrum may be growing in the string phase, $f > f_s$, we have thus to take into account also the experimental upper bound on the spectrum imposed by recent data of the LIGO-Virgo-KAGRA (LVK) network [116], namely:

$$\Omega_{\rm GW}(f_{\rm LVK}) < 4.12 \times 10^{-8}, \qquad\qquad f_{\rm LVK} \simeq 35.4\,{\rm Hz}\,. \tag{E.15}$$

From the theoretical side, on the other hand, we have constraints on the values of the physical parameters H_1, σ_i, m which control, respectively, the high-curvature bouncing scale, the scale $H_\sigma \sim m(\sigma_i/Mp)^4$ of the dust-like axion-dominated oscillations, and the axion-decay scale $H_d \sim (m/M_{\rm Pl})^2$. Here we adopt, in particular, the same constraints used in [179]:

$$10^{-3} \lesssim \frac{H_1}{M_{\rm Pl}} \lesssim 10^{-1}, \qquad\qquad 10^{-3/2} \lesssim \frac{\sigma_i}{M_{\rm Pl}} \lesssim 1, \tag{E.16}$$

which, by expressing σ_i and m in terms of the parameters z_i of Eq. (E.13),

$$\frac{m}{M_{\rm Pl}} \simeq \left(\frac{H_1}{M_{\rm Pl}}\right)^{1/3} z_d^{-1} z_\sigma^{1/3}, \qquad\qquad \frac{\sigma_i}{M_{\rm Pl}} \simeq \left(\frac{H_1}{M_{\rm Pl}}\right)^{1/6} z_d^{1/4} z_\sigma^{-7/12}, \tag{E.17}$$

provide strong constraints on the possible spectral distribution.

There are further important constraints arising from the self-consistency of the

considered pre-big bang scenario, and from its consistency with standard cosmological phenomenology. In particular: the axion decay scale H_d must be larger than the scale $H_N \sim (1\text{Mev})^2/M_{\rm Pl}$ of standard nucleosynthesis. Also, the typical frequency scale of $f_{\rm LSS}$ of Large Scale Structures, related to the *pivot* frequency scale $f_* \simeq 0.05\,\text{Mpc}^{-1}$ by $f_{\rm LSS} \simeq 60 f_*$, must be smaller than the spectral scale f_s marking the beginning of the string phase: namely, $f_* < f_{\rm LSS} \lesssim f_s$. Finally, the normalisation of the scalar spectrum at the *pivot* scale, written in terms of the observed scalar spectral index $n_s \simeq 0.965$ and of the scalar amplitude $P_s(f_*) \simeq 2.1 \times 10^{-9}$, gives a phenomenological condition which automatically fixes H_1 in terms of all the other spectral parameters.

All the above-mentioned constraints have been explicitly written (in a convenient logarithmic form) and applied to the parameters of the GW spectrum (E.11), for a general (dual and non-dual) non-minimal scenario, in previous papers (see in particular [179] for an updated discussion). The resulting allowed regions of the spectral parameters has been used in this paper to select the explicit examples of non-minimal models and the related spectra presented in Sects. 8.3.1, 8.3.2.

Bibliography

[1] E. Pavone and L. Tedesco, *Viscosity in isotropic cosmological backgrounds in general relativity and starobinsky gravity*, *Journal of Cosmology and Astroparticle Physics* **2025** (2025) 065.

[2] P. Conzinu, M. Gasperini and E. Pavone, *A simple example of "non-minimal" Pre-Big Bang scenario*, *JCAP* **11** (2025) 027 [2506.00995].

[3] P. Conzinu, G. Fanizza, M. Gasperini, E. Pavone, L. Tedesco and G. Veneziano, *Constraints on the Pre-Big Bang scenario from a cosmological interpretation of the NANOGrav data*, *JCAP* **02** (2025) 039 [2412.01734].

[4] I. Ben-Dayan, G. Calcagni, M. Gasperini, A. Mazumdar, E. Pavone, U. Thattarampilly et al., *Gravitational-wave background in bouncing models from semi-classical, quantum and string gravity*, *JCAP* **09** (2024) 058 [2406.13521].

[5] P. Conzinu, G. Fanizza, M. Gasperini, E. Pavone, L. Tedesco and G. Veneziano, *From the string vacuum to FLRW or de Sitter via α' corrections*, *JCAP* **12** (2023) 019 [2308.16076].

[6] G. Fanizza, M. Gasperini, E. Pavone and L. Tedesco, *Linearized propagation equations for metric fluctuations in a general (non-vacuum) background geometry*, *JCAP* **07** (2021) 021 [2105.13041].

[7] G. Fanizza, E. Pavone and L. Tedesco, *Freeze-out and spectral running of primordial gravitational waves in viscous cosmology*, *Submitted to JCAP* (2025) [2512.04011].

[8] G. Fanizza, E. Pavone and L. Tedesco, *Gravitational wave luminosity distance in viscous cosmological models*, *JCAP* **08** (2022) 064.

[9] S. Longo, G.M. Longo, E. Pavone and F. Schiavone, *Deterministic models of minority neutral particle kinetics close to a catalytic surface, based on the formalism of radiative transfer*, *Plasma Sources Science and Technology* **28** (2019) 125008.

[10] L.P. Grishchuk, *Amplification of gravitational waves in an isotropic universe*, *Soviet Physics JETP* **40** (1975) 409.

[11] A.A. Starobinsky, *Spectrum of relict gravitational radiation and the early state of the universe*, *JETP Letters* **30** (1979) 682.

[12] V.F. Mukhanov, H.A. Feldman and R.H. Brandenberger, *Theory of cosmological perturbations*, *Phys. Rept.* **215** (1992) 203.

[13] V.F. Mukhanov and G.V. Chibisov, *Quantum fluctuations and a nonsingular universe*, *JETP Letters* **33** (1981) 532.

[14] S.W. Hawking, *The development of irregularities in a single bubble inflationary universe*, *Phys. Lett. B* **115** (1982) 295.

[15] A.H. Guth and S.-Y. Pi, *Fluctuations in the new inflationary universe*, *Phys. Rev. Lett.* **49** (1982) 1110.

[16] J.M. Bardeen, P.J. Steinhardt and M.S. Turner, *Spontaneous creation of almost scale-free density perturbations in an inflationary universe*, *Phys. Rev. D* **28** (1983) 679.

[17] S.W. Hawking, *Particle Creation by Black Holes*, *Commun. Math. Phys.* **43** (1975) 199.

[18] A.D. Linde, *A new inflationary universe scenario: A possible solution of the horizon, flatness, homogeneity, isotropy and primordial monopole problems*, *Phys. Lett. B* **108** (1982) 389.

[19] M. Gasperini and G. Veneziano, *O(d,d) covariant string cosmology*, *Phys. Lett. B* **277** (1992) 256 [hep-th/9112044].

[20] M. Gasperini and G. Veneziano, *Pre-big bang in string cosmology*, *Astropart. Phys.* **1** (1993) 317 [hep-th/9211021].

[21] M. Gasperini and G. Veneziano, *The pre-big bang scenario in string cosmology*, *Phys. Rept.* **373** (2003) 1 [hep-th/0207130].

[22] LISA Fundamental Physics Working Group collaboration, *Prospects for fundamental physics with lisa*, *Gen. Relativ. Gravit.* **52** (2020) 81 [2001.09793].

[23] M. Colpi et al., *Lisa definition study report*, 2402.07571.

[24] LISA Cosmology Working Group collaboration, *Cosmology with the laser interferometer space antenna*, *Living Rev. Relativ.* **26** (2023) 5 [2204.05434].

[25] M. Maggiore et al., *Science case for the einstein telescope*, *JCAP* **2003** (2020) 050 [1912.02622].

[26] M. Branchesi et al., *Science with the einstein telescope: a comparison of different designs*, *JCAP* **2307** (2023) 068 [2303.15923].

[27] N. Seto, S. Kawamura and T. Nakamura, *Possibility of direct measurement of the acceleration of the universe using 0.1-hz band laser interferometer gravitational wave antenna in space*, *Phys. Rev. Lett.* **87** (2001) 221103 [astro-ph/0108011].

[28] S. Kawamura et al., *The japanese space gravitational wave antenna: Decigo*, *Class. Quantum Grav.* **28** (2011) 094011.

[29] S. Kawamura et al., *Current status of space gravitational wave antenna decigo and b-decigo*, *Prog. Theor. Exp. Phys.* **2021** (2021) 05A105 [2006.13545].

[30] NANOGrav collaboration, *The nanograv 15-year data set: evidence for a gravitational-wave background*, *Astrophys. J. Lett.* **951** (2023) L8 [2306.16213].

[31] NANOGrav collaboration, *The nanograv 15 yr data set: Observations and timing of 68 millisecond pulsars*, *Astrophys. J. Lett.* **951** (2023) L9 [2306.16217].

[32] PPTA collaboration, *Search for an isotropic gravitational-wave background with the parkes pulsar timing array*, *Astrophys. J. Lett.* **951** (2023) L6 [2306.16215].

[33] A. Zic et al., *The parkes pulsar timing array third data release*, *Publ. Astron. Soc. Aust.* **40** (2023) e049 [2306.16230].

[34] EPTA collaboration, *The second data release from the european pulsar timing array - i. the dataset and timing analysis*, *Astron. Astrophys.* **678** (2023) A48 [2306.16224].

[35] EPTA AND INPTA collaboration, *The second data release from the european pulsar timing array iii. search for gravitational wave signals*, *Astron. Astrophys.* **678** (2023) A50 [2306.16214].

[36] CPTA collaboration, *Searching for the nano-hertz stochastic gravitational wave background with the chinese pulsar timing array data release i*, *Res. Astron. Astrophys.* **23** (2023) 075024 [2306.16216].

[37] M. Gasperini, *Theory of Gravitational Interactions*, Undergraduate Lecture Notes in Physics, Springer (2013), 10.1007/978-88-470-2691-9.

[38] PLANCK collaboration, *Planck 2018 results. VI. Cosmological parameters*, *Astron. Astrophys.* **641** (2020) A6 [1807.06209].

[39] A.G. Riess, S. Casertano, W. Yuan, J.B. Bowers, L. Macri, J.C. Zinn et al., *Cosmic distances calibrated to 1% precision with gaia edr3 parallaxes and hubble space telescope photometry of 75 milky way cepheids confirm tension with λcdm*, *Astrophys. J. Lett.* **908** (2021) L6 [2012.08534].

[40] W.L. Freedman, B.F. Madore, D. Hatt, T.J. Hoyt, I.S. Jang, R.L. Beaton et al., *The carnegie-chicago hubble program. viii. an independent determination of the hubble constant based on the tip of the red giant branch*, *Astrophys. J.* **882** (2019) 34.

[41] W.L. Freedman, B.F. Madore, T. Hoyt, I.S. Jang, R. Beaton, M.G. Lee et al., *Calibration of the tip of the red giant branch (trgb)*, *Astrophys. J.* **891** (2020) 57.

[42] K.C. Wong, S.H. Suyu, G.C.-F. Chen, C.E. Rusu, M. Millon, D. Sluse et al., *H0licow xiii. a 2.4% measurement of h_0 from lensed quasars: 5.3σ tension between early- and late-universe probes*, *MNRAS* **498** (2020) 1420.

[43] W. Yuan, A.G. Riess, L.M. Macri, S. Casertano and D.M. Scolnic, *Consistent calibration of the tip of the red giant branch in the large magellanic cloud on the hst f814w system and a re-determination of the hubble constant*, *Astrophys. J.* **886** (2019) 61.

[44] D.W. Pesce, J.A. Braatz, M.J. Reid, A.G. Riess, D. Scolnic, J.J. Condon et al., *The megamaser cosmology project. xiii. combined hubble constant constraints*, *Astrophys. J.* **891** (2020) L1.

[45] DESI Collaboration collaboration, *Desi dr2 results ii: Measurements of baryon acoustic oscillations and cosmological constraints*, 2503.14738.

[46] C.G. Callan, D. Friedan, E.J. Martinec and M.J. Perry, *Strings in background fields*, *Nucl. Phys. B* **262** (1985) 593.

[47] E.S. Fradkin and A.A. Tseytlin, *Effective field theory from quantized strings*, *Phys. Lett. B* **158** (1985) 316.

[48] B. Zwiebach, *Curvature squared terms and string theories*, *Phys. Lett. B* **156** (1985) 315.

[49] D.J. Gross and J.H. Sloan, *The quartic effective action for the heterotic string*, *Nucl. Phys. B* **291** (1987) 41.

[50] R.R. Metsaev and A.A. Tseytlin, *Order α' (two-loop) equivalence of the string equations of motion and the σ-model weyl invariance conditions: Dependence on the dilaton and the antisymmetric tensor*, *Nucl. Phys. B* **293** (1987) 385.

[51] A.D. Felice and S. Tsujikawa, *f(r) theories*, *Living Rev. Rel.* **13** (2010) 3.

[52] T.P. Sotiriou and V. Faraoni, *f(r) theories of gravity*, *Rev. Mod. Phys.* **82** (2010) 451.

[53] M. Gasperini, *Lezioni di Cosmologia Teorica*, Springer-Verlag Mailand (2012), 10.1007/978-88-470-2253-9.

[54] M. Maggiore, *Gravitational Waves: Volume 2: Astrophysics and Cosmology*, Oxford University Press, Oxford (2018), 10.1093/oso/9780198570899.001.0001.

[55] LIGO Scientific Collaboration and Virgo Collaboration collaboration, *Multi-messenger observations of a binary neutron star merger*, *Astrophys. J. Lett.* **848** (2017) L12 [1710.05833].

[56] R.J. Adler, B. Casey and O.C. Jacob, *Vacuum catastrophe: An elementary exposition of the cosmological constant problem*, *Am. J. Phys.* **63** (1995) 620.

[57] A.A. Penzias and R.W. Wilson, *A measurement of excess antenna temperature at 4080 mc/s*, *Astrophys. J.* **142** (1965) 419.

[58] M. Gasperini, *Relic gravitons from the pre-big bang: What we know and what we do not know*, in *String Theory in Curved Spacetimes*, N. Sanchez, ed., (Singapore), p. 333, World Scientific (1998), DOI [hep-th/9607146].

[59] M. Gasperini, *Elementary introduction to pre-big bang cosmology and to the relic graviton background*, in *Gravitational Waves: Proc. of the Second SIGRAV School on Gravitational Waves in Astrophysics, Cosmology and String Theory*, (Bristol), IOP Publishing (2001) [hep-th/9907067].

[60] M. Gasperini, *Elements of String Cosmology*, Cambridge University Press, Cambridge, UK (2007).

[61] J. Polchinski, *String Theory. Vol. 1: An Introduction to the Bosonic String*, Cambridge University Press (1998).

[62] J. Polchinski, *String Theory. Vol. 2: Superstring Theory and Beyond*, Cambridge University Press (1998).

[63] M.B. Green, J.H. Schwarz and E. Witten, *Superstring Theory. Vol. 1: Introduction*, Cambridge University Press (1987).

[64] M.B. Green, J.H. Schwarz and E. Witten, *Superstring Theory. Vol. 2: Loop Amplitudes, Anomalies and Phenomenology*, Cambridge University Press (1987).

[65] K. Becker, M. Becker and J.H. Schwarz, *String Theory and M-Theory: A Modern Introduction*, Cambridge University Press (2007).

[66] E. Kiritsis, *String Theory in a Nutshell*, Princeton University Press, 2 ed. (2019).

[67] B. Zwiebach, *A First Course in String Theory*, Cambridge University Press, 2 ed. (2009).

[68] M. Gasperini, *Elements of String Cosmology*, Cambridge University Press, Cambridge (2007).

[69] M. Gasperini and G. Veneziano, *String theory and pre-big bang cosmology*, *Nucl. Phys. B Proc. Suppl.* **171** (2007) 957 [hep-th/0703055].

[70] K.A. Meissner and G. Veneziano, *Symmetries of cosmological superstring vacua*, *Phys. Lett. B* **267** (1991) 33.

[71] G. Veneziano, *Scale factor duality for classical and quantum strings*, *Phys. Lett. B* **265** (1991) 287.

[72] R. Brustein, M. Gasperini, M. Giovannini and G. Veneziano, *Relic gravitational waves from string cosmology*, *Phys. Lett. B* **361** (1995) 45 [hep-th/9507017].

[73] M. Gasperini, *Tensor perturbations in high curvature string backgrounds*, *Phys. Rev. D* **56** (1997) 4815 [gr-qc/9704045].

[74] E.J. Copeland, J.E. Lidsey and D. Wands, *S-duality invariant perturbations in string cosmology*, *Nucl. Phys. B* **506** (1997) 407 [hep-th/9705050].

[75] D.H. Lyth and D. Wands, *Generating the curvature perturbation without an inflaton*, *Phys. Lett. B* **524** (2002) 5 [hep-ph/0110002].

[76] O. Hohm and B. Zwiebach, *Duality invariant cosmology to all orders in α'*, *Phys. Rev. D* **100** (2019) 126011 [1905.06963].

[77] K.A. Meissner and G. Veneziano, *Manifestly o(d,d) invariant approach to space-time dependent string vacua*, *Mod. Phys. Lett. A* **6** (1991) 3397 [hep-th/9110004].

[78] J. Maharana and J.H. Schwarz, *Noncompact symmetries in string theory*, *Nucl. Phys. B* **390** (1993) 3 [hep-th/9207016].

[79] A. Sen, *O(d) x o(d) symmetry of the space of cosmological solutions in string theory, scale factor duality and two-dimensional black holes*, *Phys. Lett. B* **271** (1991) 295.

[80] K.A. Meissner, *Symmetries of higher order string gravity actions*, *Phys. Lett. B* **392** (1997) 298 [hep-th/9610131].

[81] T. Codina, O. Hohm and D. Marques, *String dualities at order α'^3*, *Phys. Rev. Lett.* **126** (2021) 171602 [2012.15677].

[82] T. Codina, O. Hohm and D. Marques, *General string cosmologies at order α'^3*, *Phys. Rev. D* **104** (2021) 106007 [2107.00053].

[83] A.A. Tseytlin, *Duality and dilaton*, *Mod. Phys. Lett. A* **6** (1991) 1721.

[84] O. Hohm and B. Zwiebach, *Non-perturbative de sitter vacua via α' corrections*, *Int. J. Mod. Phys. D* **28** (2019) 1943002 [1905.06583].

[85] J. Quintin, H. Bernardo and G. Franzmann, *Cosmology at the top of the α' tower*, *JHEP* **07** (2021) 149 [2105.01083].

[86] T. Codina, O. Hohm and B. Zwiebach, *2d black holes, bianchi i cosmologies, and α'*, *Phys. Rev. D* **108** (2023) 026014 [2304.06763].

[87] H. Bernardo, R. Brandenberger and G. Franzmann, *String cosmology backgrounds from classical string geometry*, *Phys. Rev. D* **103** (2021) 043540 [2005.08324].

[88] C.A. Núñez and F.E. Rost, *New non-perturbative de sitter vacua in α'-complete cosmology*, *JHEP* **03** (2021) 007 [2011.10091].

[89] P. Bieniek, J. Chojnacki, J.H. Kwapisz and K.A. Meissner, *Stability of the nonperturbative o(d,d) de sitter spacetime: The isotropic case*, *Phys. Rev. D* **106** (2022) 106009 [2208.06010].

[90] P. Bieniek, J. Chojnacki, J.H. Kwapisz and K.A. Meissner, *Stability of the de-Sitter spacetime. The anisotropic case*, *Phys. Lett. B* **850** (2024) 138537 [2301.06616].

[91] L. Song and D. Chen, *Two non-perturbative α' or loop corrected string cosmological solutions*, *Chin. Phys. C* **47** (2023) 095102 [2306.07031].

[92] H. Bernardo, P.R. Chouha and G. Franzmann, *Kalb-ramond backgrounds in α'-complete cosmology*, *JHEP* **09** (2021) 109 [2104.15131].

[93] M. Gasperini and G. Veneziano, *Non-singular pre-big bang scenarios from all-order α' corrections*, *JHEP* **07** (2023) 144 [2305.00222].

[94] S.R. Das and B. Sathiapalan, *New infinities in two-dimensional nonlinear σ models and consistent string propagation*, *Phys. Rev. Lett.* **57** (1986) 1511.

[95] T. Codina, O. Hohm and B. Zwiebach, *Black hole singularity resolution in D=2 via duality-invariant α' corrections*, *Phys. Rev. D* **108** (2023) 126006 [2308.09743].

[96] P. Wang, H. Wu, H. Yang and S. Ying, *Non-singular string cosmology via α' corrections*, *JHEP* **10** (2019) 263 [1909.00830].

[97] P. Wang, H. Wu, H. Yang and S. Ying, *Construct α' corrected or loop corrected solutions without curvature singularities*, *JHEP* **01** (2020) 164 [1910.05808].

[98] A. Buonanno, T. Damour and G. Veneziano, *Pre-big bang bubbles from the gravitational instability of generic string vacua*, *Nucl. Phys. B* **543** (1999) 275 [hep-th/9806230].

[99] A. Feinstein, K.E. Kunze and M.A. Vázquez-Mozo, *Initial conditions and the structure of the singularity in pre-big bang cosmology*, *Class. Quant. Grav.* **17** (2000) 3599 [hep-th/0002070].

[100] M. Gasperini, *On the initial regime of pre-big bang cosmology*, *JCAP* **09** (2017) 001 [1707.05763].

[101] R. Brustein and G. Veneziano, *The graceful exit problem in string cosmology*, *Phys. Lett. B* **329** (1994) 429 [hep-th/9403060].

[102] N. Kaloper, R. Madden and K.A. Olive, *Axions and the graceful exit problem in string cosmology*, *Phys. Lett. B* **371** (1996) 34 [hep-th/9510117].

[103] R. Easther, K. Maeda and D. Wands, *Tree level string cosmology*, *Phys. Rev. D* **53** (1996) 4247 [hep-th/9509074].

[104] M. Gasperini and G. Veneziano, *Singularity and exit problems in two-dimensional string cosmology*, *Phys. Lett. B* **387** (1996) 715 [hep-th/9607126].

[105] L.D. Landau and E.M. Lifshitz, *Mechanics*, Pergamon Press, 3rd ed. (1976).

[106] M. Gasperini, F. Piazza and G. Veneziano, *Quintessence as a runaway dilaton*, *Phys. Rev. D* **65** (2002) 023508 [gr-qc/0108016].

[107] T. Damour, F. Piazza and G. Veneziano, *Runaway dilaton and equivalence principle violations*, *Phys. Rev. Lett.* **89** (2002) 081601 [gr-qc/0204094].

[108] T. Damour, F. Piazza and G. Veneziano, *Violations of the equivalence principle in a dilaton runaway scenario*, *Phys. Rev. D* **66** (2002) 046007 [hep-th/0205111].

[109] G. Veneziano, *Large n bounds on, and compositeness limit of, gauge and gravitational interactions*, *JHEP* **06** (2002) 051 [hep-th/0110129].

[110] V. Bozza, M. Gasperini, M. Giovannini and G. Veneziano, *Assisting pre-big bang phenomenology through short lived axions*, *Phys. Lett. B* **543** (2002) 14 [hep-ph/0206131].

[111] V. Bozza, M. Gasperini, M. Giovannini and G. Veneziano, *Constraints on pre-big bang parameter space from cmbr anisotropies*, *Phys. Rev. D* **67** (2003) 063514 [hep-ph/0212112].

[112] K.E. Kunze and R. Durrer, *Anisotropic "hairs" in string cosmology*, *Class. Quant. Grav.* **17** (2000) 2597 [gr-qc/9912081].

[113] C. Ganguly and J. Quintin, *Microphysical manifestations of viscosity and consequences for anisotropies in the very early universe*, *Phys. Rev. D* **105** (2022) 023532 [2109.11701].

[114] M. Gasperini, *Looking back in time beyond the big bang*, *Mod. Phys. Lett. A* **14** (1999) 1059 [gr-qc/9905062].

[115] R.H. Brandenberger and J. Martin, *Trans-planckian issues for inflationary cosmology*, *Class. Quant. Grav.* **30** (2013) 113001 [1211.6753].

[116] LIGO Scientific, VIRGO and KAGRA collaboration, *Gwtc-3: compact binary coalescences observed by ligo and virgo during the second part of the third observing run*, *Phys. Rev. X* **13** (2023) 041039 [2111.03606].

[117] LIGO Scientific, VIRGO and KAGRA collaboration, *Tests of general relativity with gwtc-3*, 2112.06861.

[118] NANOGrav collaboration, *The nanograv 15 yr data set: search for signals from new physics*, *Astrophys. J. Lett.* **951** (2023) L11 [2306.16219].

[119] International Pulsar Timing Array collaboration, *Comparing recent pta results on the nanohertz stochastic gravitational wave background*, *Astrophys. J.* **966** (2024) 105 [2309.00693].

[120] I. Ben-Dayan, U. Kumar, U. Thattarampilly and A. Verma, *Probing the early universe cosmology with nanograv: Possibilities and limitations*, *Phys. Rev. D* **108** (2023) 103507 [2307.15123].

[121] LISA Fundamental Physics Working Group collaboration, *New horizons for fundamental physics with lisa*, *Living Rev. Relativ.* **25** (2022) 4 [2205.01597].

[122] S. Mirshekari, N. Yunes and C.M. Will, *Constraining generic lorentz violation and the speed of the graviton with gravitational waves*, *Phys. Rev. D* **85** (2012) 024041 [1110.2720].

[123] P. Canizares, J.R. Gair and C.F. Sopuerta, *Testing chern–simons modified gravity with gravitational-wave detections of extreme-mass-ratio binaries*, *Phys. Rev. D* **86** (2012) 044010 [1205.1253].

[124] J. Ellis, N.E. Mavromatos and D.V. Nanopoulos, *Comments on graviton propagation in light of gw150914*, *Mod. Phys. Lett. A* **31** (2016) 1650155 [1602.04764].

[125] N. Yunes, K. Yagi and F. Pretorius, *Theoretical physics implications of the binary black-hole merger gw150914*, *Phys. Rev. D* **94** (2016) 084002 [1603.08955].

[126] M. Arzano and G. Calcagni, *What gravity waves are telling about quantum spacetime*, *Phys. Rev. D* **93** (2016) 124065 [1604.00541].

[127] G. Calcagni, S. Kuroyanagi, S. Marsat, M. Sakellariadou, N. Tamanini and G. Tasinato, *Gravitational-wave luminosity distance in quantum gravity*, *Phys. Lett. B* **798** (2019) 135000 [1904.00384].

[128] V. Cardoso and P. Pani, *Testing the nature of dark compact objects: a status report*, *Living Rev. Relat.* **22** (2019) 4 [1904.05363].

[129] LISA Cosmology Working Group collaboration, *Testing modified gravity at cosmological distances with lisa standard sirens*, *JCAP* **2019** (2019) 024 [1906.01593].

[130] G. Calcagni, S. Kuroyanagi, S. Marsat, M. Sakellariadou, N. Tamanini and G. Tasinato, *Quantum gravity and gravitational-wave astronomy*, *JCAP* **2019** (2019) 012 [1907.02489].

[131] P. Auclair et al., *Probing the gravitational wave background from cosmic strings with lisa*, *JCAP* **2020** (2020) 034 [1909.00819].

[132] E. Belgacem, Y. Dirian, A. Finke, S. Foffa and M. Maggiore, *Gravity in the infrared and effective nonlocal models*, *JCAP* **2020** (2020) 010 [2001.07619].

[133] G. Calcagni and S. Kuroyanagi, *Stochastic gravitational-wave background in quantum gravity*, *JCAP* **2021** (2021) 019 [2012.00170].

[134] A. Addazi et al., *Quantum gravity phenomenology at the dawn of the multi-messenger era – a review*, *Prog. Part. Nucl. Phys.* **125** (2022) 103948 [2111.05659].

[135] LISA Cosmology Working Group collaboration, *Measuring the propagation speed of gravitational waves with lisa*, *JCAP* **2022** (2022) 031 [2203.00566].

[136] G. Calcagni and L. Modesto, *Testing quantum gravity with primordial gravitational waves*, 2206.07066.

[137] T. Baker, E. Barausse, A. Chen, C. de Rham, M. Pieroni and G. Tasinato, *Testing gravitational wave propagation with multiband detections*, *JCAP* **2023** (2023) 044 [2209.14398].

[138] G. Calcagni and S. Kuroyanagi, *Log-periodic gravitational-wave background beyond einstein gravity*, *Class. Quantum Gravity* **41** (2023) 015031 [2308.05904].

[139] N. Christensen, *Stochastic gravitational wave backgrounds*, *Rept. Prog. Phys.* **82** (2019) 016903 [1811.08797].

[140] A.I. Renzini, B. Goncharov, A.C. Jenkins and P.M. Meyers, *Stochastic gravitational-wave backgrounds: current detection efforts and future prospects*, *Galaxies* **10** (2022) 34 [2202.00178].

[141] N. van Remortel, K. Janssens and K. Turbang, *Stochastic gravitational wave background: methods and implications*, *Prog. Part. Nucl. Phys.* **128** (2023) 104003 [2210.00761].

[142] A.S. Koshelev, L. Modesto,
L. Rachwa⟨*andA.A. Starobinsky*, *Occurrence of exact* r^2 *inflation in non-local uv-complete gravi*

[143] A.S. Koshelev, K.S. Kumar and A.A. Starobinsky, r^2 *inflation to probe non-perturbative quantum gravity*, *JHEP* **03** (2018) 071 [1711.08864].

[144] R. Brandenberger and P.-M. Ho, *Noncommutative spacetime, stringy spacetime uncertainty principle, and density fluctuations*, *Phys. Rev. D* **66** (2002) 023517 [hep-th/0203119].

[145] G. Calcagni, S. Kuroyanagi, J. Ohashi and S. Tsujikawa, *Strong planck constraints on braneworld and non-commutative inflation*, *JCAP* **03** (2014) 052 [1310.5186].

[146] R. Brandenberger and Z. Wang, *Nonsingular ekpyrotic cosmology with a nearly scale-invariant spectrum of cosmological perturbations and gravitational waves*, *Phys. Rev. D* **101** (2020) 063522 [2001.00638].

[147] R. Brandenberger and Z. Wang, *Ekpyrotic cosmology with a zero-shear s-brane*, *Phys. Rev. D* **102** (2020) 023516 [2004.06437].

[148] R. Brandenberger, K. Dasgupta and Z. Wang, *Reheating after s-brane ekpyrosis*, *Phys. Rev. D* **102** (2020) 063514 [2007.01203].

[149] R.H. Brandenberger, A. Nayeri, S.P. Patil and C. Vafa, *Tensor modes from a primordial hagedorn phase of string cosmology*, *Phys. Rev. Lett.* **98** (2007) 231302 [hep-th/0604126].

[150] R.H. Brandenberger, *String gas cosmology: progress and problems*, *Class. Quantum Gravity* **28** (2011) 204005 [1105.3247].

[151] R.H. Brandenberger, *Unconventional cosmology*, in *Lect. Notes Phys.*, vol. 863, p. 333 (2013), DOI [1203.6698].

[152] R.H. Brandenberger, A. Nayeri and S.P. Patil, *Closed string thermodynamics and a blue tensor spectrum*, *Phys. Rev. D* **90** (2014) 067301 [1403.4927].

[153] H. Bernardo, R. Brandenberger and G. Franzmann, *Solution of the size and horizon problems from classical string geometry*, *JHEP* **10** (2020) 155 [2007.14096].

[154] G. Calcagni, S. Kuroyanagi and S. Tsujikawa, *Cosmic microwave background and inflation in multi-fractional spacetimes*, *JCAP* **08** (2016) 039 [1606.08449].

[155] M. Gasperini, *Observable gravitational waves in pre-big bang cosmology: an update*, *JCAP* **12** (2016) 010 [1606.07889].

[156] M. Gasperini, M. Giovannini and G. Veneziano, *Dilaton contributions to the cosmic gravitational wave background*, *Phys. Rev. D* **47** (1993) 1519 [gr-qc/9211021].

[157] R. Brustein, M. Gasperini and G. Veneziano, *Peak and endpoint of the relic graviton background in string cosmology*, *Phys. Rev. D* **55** (1997) 3882 [hep-th/9604084].

[158] Einstein Telescope, "Sensitivity study documentation." https://apps.et-$\overline{\sigma}$gw.eu/tds/?r=18213, 2023.

[159] T. Papanikolaou, S. Banerjee, Y.-F. Cai, S. Capozziello and E.N. Saridakis, *Primordial black holes and induced gravitational waves in non-singular matter bouncing cosmology*, *JCAP* **06** (2024) 066 [2404.03779].

[160] Planck collaboration, *Planck 2018 results. X. Constraints on inflation*, *Astron. Astrophys.* **641** (2020) A10 [1807.06211].

[161] Planck collaboration, *Planck 2018 results. vi. cosmological parameters*, *Astronomy & Astrophysics* **641** (2020) A6 [1807.06209].

[162] Particle Data Group collaboration, *Review of Particle Physics*, *Prog. Theor. Exp. Phys.* **2022** (2022) 083C01.

[163] BICEP/Keck Collaboration collaboration, *Improved constraints on primordial gravitational waves using planck, wmap, and bicep/keck observations through the 2018 observing season*, *Phys. Rev. Lett.* **127** (2021) 151301 [2110.00483].

[164] M.S. Turner, M.J. White and J.E. Lidsey, *Tensor perturbations in inflationary models as a probe of cosmology*, *Phys. Rev. D* **48** (1993) 4613 [astro-ph/9306029].

[165] Y. Watanabe and E. Komatsu, *Improved calculation of the primordial gravitational wave spectrum in the standard model*, *Phys. Rev. D* **73** (2006) 123515 [astro-ph/0604176].

[166] S. Kuroyanagi, T. Chiba and N. Sugiyama, *Precision calculations of the gravitational wave background spectrum from inflation*, *Phys. Rev. D* **79** (2009) 103501 [0804.3249].

[167] M. Gasperini, *From pre- to post-big bang: an (almost) self-dual cosmological history*, *Phil. Trans. Roy. Soc. Lond. A* **380** (2022) 20210179 [2106.12865].

[168] P. Conzinu, M. Gasperini and G. Marozzi, *Primordial black holes from pre-big bang inflation*, *JCAP* **08** (2020) 031 [2004.08111].

[169] B. Allen, *Stochastic gravity-wave background in inflationary-universe models*, *Phys. Rev. D* **37** (1988) 2078.

[170] J. Garriga and E. Verdaguer, *Particle creation due to cosmological contraction of extra dimensions*, *Phys. Rev. D* **39** (1989) 1072.

[171] V. Sahni, *Energy density of relic gravity waves from inflation*, *Phys. Rev. D* **42** (1990) 453.

[172] M. Gasperini, M. Maggiore and G. Veneziano, *Towards a nonsingular pre-big bang cosmology*, *Nucl. Phys. B* **494** (1997) 315 [hep-th/9611039].

[173] T. Moroi and T. Takahashi, *Effects of cosmological moduli fields on cosmic microwave background*, *Phys. Lett. B* **522** (2001) 215 [hep-ph/0110096].

[174] K. Enqvist and M.S. Sloth, *Adiabatic cmb perturbations in pre-big bang string cosmology*, *Nucl. Phys. B* **626** (2002) 395 [hep-ph/0109214].

[175] V. Kaspi, J. Taylor and M. Ryba, *High-precision timing of millisecond pulsars. iii: Long-term monitoring of psrs b1855+09 and b1937+21*, *Astrophys. J.* **428** (1994) 713.

[176] S. Kuroyanagi, T. Chiba and T. Takahashi, *Probing the universe through the stochastic gravitational wave background*, *JCAP* **11** (2018) 038 [1807.00786].

[177] M. Braglia et al., "Gravitational waves from inflation in lisa: reconstruction pipeline and physics interpretation."

[178] C. Caprini, D.G. Figueroa, R. Flauger, G. Nardini, M. Peloso, M. Pieroni et al., *Reconstructing the spectral shape of a stochastic gravitational wave background with lisa*, *JCAP* **11** (2019) 017 [1906.09244].

[179] Q. Tan, Y. Wu and L. Liu, *Constraining string cosmology with the gravitational-wave background using the NANOGrav 15-year data set*, *Eur. Phys. J. C* **85** (2025) 327 [2409.17846].

[180] J.E. Lidsey, D. Wands and E.J. Copeland, *Superstring cosmology*, *Phys. Rep.* **337** (2000) 343 [hep-th/9909061].

[181] M. Gasperini and G. Veneziano, *String theory and pre-big bang cosmology*, *Nuovo Cim. C* **38** (2016) 160 [hep-th/0703055].

[182] P. Conzinu and G. Marozzi, *Primordial black holes formation in an early matter dominated era from the pre-big-bang scenario*, *Phys. Rev. D* **108** (2023) 043533 [2305.01430].

[183] M. Gasperini and G. Veneziano, *Dilaton production in string cosmology*, *Phys. Rev. D* **50** (1994) 2519 [gr-qc/9403031].

[184] R. Brustein, M. Gasperini, M. Giovannini, V.F. Mukhanov and G. Veneziano, *Metric perturbations in dilaton driven inflation*, *Phys. Rev. D* **51** (1995) 6744 [hep-th/9501066].

[185] S. Kawai, M.-a. Sakagami and J. Soda, *Instability of one loop superstring cosmology*, *Phys. Lett. B* **437** (1998) 284 [gr-qc/9802033].

[186] G. Veneziano, *A model for the big bounce*, *JCAP* **2004** (2004) 004 [hep-th/0312182].

[187] J. Quintin, R.H. Brandenberger, M. Gasperini and G. Veneziano, *Stringy black-hole gas in α'-corrected dilaton gravity*, *Phys. Rev. D* **98** (2018) 103519 [1809.01658].

[188] D. Bitnaya, P. Conzinu and G. Marozzi, *On the stability of string-hole gas*, *JCAP* **2024** (2024) 025 [2308.16764].

[189] G. Janssen, G. Hobbs, M. McLaughlin, C. Bassa, A. Deller, M. Kramer et al., *Gravitational wave astronomy with the ska*, in *PoS (AASKA14)*, p. 037, 2015, DOI.

[190] A.B. Green, *Primordial black holes as a dark matter candidate - a brief overview*, 2024.

[191] Z. Yi and Q. Fei, *Constraints on primordial curvature spectrum from primordial black holes and scalar-induced gravitational waves*, *Eur. Phys. J. C* **83** (2023) [2210.0641].

[192] E. Belgacem, Y. Dirian, S. Foffa and M. Maggiore, *Gravitational-wave luminosity distance in modified gravity theories*, *Phys. Rev. D* **97** (2018) 104066 [1712.08108].

[193] M. Maggiore, *Gravitational Waves. Vol. 2: Astrophysics and Cosmology*, Oxford University Press (3, 2018).

[194] E. Belgacem, Y. Dirian, S. Foffa and M. Maggiore, *Modified gravitational-wave propagation and standard sirens*, *Phys. Rev. D* **98** (2018) 023510 [1805.08731].

[195] LISA Cosmology Working Group collaboration, *Testing modified gravity at cosmological distances with LISA standard sirens*, *JCAP* **07** (2019) 024 [1906.01593].

[196] S. Mukherjee, B.D. Wandelt and J. Silk, *Testing the general theory of relativity using gravitational wave propagation from dark standard sirens*, *Mon. Not. Roy. Astron. Soc.* **502** (2021) 1136 [2012.15316].

[197] A. Begnoni, L. Valbusa Dall'Armi, D. Bertacca and A. Raccanelli, *Gravitational wave luminosity distance-weighted anisotropies*, *JCAP* **10** (2024) 087 [2404.12351].

[198] M. Pantiri, M. Foglieni, E. Di Dio and E. Castorina, *The power spectrum of luminosity distance fluctuations in General Relativity*, *JCAP* **11** (2024) 021 [2407.01486].

[199] J. Fonseca, S. Zazzera, T. Baker and C. Clarkson, *The observed number counts in luminosity distance space*, *JCAP* **08** (2023) 050 [2304.14253].

[200] A. Lizardo, J. Chagoya and C. Ortiz, *On phenomenological parametrizations for the luminosity distance of gravitational waves*, *Int. J. Mod. Phys. D* **31** (2022) 2250109 [2107.09143].

[201] C. García, C. Santa and A.E. Romano, *Deep learning reconstruction of the large-scale structure of the Universe from luminosity distance*, *Mon. Not. Roy. Astron. Soc.* **518** (2022) 2241 [2107.05771].

[202] D. Bertacca, A. Raccanelli, N. Bartolo and S. Matarrese, *Cosmological perturbation effects on gravitational-wave luminosity distance estimates*, *Phys. Dark Univ.* **20** (2018) 32 [1702.01750].

[203] J. Yoo and F. Scaccabarozzi, *Unified Treatment of the Luminosity Distance in Cosmology*, *JCAP* **09** (2016) 046 [1606.08453].

[204] C. Deffayet and K. Menou, *Probing Gravity with Spacetime Sirens*, *Astrophys. J. Lett.* **668** (2007) L143 [0709.0003].

[205] I.D. Saltas, I. Sawicki, L. Amendola and M. Kunz, *Anisotropic Stress as a Signature of Nonstandard Propagation of Gravitational Waves*, *Phys. Rev. Lett.* **113** (2014) 191101 [1406.7139].

[206] J. Chi, Y. Wu, Y. Sang et al., *Gravitational wave luminosity distance for starobinsky gravity in viscous cosmological models*, *Eur. Phys. J. C* **85** (2025) 22.

[207] G. Fanizza, G. Franchini, M. Gasperini and L. Tedesco, *Comparing the luminosity distance for gravitational waves and electromagnetic signals in a simple model of quadratic gravity*, *Gen. Rel. Grav.* **52** (2020) 111 [2010.06569].

[208] A. Starobinsky, *A new type of isotropic cosmological models without singularity*, *Phys. Lett. B* **91** (1980) 99.

[209] S. Nojiri and S.D. Odintsov, *Unified cosmic history in modified gravity: from f(r) theory to lorentz non-invariant models*, *Phys. Rept.* **505** (2011) 59 [1011.0544].

[210] S. Nojiri, S.D. Odintsov and V.K. Oikonomou, *Modified gravity theories on a nutshell: Inflation, bounce and late-time evolution*, *Phys. Rept.* **692** (2017) 1 [1705.11098].

[211] G. Cognola, E. Elizalde, S. Nojiri, S.D. Odintsov and S. Zerbini, *One-loop f(r) gravity in de sitter universe*, *JCAP* **0502** (2005) 010 [hep-th/0501096].

[212] S. Bahamonde, S.D. Odintsov, V.K. Oikonomou and M. Wright, *Correspondence of f(r) gravity singularities in jordan and einstein frames*, *Annals Phys.* **373** (2016) 96 [1603.05113].

[213] S. Bahamonde, S.D. Odintsov, V.K. Oikonomou and P.V. Tretyakov, *Deceleration versus acceleration universe in different frames of $f(r)$ gravity*, *Phys. Lett. B* **766** (2017) 225 [1701.02381].

[214] S. Capozziello, S. Nojiri and S.D. Odintsov, *Dark energy: The equation of state description versus scalar-tensor or modified gravity*, *Phys. Lett. B* **634** (2006) 93 [hep-th/0512118].

[215] S.D. Odintsov and V.K. Oikonomou, *Generalized rp-attractor cosmology in the jordan and einstein frames: New type of attractors and revisiting standard jordan frame rp inflation*, *Int. J. Mod. Phys. D* **32** (2023) 2250135 [2210.11351].

[216] A. Muronga, *Causal theories of dissipative relativistic fluid dynamics for nuclear collisions*, *Phys. Rev. C* **69** (2004) 034903 [nucl-th/0309055].

[217] N. Deruelle and M. Sasaki, *Conformal equivalence in classical gravity: the example of 'veiled' General Relativity*, in *Springer Proceedings in Physics*, vol. 137, pp. 247–260, Springer, 2011 [1007.3563].

[218] T. Chiba and M. Yamaguchi, *Conformal-frame (in)dependence of cosmological observations in scalar-tensor theory*, *JCAP* **10** (2013) 040 [1308.1142].

[219] F. Rondeau and B. Li, *Conformal frame dependence of inflation*, *Phys. Rev. D* **96** (2017) 124009 [1709.07087].

[220] M. Gasperini and G. Veneziano, *Inflation, deflation, and frame independence in string cosmology*, *Mod. Phys. Lett. A* **8** (1993) 3701 [hep-th/9309023].

[221] M. Gasperini, N.G. Sanchez and G. Veneziano, *Highly unstable fundamental strings in inflationary cosmologies*, *Int. J. Mod. Phys. A* **6** (1991) 3853.

[222] M. Gasperini, N.G. Sanchez and G. Veneziano, *Selfsustained inflation and dimensional reduction from fundamental strings*, *Nucl. Phys. B* **364** (1991) 365.

[223] J. Quintin and R. Brandenberger, *Black hole formation in a contracting universe*, *JCAP* **2016** (2016) 029.

[224] P. Conzinu, *Echoes from the Early Universe*, Ph.D. thesis, University of Pisa, 2024.

[225] P.S. Letelier, *Anisotropic fluids with two-perfect-fluid components*, *Phys. Rev. D* **22** (1980) 807.

[226] L. Herrera and N.O. Santos, *Local anisotropy in self-gravitating systems*, *Phys. Rept.* **286** (1997) 53.

[227] L.H. Ford and L. Parker, *Quantized gravitational wave perturbations in robertson–walker universes*, *Phys. Rev. D* **16** (1977) 1601.